mTOR-Mediated Regulation
of
Group 3 Innate Lymphoid Cell Numbers
and
Cytokine Responses

Inauguraldissertation

zur

Erlangung der Würde eines Doktors der Philosophie

vorgelegt der

Philosophisch-Naturwissenschaftlichen Fakultät

der Universität Basel

von

Claudia Cornelia Teufel

2020

Genehmigt von der Philosophisch-Naturwissenschaftlichen Fakultät

auf Antrag von

Prof. Dr. Daniela Finke

Prof. Dr. Jean Pieters

Prof. Dr. Christoph Müller

Basel, den 23.06.2020

Prof. Dr. Martin Spiess

Dekan

Table of Contents

1 Summary

Group 3 innate lymphoid cells (ILC3s) are most abundant at surface barrier regions, particularly in the mucosa of the intestinal tract. ILC3 subsets produce various cytokines under homeostatic and activating conditions and act as inducers of lymphoid tissue development. ILC3-derived IL-22 contributes to tissue homeostasis, tissue repair and protection against infections. On the other hand, ILC3-mediated IFN-γ responses participate in the pathogenesis of intestinal inflammatory diseases. It is not fully understood which molecular pathways regulate the protective versus the pathogenic outcome of ILC3 immune responses in the intestine.

Mechanistic target of rapamycin complexes (mTORC) 1 and 2 integrate activation signals and environmental cues, drive activation-induced metabolic adaptation and shape immune responses by regulating proliferation, differentiation and cytokine responses. Results obtained in T cells demonstrate that mTOR signaling incorporates cues from various sources including nutrient-, cell- and microbiota-derived metabolites and critically affects cell function. Given the known impact of these factors on the generation, differentiation and function of ILC3s, I hypothesized that mTORC1 and/or mTORC2 are critical regulators of ILC3 differentiation and function. To investigate the impact of mTOR signaling on ILC3s, I generated wildtype and $Rag2^{-/-}$ lymphopenic mouse strains with a conditional $RORc$ promoter-driven deletion of $Rptor$ and/or $Rictor$, the essential subunits of mTORC1 and mTORC2, respectively.

mTORC1 and mTORC2 had a tissue-specific impact on ILC3 development and proliferation. Whereas small intestinal ILC3s required mTORC1 and to a lesser extent mTORC2, maintenance of colonic ILC3 numbers was independent of mTOR signaling. Small intestinal ILC3s from $Rag2^{-/-}$ mice exhibited a higher dependency on both mTORCs than small intestinal ILC3s from wildtype mice, indicating that mTOR is differentially regulated in ILC3s from lymphopenic and wildtype mice. $Rptor$- and $Rictor$-deficient ILC3s displayed significantly impaired IL-23/IL-1β-mediated IFN-γ production, while IL-22 production was only marginally affected. Consistently, $Rag2^{-/-}$ mice with ILC3-specific deletion of $Rptor$ or $Rictor$ were more resistant to IFN-γ-dependent α-CD40 colitis, but exhibited no obvious defects in IL-22-mediated defense against *Citrobacter rodentium* infection. Taken together, those findings suggest that mTORC1 and mTORC2 signaling occupy a critical role in IFN-γ production of ILC3s

in vitro and *in vivo* and thus represent central regulators of protective versus inflammatory responses in the intestine. This implies that therapeutic mTOR blockade may have beneficial effects in colitis patients by downmodulating the IFN-γ response of ILC3s.

2 Introduction

2.1 The innate and adaptive immune system

The mammalian immune system evolved to protect the body from co-evolving harmful pathogens such as bacteria, fungi, parasites and viruses. The immune system consists of a so called "innate" and "adaptive" cellular and humoral component.

Cells of the innate immunity respond immediately to damage-associated molecular patterns (DAMPs), pathogen-associated molecular patterns (PAMPs) and microbe-associated molecular patterns (MAMPs) through germline-encoded unspecific pattern recognition receptors (PRRs). Those PRRs include Toll-like receptors (TLRs), NOD-like receptors (NLRs) and RIG-I-like receptors (RLRs). PRRs recognize various molecular structures, for example carbohydrates, free nucleic acids, peptides, lipoproteins, peptidoglycans or extracellular adenosine triphosphate (ATP), which are released by bacteria, fungi, viruses or damaged cells or tissues. Macrophages (MΦ), granulocytes and dendritic cells (DCs) belong to the group of innate immune cells. MΦ and neutrophil granulocytes are specialized in phagocytosis, a process which leads to uptake and intracellular destruction of pathogens. DCs are professional antigen-presenting cells, which are essential to activate adaptive immune cells. As PRRs are limited to recognition of common molecular patterns, cells of the innate immune system only distinguish classes of pathogens, and their response is therefore unspecific. Still, innate immune cells are essential to mount a very rapid immune response and to help the adaptive immune system to respond later.

In contrast to innate immune cells, the adaptive immune cells recognize antigens (Ags) via Ag-specific receptors. Each adaptive immune cell harbors a unique rearranged Ag-receptor, and consequently detects one specific epitope of a single pathogen. Thus, adaptive immune responses are highly specific. The two major subsets of the adaptive immune system are B and T cells. B cells develop in the bone marrow (BM) while T cells mature in the thymus. Both the BM and the thymus are primary lymphoid structures. B cells capture extracellular Ags and, once activated, differentiate into antibody (Ab)-secreting plasma cells. Abs are part of the so-called humoral immune response and can neutralize extracellular pathogens. Moreover, Abs mark infected, transformed or damaged cells for destruction by innate immune cells or the complement system (serum proteins belonging to the humoral innate immune system). T

cells can be subdivided into CD8^{+} and CD4^{+} T cells. Cytotoxic CD8^{+} T cells detect Ags presented by major histocompatibility complex (MHC)-I expressed on all nucleated cells while CD4^{+} T cells recognize Ags in the context of MHC-II expressed on professional Ag-presenting DCs, activated B cells or MΦs. Whereas CD8^{+} T cells directly kill infected or degenerated cells, different subclasses of CD4^{+} T cells support the humoral responses by B cells, proliferation of CD8^{+} T cells and activation of MΦs. In contrast to classical CD4^{+} T helper (Th) responses, CD4^{+} regulatory T cells (Tregs) downmodulate immune responses. Thereby, Tregs prevent inappropriate immune responses towards self-Ags and commensal bacteria, viruses and fungi, which otherwise might cause inflammatory and autoinflammatory diseases. The initial adaptive immune response towards new pathogens requires activation and clonal expansion of rare specific cells. Thus, the adaptive immune system reacts much slower than the innate immune response. However, adaptive immune cells form an immunological memory, which accelerates the secondary response to reinfection with pathogens.

Cytokines are humoral factors of the immune system, which are produced by both innate and adaptive immune cells. Cytokines can function as growth factors, repair proteins and as mediators of immune defense or inflammation by modulating immune cell and non-immune cell responses.

2.2 Innate lymphoid cells

Innate lymphoid cells (ILCs) represent a more recently discovered subgroup of immune cells, which were uniformly classified in 2013[1] and re-classified in 2018[2]. ILCs lack phenotypical markers of myeloid cells. They show a lymphoid morphology but, in contrast to B and T cells, lack rearranged Ag receptors. Hence, they are referred to as lineage-negative (Lin^{-}) cells. During the past decade, active research has aimed to understand the development, the identity and lineage relationship, and the function of ILCs. Current studies indicate that ILCs play a role in protection against infections, development of secondary lymphoid organs and tissue homeostasis and repair.[3,4] However, once dysregulated, they can also contribute to chronic inflammatory diseases.[5]

2.2.1 Innate lymphoid cell subsets

The ILC family comprises natural killer (NK) cells, group 1 ILCs (ILC1s), group 2 ILCs (ILC2s) and group 3 ILCs (ILC3s), which include lymphoid tissue inducer (LTi) cells. Those ILC subsets can be distinguished by their expression of different transcription factors and the release of distinct cytokines (Fig.1).[2]

NK cells, the first known ILC family members, were discovered and characterized more than half a century ago.[6,7] NK cells can be identified by their expression of T-box transcription factor T-bet and Eomesodermin (EOMES). Upon activation, NK cells release cytokines such as interferon (IFN)-γ and tumor necrosis factor (TNF)-α.[8] In addition, they produce cytolytic proteins including perforin and granzyme B.[8] NK cells participate in clearance of intracellular bacterial and viral infections and are involved in anti-cancer defense.

Similar to NK cells, ILC1s express T-bet and produce pro-inflammatory cytokines including IFN-γ. ILC1s have been shown to support defense against viral infections, intracellular parasites and cancer, but lack direct cytolytic activity.[9-11] The expression of surface molecules and the overall transcriptional program of ILC1s is highly variable between tissues and species.[12-14] Hence, there is an on-going debate whether ILC1s truly constitute only one entity.[15,16]

ILC2s are defined by their expression of GATA3 (GATA binding protein 3) and RORα (RAR-related orphan receptor alpha), and the production of interleukin (IL)-4, IL-5, Il-13 and amphiregulin.[4] The ILC2 subgroup represents the most homogenous group of the ILC family. However, expression of cytokine receptors and other surface markers can vary between tissues and upon activation of ILC2s.[2,17,18] ILC2s respond to helminth infection and ILC2-derived type 2 cytokines support worm expulsion and tissue repair.[2] On the other hand, various studies associate ILC2s with allergies and inflammatory diseases, in particular diseases of the airways such as asthma and lung fibrosis.[2]

The ILC3 family comprises LTi cells and other ILC3 subsets, which depend on the transcription factor RORγt (RAR-related orphan receptor gamma t). Like NK cells, LTi cells have been described long before the discovery of other ILCs.[19-21] LTi cells are already present in the fetus and in neonates and are absolutely required for induction of secondary lymphoid structures such as lymph nodes (LNs) and Peyer's patches (PPs).[22-24] LTi cells are the only RORγt^{+} cells detected during fetal development.[25] Moreover, LTi-like ILC3s with the capacity to induce

secondary lymphoid organs have been found in the pool of CD4$^+$ ILC3s in adults.[26-28] ILC3s are further defined by their capacity to release the Th17-related cytokines IL-17 and IL-22.[2] In addition, ILC3s can release granulocyte-macrophage colony-stimulating factor (GM-CSF, or CSF2) and IFN-γ during inflammation and infection.[29-31] The ILC3 subgroup displays the highest heterogeneity and shows a highly divergent expression profile even within one tissue.[18,32,33] A subset of ILC3s expresses the natural cytotoxicity receptor (NCR) NKp46 and hence is termed NCR$^+$ ILC3. In contrast to NCR$^+$ ILC3s which are uniformly CD4-negative, NCR$^-$ ILC3s can be subdivided into CD4$^+$ LTi-like ILC3s and CD4$^-$ ILC3s in adults.[31] Hereinafter, those two subpopulations will be referred to as CD4$^+$ ILC3s and NCR$^-$ ILC3s, respectively. Evidence from several mouse studies suggests that ILC3s play a role in tissue repair, control of T cells and defense against bacterial and fungal infections.[2,4,34] At the same time, ILC3s have been shown to promote inflammation in several mouse models of colitis and psoriasis and to be altered in patients with inflammatory diseases such as colitis, rheumatic diseases and psoriasis.[4,5]

Maintenance of all ILC subsets depends on the common cytokine receptor γ (γ_c)-chain (IL-2Rγ), a receptor subunit of IL-2, IL-4, IL-7, Il-9, IL-15 and IL-21 receptor.[3] ILC2 and ILC3 subsets strictly require IL-7 signaling as deficiency of IL-7 or IL-7Rα has detrimental effects on ILC development and survival in mice.[35] IL-15 which is absolutely required for NK cell and ILC1 development can compensate for loss of IL-7 to a low degree.[36]

Throughout the first years of ILC research, ILCs were merely described as innate counterparts of the respective Th cells of the adaptive immune system. This view was based on the close proximity of transcriptional programs and cytokines produced in ILCs and corresponding Th cells (Fig.1). Hence, ILC1s, ILC2s and ILC3s are often referred to as helper ILC subsets. However, recent findings foster the idea that ILCs are profoundly different from Th cells.[37] In particular, murine ILC subsets from various tissues and human tonsillar and circulating ILC subsets and Th cells subsets were found to differ in gene regulatory circuitries and long non-coding RNAs suggesting a significant difference in early imprinting towards specific effector functions.[38-41]

ILCs are most abundant at mucosal barrier sites.[2] Nevertheless, small numbers of ILCs are also found in other tissues such as secondary lymphoid organs, liver and skin. In the absence of inflammation, most murine ILCs represent tissue-resident immune cells being largely absent from peripheral blood.[4,37,42] Studies by Huang *et al.*, however, provided new evidence that

murine ILCs can be mobilized during inflammation and can migrate to distant infection sites.[43] Further hints that ILCs might possess migratory capacity stem from experiments showing that the inhibitor fingolimod, which targets sphingosine-1 phosphate receptor 1 (S1PR1), affected ILC distribution both in humans and mice.[44]
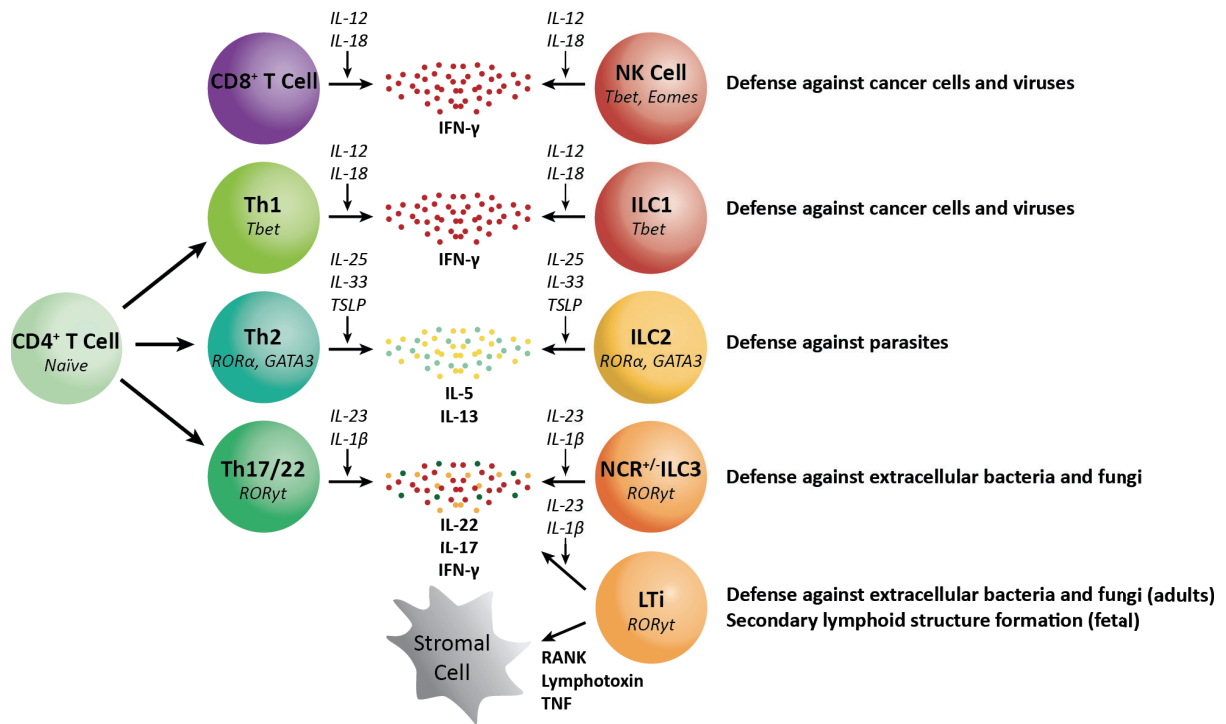
Fig.1 Innate lymphoid cells vs. differentiated T cells. Lineage defining transcription factors, activating cytokines, effector molecules and function. Adapted from Vivier *et al.*[2] and Spits *et al.*[1]

2.2.2 Innate lymphoid cell development

Since the classification of ILCs as an independent group of immune cells, extensive research has focused on the identification of ILC precursors and transcription factors involved in ILC lineage commitment. Due to ethical considerations, most of the knowledge on ILC development is based on mouse models.

Early studies demonstrated that NK and LTi cells depend on the expression of the inhibitor of DNA binding 2 (ID2) as both cell types were almost absent in *Id2*$^{-/-}$ mice.[22,45] Following up on those reports, another group found that ID2$^+$ progenitors were equally essential for the development of the newly defined helper ILC subsets.[11] This mutual dependency on ID2 hinted at the existence of a common progenitor. Indeed, all ILCs evolve from the common lymphoid progenitor (CLP) as both fetal and adult CLPs, derived from fetal liver and adult BM respectively, reconstituted ILCs as well as B and T cells in BM transplant experiments.[46,47]

According to the current model of ILC development, CLPs give rise to a sequence of progressively more and more lineage-restricted precursors such as the common ILC precursors (CILCPs) including the α-lymphoid progenitor (αLP) and the early innate lymphoid progenitor (EILP), the common helper ILC progenitor (CHILP) and the ILC precursor (ILCP) (Fig.2).[46,47]
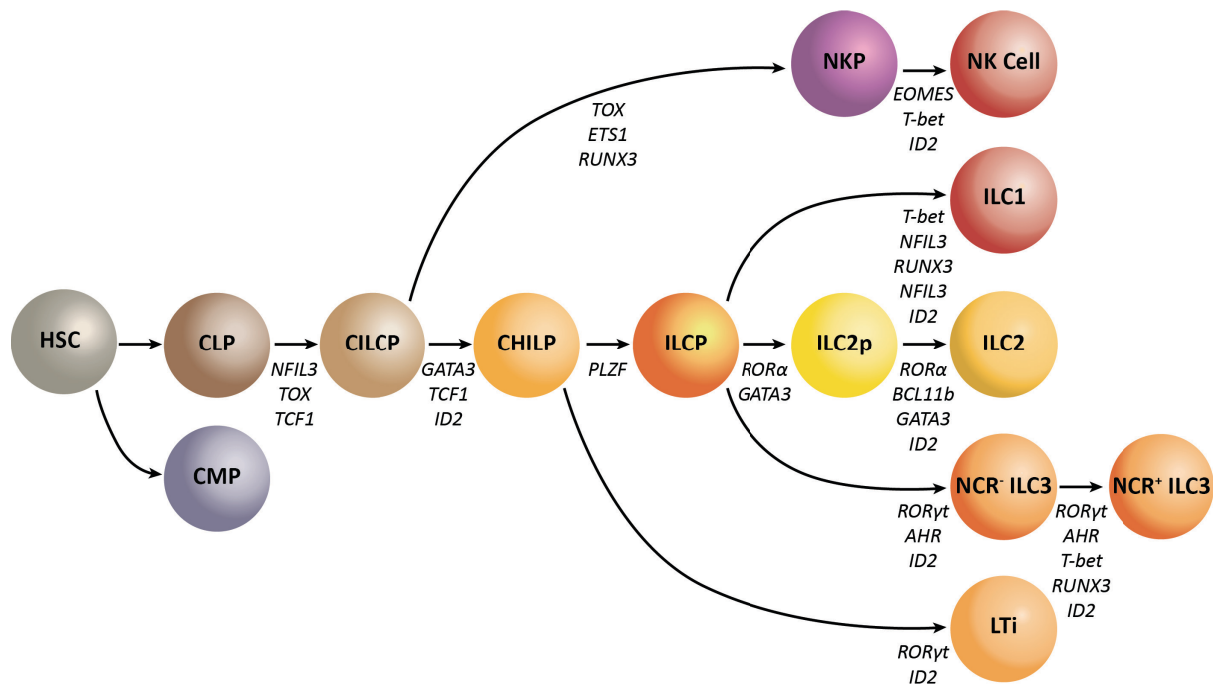
Fig.2 Innate lymphoid cell development. Progenitor cell stages and transcription factors involved in ILC differentiation. Adapted from Vivier *et al.*[2], Cherrier *et al.*[47] and Zook and Kee[46]

Transcription factors such as nuclear factor interleukin-3 regulated protein (NFIL3) and thymocyte selection-associated high mobility group box protein (TOX) are critically involved in shutting down the T cell program of CLPs and thereby promote ILC development.[47] All mature ILC subsets are severely diminished upon global loss of either NFIL3 or TOX in mice.[48-51] In a sequential cascade, NFIL3 promotes TOX, which in turn induces T cell factor 1 (TCF1).[52-54] Downstream of TCF1, αLPs and EILPs express ID2, which suppresses E protein transcription factor activity. Thereby, ID2 blocks B and T cell commitment of CLPs while promoting ILC differentiation.[45,52] Thus, αLP and EILP fail to generate T and B cells but retain the capacity to produce all ILC subsets. Accordingly, CLPs are Lin⁻ID2⁻IL-7Rα⁺α4β7⁻Flt3⁺ cells, while αLP and EILP have been described as Lin⁻ID2⁺IL-7Rα⁻/low α4β7⁺ cell stages.[11,46,52]

Though ID2 was shown to be important for maturation of NK cells, NK cell progenitors (NKP) were present in *Id2⁻/⁻* mice.[45] In contrast, CHILPs that give rise to all ILCs except NK cells were absent in those mice. This finding indicates that NK cell development and the differentiation

path of other ILCs segregates early in ILC ontogeny.[46] Accordingly, ILC development seems to divide into two distinct trajectories before the CHILP stage: one towards NK cells and another towards helper ILCs comprising ILC1s, ILC2s and ILC3s. Lineage restriction of NKPs depends on transcription factors such as runt related transcription factor 3 (RUNX3), ETS1 and EOMES.[11,47,55] Although NK cell express T-bet, which is required for NK cell effector functions, T-bet was not essential for NK cell maturation in *Tbx21(T-bet)$^{-/-}$* mice.[11] On the other hand, GATA3 represents one transcription factor which is crucial for transition of CILCPs towards CHILPs. Excluding NK cells, most ILCs express different levels of GATA3 with ILC2s displaying the highest GATA3 expression.[56] Initially, it was shown that only the differentiation into ILC2ps and ILC2s was blocked upon *Id2*-driven deletion of *Gata3*.[57] However, other publications using *Vav-* or *Ncr1*(NKp46)-driven knockout of *Gata3* demonstrated that GATA3 expression was also required for the development of ILC1s and ILC3s.[11,56] Conditional knockout of *Gata3* in all hematopoietic cells or NKp46-positive cells eradicated IL-7Rα^+ ILC progenitors and all ILCs except NK cells or ILC1s, respectively.[11,56] Furthermore, *in vitro* overexpression of GATA3 diverted differentiation of human cord blood-derived hematopoietic stem cells away from NK cells and towards helper ILCs.[58] CHILPs have been identified as Lin$^-$ID2$^+$IL-7R$\alpha^+\alpha$4β7$^+$Flt3$^-$CD25$^-$ cells.[11,47]

Deletion of *PLZF* resulted in loss of all ILCs except NK and LTi cells despite the presence of CILCPs and CHILPs.[59] Thus, Lin$^-$IL-7Rα^+cKit$^+\alpha$4β7^{high}PLZF$^+$ cells have been defined as ILCPs that can only give rise to ILC1s, ILC2s and ILC3s, but not to LTi cells *in vitro* and *in vivo*.[11,59]

The direct precursors of ILC1s and ILC3s have not been identified yet. Nevertheless, some transcription factors, which are essential for specific ILC subsets downstream of ILCPs, have been described. T-bet and NFIL3 are necessary for the maintenance of mature ILC1s.[11] Like NK cells, ILC1s and NCR$^+$ ILC3s were absent upon conditional knockout of *Runx3* in all hematopoietic cells or NCR$^+$ cells.[55] Whereas RUNX3 promotes survival of ILC1s, it controls the expression of RORγt and downstream aryl hydrocarbon receptor (AhR) in ILC3s.[55] In line with this, mice with deficiency of RORγt lacked all ILC3 subsets and LTi cells.[25,31,60,61] Ikaros-mediated inhibition of AhR impaired ILC3 development and function.[60] Moreover, the retinoic acid receptor (RAR) ligand Vitamin A controls ILC3 number and function in the small intestine (SI) in adult mice.[62] In contrast to the unknown ILC1 and ILC3 precursors, Lin$^-$ID2$^+$IL-7R$\alpha^+\alpha$4β7$^+$CD25$^+$Flt3$^-$ cells have emerged as ILC2-committed precursors (ILC2p).[57] The final

differentiation step from ILC2ps to ILC2s and the maintenance of ILC2 lineage-specification relies on expression of GATA3, RORα and B cell lymphoma-leukemia 11b protein (BCL11b).[57,63-65]

As described above, the current model of ILC development assumes a hierarchy of progenitors with increasing lineage restriction. However, two recent studies have contradicted the prevailing concept of a linear lineage commitment. Using a polychromic reporter mouse for ID2, BCL11b, GATA3, RORγt and RORα, Walker *et al.* showed that the hitherto defined progenitors displayed a higher lineage heterogeneity than estimated.[66] In this study, a fraction of adult BM-derived phenotypical CHILPs and ILCPs still possessed the potential to develop into NK cells. Moreover, the investigators discovered a promiscuous RORγt[+] ILC precursor with potential for all ILC subgroups including NK cells. This contradicts another report in which expression of RORγt could be traced back to a small proportion of CHILPs found in the fetal liver but not in adult BM in the reporter mice for PLZF-expression.[59] In the second publication, Xu et al. generated an *Id2*[RFP] reporter mouse with increased sensitivity compared to the previous *Id2*[GFP] reporter strain.[67] In a mouse strain generated by crossing *Id2*[RFP] reporter mice with *PLZF* reporter mice, ID2^{+}PLZF[+] ILCPs retained NK cell potential and thereby exhibit a higher multipotency than previously published. Those results suggest that CHILPs and ILCPs exhibit higher pluripotency than previously appreciated. However, those studies would require more detailed confirmation.

Throughout the last decade of ILC research, it was commonly assumed that most ILCs are tissue-resident cells. Hence, it was proposed that the pool of ILCs in tissues is maintained by proliferation of mature ILCs already deposited into tissues during embryonal development or by entrance of mature ILCs derived from ILC progenitors in the BM. However, a new model of ILC-poiesis was recently introduced (Fig.3a).[68-70] In this model, BM-derived ILC precursors are recruited from the blood upon local disturbances and differentiate into mature ILC subsets according to the specific tissue microenvironment. The model is based on the newer findings on the heterogeneity of murine ILC precursors and the detection of uni- and multipotent ILC precursors in human blood and tissues. Those findings raise the idea that ILC progenitors, which emerge before and after birth, might build two independent sources for ILC replenishment in tissues. In adult life, they could account in part for the huge heterogeneity of ILCs in various tissues.

2.2.3 Innate lymphoid cell plasticity

Recent research using new methods to analyze bulk and single cell transcriptomics have revealed that ILCs are overall a highly heterogenous group of immune cells both in mouse and humans.[12,13,18,32] With the new concept of ILC-poiesis, part of the extensive variability in ILC phenotypes might be explained by intermediate developmental stages of ILC precursors *in situ*.[68-70] Another explanation for the immense ILC heterogeneity is based on ILC plasticity.[70] The general term plasticity describes the property of mature cells to change their cell fate and to transit into cells of other phenotype and function in response to physiological and pathophysiological changes. Such phenotypical and functional transitions in ILCs have been described in several mouse models and human studies.[70] Recently, Pokrovskii *et al.* suggested that the ILC plasticity in the SI and large intestine of mice may be based on shared accessibility of some but not all genomic regulatory elements in different mature ILC subsets.[71] Thus, changes in expression levels of specific lineage-activating and, in particular, lineage-repressing transcription factors may cause phenotypic shifts from one ILC subset into another. Fig.3b describes the current knowledge on the plasticity between helper ILCs, though NK cell-ILC1 plasticity has also been described.[70]
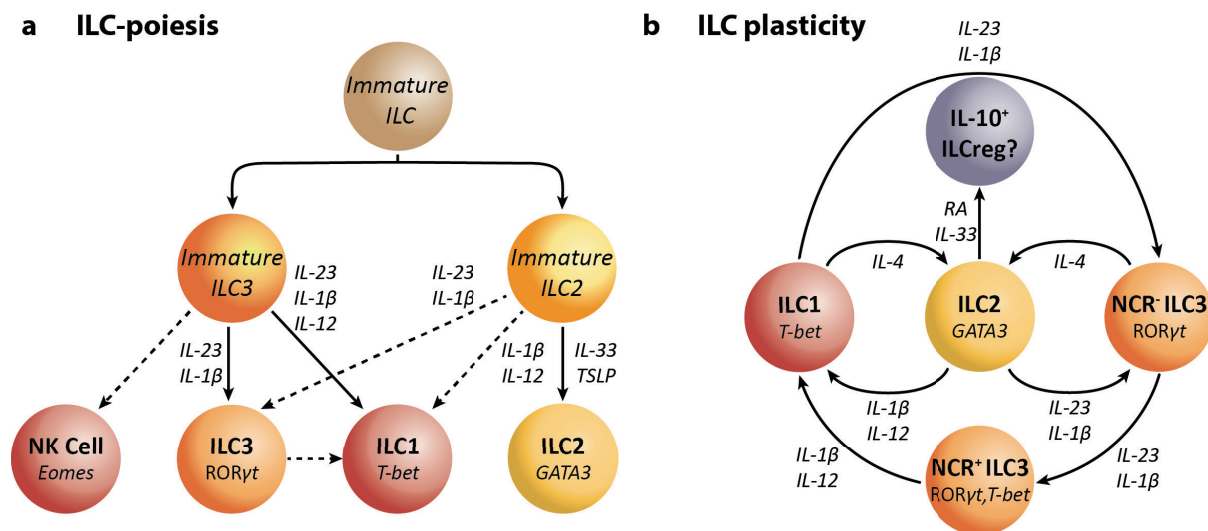
Fig.3 ILC heterogeneity – ILC-poiesis and ILC plasticity. ILC heterogeneity might be based on two different processes. a) The ILC-poiesis model is largely based on findings from human blood-derived immature ILC precursor-like cells, although recent findings also hint at existence of immature ILCs in the tissues of mice. Immature ILCs do not express ILC lineage-specific transcription factors and are incapable of producing cytokines. These immature ILCs can give rise to more restricted immature ILCs biased towards ILC2s (immature ILC2) and ILC3s (immature ILC3). Following their default developmental pathways (bold line), those cells would differentiate into ILC2s and ILC3s, respectively. However, certain cytokine environments can evoke an alternative differentiation pathway (dashed line). b) An ILC of one subtype can transdifferentiate into another ILC subtype, which has become known as ILC plasticity. This transdifferentiation is promoted by changes in cytokine environment and is often reversible. RA: retinoic acid. Adapted from Bal *et al.*[70]

ILC2-ILC1 plasticity

A reduction of ILC2s and increased ILC1-mediated IFN-γ responses to influenza A virus was first observed in patients with chronic obstructive pulmonary disease (COPD).[72,73] Under the light of the earlier discovered ILC3-ILC1 plasticity (see chapter 2.2.3 ILC3-ILC1 plasticity), these findings formed the basis of consequent studies investigating whether ILC2s might possess the potential to gain an ILC1-like phenotype. Indeed, several factors associated with exacerbation of COPD such as influenza A, *Staphylococcus aureus* or cigarette smoke were shown to induce a shift from ILC2s toward ILC1s in the lungs of mice.[72] This ILC2 conversion was conferred by gradual loss of GATA3 expression concomitant with increase in T-bet expression. In turn, T-bet induced *Il18r* and *Il12rb2* transcription and rendered mature ILC2s responsive to the respective cytokines IL-18 and IL-12. Accordingly, activated ILC2s expressed IL-13 and IFN-γ in response to IL-33 and IL-12. Although the study showed that ILC2-ILC1 transformation can occur, the signals causing the phenotypical adaptation were not analyzed.

In two papers published at the same time, cytokines were identified to promote the ILC2-ILC1 transition. In the first study, an *in vitro* screening for cytokines that activate human ILC2s revealed that IL-2/IL-1β not only increased type 2 cytokine production of ILC2s, but also induced T-bet, IL-12RB1 and IL-12RB2.[74] Coinciding with the assumption that IL-2/IL-1β primes Th1 responses in ILC2s, co-stimulation of ILC2s with IL-2, IL-1β and IL-12 induced IL-13+IFN-γ+ double-producing ILC2s. In line with this *in vitro* finding, intranasal IL-1β treatment of mice led to the generation of IL-13+IFN-γ+ hybrid ILC2s in the lung.[74] In the second report, ILC2s have been shown to be diminished in lungs of COPD patients, while patients with chronic rhino-sinusitis with nasal polyps (CRSwNP) harbored increased proportions of ILC2s in nasal tissues.[73] Adoptive transfer experiments of human cell tracer-labeled ILC2s into NOD *SCID IL2rγ⁻ᐟ⁻ (*NSG*)* mice revealed that a fraction of ILC2s lost GATA3 expression, while they gained T-bet expression.[73] Similar to the report by Ohne *et al.*[74], IL-1β-primed human ILC2s showed increased T-bet expression and IFN-γ production in response to IL-12 *in vitro*. Importantly, IL-4, which is upregulated in the nasal mucosa of patients with CRSwNP, prevented the IL-12-mediated ILC2-ILC1 plasticity.[73] IL-4 was even able to reverse the ILC2-ILC1 transition. This was shown in *in vitro* experiments in which mature ILC2s first acquired an ILC1 phenotype in response to IL-2, IL-1β and IL-12, but then recovered an ILC2 phenotype upon re-stimulation with IL-2 and IL-4.[73] Hence, the investigators concluded that

the low percentage of ILC2s in COPD and the high percentage in CRSwNP might be guided by different levels of IL-12 and IL-4. A dominant effect of IL-4 would explain why the inflammatory environment induces 'exILC2s' in COPD and not in CRSwNP patients. Furthermore, the observations imply that ILC2-ILC1 transition is reversible.

ILC2-ILC3 plasticity

Califano *et al.* reported that loss of BCL11b promotes ILC2-ILC3 transition. In their study, tamoxifen-induced *Cre-ERT2*-driven deletion of *Bcl11b* resulted in reduced expression of GATA3 and RORα and an induction of RORγt and AhR expression in mature ILC2s.[65] As a result of RORγt and AhR upregulation, murine BCL11b-deficient ILC2s produced Th17-related cytokines upon papain-induced airway inflammation.[65] This experimental model demonstrated that in a genetically susceptible setting ILC2s have the potential to adopt an ILC3-like phenotype under pro-inflammatory conditions. However, it did not answer the question whether physiological changes are sufficient to induce such phenotypical changes in ILC2s. This question was recently addressed in another work, in which the investigators analyzed changes in the ILC2 subset upon cytokine activation or helminth infection *in vivo*. IL-25 treatment or infection with the helminth *Nippostrongylus brasiliensis* induced so-called inflammatory ILC2s (iILC2s), which are phenotypically distinct from ILC2s under homeostatic conditions.[17] Interestingly, those iILC2s produced both IL-13 and IL-17, upregulated RORγt expression and improved anti-fungal defense against *Candida albicans* infection when transferred into *Rag2$^{-/-}$IL2r$\gamma^{-/-}$* mice. The transition into IL-13$^+$IL-17$^+$ hybrid cells is reversible as iILC2s were found to turn into classical ILC2 in the lung tissue.[17] These findings raise the possibility that ILC2-ILC3 transition might occur during inflammations, which are associated with IL-25.

These data from mouse models were confirmed in human studies. For example, a skin- and blood-derived CCR6$^+$cKit$^+$ ILC2 subset that can upregulate RORγt and IL-17 in response to appropriate stimulation was described in humans.[75] The conversion from ILC2s into an ILC3-like phenotype required IL-23 as well as IL-1β and, most crucially, transforming growth factor-β (TGF-β). IL-4 could revert the conversion. Of note, an enhanced percentage of IL-22, IL-17- and IFN-γ-producing ILC3s and a reduction of ILC2s was found in psoriatic lesions of patients.[75] There was, however, no direct proof that the changed ratio in ILC2s and ILC3s in patients with psoriasis was based on ILC2-ILC3 transition.[75] A similar observation comes from

a study focusing on nasal mucosal sites. Based on the finding that cystic fibrosis (CF) patients harbor increased ILC3 numbers in nasal polyps whereas patients with CRSwNP display accumulation of ILC2s, Golebski et al. hypothesized that different cytokine milieus in both diseases might drive different ILC plasticity.[76] Accordingly, they showed that pathogenic bacteria, which are characteristically found in CF patients induced expression of IL-23, IL-1β and TGF-β in human nasal epithelial cell layers.[76] In vitro co-culture with those bacteria-primed nasal epithelial cells or culture with IL-2, IL-7, IL-23, IL-1β and TGF-β was sufficient to convert a fraction of human blood-derived ILC2s into RORγt⁺IL-17⁺ ILC3s.[76] In contrast, blood-derived ILC2s were unable to differentiate into ILC3s when IL-23, IL-1β and TGF-β was supplemented with IL-4. Additionally, ILC3s from CF patients upregulated ILC2 surface markers in response to IL-2/IL-4 in vitro. Interestingly, IL-4 was only upregulated in nasal tissues from CRSwNP patients, but not in samples from CF patients.[76] This finding suggests that IL-4 was crucial to maintain the ILC2 phenotype under inflammatory conditions in CRSwNP patients.

ILC3-ILC1 plasticity

The first indication of ILC3-ILC1 plasticity was already published one decade ago. In murine adoptive transfer studies and cell culture experiments, Vonarbourg et al. demonstrated that NCR⁻ ILC3s cells gave rise to NCR⁺ ILC3s.[77] Some of these NCR⁺ ILC3s gradually lost RORγt expression in the SI, colon and spleen.[77] Analysis of *RORc(γt)-Cre^{tg}* x *Rosa26R^{Yfp/+}* reporter mice in which all cells with a history of RORγt expression were constitutively labelled by eYFP confirmed that a fraction of eYFP-positive cells in the SI, colon, spleen and LN downregulated RORγt expression. Throughout this process, RORγt⁻ 'ex-ILC3s' acquired a phenotype similar to ILC1s by downregulating IL-23 receptor (IL-23R) and IL-22 expression while upregulating IL-12RB2 and IFN-γ. Moreover, exILC3s transferred into *Rag2^{-/-}IL2rγ^{-/-}* mice, which lack adaptive immune cells and all ILCs, produced IFN-γ in response to α-CD40 Ab treatment and induced α-CD40 colitis. Using *Eomes^{Gfp/+}* x *RORc(γt)-Cre^{tg}* x *Rosa26R^{Yfp/+}* double reporter mice in which cells expressing EOMES are additionally GFP-labeled, Klose et al. verified that small intestinal (SI) NCR⁺ ILCs comprised three different subsets: classical NK cells, ILC1s and exILC3s.[11] Several studies showed that NCR⁺ ILC3s upregulated T-bet and that T-bet was required for ILC3-ILC1 plasticity.[31,78,79]

By adoptive transfer of *RORc(γt)-Cre^tg* x *Rosa26R^Yfp/+* reporter mouse-derived eYFP+RORγt⁻ exILC3s and eYFP⁻RORγt⁻ ILC1s into *Rag2^-/-IL2rγ^-/-* mice, Bernink *at al.* demonstrated that the opposite transition from exILC3s and ILC1s into ILC3s can also occur.[80] Likewise, human ILC1s stimulated with IL-23 lost their T-bet expression and IFN-γ production, but secreted IL-22. IL-1β and retinoic acid acted in synergy with IL-23 and accelerated ILC1-ILC3 plasticity.[80] These results imply that ILC3-ILC1 plasticity is bidirectional and that the ILC3 transition into exILC3s can be reverted.

The transition of ILC3s towards ILC1s was also observed in dextran sulfate sodium (DSS)-induced colitis in NSG mice reconstituted with human fetal liver hematopoietic stem cells.[81] Likewise, the transfer of pediatric tonsil-derived ILC3s gave rise to both ILC3s and ILC1s in the spleen and liver of MISTRG-6- and IL-15 humanized mice.[82] Analysis of human tonsil and SI furthermore revealed the presence of intermediate ILC3-ILC1 clusters *in vivo*.[82] Using RNA velocity analysis that estimates the future state of cells, the intermediate ILC3-ILC1 cell stages were found to be directed towards an ILC1 phenotype.[82] As observed in cell cultures with murine ILC3s, human cKit+RORγt+NKp44⁻T-bet⁻ ILC3s derived from fetal SI and pediatric tonsil could differentiate into cKit⁻RORγt⁻NKp44+T-bet+ ILC1-like ex-ILC3s in response to IL-2 and IL-12 *in vitro*.[80,81] In contrast, the ILC3 phenotype was preserved upon stimulation with IL-2, IL-23 and IL-1β. Other *in vitro* studies with human tonsil-derived ILC3s or IL-7Rα+ ILCs revealed high variability in ILC3 cytokine production depending on the cocktail of stimulating cytokines. Under appropriate activation conditions, those tonsillar ILC3s could be induced to produce Th1, Th2 or Th17-related cytokines.[83,84] These results reinforce the idea that ILC3-ILC1 transition might also occur *in vivo* in humans.

IL-10+ ILC plasticity

Research on regulatory IL-10+ ILCs is a new but highly controversial field. In 2017, Wang *et al.* described a population of IL-10-producing Lin⁻IL-7Rα+ ILCs, which were referred to as regulatory ILCs (ILCregs).[85] ILCregs existed both in mouse and human SI and colon, expanded in four different murine innate colitis models and contributed to amelioration of DSS-induced colitis when transferred into *Rag1^-/-Il10^-/-* mice.[85] However, the existence of such an ILCreg population has been opposed by another study in which the investigators failed to detect ILCregs in *Il10^eGFP* reporter mice crossed to C57BL/6J mice.[86] Furthermore, the investigators showed that mice bred in their facility and mice purchased from three other distributors were

also devoid of ILCregs. In addition, the findings on ILCreg expansion in response to intestinal inflammation to DSS could not be confirmed. In contrast, ILC2s were found to express IL-10 in response to IL-2, IL-4, IL-10, Il-27 and neuromedin U (NMU).[86] This finding was in line with a previous publication in which IL-33- or papain-mediated activation induced IL-10 production in a fraction of murine lung ILC2s *in vivo*.[87] In this model, the transition from ILC2s into IL-10^{+} ILC2s was primed by IL-2 *in vitro* and *in vivo*. This raises the possibility that ILC2s can be primed to produce IL-10 in response to other cytokines. Further investigations will be required to define whether ILC2s represent the only source of ILC-derived IL-10 or whether ILCregs truly exist.

2.3 Group 3 innate lymphoid cell immune functions

As introduced in chapter 2.2.1, ILC3s found in adult mice are defined as Lin[-]cKit^{+}RORγt^{+} ILCs and can be further subdivided into CD4^{+}, NCR^{-} and NCR^{+} ILC3s.[45] In humans, ILC3s are distinguished as Lin^{-}CD161^{+}IL-7Rα^{+}cKit^{+}CRTH^{-} cells and can be separated into NCR^{-} and NCR^{+} ILC3s.[45] ILC3s are most abundant at mucosal barrier sites of the intestinal tract. Whereas NCR[-] ILC3s are particularly enriched in cryptopatches (CPs), isolated lymphoid follicles (ILFs) and PPs of the intestinal tract, NCR[+] ILC3s are also distributed throughout the lamina propria (LP).[61,88-90] Rarer populations of ILC3s have also been reported in other organs such as tonsils, spleen, LNs, skin or decidua.[75,91-94]

2.3.1 Mediators of ILC3 expansion and activity

Since the discovery of ILC3s, results of several murine studies suggested that the number and function of ILC3s is regulated by signals derived from the microbiota, nutrients, neurons and other immune cells.

Microbiota as ILC3 regulators

Satoh-Takayama *et al.* and Sanos *et al.* demonstrated that germ-free mice harbored much lower ILC3 numbers in the SI and that the remaining ILC3s produced less IL-22 compared to wildtype mice.[61,90] In line with this finding, Vonarbourg *et al*. observed that SI ILC3 numbers were reduced in antibiotic-treated *RORc(γt)-Cre[tg]* x *Rosa26R[Yfp/+]* reporter mice.[77] Interestingly, the eYFP[+]RORγt[-] exILC3 numbers increased in the absence of microbiota.[77] This result

indicates that microbial products preserve the expression of lineage-defining RORγt to sustain the ILC3 phenotype. Contradicting those reports, Sawa *et al.* and Lee *at al.* reported that ILC3 numbers were not reduced in germ-free or antibiotic-treated mice, and that IL-22 was even increased when compared to conventional mice.[95,96] Sawa *et al.*[95] argued that microbiota-induced IL-25 repressed ILC3 activation. This is contradicted by a more recent study in which treatment with IL-25 or helminth infections induced RORγt and IL-17 expression in ILC2s.[17] The controversial findings on microbiota-mediated regulation of ILC3s might be caused by different composition of gut microbiota in mice kept under specific-pathogen-free (SPF) conditions.[30]

The microbiota in the intestine has also been shown to modulate ILC3 functions at distant sites of the body. For example, metabolites from intestinal microbiota regulated IL-22 release in pancreatic ILC3s.[97] The local induction of IL-22 increased the expression of mouse β-defensin by pancreatic endocrine cells in mice, which in turn was protective in autoimmune non-obese diabetic. Moreover, transplantation of *Bacteroides vulgatus*, a bacterium elevated in the feces of patients with polycystic ovary syndrome, has been demonstrated to impair bile-acid mediated induction of IL-22 production in SI ILC3s in female mice.[98] The reduction of systemic IL-22 was linked to disturbed ovary functions, insulin resistance and impaired fertility. Similarly, changes in the composition of the microbiota in the intestine induced resistance to acute liver injury upon repeated concanavalin A-injections.[99] The resistance induction was linked to accumulation of *Lactobacillus* species in the intestine and increased IL-22 expression in SI ILC3s. Altogether, those studies highlight that dysbiosis might affect ILC3 numbers and cytokine release in the gut and other organs.

AhR signaling in ILC3s

The aryl hydrocarbon receptor (AhR) is a ligand-activated transcription factor that controls transcription of target genes by two different modes: 1) by formation of heterodimers with AhR nuclear translocator (ARNT) and direct binding of xenobiotic response elements (XREs) in the DNA and 2) by indirect regulation of other transcription factors such as retinoic acid receptor (RAR), NF-κB, signal transducer and activator of transcription (STAT) proteins and epigenetic modulators.[100,101] AhR is activated by physiological ligands derived from vegetables, tryptophan metabolites generated by both host metabolism and commensal bacteria and exogenous toxins, so-called xenobiotic ligands. Several studies have shown that

AhR-mediated sensing of such ligands regulates ILC3s in the SI and colon. As mentioned in chapters 2.2.2 and 2.2.3, AhR is involved in induction and stabilization of the ILC3 phenotype. Activation of AhR is a critical step in development of ILCPs into ILC3s, as AhR deficiency led to reduced ILC3 numbers.[31,55,60,65,96,102] In addition, AhR-deficient ILC3s showed a reduced production of IL-22, and RORγt[+] ILC3s or LTi cells failed to induce CPs and ILFs in adult mice.[96,102] Conversely, AhR-ligand supplemented food resulted in upregulation of ILC3 numbers and higher number of ILFs.[102] Interestingly, LNs and PPs were not affected by loss of AhR suggesting that fetal LTi cell development and function do not require AHR signals.[96,102] The importance of AhR ligands for ILC3 development and maintenance was further emphasized in mice with overexpression of AhR ligand-degrading cytochrome P4501 (CYP1) in intestinal epithelial cells. In these mice, ILC3 numbers in the SI and colon were severely reduced.[103] Besides impairment of ILC3 development, deletion of AhR repressors such as BCL11b or Ikaros promoted the ILC2-ILC3 plasticity.[60,65] In line, deletion of *Ahr* in hematopoietic cells led to increased ILC2 numbers and type 2 cytokine production in SI and colon.[104] *RORc*-driven knock-in of a constitutively active *Ahr* expanded intestinal ILC3s and promoted ILC3 cytokine release.[104] Altogether, those studies demonstrate that food-derived ligands and toxins binding to AhR harbor a large potential to modulate ILC3 number and function in the intestine.

Regulation of ILC3s by neurotransmitters

Recent studies show that a proportion of ILC3s in the intestine express several receptors for neurotransmitters, and that ILC3 compartments such as CPs and ILFs are highly innervated. Indeed, neuronal signals form an additional layer of ILC3 regulation.[105] In the SI of mice, ILC3s express the neuroregulatory receptor RET and co-locate with glial cells releasing glial-derived neurotrophic factor (GDNF) family ligands (GFLs).[106] Global and *RORc*-driven deletion of *Ret* reduced IL-22 production specifically in ILC3s but not Th17 cells due to impaired p38 MAPK/ERK-AKT and STAT3 signaling.[106] In addition to RET, ILC3s express the neuroregulatory receptor vasoactive intestinal peptide receptor (VIPR) 2. Like GFLs, binding of the neural-derived VIPR-ligand VIP, which is induced by food intake, enhanced IL-22 production of ILC3s but not T cells.[107] VIP expression in the intestine oscillates according to the food-intake and this contributes to fluctuating IL-22 levels in the intestine throughout the day. Another study demonstrated that neuronal cues are also involved in ILC3 regulation at other sites of the

body. Resection of one vagus trunk was followed by the decrease of acetylcholine (ACh) in the peritoneum. Reduction of ACh resulted in lower numbers of ILC3s in the peritoneum, diminished protective PCTR1 (protectin conjugates in tissue regeneration 1) release by ILC3s and a subsequent increase in inflammatory MΦ.[108] This effect can possibly be extended to humans, as ACh also enhanced PCTR1 pathways in human-derived ILC3s.

Innate immune cell-derived cytokine signals as regulators of ILC3 function

In 2009, Takatori *et al.* reported that IL-23, which was previously known to induce and maintain Th17 responses, also elicited IL-17 and IL-22 production by ILC3s *in vitro* and *in vivo*.[109] Later, BM chimera experiments with wildtype, *Il22*^{-/-}, *Tlr5*^{-/-}, *CD11cDTR* (diphteria toxin-induced depletion of DCs) and *Ccr2DTR* (diphteria toxin-induced depletion of monocytes) mice demonstrated that flagellin-mediated IL-22 production in the SI required TLR5-mediated IL-23 release by CD11c^{+} phagocytes.[110] Subsequent studies concluded that CX3CR1^{+} mononuclear phagocytes (MNPs), which are found in close proximity to CPs, activate ILC3s in the large intestine.[111-115] *In vivo* and *in vitro* studies on both mouse- and human-derived large intestinal MNPs revealed that TLR agonists and microbial commensals or pathogens triggered MNP-derived IL-23 and IL-1β production.[111-114,116] IL-23 and IL-1β synergistically induce IL-22 production by ILC3s *in vivo*.[111-114,116] In addition, IL-23 and IL-1β from MNPs promote ILC1-ILC3 transition *in vitro*.[80] The IL-23/IL-1β-mediated ILC3 cytokine response is further potentiated by TNF-like ligand 1A (TL1A) produced by CX3CR1^{+} MNPs.[111] Of note, MNPs can also trigger release of other cytokines by ILC3s. Mincle- and Syk-dependent recognition of microbiota by CD11c^{+} phagocytes contributed to IL-22 and IL-17 production in ILC3s under steady state and prevented microbial translocation to other organs.[117] Moreover, it has been shown that bacterial Ags also induced IFN-γ production in human intestinal NKp46^{+} ILC3s *in vitro*.[118] This IFN-γ induction was mediated by CD14^{+} MΦ in an IL-23-, TL1A- and contact-dependent manner.[118] Finally, Mortha *et al.* showed that under homeostatic conditions ILC3s represented the major source of GM-CSF in the SI and colon of mice.[119] The production of GM-CSF by ILC3s required microbiota-induced, MyD88-dependent release of IL-1β by MNPs. Genetic deletion of GM-CSF and depletion of ILCs decreased DC and MΦ regulatory functions suggesting positive feedback loops between ILC3s and cells of the myeloid lineage.[119] Collectively, these results imply that activated innate immune cells enhance ILC3 cytokine production via release of cytokines. In turn, myeloid cells themselves

are regulated by ILC3s. Nevertheless, those studies could not exclude that ILC3s can sense PAMPs and DAMPs through direct receptor recognition.

T cells as regulators of ILC3s

Accumulating evidence suggests that ILC3 number and functions are locally regulated by T cells.[120,121] The regulation of ILC3s and T cells are closely entangled and bidirectional. As the cross-talk between ILC3s and T cells is related to ILC3s functions in tissue homeostasis, the detailed processes are described in Chapter 2.3.2. *ILC3s and the adaptive immune system*.

2.3.2 ILC3s in homeostasis and tissue repair

As described before (chapter 2.3.1), ILC3s integrate various environmental signals and adapt their cytokine responses accordingly. The functional ILC3 output, often but not always in form of soluble cytokines, has significant impact on non-hematopoietic cell and immune cell functions for tissue homeostasis and during tissue repair (Fig.4).[122]

ILC3-derived cytokines as modulators of epithelial cells

Epithelial layers form a physical barrier towards commensal and pathogenic microbes. Ample evidence emphasizes that IL-22 plays a crucial role in maintaining integrity of epithelial cells. IL-22 binds to the IL-22 receptor, a heterodimeric transmembrane receptor composed of IL-22R1 and IL-10R2.[123,124] IL-22R is particularly expressed in epithelial cells at barrier sites (lung, gastrointestinal tract, skin) and is also found in the liver, pancreas and kidney, but not on hematopoietic cells.[123,124] In the murine SI, IL-22 production is initiated after birth and, under homeostasis, the majority of SI IL-22 is produced by ILC3s in humans, rhesus macaques and mice.[95,112,125,126] In contrast to the SI, only about one third of IL-22 is produced by ILC3s in the colon of mice under homeostatic conditions.[126] Various classical and innate-like T cells contribute to IL-22 production.[124,126] Both SI and colonic ILC3s readily upregulate IL-22 early upon inflammation or infection.[95,123,127-129]

IL-22 stimulates the production of antibacterial proteins in epithelial cells. IL-22-induced antibacterial proteins encompass lipocalin-2 (LP2), S100A8, S100A9, β-defensins and regenerating islet-derived proteins (Reg) such as RegIα, RegIIIβ and RegIIIγ.[90,124,125,129] Moreover, IL-22 elicits goblet cell expression of mucus-associated proteins including mucins and strengthens tight-junctions between epithelial cells.[124] Antibacterial proteins, mucins and

interepithelial tight-junctions reinforce the intestinal physical barrier and prevent bacterial translocation. Additionally, IL-22 and lymphotoxin (Lt)α corporately enhance fucosylation of intestinal epithelia which is associated with colonization by commensal bacteria that hinder intestinal colonization by pathogens.[130-133] IL-17 can further promote IL-22-mediated protective mechanisms.[2,4,134] ILC3-mediated IL-17 release is low under homeostatic conditions in adult mice, but is upregulated under inflammatory circumstances.[4,61,95]

IL-22 also regulates and protects intestinal epithelial stem cells (ISCs) during tissue damage and repair. ILC3s upregulated cytokine production in response to methotrexate-mediated tissue damage and instructed activation and proliferation of epithelial cells.[135] In the absence of ILC3s, proliferation of epithelial cells was impaired. Hence, *RORγt$^{-/-}$* mice failed to resolve methotrexate-induced tissue damage and displayed exacerbated colitis. Additionally, ILC3s prevented methotrexate-mediated loss of ISCs in an IL-22-dependent manner, which may contribute to the defective tissue repair in *RORγt$^{-/-}$* mice.[135] ILC3-derived IL-22 also induced expansion of epithelial cells and ISCs in human and mouse SI organoids, accelerated intestinal regeneration after allogenic BM transplantation and lowered the risk of graft-versus-host disease in BM-transplanted mice.[136] Moreover, IL-22 has been demonstrated to play an essential role in augmentation of DNA damage responses (DDR) in colonic ISCs.[126] Gronke *et al.* made use of a mouse model with tamoxifen-inducible sporadic deletion of *Il22r1* in ISCs, in which progeny of single *Il22r1$^{-/-}$* ISCs could be traced by a Confetti reporter gene.[126] Upon treatment with pro-carcinogen azoxymethane or DSS, tumors were preferentially derived from *Il22r1$^{-/-}$* ISCs. Furthermore, *Il22r1$^{-/-}$* ISCs were more resistant to irradiation-induced cell death when compared to *Il22r1$^{+/+}$* ISCs in the same mouse or *Il22r1$^{+/-}$* mice. In line, ISCs from *Il22$^{-/-}$* mice were less susceptible to irradiation-induced DRR-mediated apoptosis and accumulated mutations, which rendered *Il22$^{-/-}$* mice more prone to development of colon cancer.[126]

Low levels of IL-22 seem to be sufficient to maintain gut barrier integrity under homeostatic conditions.[106,107,127] In *RORc(γt)-Cre^{tg}* x *Ret$^{fl/fl}$* mice, in which ILC3-derived IL-22 is reduced due to impaired sensing of neurotrophic factors, morphology, proliferation and permeability of the intestinal epithelial barrier was not changed.[106] Those mice, however, displayed higher susceptibility to DSS-mediated colitis. Similarly, VIP2-deficiency in ILC3s diminished IL-22

release in response to food-mediated neuronal VIP release, which impaired the protection against DSS-induced colitis.[107]

ILC3s and the adaptive immune system

Recent studies propose that ILC3s and cells of the adaptive immune system regulate each other in a contact-dependent and contact-independent manner. The ILC3-T/B cell crosstalk is important to maintain tissue homeostasis. In adult wildtype mice, ILC3s are situated in the interfollicular space of mesenteric LNs, are placed next to the marginal zone in the spleen and co-localize with T and B cells in the PPs, ILFs and CPs.[61,88-92,137] Thereby, the intercellular communication is facilitated by the close proximity of ILC3s and cells of the adaptive immune system.

In the spleen, ILC3s directly support B cell survival and homeostatic T cell-independent B cell immunoglobulin G (IgG) responses. In mice and humans, splenic ILC3s enhance marginal reticular cell-mediated B cell help by expression of LTα1β2 and TNF and provide B cell-activation factor (BAFF), CD40L and the Notch ligand Delta-like 1 (DLL1).[91] Moreover, ILC3-derived GM-CSF recruits neutrophils, which further assist formation of marginal zone B cells (MZBs) and MZB-derived plasma cells. Ab-mediated depletion of ILC3s in mice impairs differentiation of IgG-producing plasmablasts and plasma cells. [91]

Beyond regulation of T cell-independent IgG responses, ILC3s further modulate T cell-dependent IgG production in the spleen. ILC3s have been shown to take up, process and present peptide-derived Ags and thus can act as bona fide APCs.[138,139] Human ILCs from secondary lymphoid tissues and IL-1β activated murine splenic ILC3s express both MHC-II and T cell co-stimulatory receptor ligands and promote T cell proliferation and activation *in vitro*.[33,138] However, *in vivo* results on the effect of crosstalk between T cells and splenic MHC-II$^+$ ILC3s in mice are contradictory. In one study, *RORc*-driven deletion of *MHC-II* in ILC3s reduced proliferation of splenic OVA-specific CD4$^+$ T cells upon immunization with OVA peptide, OVA protein and TLR9-agonist CpG.[138] In line with this, loss of MHC-II in ILC3s led to decreased T cell-dependent B cell IgG responses in the spleen of mice immunized with alum-precipitated NP-OVA and CpG.[138] These findings suggested that ILC3s drive T cell-dependent IgG responses. In contrast, another group reported that *RORc*-driven deletion of *MHC-II* in ILC3 induced proliferation of Ag-specific T cells and led to increased B cell IgG responses against commensal Ags, which would indicate that ILC3s suppress IgG Ab production.[139] It has

been shown that CpG induces IL-1β production in MNPs[111,140] and that splenic ILC3s upregulated co-stimulatory receptors upon activation with IL-1β[138]. Thus, the discrepancy between those results might be explained by differences in the activation status of splenic ILC3s in the two different mouse models.

Apart from modulating IgG responses, ILC3s participate in the regulation of immunoglobulin A (IgA) Ab release by B cells at mucosal barrier sites. IgA Abs are particularly enriched at mucosal sites and are involved in controlling pathogens and colonization by commensal bacteria. ILC3s have been shown to promote T cell-independent IgA production in B cells in the SI in a LTα1β2-dependent manner.[141-143] At the same time, ILC3-mediated LTα3 production controls T cell recruitment to the SI and thereby supports T cell-dependent IgA production.[143] *RORc*-driven deletion of *LTa* in wildtype and T cell-deficient mice diminished fecal and serum IgA levels and caused a change in microbiota composition with an outgrowth of segmented filamentous bacteria (SFB).[143] Interestingly, MHC-II deletion in ILC3s resulted in an increase of follicular T helper cells (Tfh) and IgA$^+$ plasma cells exclusively in the colonic mLN, but not in mLNs draining the SI.[137] From these data, the authors conclude that MHC-II$^+$ ILC3s suppress IgA production in the large intestine. Further studies using *in vivo* infection models are required to confirm these data, and to determine signals for ILC3s to either promote or prevent IgA production in a tissue-dependent manner.

ILC3s not only regulate B cell responses, but also directly modulate T cell responses in the intestine. Like splenic ILC3s, a fraction of ILC3s in the mLN, SI and colon express MHC-II and have the capacity to process and present Ags.[139,144] However, ILC3s in the intestine and mLN lack T cell co-stimulatory receptor ligands and were shown to reduce T cell responses against the microbiota.[139,144] Accordingly, genetic ablation of *MHC-II* in ILC3s led to microbiota-dependent, unrestrained Th1 and Th17 T cell responses towards commensal Ags and induced intestinal inflammation.[139,144,145] Supporting the notion that ILC3s are required to dampen T cell responses against commensal bacteria, *Ahr$^{-/-}$* mice which have less ILC3s and impaired ILC3 function (see chapter 2.3.1) displayed an increase in Th17 cell numbers and enhanced IL-17 and IFN-γ production in the SI.[146] In this model, reduced levels of ILC3-derived IL-22 caused a specific outgrowth of SFB but not other commensals, which in turn induced Th17 cells. Further reduction of IL-22$^+$ ILC3s in *RORγt$^{gfp/+}$Ahr$^{-/-}$* mice with haploinsufficiency for RORγt culminated in spontaneous colitis, which emphasized the importance of ILC3s in

maintaining intestinal homeostasis.[146] Similarly, T cell responses against the intracellular parasite *Toxoplasma gondii* and commensal Ags is balanced by AhR-dependent, ILC3-mediated IL-22 release and upregulation of MHC-II on ILC3s.[147] This has been shown in AhR-deficient mice in which T cells exhibited a hyperactive phenotype.[147] Altogether, those results illustrate an interplay of both IL-22 mediated containment of bacteria and MHC-II-dependent regulation of T cells under homeostasis. Interestingly, Martin *et al.* demonstrated that IL-7R-expressing ILCs can also constrain T cell proliferation *in vivo* by serving as 'IL-7 cytokine sink'.[148] IL-7 is involved in T cell expansion while ILC2 and ILC3 maintenance requires IL-7. Helper ILCs express large amounts of IL-7R on the surface and, in contrast to T cells, do not downregulate surface IL-7R upon IL-7 ligation.[148] Therefore, ILCs efficiently deprive T cells of IL-7. Given that ILCs are abundantly present at mucosal sites, ILC-mediated IL-7 depletion could further attenuate T cell responses in the intestinal tract.

Further evidence indicates that ILC3s also restrain inappropriate T cell responses by promoting regulatory T cell (Treg) functions. Under homeostasis, ILC3-derived GM-CSF contributes to maintenance of tolerogenic DCs and MΦ in the SI and large intestine and promotes IL-10 and retinoic acid (RA) production by DCs and MΦ, which is important to preserve the intestinal Treg pool.[119] In addition, microbiota induces IL-2 expression in ILC3s, which further supports the expansion of SI Tregs.[149] Consequently, the disruption of the circuit between myeloid cells, ILC3s and Tregs or compromised IL-2 production in ILC3s has been shown to impair oral tolerance to dietary Ags in mice.[119,149] Thus, ILC3s in the mLN are critical contributors to the maintenance of tolerance towards the intestinal microbiota and food Ags under homeostasis. Of note, Tregs inhibit exaggerated ILC3 responses under inflammatory conditions by suppressing IL-23 and IL-1β production in CX3CR+ MNPs and thereby form a negative feedback loop which constrains ILC3s and T cells to preserve tissue homeostasis.[120,121]

Even though ILC3s have been described to modulate various aspects of tissue homeostasis, a recent study by Mao *et al.* demonstrated that murine ILC3s were only transiently active after birth and that Th17 cells and Tregs collaboratively suppressed ILC effector functions.[121] Consequently, SI IL-22, RegIIIβ and RegIIIγ expression was much lower in wildtype mice compared to *Rag1-/-* mice.[121]
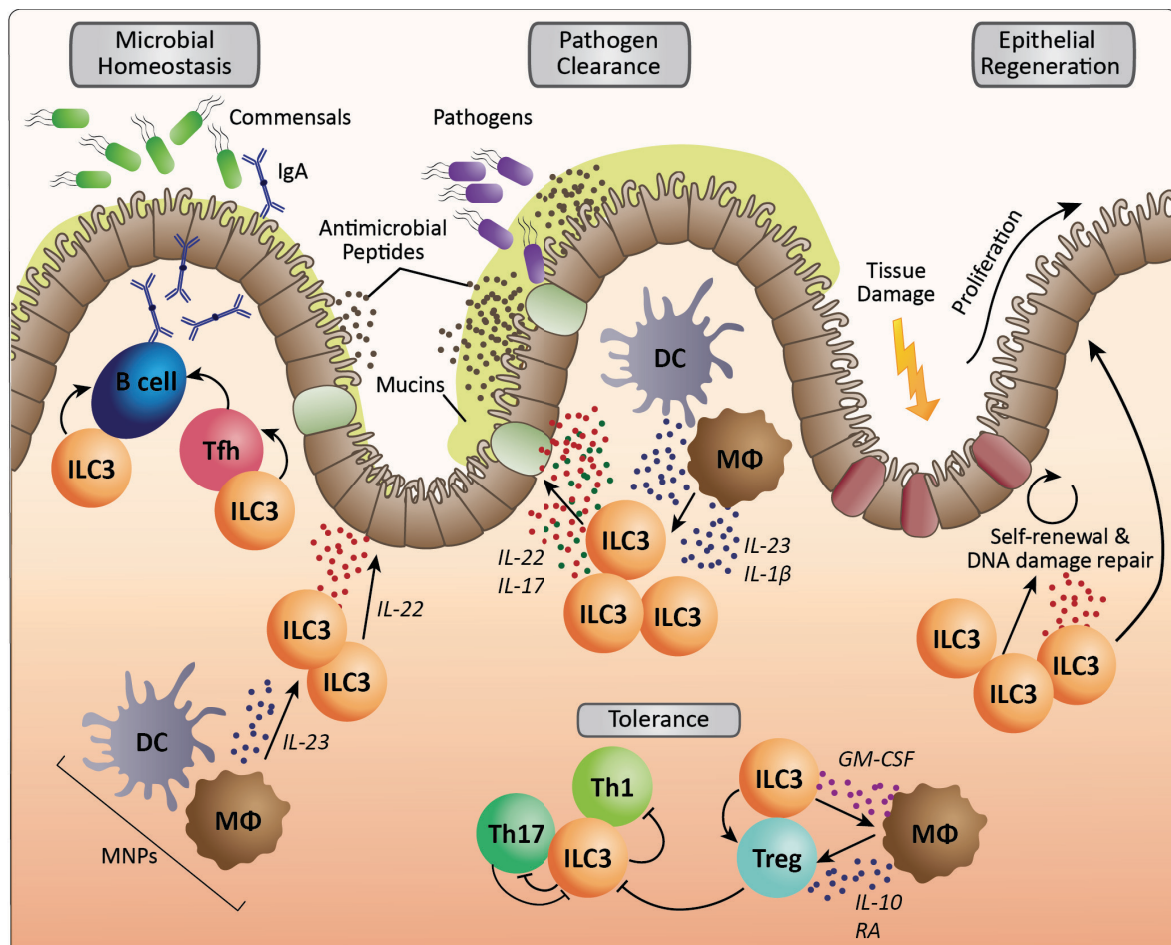
Fig.4 Small intestinal ILC3s in tissue homeostasis, tissue repair and infection. During homeostasis, ILC3s produce low amounts of IL-22. IL-22 promotes epithelial cell barrier integrity, basal expression of antimicrobial peptides such as RegIα, RegIIIβ, RegIIIγ, S100A8 and S100A9 in epithelial cells (brown cells) and mucin production by goblet cells (green cells). Moreover, ILC3s supports T cell-independent and T cell-dependent IgA production. ILC3s induce tolerance toward commensals and food antigens by suppressing Th1 and Th17 responses and by directly and indirectly enhancing Treg development and function. ILC3s are in turn regulated by Th17 cells and Tregs. During infection, mononuclear phagocytes (MNPs) induce upregulation of IL-22 and IL-17 production in ILC3s, which reinforces antimicrobial response mechanisms in epithelial cells. Tissue damage increases ILC3-mediated IL-22 production, which regulates tissue regeneration by protecting intestinal epithelial stem cells (ISCs, red cells) and by promoting epithelial cell proliferation. Adapted from Klose and Artis[4] and Hernandez *et al.*[150]

One report suggested the dispensability of ILCs for protection against infections and inflammation in humans, at least under modern hygiene conditions. This assumption was based on the observation that blood circulating ILCs were not reconstituted in SCID patients with mutation in IL-2Rγ and Janus kinase (JAK) 3 after hematopoietic stem cell transplantation (HSCT).[151] Despite the apparent lack of ILCs, patients were not more susceptible to infectious or inflammatory diseases.[151] Importantly, reconstitution of tissue-resident ILCs was still detected in patients who received myeloablative treatment before HSCT.[151] In line with the earlier described concept of ILC-poiesis (2.2.2 and Fig.3), this finding raises the possibility that donor-derived ILC progenitors might directly migrate into tissue where they can give rise to

tissue-resident ILCs. Moreover, tissue-resident ILCs were barely or not reconstituted after non-myeloablative allogenic HSCT in the intestine of two patients and the skin of one patient. However, the two earlier patients received intravenous immunoglobulin replacement. Therefore, it cannot be concluded that lack of ILCs does not impair protection against infections. More extensive clinical studies including larger cohorts of tissue biopsies will be required to draw definite conclusions on ILC redundancy in humans.

2.3.3 ILC3s in defense against infection

ILC3s are not solely participating in reinforcement of physical barriers, but also essentially contribute to the immediate immune responses upon translocation of commensals or invasion of pathogens into mucosal tissues (Fig.4). The impact of ILC3s in defense against extracellular pathogens has been demonstrated in several murine infection models.

Citrobacter rodentium is a gram-negative, attaching-and-effacing mouse pathogen, which is used to model human infections with enteropathogenic *Escherichia coli* (EPEC) and enterohemorrhagic *E. coli* (EHEC).[152] IL-22 is induced in the colon early after infection with *C. rodentium* and peaks at 4 days post-infection in an IL-23-dependent manner.[128,129,153] It has been shown that this immediate IL-22 response was provided by STAT3-dependent activation of ILC3s but not T cells.[129,153] Even though T cells are crucial to clear *C. rodentium* infection, the rapid ILC3-mediated IL-22 release is absolutely required to induce antimicrobial proteins such as S100A8, S100A9, RegIIIβ and RegIIIγ and to restrict the infection until the adaptive immune reaction is established.[61,128,129] *Il23*$^{-/-}$ mice and *Il22*$^{-/-}$ mice displayed higher histological colitis scores and died within one to two weeks post-infection. In contrast to IL-22, IL-23-independent IL-17 production is initiated only one week after infection and deletion of IL-17 did not affect the course of infection.[128,129] In line with an essential role of ILC3s in defense against infection, deletion of various genes, which are associated with ILC3 development and function, rendered mice susceptible to *C. rodentium* infection.[96,102,103,106,129] For example, *RORc*-driven depletion of *Stat3* weakened defense against *C. rodentium* infection.[106,129] The defect in the control of *C. rodentium* infection was based on reduced ILC3-mediated IL-22 production. Defense against *C. rodentium* was restored upon IL-22 injection. Of note, deletion of MyD88 in CX3CR1$^+$ MNPs or loss of CX3CR1$^+$ MNPs led to impaired defense against *C. rodentium* infection and exacerbated *C. rodentium*-mediated

colitis.[111,113,114] This susceptibility to *C. rodentium* infection was associated with decreased levels of IL-22, highlighting the importance of the crosstalk between myeloid cells and ILC3s during infection.

ILC3-mediated IL-22 and IL-17 have further been shown to contribute to defense against infections in other organs. Ardain *et al.* found that infection with *Mycobacterium tuberculosis* was marked by a depletion of blood circulating ILC1s and ILC3s and accumulation of ILC3s in the lung of humans.[154] Using a *M. tuberculosis* mouse infection model, the investigators found that recruitment of ILC3s to the lung was associated with an upregulation of neutrophil- and macrophage-attracting chemokines, higher alveolar macrophage numbers and an increase in formation of inducible bronchus-associated lymphoid tissues (iBALT).[154] These immediate *M. tuberculosis*-induced responses were impaired in *Rag2$^{-/-}$IL2r$\gamma^{-/-}$* mice*, Il17$^{-/-}$/Il22$^{-/-}$* mice and mice with *RORc*-driven deletion of *Ahr*. Thus, ILC3s may be involved in early responses towards *M. tuberculosis*.

Moreover, regulation of ILC3s through the vagus nerve modulated ILC3-mediated release of PCTR, the neutrophil influx and the time until resolution upon *E. coli* infection in the peritoneum of mice.[108]

ILC3-derived IL-17 responses are not only important for defense against bacterial infections but ILC3s represent the major source of IL-17 during oropharyngeal infections with the fungus *Candida albicans*. Gladiator *et al.* have demonstrated that *Rag1*-deficient mice showed an undisturbed defense against *C. albicans*.[155] ILC3s were the major producer of IL-17 in response to fungal infection. Accordingly, Ab-mediated depletion of ILCs or IL-17 hampered clearance of *C. albicans* infection.

Many of the protective functions of ILC3s have been attributed to activation-induced IL-22 and IL-17 responses. Nevertheless, ILC3s have also been shown to upregulate IFN-γ production during some infections. For example, ILC1 and NCR$^+$ ILC3 expansion and STAT4-dependent IFN-γ production by ILC1s and NCR$^+$ ILC3s occurs early after infection with *Listeria monocytogenes*.[156] Ab-mediated ILC depletion or genetic deletion of *Stat4* in wildtype mice and *Rag1$^{-/-}$* mice led to increased lethality. Hence, ILC3s essentially contribute to favorable IFN-γ responses during *L. monocytogenes* infection. Similarly, NCR$^+$ ILC3s expanded upon infection with *Salmonella typhimurium*.[31] NCR$^+$ ILC3s represented the major producers of IFN-γ throughout the intestine during *Salmonella* infection. Furthermore, ILC3s augmented

mucus production in goblet cells. Although ILC3s protect mice from *Salmonella* infection, *S. thyphimurium*-induced IFN-γ production by ILC3s exacerbated inflammation in the SI.[31] Thus, IFN-γ responses by ILC3s need to be tightly regulated.

Altogether, those studies demonstrate that ILC3s are activated by invading pathogens at different barrier sites. Immediate ILC3-mediated cytokine responses augment the barrier functions, enhance production of antibacterial proteins and promote other immune cells during infection. Therefore, ILC3s play an important role in the containment of bacterial and fungal infections.

2.3.4 ILC3s in colitis

Dysbiosis and dysregulation of the mucosal immune system is often discussed as cause of the development of a group of inflammatory diseases of the intestinal tract collectively termed inflammatory bowel disease (IBD). IBD contains different clinical entities, such as Crohn's disease (CD) and ulcerative colitis (UC). Even though it is not clear whether dysbiosis or dysregulation of immune cells initiate IBD, results from murine colitis models and human studies imply that dysregulation of ILC3s contributes to inflammatory diseases of the intestinal tract.

ILC3s in mouse colitis models

In contrast to the beneficial effects during homeostasis and tissue repair, cytokine production by ILC3s has been shown to participate in intestinal inflammation in murine models of colitis. In several of these colitis models, inflammation is associated with increased levels of IL-23, IL-1β, IL-17 and IFN-γ.

In *Helicobacter hepaticus*-induced colitis in 129SvEv *Rag2*$^{-/-}$ mice, intestinal inflammation is restricted to the cecum and colon.[157] The inflammation is linked to IL-23- and IL-1β-mediated activation of ILC3s and ILC3-derived IL-17 and IFN-γ.[29,157] Accordingly, Ab-mediated depletion of IL-1β, IL-17, IFN-γ or CD90(Thy1)$^+$ cells almost completely prevented this form of colitis and attenuated the colitis-associated recruitment of inflammatory granulocytes.[157]

Harmful ILC3s responses have also been demonstrated in mouse models with spontaneous colitis. For example, loss of the G protein-coupled receptor Gpr109a in *Rag1*$^{-/-}$ mice led to a changed composition of the intestinal microbiota, microbiota-mediated augmentation of IL-23 production in MNPs, increase in IL-17$^+$ ILC3 numbers and spontaneous colonic

inflammation and rectal prolapse.[158] Antibiotics and depletion of IL-23 or CD90.2(Thy1.2)$^+$ ILCs prevented the upregulation of IL-17 and inflammation and thereby create a causal link between dysbiosis and the dysregulation of ILC3 cytokine release.

ILC3s have been further shown to be involved in inflammation in a mouse model of acute innate colitis. α-CD40 Ab injection into *Rag1*- or *Rag2*-deficient mice induces an acute colitis.[29,159] In this form of colitis, MNP-derived IL-23 induces IL-22 and IFN-γ in ILC3s and a conversion of NCR$^+$ ILC3s into ex-ILC3s.[29,77,160,161] Of note, IL-17 is not involved in this acute colitis model.[29,160,161] Transfer of exILC3s into *Rag2$^{-/-}$IL2r$\gamma^{-/-}$* mice was sufficient to drive α-CD40 colitis and exILC3s seemed to be the prominent source of IFN-γ in this model.[29,77,160] Genetic or Ab-mediated depletion of CD90$^+$ ILCs, RORγt$^+$ ILC3s or IFN-γ significantly decreased inflammation in the α-CD40 colitis model.[29,160,162] However, ILC3-mediated IL-22 might also enhance α-CD40 colitis as α-IL-22 treatment slightly attenuated inflammation.[161] Accordingly, forced expression of IL-22 by microinjection of an IL-22 plasmid aggravated inflammation through further upregulation of IFN-γ and increased recruitment of neutrophils.[161] Hence, exaggerated IL-22 levels may contribute to pathogenic IFN-γ responses during colitis. The source of IFN-γ was not defined in this study. Nevertheless, the collective findings highlight the importance of ILC3s and ILC3-derived IFN-γ in acute α-CD40 colitis.

Results from several mouse colitis models support the idea that ILC3s promote inflammatory diseases. However, ILC3 cytokines have also been attributed to beneficial functions during colitis. The mode of activation of ILC3s appears to determine whether ILC3s play a beneficial or detrimental role during the course of inflammation. This has been illustrated in a publication by Castellanos *et al*. in which the role of ILC3s was directly compared between two different colitis models: 1) an acute colitis model in which inflammation is induced by DSS supplementation in the drinking water and 2) a chronic T cell colitis model in which inflammation is triggered by T cell transfer into *Rag2$^{-/-}$* mice.[163] On one hand, ILC3 activation was protective in DSS-induced acute colitis. In this form of acute colitis, synergistic IL-23/TL1A-mediated stimulation of IL-22 in ILC3s essentially contributed to mucosal healing, while IL-17 and IFN-γ production in ILC3s remained unchanged. On the other hand, ILC3s exacerbated inflammation in chronic T cell colitis. In this model, CX3CR1$^+$ MNP-mediated TL1A release induced OX40L expression on MHC-II$^+$ ILC3s, which in turn promoted harmful Th1 responses in T cells.[163] Findings from similar studies, however, oppose the opinion that ILC3s

harbor detrimental effect in chronic T cell colitis. Instead, IL-23R- and RORγt-deficient mice even displayed enhanced colitis scores suggesting a protective role of ILC3s in chronic T cell colitis.[161,162] Altogether, the relevance of ILC3s in promotion and attenuation of colitis varies between colitis models. The contradicting results might be based on differences in underlying pathogenic mechanisms elicited in different colitis models.

ILC3s in IBD in humans

Several lines of evidence indicate that dysregulation of ILC3 biology and function promotes inflammation in the intestinal tract in humans. In human fetal intestine samples and in non-inflamed ileum sections from adult controls, NCR⁺ILC3s are most abundant while NCR⁻ ILC3s and ILC1s each represent only about 10 % of ILCs.[81] In patients with CD, this ratio is almost reversed: IFN-γ producing ILC1-like ILCs accumulate in the inflamed tissue whereas NCR⁺ ILC3s are severely reduced.[81,118,164-166] Furthermore, NCR⁺ ILC3s derived from inflamed regions of the ileum of CD patients displayed reduced AhR protein levels compared to ILC3s from non-inflamed regions.[167] As previously described (2.2.3), ILCs are highly plastic cells and AhR expression has been shown to stabilize the ILC3 phenotype in murine ILCs. Thus, these findings raise the possibility that ILC3s undergo a transition into exILC3s in CD patients and thereby contribute to the pool of IFN-γ-producing ILCs which exacerbate inflammation.[118] In contrast to CD patients, UC patients exhibit no increase in ILC1-like ILCs.[118,166] However, NKp46⁺ ILC3s from both CD and UC patients showed hypersensitivity to stimulation with *Enterococcus faecalis* and *Escherichia coli*, two commensal bacteria, *in vitro*.[118] Hence, dysregulation of ILC3 cytokine production might also participate in inflammatory responses in UC patients.

Moreover, dissection of Th17 subsets and ILC subsets in the ileum of adult CD patients and the colon of pediatric CD patients revealed a reduction of human leucocyte Ag D-related (HLA-DR) protein, a human MHC-II molecule, on the surface of ILC3s. This correlated with increased numbers of pathogenic Th17 cells.[144,165] Given that MHC-II⁺ ILC3s are assumed to be involved in maintaining the tolerance towards microbiota of the intestine in mice (chapter 2.3.2), the loss of MHC-II in ILC3s might at least in part account for failure to restrain pathogenic T cell responses.

Many findings from human IBD studies suggest that ILC3s might promote inflammation in IBD patients via IL-17 and IFN-γ. However, some results from patients also associate IL-22 with

disease severity. For example, TL1A and IL-22 were found to be elevated in colon-derived CX3CR1[+] MNPs and ILC3 from CD patients.[111,163] These findings imply that cytokines which have been proposed to be beneficial under homeostasis might contribute to inflammation in IBD. As described above, results from mouse colitis studies suggest that TL1A and IL-22 can be both protective or harmful depending on the context.[163] Therefore, further studies would need to address whether the observed association between TL1A, ILC3-derived IL-22 and GM-CSF and inflammation indicates that ILC3s have harmful effects in the context of IBD or whether the changes in ILC3 cytokine production may counteract inflammation.

2.4 mTOR

In the 1970s, analysis of soil samples from 'Rapa Nui' (Easter Islands) led to the discovery of an antifungal compound called rapamycin, which later proved to be a potent antiproliferative and immunosuppressive compound in mammals. In the 1990s, TOR1 and TOR2 were described as molecular targets after target screens for rapamycin in yeast.[168,169] Soon after, mechanistic target of rapamycin (previously called mammalian target of rapamycin) (mTOR) was also isolated from mammalian cells.[170-172] Today, it is known that mTOR is an atypical serine/threonine kinase of the phosphoinositide 3-kinase (PI3K)-related family, which is conserved throughout mammalian evolution. The mTOR signaling pathway is involved in the integration of various environmental signals.[173,174] mTOR signaling has a major impact on cellular functions and the outcome of mTOR activation is highly cell type-specific.

2.4.1 The mTOR complexes and mTOR signaling

The mTOR kinase represents the enzymatically active core subunit of two cytoplasmic protein complexes, mTOR complex (mTORC) 1 and 2, which control different pathways and differ in drug sensitivities (Fig.5).[173,174] mTORC1 and mTORC2 are formed by six and seven protein subunits, respectively. Besides the catalytic mTOR subunit, mTORC1 and mTORC2 share the three subunits mLST8 (mammalian lethal with sec-13 protein 8), Deptor (DEP domain containing mTOR-interacting protein) and Tti/Tel2 complex. Raptor (regulatory-associated protein of mTOR) and PRAS40 (prolin-rich Akt substrate 40 kDa) represent mTORC1-specific subunits, whereas Rictor (rapamycin-insensitive companion of mTOR), mSIN1 (mammalian stress-activated map kinase-interacting protein) and Protor1/2 (protein observed with Rictor

1 and 2) are mTORC2-specific subunits. Raptor (encoded by *Rptor*) and Rictor (encoded by *Rictor*) serve as scaffolds for their respective complex. They are essential for the complex assembly and substrate binding.[174] Consequently, mTORC1 is lost upon genetic deletion of *Rptor* while knockout of *Rictor* prevents the formation and function of mTORC2.

mTORC1 is an intracellular hub sensing and integrating at least five major intracellular and extracellular inputs: 1) signaling through growth factor receptors, 2) cellular stress signals, 3) intracellular energy status, 4) oxygen availability and 5) amino acid availability (Fig.5).[173,174] mTORC1 activation is usually followed by an upregulation of protein and lipid synthesis, increased energy metabolism and enhanced ribosome biogenesis, whereas other processes such as autophagy and lysosome biogenesis are inhibited. By inducing the synthesis of cellular building blocks and enhancing mRNA translation, mTORC1 signaling promotes cell cycle progression and cell growth in various cell types. Many cellular signals modify mTORC1 indirectly by suppression of the GTPase-activating protein heterodimer TSC1/2 (tuberous sclerosis 1/2), which inhibits the mTORC1-activating protein Rheb (Ras homolog enriched in brain).[173,174] In contrast to other signals, mTORC1-inducing amino acids such as leucine and arginine exploit an alternative activation pathway, which involves the Ragulator complex-mediated recruitment of mTORC1 to the surface of lysosomes. Conversely, mTORC1 deactivation is often achieved by induction of TSC1/2 and AMPK (AMP activated protein kinase), which downmodulate mTORC1 activity. The mTORC1 inhibitor rapamycin forms a complex with FKBP12 (12-kDa FK506-binding protein). This complex specifically binds and inhibits mTORC1, although long-term exposure also downmodulates mTORC2 activity.[173] Of note, mTORC1 dampens its own activity as well as mTORC2 activation by inhibiting PI3K signaling.[173,174]

Many results on mTORC1-related functions are based on the application of mTORC1-specific inhibitors. Since mTORC2-specific inhibitors are still not available, much less is known about the biology of mTORC2. Newly synthesized mTOR inhibitors target the ATP binding site of mTOR, thereby block activity of both mTORCs, and have revealed further rapamycin-insensitive effects of mTOR.[173,174] It is generally accepted that mTORC2 is activated by PI3K-dependent pathways and that mTORC2 regulates mTORC1, cell metabolism, cytoskeletal organization, cell migration, mitochondrial fitness, differentiation and cell survival (Fig.5).[173-175] More recent studies show that mTORC2 can be found close to the plasma membrane but also in organelles like mitochondria and vesicles.[175]

2.4.2 mTOR and the immune system

Immune cells constantly receive survival and differentiation signals from their microenvironment and rapidly need to adjust their proliferative, migratory and functional programs in response to infection and inflammation. Several studies have shown that mTOR is integrating environmental cues in both innate and adaptive immune cells.[176-181] In immune cells, mTOR is important for transcriptional regulation and metabolic adaptation upon activation. Modulation of mTOR signaling changes the pro- and anti-inflammatory behavior of immune cells, the differentiation capacity and memory formation (Fig.5). Importantly, blocking the mTOR pathway hampers metabolic adaptation of cells and thereby either impairs immune cell functions or diverts cytokine profiles.
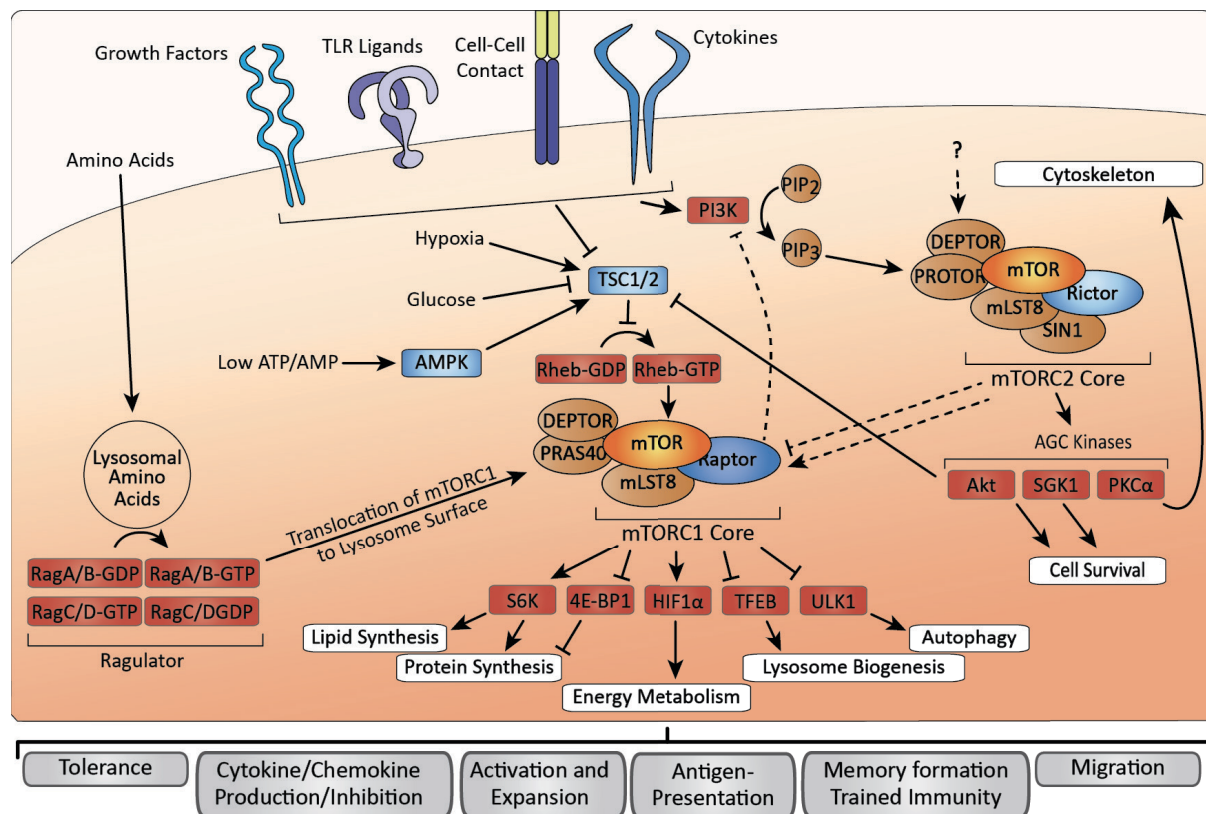
Fig.5 Simplified scheme of mTORC1 and mTORC2 signaling in immune cells. Receptor signaling, energy status, and hypoxia indirectly induces mTORC1 and mTORC2 by modulating TSC1/2 activity and PI3K signaling. Amino acids promote mTORC1 recruitment to the lysosome. mTORC1 and mTORC2 in turn regulate kinases and transcription and thereby adapt cellular processes. The sum of mTORC1 and mTORC2 activation and inhibition defines immune cell type-specific differentiation programs and immune cell functions. Depending on immune cell subgroup, mTORC1 and mTORC2 regulate each other in positive or negative feedback loops (dashed lines). Adapted from Shimobayashi and Hall[174], Laplante and Sabatini[173], Weichhart *et al.* [176], Keating and McGargill[177].

mTOR in T cells

In T cells, mTOR is induced upon T cell receptor activation and is enhanced by co-stimulation, cytokines and other environmental cues such as nutrient availability and growth factors (Fig.5). Metabolic adaptation is crucial for activated T cells to support expansion and effector functions such as cytokine production. Part of this metabolic switch is mediated via mTOR.[178,180-183] However, mTOR-driven changes in metabolism are also critically involved in shaping the differentiation of T cells and thereby adjust the type of immune response.

Based on multiple *in vitro* and *in vivo* studies with mTOR inhibitors and *Lck-* or *CD4*-driven genetic ablation of mTORC components or mTOR suppressors, it is now commonly accepted that the two mTORCs differentially affect activation-induced CD4^{+} T cell differentiation.[177,180,182-184] Loss of mTORC1 signaling results in defective Th1 and Th17 differentiation while ablation of mTORC2 prevents Th2 differentiation.[185] Moreover, mTOR deficiency in CD4 T helper cells promotes Treg differentiation while impairing Th1, Th2 and Th17 differentiation.[186] mTORC1 and mTORC2 further participate in differentiation of Tfh cells.[187] Although silencing of mTORC1 or mTORC2 only partially overlap in the effect on gene expression profiles of Tfh cells, they are both involved in Tfh differentiation.[187]

Of note, mTOR is not only guiding T cell differentiation but also modulates functionality of differentiated T cells. For example, Tregs displayed impaired immunosuppressive capacity upon loss of mTORC1 signaling[188-191], whereas deletion of both mTORCs preserved Treg functions.[188] This seemingly contradictive finding might be based on an increased phosphorylation of mTORC2 target Akt in mTORC1-deficient Tregs.[188] Accordingly, hyperactivity of PI3K signaling, mTORC2 and Akt in Tregs has been associated with dampened immunosuppressive functions.[192,193] Altogether, this example illustrates that a fine-tuned balance of mTORC1 and mTORC2 activity is required to maintain immune cell functions.

Interestingly, the dual mTORC1/2 inhibitor AZD8055 ameliorates DSS-induced colitis in mice.[194] In this study, mTOR inhibition was linked to reduced numbers of Th1 and Th17 T cells, decreased levels of pro-inflammatory cytokines such as IL-1β, IL-6 and TNF-α and Treg expansion.

While many mTOR studies in CD4^{+} T cells have focused on differentiation towards specific Th effector programs, research on CD8^{+} T cells revealed that the level of mTOR activation controls whether activated T cells enter effector or memory T cell stage.[184,195] On the one hand, a strong mTOR signal during activation mediates a metabolic shift towards increased

glycolysis and T cell effector fate. Conversely, low levels of mTOR result in an upregulation of mitochondrial oxidative phosphorylation in T cells promoting memory phenotype. Moreover, deletion of mTORC2 drives memory phenotype in CD8^{+} T cells marked by more potent memory responses during infection.[196] A similar model in which the strength of mTOR activation determines whether activated T cells follow the effector or memory trajectory has been suggested for CD4^{+} T cells.[180,183,191]

mTOR activity might also modulate migration of T cells. mTORC1 has been shown to differentially regulate migration of conventional CD4^{+} T cells and Tregs. While expression of the gut homing receptors CCR9 and $\alpha 4\beta 7$ in conventional CD4^{+} T cells does not require mTORC1 *in vitro*, expression of both receptors in Tregs depends on mTORC1.[197] Accordingly, Treg migration to the intestine is impaired when rapamycin-treated Tregs are adoptively transferred into mice.

mTOR in innate immunity

In MΦ and DCs, mTOR is activated in response to extracellular signals such as growth factors, TLR ligands and cytokines, links activation signals to glucose, amino acid and energy availability and thereby modulates effector functions such as cytokine responses and memory formation (Fig.5).[176] In general, mTOR activation in innate immune cells is associated with a metabolic shift from oxidative phosphorylation towards glycolysis.[176,179,181]

It is not yet entirely clear if this metabolic shift renders MΦ pro- or anti-inflammatory. On one hand, several studies suggest that mTOR-mediated metabolic changes result in increased pro-inflammatory cytokine release by MΦ.[180,181] Accordingly, IL-10 exerted its immuno-suppressive functions on TLR ligand-induced MΦ by downregulation of mTORC1 signaling.[198] This mTORC1 inhibition led to a block in metabolic adaptation and impaired pro-inflammatory cytokine production in mouse and human MΦ *in vitro*.[198] On the other hand, there is also experimental evidence that mTORC1 activation drives an anti-inflammatory phenotype in MΦ. In several studies, IL-12 expression was suppressed by mTOR signaling, whereas pharmacological or genetic inhibition of mTORC1 or mTORC2 promoted IL-12 production by MΦ.[176,180,181] Cytokines such as IL-4 promote TSC1/2 activity, thereby suppressing a metabolic shift and inducing production of anti-inflammatory cytokines.[176,179,181] Those adverse results might be explained by different methods and variations in activating conditions.[176] This emphasizes the complexity of the regulation of pro- and anti-inflammatory cytokines in MΦ.

In activated DCs, mTORC1 inhibition or deletion of Rictor promotes immune-stimulatory effects. This immune-stimulatory effect is linked to impaired IL-10 release by DCs, increase in IL-12 production, a concomitant enhancement of MHC-II-Ag presentation and upregulation of co-stimulatory ligands such as CD86.[176,179-181]

In addition, mTORC1 differentially modulates MΦ and DC migration as mTORC1 promotes migration of MΦ, but inhibits DC migration.[176]

Moreover, defying old dogmas, research of the past decade has demonstrated that activated innate immune cells can acquire an unspecific memory that augments the response to a second infection with unrelated pathogens. The development of this so-called 'trained immunity' depends on metabolic switches mediated through mTOR. Cheng *et al.* have shown that a single injection with the immunogenic *C. albicans* component β-glucan protected mice from a secondary lethal infection with *C. albicans* or *Staphylococcus aureus* one week later.[199] Mechanistically, β-glucan-mediated activation of the receptor Dectin-1 activated mTORC1 which in turn induced HIF-1α. HIF-1α activation led to a metabolic shift from oxidative phosphorylation towards glycolysis in MΦ. This trained immunity could be reverted upon treatment with rapamycin or rapamycin-loaded high-density lipoprotein (HDL) nanobiologics.[199-201] Treatment of heart-transplanted mice with rapamycin-loaded HDL nanobiologics similarly prevented trained immunity in an allogenic heart transplant model and redirected MΦ into tolerogenic MΦ, which induced allograft tolerance.[200]

While there is some evidence that mTOR is involved in modulation of DC and MΦ functions, the impact of mTOR on ILC activation has not yet been studied in depth. Nevertheless, there are some implications that activated ILCs also undergo metabolic adaptations prior to maximizing cytokine production, and that part of this metabolic shift is mediated via mTOR signaling.[202,203]

Accordingly, sustained IFN-γ and granzyme B production by NK cells was enhanced by mTORC1-dependent upregulation of glycolysis in response to Poly I:C, IL-12 or high-doses of IL-15.[176,204,205] Moreover, intestinal ILC1s exhibit an enrichment of RNA transcripts related to mTOR signaling, though the functional importance for ILC1s has not yet been investigated.[32] Cytokine-activation of ILC2s was shown to depend on glycolysis and fatty acid oxidation in the lung and intestine, respectively.[202,206,207] Later, it was reported that uptake of glucose was required to activate mTORC1 in activated ILC2s.[208] Both glucose uptake and mTORC1 were

regulating fatty acid metabolism.[208] Thus, reduction of glucose availability by ketonic diet suppressed ILC2-mediated airway inflammation.[208] The authors propose that glucose metabolism is required for inflammatory ILC2 responses in the lung. However, they did not test whether mTORC1 was involved in such ILC2 responses and airway inflammation. Similar to ILC2s, ILC3s take up low levels of fatty acids.[206] Murine intestinal ILC3 RNA transcript profiles show enrichment for glycolysis-associated genes.[32,202] Di Luccia *et al.* have recently reported that mTORC1 signaling was required for HIF-1α-mediated *in vitro* proliferation and IL-22 and IL-17 production by the ILC3-like MNK3 cell line.[209] In MNK3 cells, mTORC1 activation led to an upregulation of glycolysis and increased reactive oxygen production in mitochondria. This metabolic shift was required for maximal ILC3 cytokine production. Accordingly, wildtype and *Rag1*$^{-/-}$ mice with *RORc*-driven deletion of *Rptor* had lower numbers of ILC3s in the SI and exhibited reduced protection against infection with *C. rodentium*.

3 Aim of the project

Group 3 innate lymphoid cells (ILC3s) are present in multiple organs but are most abundant in mucosal tissues of the gastrointestinal tract. ILC3s respond to innate stimulation with the secretion of cytokines such as IL-22, IL-17 and IFN-γ. Under homeostatic conditions, ILC3s are often associated with protective functions and preserve homeostasis at mucosal barrier sites. However, ILC3s can also downmodulate their transcriptional identity and switch to a proinflammatory cytokine profile contributing to chronic inflammation and tissue damage. The mechanisms by which ILC3 responses in the intestinal tract can be modulated is not yet fully understood. Activation-induced immune cell functions are often based on metabolic changes. The serine/threonine kinase mechanistic target of rapamycin (mTOR) drives such metabolic changes and integrates environmental signals in several immune cell subtypes. mTOR signaling modulates the expansion, differentiation and the pro- and anti-inflammatory behavior of cells. Accordingly, inhibition of the mTOR pathway hampers metabolic adaptation of cells and thereby affects immune cell functions. mTOR forms two complexes, mTORC1 and mTORC2, with distinct and overlapping functions.

The present work aimed to elucidate three major questions: 1) whether the two mTORCs play a role in ILC3 differentiation and proliferation, 2) whether mTORCs regulate activation-induced cytokine responses, and 3) whether mTOR deficiency has an effect on ILC3 immune responses during acute colitis and bacterial infection *in vivo*. To address these questions, I established immune-sufficient and lymphopenic mice harboring a conditional *RORc* promoter-driven knockout for the essential mTORC1 component *Rptor* and/or the mTORC2 component *Rictor*. Using mixed BM chimeras, I determined whether disruption of mTORC1 or mTORC2 signaling impairs competitive reconstitution of ILC3s. To assess whether mTOR deficiency is associated with defects in proliferation, knockout strains were tested *in vivo* for their ILC3 proliferative capacity in response to IL-2/α-IL-2 complex. The effect of mTOR on ILC3 plasticity was investigated by injecting mTORC1 inhibitor rapamycin into *RORγt^{eYFP}Rag2$^{-/-}$* fate map reporter mice. To understand the role of mTOR for ILC3 activation, *in vitro* ILC3 cultures from knockout mice or rapamycin-treated ILC3s were exposed to inflammatory cytokines. Finally, I studied the effect of mTOR deficiency on ILC3 immune responses during α-CD40 colitis and *Citrobacter rodentium* infection *in vivo*.

4 Materials and methods

4.1 Materials

4.1.1 Reagents and chemicals

2-mercaptoethanol (50 mM)	Gibco
2 N sulfuric acid (H_2SO_4)	Roth
Agarose	Sigma-Aldrich
Agar for microbiology	AppliChem
Ammonium chloride (NH_4Cl)	Sigma-Aldrich
Ammonium sulfate ((NH_4)$_2SO_4$)	Roth
Baytril	Provet AG
Bovine serum albumin (BSA)	Sigma-Aldrich
Brefeldin A (BFA)	Sigma-Aldrich
Cell Tak	BD Biosciences
Ciproxine (0.2%)	Bayer
Collagenase D	Roche
Collagenase VIII	Roche
Dimethyl sulfoxide (DMSO)	Sigma-Aldrich
Di-potassium hydrogen phosphatate (K_2HPO_4)	Merck KgaA
Di-sodium hydrogen phosphatate (Na_2HPO_4 x 2 H_2O)	Merck KgaA
dT20	Microsynt
DMEM (1x) GlutaMax^{TM}-I	Gibco
DNase	Promega
DNase I	Roche
EDTA disodium salt dihydrate	AppliChem
Erythromycin	Sigma-Aldrich
Ethanol (C_2H_5OH)	Sigma-Aldrich
Ethanol (C_2H_5OH), absolute	Merck KgA
Fetal calf serum (FCS, heat-inactivated)	Gibco
HEPES (1 M)	Gibco
Hydrochloric acid (HCl)	Sigma-Aldrich
Insulin Transferrin Selenium	Gibco
Iscove's modified Dulbecco`s medium (IMDM)	Sigma-Aldrich

Kanamycin	Sigma-Aldrich
Luria-Bertani broth (Lennox)	Sigma-Aldrich
Magnesium chloride hexahydrate (MgCl$_2$ x 6 H$_2$O)	AppliChem
Natriumhydroxid	Roth
Non-essential amino acids (NEAA) (100 x)	Gibco
Nuclease-free H2O	Thermo Fisher Scientific
Oligo dT	Promega
Phosphate buffered saline (PBS)	Biochrom AG
Penicillin Streptomycin (Pen/Step)	Gibco
Percoll	GE Healthcare
Paraformaldehyde (PFA)	AppliChem
Potassium bicarbonate (KHCO$_3$)	Sigma-Aldrich
Potassium chloride (KCl)	AppliChem
Primatone	Sigma-Aldrich
Primers	Sigma-Aldrich
Proteinase K	Merck Millipore
Random hexamers	Sigma-Aldrich
RNaseOUT	Invitrogen
Roti-Histofix	Roth
Saponin	Sigma-Aldrich
Sodium azide (NaN$_3$)	Merck KgaA
Sodium chloride (NaCl)	AppliChem
Sodium dodecyl sulfate (SDS)	Bio-Rad
Sodium hydrogen carbonate (NaHCO$_3$)	Merck KgaA
Sodium hydroxide (NaOH)	Merck KgaA
Taq Polymerase Sigma-Aldrich	Sigma-Aldrich
Tris (C$_4$H$_{11}$NO$_3$)	Carl Roth GmbH
Trypan blue	Sigma-Aldrich
Tween-20	AppliChem
Triton X100	AppliChem
Unbuffered RPMI-1640 Medium (without sodium bicarbonate)	Sigma-Aldrich

4.1.2 Buffers, solutions and media

1x PBS	137 mM NaCl
(magnesium- and calcium-free)	2.7 mM KCl
	10 mM Na_2HPO_4 x 2 H_2O
	2 mM KH_2PO_4
	in ddH_2O

1x TE buffer	10 mM Tris
	1 mM EDTA
	in ddH_2O

10x reaction buffer	500 mM Tris HCl
	160 mM $(NH_4)_2SO_4$
	25 mM $MgCl_2$
	1 % Tween-20
	in ddH_2O

4 % PFA	1 x PBS
	4 % PFA

DMEM (1x) GlutaMax^{TM}-I	(+) 4.5 g/L D-Glucose
	(-) Pyruvate

dNTP mix	10 mM sATP
	10 mM sCTP
	10 mM sGTP
	10 mM sTTP
	in nuclease-free H_2O

ELISA reagent dilutent	1 % BSA
	in 1x PBS

ELISA wash buffer	0.05 % Tween-20
	in ddH_2O

Erythrolysis buffer	0.15 M NH_4Cl
	10 mM $KHCO_3$
	0.1 mM EDTA
	in ddH_2O (pH 7.2 – 7.4)
FACS buffer	1x PBS
	3 % FCS
IMDM (SF)	IMDM (powder)
	3.02 g $NaHCO_3$
	1 % Pen/Strep
	1 % Ciproxine
	0.1 % Kanamycin
	1 % Insulin Transferrin Selenium
	0.3 % Primatone
	1 % NEAA
	0.1 % 2-mercaptoethanol
	In ddH_2O
IMDM 5 % FCS	IMDM (SF)
	5 % FCS
lysis buffer	100 mM Tris (pH 8.0)
(for gDNA isolation from	200 mM NaCl
mouse biopsies)	5 mM EDTA (pH 8.0)
	0.2 % SDS
	in ddH_2O
Permeabilization buffer for	0.5 % Saponin
intracellular FACS staining	0.01 % NaN_3
	in FACS buffer

4.1.3 Cytokines, inhibitors and antibodies for *in vitro* and *in vivo* application

2-Deoxy-D-glucose	Sigma-Aldrich
α-IL-2 mAb JES6-1A12	BioXCell
α-CD40 Ab (Clone FGK45.5)	home-made, purified from hybridoma tissue culture supernatant (provided by Antonius Rolink)
Carbonyl cyanide 4-(trifluoromethoxy) phenylhydrazone (FCCP)	Sigma-Aldrich
Etomoxir	Sigma-Aldrich
Oligomycin	Sigma-Aldrich
PP242	Chemdea
Rapamycin	LC Laboratories
Recombinant murine IL-1β	Biovision
Recombinant murine IL-2	BioXCell
Recombinant murine IL-23	eBioscience
Rotenone	Sigma-Aldrich

4.1.4 Antibodies

Abs used for flow cytometry analysis (directed against murine Ags)

Specificity	clone	conjugates
α4β7 (LPAM-1)	DATK32	Biotin
active Caspase-3	C92-605	V450
B220 (CD45R)	RA3-6B2	FITC, PE/Cy7, PE-CF594
CCR2	475301	PE
CD103	2E7	PE/Dazzle 594
CD117	2B8	BV421^{TM}
CD11b	M1/70	BV421^{TM}, PE/Cy7
CD11c	N418	BV605^{TM}, BV650^{TM}, FITC
CD127 (IL-7Rα)	A7R34	BV605^{TM}, PE/Cy7
CD135 (FLT3)	A2F10	PE
CD19	6D5	APC/Cy7, BV785^{TM}, FITC
CD21 (FcεRII)	7G6	APC

CD23	B3B4	Biotin
CD24	M1/69	PE/Cy7
CD25	PC61	APC/Cy7, PE/Cy5
CD3ε	145-2C11	APC/Cy7, FITC, PE/Cy7
CD4	RM4-5	BV650™, PE, PE-Texas Red®
CD44	IM7	PE/Cy7
CD45	30-F11	PerCP/Cy5.5
CD45.1	A20	APC/Cy7, BV605™, PE/Cy7
CD45.2	104	BV650™
CD62L	MEL-14	Per/CpCy5.5
CD64 (FcγRI)	X54-5/7.1	APC
CD8α	53-6.7	APC, FITC
CD90.2	30-H12	APC/Cy7, AF700®, BV785™, PE
Eomes	Dan11mag	PE
F4/80	BM8	APC/Cy7
FoxP3	FJK-16s	PE
GL7	GL7	FITC
IFN-γ	XMG1.2	BV650™
IgD	11-26c.2a	PE
IgM	II/41	AF700®
IL-17A	TC11-18H10.1	AF700®
IL-22	1H8PWSR	PE, PerCP-eFluor710
Ki-67	B56	BV786™
KLRG1	2F1	PE-eFluor610
Ly-6C	HK1.4	AF488
Ly-6G (Gr-1)	1A8	APC/Cy7
Ly-6G (Gr-1)	RB6-8C5	FITC, PE
MHC-II (I-A/I-E)	M5/114.15.2	BV785™, FITC
NK1.1	PK136	APC/Cy7, FITC, PE/Cy7
NKp46 (CD335)	29A1.4	BV421™, BV605™, eFluor660
Phospho-Akt (pS473)	M89-61	V450
Phospho-mTOR (pS2448)	MRRBY	PerCP-eFluor710

Phospho-S6 (pS235/236)	D57.2.2E	AF647
Phospho-STAT3 (pY705)	13A3-1	PE
Phospho-STAT4 (pY693)	38/p-Stat4	APC, PE
RORγt	Q31-378	BV785™
RORγt	B2D	PerCP-eFluor710
Sca-1 (Ly-6A)	D7	BV510™
Siglec H	eBio440c	PE
Sirpα (CD127a)	P84	PerCP-eFluor710
T-bet	eBio4B10	PE/Cy7
TCRβ	H57-597	Biotin, FITC
TCRγδ	UC7-13D5	FITC
TER-119	TER-119	FITC
XCR1	ZET	BV421™

All monoclonal Abs were purchased from BD Biosciences, eBioscience, Biolegend, Invitrogen, R&D Systems and Cell Signaling Technology. Biotin-conjugated primary antibodies were detected using Streptavidin conjugated either to APC or BV650™ (Biolegend).

Abs used for In-Cell Western

Phospho-Akt (Ser473) Rabbit mAb	193H12	Cell Signaling Technology
Phospho-S6 Ribosomal Protein (Ser235/236) Rabbit mAb	2F9	Cell Signaling Technology
mouse anti-alpha-Tubulin	DM1A	Sigma-Aldrich
IRDye® 680RD goat a-mouse IgG secondary Ab	polyclonal	LI-COR Biosciences
IRDye® 800RD goat a-rabbit IgG secondary Ab	polyclonal	LI-COR Biosciences

4.1.5   Primers for quantitative real-time polymerase chain reaction (RT qPCR)

Il22 fwd primer   5' GAGTCAGTGCTAAGGATCAG 3'

Il22 rev primer   5' TCAGAGACATAAACAGCAGG 3'

Ifng fwd primer   5' CTGAGACAATGAACGCTACAC 3'

Ifng rev primer   5' TTTCTTCCACATCTATGCCAC 3'

4.1.6 Kits

2x SensiMix SYBR Hi-ROX Kit	Bioline
BD Perm Buffer III	BD Bioscience
Deoxynucleotide triphosphates (dNTPs)	Roche
Foxp3 Transcription Factor Staining Buffer Set	eBiosciences
LEGENDplex™ Mouse Th Cytokine Panel (13-plex) with V-bottom Plate V02	Biolegend
LIVE/DEAD® Fixable Aqua Dead Cell Stain Kit	Molecular Probes
mouse Lipocalin-2/NGAL DuoSet ELISA Kit	R&D Systems
RNeasy Micro Kit	Qiagen
Seahorse XFe96 FluxPak	Agilent Technologies / Bucher Biotec
SuperScript™ III Reverse Transcriptase	Invitrogen
TMB Substrate Set	Biolegend

4.1.7 Tools and instruments

BD FACS Aria™	BD Biosciences
BD Microtainer SST™ Tubes	BD Biosciences
BD LSRFortessa™	BD Biosciences
black flat-bottom 96 well carrier plates with transparent bottom	Falcon
Cell strainer (70 μm / 100 μm)	Falcon
Cell counter CASY INNOVATIS	Roche
CO_2 - incubator	Binder
Cs-137 radiator	Gammacell
Cytoflex S	Beckman Coulter
Disposable Cuvettes, semi-micro	Brandtech Scientific
Eppendorf centrifuge 5810 R, 5415 R, 5417 R	Eppendorf
Eppendorf Thermomixer Comfort	Eppendorf
Eppendorf Mastercycler Gradient	Eppendorf
Flask 250 "rapid"-FILTERMAX	TPP
Flask 500 "rapid"-FILTERMAX	TPP

gentleMACS™ Octo Dissociator	Miltenyi Biotec
MAXI sorb 96 well plates for ELISA	Nunc
Micro tubes PP (1.5 ml)	Sarstedt
MP FastPrep-24 device	MP Biomedical
Nanodrop 2000c	Thermo Scientific Inc.
Odyssey CLx Infrared Scanning System	LI-COR Biosciences
Rotor-Gene RG-3000A	Corbett Research
Seahorse XF96 flux analyzer	Agilent Technologies/ Bucher Biotec
Shaker Polymax 1040	Heidolph
SmartSpec 3000	Bio-Rad
SpectraMax 340 microplate reader	Molecular Devices
Syringes 1 ml BD MicroFine[+]	BD Biosciences
Thermocyler Biometra	BIOLABO
Vortex Genie	Scientific Industries
Waterbath	GFL
ZIRCONIA beads (20 mm diameter)	Biospec

4.1.8 Software

BD FACS Diva Software Version 8.0	BD Biosciences
CytExpert Version 2.1	Beckman Coulter
FlowJo[TM] Version 10.6.1	BD Biosciences
Adobe® Illustrator CS6 Version 16.0.4	Adobe
Image Studio[TM] Version 5.2	LI-COR, Inc
LEGENDplex[TM] V8.0 Software	VigeneTech
Prism 8 Software Version 8.4.1	GraphPad Software, Inc
Microsoft® Office for Mac Version16.16.20	Microsoft
Rotor-Gene 6	Corbett Research
SoftMax Pro Software	Molecular Devices

4.1.9 Mice

C57Bl/6J (wildtype) mice and *Rag2*^{-/-} mice (Rag2-Model RAGN12) were purchased from Janvier Labs and Taconic, respectively. *Rptor*^{fl/fl} and *Rictor*^{fl/fl} mice[210] (provided by M. N. Hall, Biocentre, University of Basel), *RORc(γt)-Cre*[tg] mice[25] (B6.FVB-Tg(Rorc-cre)1Litt/J, The Jackson Laboratory), *RORγt*^{-/-} mice[23] (B6.129P2-Rorc[tm1Litt]/J mice, The Jackson Laboratory), *RORγt*[eYFP]*Rag2*^{-/-} fate map (FM) reporter mice[25,211] (generated by in-house cross-breeding of *Rag2*^{-/-} mice, *RORc(γt)-Cre*[tg] and B6.129X1-Gt(ROSA)26Sor[tm1(EYFP)Cos]/J, The Jackson Laboratory) and *Flt3*[tg] mice[212] (provided by A. Rolink, University of Basel, Switzerland) were kept under specific-pathogen-free (SPF) condition. The animal experiments received the approval of the Cantonal Veterinary Office of the city of Basel, Switzerland.

4.2 Methods

4.2.1 Generation of knockout mice

4.2.1.1. *Rptor*[ΔRORγt] mice

For conditional *in vivo* deletion of mTORC1, the transgenic mouse strain *Rptor*^{fl/fl} bearing loxP sequences encompassing exon 6 of *Rptor* (encoding for Raptor, regulatory-associated protein of mTOR)[210] was crossed with a transgenic mouse strain harboring a *RORc* promoter-driven Cre recombinase (*RORc(γt)-Cre*[tg] mouse)[25]. The Cre-positive F1 generation was backcrossed to *Rptor*^{fl/fl} mice to receive mice homozygous for the floxed *Rptor* allele and heterozygous for the *Cre* transgene. Raptor is a subunit specific for mTORC1 and is essential for localization, assembly and substrate binding of the complex.[174] Loss of Raptor leads to a disruption of mTORC1 in RORγt-expressing cells.

4.2.1.2. *Rictor*[ΔRORγt] mice

To specifically abolish the mTORC2 pathway, rapamycin-insensitive companion of mTOR (Rictor) was deleted by crossing the *RORc(γt)-Cre*[tg] mouse strain with *Rictor*^{fl/fl} mice containing loxP sites enclosing *Rictor* exon 4 and 5.[210] To generate mice homozygous for the floxed *Rictor* allele and heterozygous for the *Cre* transgene, Cre-positive mice from the F1 generation were backcrossed with *Rictor*^{fl/fl} mice. Rictor is necessary for a functional mTORC2 as it is important

for complex assembly and substrate binding.[174] Loss of Rictor is deleterious for mTORC2 function in targeted cells.

4.2.1.3. *Rictor/Rptor*$^{\Delta ROR\gamma t}$ mice

For double-knockout mice, *Rptor*$^{fl/fl}$ and *Rictor*$^{fl/fl}$ mice were cross-bred. Litters were mated to *RORc(γt)-Cre*^{tg} mice. This F1 generation was then bred with homozygous *Rictor/Rptor*$^{fl/fl}$ mice. *Rictor/Rptor*$^{\Delta ROR\gamma t}$ mice are homozygous for both the floxed *Rptor* and *Rictor* allele and heterozygous for the *Cre* transgene.

4.2.1.4. *Rptor*$^{\Delta ROR\gamma t}$*Rag2*$^{-/-}$ mice

Rptor$^{\Delta ROR\gamma t}$ mice were crossed with *Rag2*$^{-/-}$ mice. Cre-positive F1 generation mice were crossed to Cre-negative F1 generation mice. *Rptor*$^{\Delta ROR\gamma t}$*Rag2*$^{-/-}$ mice are heterozygous for the *Cre* transgene and homozygous for floxed *Rptor* and *Rag2*$^{-/-}$ alleles.

4.2.1.5. *Rictor*$^{\Delta ROR\gamma t}$*Rag2*$^{-/-}$ mice

Rag2$^{-/-}$ mice were mated with *Rictor*$^{\Delta ROR\gamma t}$ mice. Cre-positive and Cre-negative F1 generation mice were crossed to receive mice heterozygous for *Cre* transgene and homozygous for floxed *Rictor* and *Rag2*$^{-/-}$ alleles.

4.2.1.6. *Rictor/Rptor*$^{\Delta ROR\gamma t}$*Rag2*$^{-/-}$ mice

Rictor/Rptor$^{\Delta ROR\gamma t}$ mice were crossed to *Rag2*$^{-/-}$ mice. Cre-negative and Cre-positive mice from the F1 generation were mated to generate mice heterozygous for the *Cre* transgene and homozygous for floxed *Rptor* and *Rictor* alleles and the *Rag2*$^{-/-}$ allele.

4.2.2 Genotyping

For genomic DNA isolation, 500 µl of lysis buffer supplemented with 300 µg/ml Proteinase K was added to each toe biopsy. Biopsies were then incubated for at least 3 h at 56 ºC on a heating block. After digestion, 500 µl ddH$_2$O was added and the DNA was stored at 4 ºC.

4.2.2.1. BacCre PCR

BacCre fwd primer   5' CGTACTGACGGTGGGAGAAT 3'

BacCre rev primer   5' TGCATGATCTCCGGTATTGA 3'

PCR reaction mix

2.5 μl   10x reaction buffer

0.5 μl   dNTP (10 mM)

0.5 μl   *BacCre* fwd primer (10 μM)

0.5 μl   *BacCre* rev primer (10 μM)

0.1 μl   Taq Polymerase

1 μl   genomic DNA

19.9 μl   ddH$_2$O

PCR program

Initialization	94 ºC	5 min
35 amplification cycles	94 ºC	30 s
	58 ºC	45 s
	72 ºC	60 s
Final replication	72 ºC	10 min
Storage	10 ºC	hold

PCR product length

~ 400 bp

4.2.2.2. *Rptor* flox PCR

Rptor^{fl} fwd primer   5' ATGGTAGCAGGCACACTCTTCATG 3'

Rptor^{fl} rev primer   5' GCTAAACATTCAGTCCCTAATC 3'

PCR reaction mix

2.5 μl   10x reaction buffer

0.5 μl   dNTP (10 mM)

0.5 μl   *Rptor^{fl}* fwd primer (10 μM)

0.5 μl   *Rptor^{fl}* rev primer (10 μM)

0.1 μl   Taq Polymerase

1 μl   genomic DNA

19.9 μl   ddH$_2$O

PCR program

See 4.2.2.1

PCR product length

Wildtype   141 bp

Floxed   228 bp

4.2.2.3. *Rptor* excision PCR

Rptor^{fl} fwd primer   5' ATGGTAGCAGGCACACTCTTCATG 3'

Rptor^{ex} rev primer   5' CTCAGAGAACTGCAGTGCTGAAGG 3'

PCR reaction mix

2.5 μl   10x reaction buffer

0.5 μl   dNTP (10 mM)

0.5 μl   *Rptor^{fl}* fwd primer (10 μM)

0.5 μl   *Rptor^{ex}* rev primer (10 μM)

0.1 μl   Taq Polymerase

1 μl   genomic DNA

19.9 μl   ddH$_2$O

PCR program

See 4.2.2.1

PCR product length

Wildtype   ~ 800 bp

Excised   204 bp

4.2.2.4. *Rictor* flox PCR

Rictor^{fl} fwd primer   5' TTATTAACTGTGTGTGGGTTG 3'

Rictor^{fl} rev primer   5' CGTCTTAGTGTTGCTGTCTAG 3'

PCR reaction mix

2.5 μl   10x reaction buffer

0.5 μl   dNTP (10 mM)

0.5 μl   *Rictor^{fl}* fwd primer (10 μM)

0.5 μl   *Rictor^{fl}* rev primer (10 μM)

0.1 μl   Taq Polymerase

1 μl   genomic DNA

19.9 μl   ddH$_2$O

PCR program

See 4.2.2.1

PCR product length

Wildtype	197 bp
Floxed	295 bp

4.2.2.5. *Rictor* excision PCR

Rictor^{fl} fwd primer   5' TTATTAACTGTGTGTGGGTTG 3'

Rictor^{ex} rev primer   5' CAGATTCAAGCATGTCCTAAGC 3'

PCR reaction mix

2.5 µl	10x reaction buffer
0.5 µl	dNTP (10 mM)
0.5 µl	*Rictor^{fl}* fwd primer (10 µM)
0.5 µl	*Rictor^{ex}* rev primer (10 µM)
0.1 µl	Taq Polymerase
1 µl	genomic DNA
19.9 µl	ddH$_2$O

PCR program

See 4.2.2.1

PCR product length

Wildtype	no band
Excised	280 bp

4.2.2.6. *Rag2* wt PCR

Rag2wt fwd primer 5' CTGACTGCCTACCCCATGTT 3'

Rag2wt rev primer   5' CCATGTTGCTTCCAAACCAT 3'

PCR reaction mix

2.5 µl	10x reaction buffer
0.5 µl	dNTP (10 mM)
1 µl	*Rag2wt* fwd primer (10 µM)
1 µl	R*ag2wt* rev primer (10 µM)
0.1 µl	Taq Polymerase

1 μl   genomic DNA

18.9 μl   ddH$_2$O

PCR program

Initialization	94 ºC	5 min
35 amplification cycles	94 ºC	30 s
	60 ºC	30 s
	72 ºC	30 s
Final replication	72 ºC	2 min
Storage	10 ºC	hold

PCR product length

441 bp

4.2.2.7. *Rag2*$^{-/-}$ **PCR**

Rag2$^{-/-}$ fwd primer   5' GCAACATGTTATCCAGTAGCCGGT 3'

Rag2$^{-/-}$ rev primer   5' GCTTCCTCTTGCAAAACCACACTG 3'

PCR reaction mix

2.5 μl   10x reaction buffer

0.5 μl   dNTP (10 mM)

0.5 μl   *Rag2*$^{-/-}$ fwd (10 μM)

0.5 μl   *Rag2*$^{-/-}$ rev primer (10 μM)

0.1 μl   Taq Polymerase

1 μl   genomic DNA

19.9 μl   ddH$_2$O

PCR program

Initialization	94 ºC	5 min
33 amplification cycles	94 ºC	20 s
	64 ºC	30 s
	72 ºC	45 s
Final replication	72 ºC	10 min
Storage	10 ºC	hold

PCR product length

425 bp

4.2.3 Cell isolation from small intestine, colon, spleen, lymph nodes, thymus and bone marrow

Small intestinal lamina propria (SI LP) cells were isolated from the small intestine (SI) of adult mice. In short, mesenteric tissue was removed from the dissected SI. The SI was opened longitudinally, cut into pieces and incubated in 30 mM Ethylenediaminetetraacetic acid (EDTA) in calcium- and magnesium-free phosphate-buffered saline (PBS) for 30 min on ice. The tissue pieces were washed repeatedly in cold PBS until the PBS remained clear. The tissue was placed in cell culture plates, cut into smaller pieces and digested four times for 15 min at 37 ºC in 3 ml Dulbecco's Modified Eagle medium (DMEM, Gibco) containing 0.025 mg/ml DNase I (Roche) and 1 mg/ml Collagenase D (Roche). Before and after each digestion step, the tissue was homogenized by pipetting up and down. After addition of 3 ml DMEM, supernatant of each digestion step was pooled through a 100 μM cell strainer into a tube containing DMEM supplemented with 5 % fetal bovine serum (FBS) and 2 mM EDTA. After the final digestion step, remaining tissue was transferred onto the cell strainer and mashed through. Cell suspension was pelleted, resuspended in 40 % of isotonic Percoll (GE Healthcare), underlaid with 80 % isotonic Percoll and centrifuged (30 min, 4 ºC, 1.800 rpm, acceleration speed 4, deceleration speed 1). After gradient centrifugation, the cell interphase was collected, washed and used for direct staining or for sorting.

For colonic lamina propria (cLP) cell isolation, the colon was opened longitudinally, washed in PBS, cut into pieces and incubated on a shaker in 5 μM EDTA and 10 mM HEPES in PBS for 20 min at 37 ºC. This wash step with 5 μM EDTA and 10 mM HEPES in PBS was repeated another three times. The tissue was transferred into a gentleMACS™ C Tube (Miltenyi Biotec) filled with 10 ml DMEM supplemented with 0.025 mg/ml DNase I, 1 mg/ml Collagenase D and 0.25 mg/ml Collagenase VIII (Roche). The tube was incubated 30 min at 37 ºC on a shaker. The colon pieces were dissociated using gentleMACS™ Octo Dissociator (Miltenyi pre-defined program: m_intestine_01, Miltenyi Biotec). Incubation and shredding procedure were repeated once more. Finally, the tissue solution was transferred onto a 100 μM cell strainer and subjected to gradient centrifugation as described for the SI LP cells.

Spleen and LNs were washed in PBS, diced and digested three times as described for SI. Cell pellets from spleens were resuspended in erythrocyte lysis buffer for 2 min at room temperature and washed in 3 % FBS in PBS.

Mesenteric tissue was removed from the thymus. The organ was smashed through a grid in 3 % FBS in PBS and filtered.

To obtain BM cells, femur and tibia from one hind leg were removed. Bones were cleaned and grounded in a mortar in 3 % FBS in PBS. Erythrocytes were lysed as described for spleen.

4.2.4 Fluorescence-activated cell sorting (FACS) and flow cytometry

Fluorochrome-conjugated or biotinylated Abs were diluted in a staining solution consisting of a 1:1 mixture of 3 % FBS in PBS and anti-mouse FcγRII/III monoclonal Ab (clone 2.4G2, purified cell supernatant). Cells were stained for 30 min at 4 ºC and washed with PBS. Where applicable, surface staining was followed by an incubation with fluorochrome-conjugated streptavidin (20 min, 4 ºC). For exclusion of dead cells, cells were washed in PBS and stained with LIVE/DEAD® Fixable Aqua Dead Cell Stain kit (Molecular Probes) according to manufacturer's protocol.

For cytokine staining, cells were incubated with 10 μg/ml Brefeldin A in complete IMDM medium supplemented with 5 % FBS at 37 ºC for 2 h prior to surface staining. After staining with LIVE/DEAD® Fixable Aqua Dead Cell Stain kit, cells were fixed in 4 % paraformaldehyde in PBS for 10 min at room temperature. Cells were washed twice in permeabilization solution (0.5 % Saponin, 0.01 % sodium azide and 3 % FBS in PBS) and stained with antibodies against cytokines diluted in permeabilization solution at 4 ºC for 1 h.

Transcription factor staining was performed using Foxp3 Transcription Factor Staining Buffer Set (eBioscience) according to manufacturer's protocol.

For phosphoFlow analysis, sort-purified cells were cultured with IL-23/IL-1β for 17 h. After 17 h, cells were washed in PBS and stained with LIVE/DEAD® Fixable Aqua Dead Cell Stain kit supplemented with 20 mg/ml IL-23/IL-1β. Cells were washed with 3 % FBS in PBS and immediately fixed with 2 % PFA in PBS for 10 min at 37 ºC. Cells were washed twice and resuspended in BD Perm Buffer III (pre-chilled to -20 ºC). Cells were permeabilized 30 min on ice, washed twice and stained with Abs for 30 min on ice. After two final wash steps, cells were analyzed immediately.

Cells were acquired with FACS Fortessa (BD Biosciences) using BD High Throughput sampler (HTS) and analyzed with FlowJo 10 software (Tree Star).

Cell sorting was performed using FACS Aria (BD Biosciences). Purity of isolated cells was $\geq 98 \%$.

4.2.5 *In vitro* stimulation and cell culture

Sorted Lin⁻CD90.2⁺KLRG1⁻ ILC3s, SI LP or cLP cells were cultured in complete IMDM medium supplemented with 5 % FBS at 37 ºC under 95 % humidity and with 5 % CO_2. Where indicated, cells were stimulated with 20 ng/ml IL-23 and 20 ng/ml IL-1β. mTORC1 inhibitor rapamycin was added to a final concentration of 10 nM or 100 nM. PP242 was diluted to a final concentration of 10 nM, 100 nM or 1 μM. Glycolysis inhibitor 2-Deoxy-D-glucose, fatty acid oxidation inhibitor etomoxir, mitochondrial complex I inhibitor oligomycin and mitochondrial ATP-synthase inhibitor rotenone were used at 10 mM, 10 μM, 0.1 μM and 1 μM, respectively.

4.2.6 In-Cell Western analysis of phosphorylated proteins

SI Lin⁻CD90.2⁺KLRG1⁻ ILC3s of *Flt3^{tg}* mice were cultured for 48 h in black flat-bottom 96 well carrier plates with transparent bottom with or without 20 ng/ml IL-23/IL-1β, rapamycin (10 nM) or PP242 (1 μM). For fixation and cell cross-linkage, 10 % paraformaldehyde in PBS was added directly into the wells (final paraformaldehyde concentration 3.75 %) and incubated for 30 min at room temperature. Cells were washed twice with 1x PBS/1 % BSA and permeabilized for 30 min with 1x PBS/1 % BSA/0.1 % Triton X100. Following one wash with 1x PBS/1 % BSA/0.1 % Triton X100, cells were blocked with 1x PBS/1 % BSA/1 % goat serum for 1 h and incubated overnight with primary mouse α-tubulin (Sigma Aldrich) and rabbit α-pS6 (Ser235/236) or α-pAkt (Ser473) (Cell Signaling Technology) antibodies diluted in 1x PBS/1 % BSA/1 % goat serum. Cells were washed three times with 1x PBS/1 % BSA/ 0.1 % Triton X100 and incubated for 1 h with secondary goat α-mouse IgG IRDye680 (LI-COR Biosciences) and goat α-rabbit IgG IRDye800 (LI-COR Biosciences) antibodies diluted in 1x PBS/1 % BSA/0.1 % Triton X100. Finally, cells were washed five times with 1x PBS/1 % BSA/ 0.1 % Triton X100. All supernatant was removed before scanning the cells with the Odyssey CLx Infrared Scanning System (LI-COR Bioscience).

4.2.7 Metabolic analysis with Agilent Seahorse platform

Lin⁻CD90.2⁺KLRG1⁻ ILC3s from the SI of *Flt3^{tg}* mice were cultured for 48 h with or without stimulus and inhibitors as indicated. One day prior to Seahorse analysis, 200 μl/well of Seahorse XF Calibrant Solution was added into Seahorse XFe96 sensor cartridges (Seahorse XFe96 FluxPak, Agilent Technologies) and the plate was incubated overnight at 37 ºC in a CO_2-free incubator. 1.5 ml of 0.1 M sodium bicarbonate (pH 8.0) was mixed with 100 μl Cell Tak (BD Biosciences). 12.5 μl/well Cell Tak were distributed onto a XF96 cell culture microplate. The plate was stored at 4 ºC overnight.

On the day of analysis, Cell Tak was removed, the XF96 cell culture microplate was washed once with ddH$_2$O and dried for at least one hour. Cultured cells were resuspended and transferred into tubes. 3 ml of unbuffered RPMI was added to each sample. After centrifugation (1.400 rpm, 10 min), the supernatant was discarded and cells were resuspended with 170 μl unbuffered RPMI. An aliquot of cells was mixed with trypan blue and counted in a Neubauer counting chamber. All samples were diluted to a final concentration of 2×10^6 cells/ml and 50 μl/well (= 100.000 cell) was plated into the dried XF96 cell culture microplate. Cells were centrifuged at 450 rpm (acceleration speed 4, deceleration speed 3) for 1 s. Afterwards, the plate was rotated by 180 º and spun at 650 rpm (acceleration speed 4, deceleration speed 3) for 1 s). Each well was filled up with unbuffered RPMI to a final volume of 175 μl/well. Cells were stored at 37 ºC in a CO_2-free incubator. 25 μl of 8 μM oligomycin, 18 μM FCCP and 10 μM rotenone was added to Port A, B and C of the Seahorse XFe96 sensor cartridges, respectively. The Seahorse XF96 flux analyzer was programed (see program below) and calibrated with the Seahorse XFe96 sensor cartridge. The XF96 cell culture microplate was loaded and analyzed.

Seahorse program

Baseline Measurement	4 cycles: 3 min mix, 6 min measure
Injection Port A	3 cycles: 3 min mix, 6 min measure
Injection Port B	3 cycles: 3 min mix, 6 min measure
Injection Port C	3 cycles: 3 min mix, 6 min measure

4.2.8 RNA isolation, cDNA synthesis and quantitative real-time polymerase chain reaction (RT qPCR) from cultured cells

For RNA extraction from cultured cells, RNeasy Micro Kit (Qiagen) was used according to manufacturer's protocol. In short, cultured cells were transferred into 1.5 ml reaction tubes, centrifuged at 3.500 rpm for 5 min at 7 ºC and resuspended in 350 µl RLT buffer. Cells were frozen at -20 ºC for several hours or at -80 ºC for 10 min. Lysates were mixed with 350 µl 70 % ethanol and transferred to a RNeasy MinElute spin column. Columns were centrifuged at 10.000 rpm for 15 s, washed with 350 µl Buffer RW1 and centrifuged again. 10 µl DNase I stock solution and 70 µl Buffer RDD were mixed per sample and added directly on top of the column membrane. After 15 min incubation at room temperature, 350 µl Buffer RW1 was added to each column and samples were centrifuged. Columns were transferred to a new collection tube and washed with 500 µl Buffer RPE. After centrifugation (10.000 rpm, 15 s), 500 µl of 80 % ethanol was added to each column and spun at 10.000 rpm for 2 min. Columns were dried by spinning at full speed for 5 min. RNA was eluted from the column by adding 14 µl RNase-free water directly on the membrane and centrifuging the RNA into collection tubes (full speed, 1 min). RNA was stored at -80 C.

cDNA synthesis was performed using dNTPs (Roche), random hexamers (Sigma-Aldrich), oligo(dT)$_{20}$ (Promega), RNaseOUT (Invitrogen) and Superscript III Reverse Transcriptase (Invitrogen) according to manufacturer's protocol.

Quantitative transcript analysis was performed by RT qPCR on a Rotor-Gene RG-3000A (Corbett Research) using SensiMix SYBR Hi-Rox Kit (Bioline) (threshold 0.1). Ct results of genes of interest were normalized to TBP housekeeping gene using the comparative threshold cycle method (ΔC_T) for relative quantification.

RT qPCR program

Initialization	95 ºC	1 min
40 amplification cycles	95 ºC	10 s
	60 ºC	15 s
	72 ºC	20 s

4.2.9 Bone marrow chimeras

For generation of BM chimeras, *Rag2*$^{-/-}$ mice heterozygous for the congenic marker CD45.1 (Ly5.1) and CD45.2 (Ly5.2) (*Rag2*$^{-/-}$*Ly5.1/Ly5.2* mice) were lethally irradiated with two doses of 450 rad from a γ-source (Cs 137 source) with a resting period of four hours between the two irradiations.

One day after irradiation, *Rag2*$^{-/-}$*Ly5.1* donor mice and knockout or control mice of interest (*Ly5.2*) were sacrificed and both hind legs were removed. Bones were cleaned and grounded in a mortar containing DMEM. The cell suspension was filtered through a 70 μm cell strainer, centrifuged (1.400 rpm, 10 min) and erythrocytes were lysed as described before. Cells were washed twice in PBS, filtered through a 40 μm filter and counted. The donor cells from *Rag2*$^{-/-}$*Ly5.1* mice and knockout or control mice were mixed in a 1:1 ratio. 1.5 x 10^7 cells/200 μl were injected into the tail vein of irradiated recipient mice.

During the first 10 days post-irradiation, recipient mice received Baytril (570 mg/l drinking water = 85 mg/kg bodyweight). Mice were sacrificed and analyzed 5 weeks after experiment initiation.

4.2.10 IL-2/α-IL-2 complex treatment

To prepare the IL-2/α-IL-2 complex, 2.5 μg recombinant murine IL-2 (0.67 mg/ml) and 7.5 μg anti-IL-2 mAb JES6-1A12 (3 mg.ml, BioXCell) per mouse were mixed and incubated at 37 ºC for 30 min. The IL-2/α-IL-2 complex was adjusted to 200 μl with sterile PBS and intraperitoneally (i.p.) injected into mice. Mice were analyzed one day post-injection.

4.2.11 Rapamycin treatment

Rapamycin (LC Laboratories) was diluted to 200 mg/ml in dimethyl sulfoxide (DMSO). For *in vivo* use, the rapamycin stock was prediluted to 10 mg/ml in 100 % ethanol and then further diluted to 250 μg/ml in sterile PBS. Mice were weighted and i.p. injected with mock solution (PBS with 0.125 % DMSO and 2.5 % ethanol) or 2.5 mg/kg rapamycin (= 10 μl/g of 10 mg/ml preparation) every other day for three weeks.

4.2.12 α-CD40 colitis model

α-CD40 Ab (Clone FGK45.5) was diluted to 1 mg/ml in sterile PBS. Mice were weighted and i.p. injected with 140 μg α-CD40 Ab. Weight and health condition of mice was monitored daily (Table 1).

Score	Weight
0	no weight loss (≥ 100% of initial weight)
1	95-99.9% of initial weight
2	90-94.9% of initial weight
3	85-89.9% of initial weight
4	80-84.9% of initial weight
6	< 80% of initial weight
Score	Diarrhea
0	Normal stool
1	"loose stool"
2	extreme diarrhea 24 hours
6	extreme diarrhea for > 2 days
Score	Feces
0	no blood in feces
3	few blood in feces or perianal traces of blood
6	blood in feces
Score	Prolapse
0	no rectal prolapse
2	Partial rectal prolapse
6	Rectal prolapse
Score	Behavior
0	Normal behavior
2	Changed behavior (reduced activity)
4	Changed behavior > 2 days
6	pain (nose bulge, orbital tightening, hunchback)
Abort Criterion: total of all single scores ≥ 6	

Table 1 Monitoring abortion criteria

4.2.13 Infection with *Citrobacter rodentium*

Two days before infection, a stock of nalidixic acid-resistant *Citrobacter rodentium* strain ICC169 (containing a bioluminescence construct kindly provided by Dr. Jan Niess) was plated on LB agar plates with 300 μg/ml erythromycin (Sigma Aldrich) and incubated overnight at 37 ºC. One colony was picked and grown in LB medium with 300 μg/ml erythromycin overnight at 37 ºC. At the day of infection, the bacterial culture was diluted back to OD_{600} 0.1 and grown to exponential phase (between OD_{600} 1.0 and 1.7). 2 x 10^9 CFU/mouse were collected and washed twice with sterile PBS. Mice were infected by oral gavage with

2×10^9 CFU/200 µl/PBS. After infection, health condition and weight of mice was monitored daily (Table 1).

4.2.14 Hematoxylin and eosin staining and histological colitis scoring

Whole cecum or colon pieces were cleaned with PBS using a syringe with gavage needle, placed on a filter paper into a histology cassette and fixed in 4 % paraformaldehyde (histology grade, Roth) for 48 h to 72 h. Organs were washed and stored in PBS. Standard dehydration series with ethanol, paraffine-embedding and hematoxylin/eosin staining was performed in the laboratory of Dr. Salvatore Piscuoglio (Institute for Pathology, University Hospital Basel). Histology colitis scores were determined by experienced gastroenterologists (Luigi Terracciano and Caner Ercan, Institute for Pathology, University Hospital Basel) in a blinded fashion according to the criteria in Table 2 (adapted from Bouladoux et al.[152]).

	Epithelium		
Score	**Hyperplasia**		**Goblet cell depletion**
0	None		None
1	Mild (1.5 x of normal length)	and/or	Mild (25 %)
2	Moderate (2-3 x of normal length)		Moderate (25-50 %)
3	Severe (> 3 x of normal length)		Severe (50 %)
	***Lamina propria* infiltration**		
Score	**Finding**		
0	None		
1	Mild (some leukocytes at villi tips or many lymphoid follicles)		
2	Moderate (marked leukocyte infiltrate, crypt broadening)		
3	Severe (dense leukocyte infiltrate)		
	Area affected (% of section)		
Score	**Finding**		
0	None		
1	0-25 %		
2	25-50		
3	> 50 %		
	Severe markers		

Score	**Submucosal inflammation**		**Crypt abscesses**		**Crypt branching**	**Ulceration or fibrosis**
0	None		0		No	No
1	Mild	or	< 5		No	No
2	Mild	and	< 5		No	No
2	Severe	or	> 5	or	Yes	No
3	Severe	and	> 5	or	Yes	No
3	-		-		-	Yes
	Histological colitis score: total of all single scores max. 12					

Table 2 Histological Colitis Scores. Adapted from Bouladoux et al.[152]

4.2.15 Cytokine analysis of cell culture supernatants – LEGENDplex^{TM} Mouse Th Cytokine Panel

Cell culture supernatants were collected at the time points indicated and stored at -80 ºC until analyzed.

To determine cytokines in cell culture supernatants, LEGENDplex Multi-Analyte Flow Assay Kit Mouse Th Cytokine Panel (13-plex) (Biolegend) was used according to manufacturer's protocol. In short, samples or cytokine standards were mixed with assay buffer, capture antibodies and detection antibodies and incubated on a plate rocker for 2 h at room temperature in the dark. Streptavidin-PE was added and the plate was incubated 30 min at room temperature in the dark. Beads were centrifuged, washed once with wash buffer and resuspended in wash buffer. Samples were acquired with Cytoflex S and CytExpert Software and analyzed with LEGENDplex V8.0 Software (VigeneTech).

4.2.16 Lipocalin-2 enzyme-linked immunosorbent assay

Feces were collected into weighted 1.5 ml reaction tubes. Tubes were weighted again and sterile PBS was added to each tube to reach a final ratio of 0.1 g of feces per 1 ml. Fecal samples were incubated for 15 min at room temperature, disrupted with pipette tips and vortexed. After centrifugation (13.000 g, 3 min), supernatants were transferred into new tubes and stored at -20 ºC.

To determine fecal Lipocalin-2 concentrations, mouse Lipocalin-2/NGAL DuoSet ELISA Kit (R&D) was used according to manufacturer's protocol. In brief, 96 well Microwell MaxiSorp plates were coated with capture antibodies in PBS at 4 ºC overnight. Plates were then blocked 1 h with 1 % BSA in PBS. Fecal samples and standards were diluted with 1 % BSA in PBS, plated on capture Ab-coated plates and incubated for 2 h at room temperature. Plates were washed three times with ELISA wash buffer and detection Ab was added to each well. After 1.5 hours incubation, plates were washed again and incubated with Streptavidin-HRP for 20 min at room temperature. Plates were washed three times. TMB substrate (Biolegend) was added for ~ 15 min and the enzymatic reaction was stopped with 2 N sulfuric acid (H_2SO_4).

Optical density at 450 nm was measured using SpectraMax 340 microplate reader (Molecular Devices). Wavelength correction was performed by subtraction of optical density measurements at 570 nm.

4.2.17 Bacterial counts from feces and spleen

Feces were collected into 1.5 ml reaction tubes and weighted. Sterile PBS was added to each tube to reach a final ratio of 0.1 g of feces per 1 ml. Fecal samples were incubated for 15 min at room temperature, homogenized with pipette tips and vortexed.

Spleens were placed into pre-weighted tubes containing 7-8 ZIRCONIA beads (20 mm diameter, Biospec). The weight of each spleen was determined and samples were homogenized using a MP FastPrep-24 device (6.5 m/s, 60 s, 1 run; MP Biomedical).

Feces and spleen homogenates were centrifuged for 1 min a 400 x g. Serial 1:100 dilutions (up to 10^6) and 1:10 dilutions (up to 10^3) were performed for feces and spleen, respectively. Undiluted and diluted samples were plated on LB agar plates with 300 μg/ml erythromycin and incubated overnight at 37 ºC. Colony numbers were determined and the bacterial load was calculated as CFU/g feces or spleen:

$$\frac{CFU}{g \ (feces \ or \ spleen)} = \frac{CC \ x \ VT}{Vp \ x \ DF \ x \ W}$$

CC = colony count, VT = total volume of sample, Vp = volume plated, DF = dilution factor, W = weight of sample.

4.2.18 Statistical analysis

Depending on sample size normality of values was tested with D'Agostino & Pearson test (n > 7) or Shapiro-Wilk test (n $\leq$ 7). Mann Whitney U test, two-tailed unpaired t test or One-Way ANOVA with multiple comparison (Dunnett) were used for statistical analysis. All tests were performed with Prism 8 Software (GraphPad Software, Inc). Unless specified otherwise, data is shown as mean values $\pm$ SD.

5 Results

5.1 Characterization of wildtype and lymphopenic mice with *RORc*-driven deletion of *Rptor* and/or *Rictor*

To address the question whether mTORC1 and mTORC2 signaling are important for the development and cytokine production of ILC3s *in vivo*, conditional knockout mice were generated by cross-breeding of previously published mouse strains.

In brief, six mouse strains with disrupted mTORC1 and/or mTORC2 signaling in ILC3s both on an immune-competent C57Bl/6J background (*Rptor*$^{\Delta ROR\gamma t}$, *Rictor*$^{\Delta ROR\gamma t}$ and *Rictor/Rptor*$^{\Delta ROR\gamma t}$) and a T and B cell-deficient C57Bl/6J *Rag2*$^{-/-}$ background (*Rptor*$^{\Delta ROR\gamma t}$*Rag2*$^{-/-}$, *Rictor*$^{\Delta ROR\gamma t}$*Rag2*$^{-/-}$ and *Rictor/Rptor*$^{\Delta ROR\gamma t}$*Rag2*$^{-/-}$) (Fig.6) were generated. Therefore, a transgenic mouse strain bearing loxP sequences encompassing exon 6 of *Rptor* (encoding for Raptor, essential subunit for mTORC1)[210] or a transgenic mouse containing loxP sites enclosing *Rictor* (encoding for Rictor, essential subunit for mTORC2) exon 4 and 5[210] was crossed to a transgenic mouse strain harboring a *RORc* promoter-driven Cre recombinase (*RORc(γt)-Cre*^{tg} mouse)[25] on C57Bl/6J or C57Bl/6J *Rag2*$^{-/-}$ background.

Under SPF conditions, all six knockout mice were healthy.

RORc(γt)Cre^{tg} x *Rptor*$^{fl/fl}$ *RORc(γt)Cre*^{tg} x *Rictor*$^{fl/fl}$ *RORc(γt)Cre*^{tg} x *Rictor*$^{fl/fl}$ x *Rptor*$^{fl/fl}$

Rptor$^{\Delta ROR\gamma t}$ **Rictor$^{\Delta ROR\gamma t}$**   **Rictor/Rptor$^{\Delta ROR\gamma t}$**

Rptor$^{\Delta ROR\gamma t}$ x *Rag2*$^{-/-}$ *Rictor*$^{\Delta ROR\gamma t}$ x *Rag2*$^{-/-}$ *Rictor/Rptor*$^{\Delta ROR\gamma t}$ x *Rag2*$^{-/-}$

Rptor$^{\Delta ROR\gamma t}$Rag2$^{-/-}$ **Rictor$^{\Delta ROR\gamma t}$Rag2$^{-/-}$**   **Rictor/Rptor$^{\Delta ROR\gamma t}$Rag2$^{-/-}$**
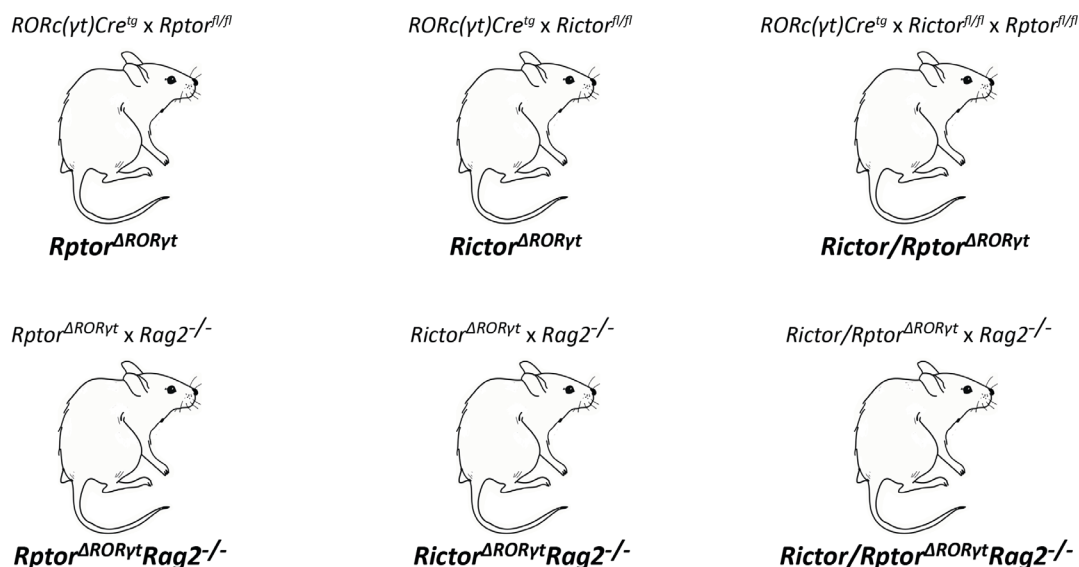
Fig.6 Conditional knockout mouse strains generated by crossbreeding.

5.1.1 Deletion of *Rptor* and *Rictor* efficiently ablates mTORC1 and mTORC2 signaling in ILC3s

To determine whether *Rptor* and *Rictor* deletion was efficient in ILC3s, sort-purified ILC3s from *Rptor*$^{\Delta ROR\gamma t}$*Rag2*$^{-/-}$, *Rictor*$^{\Delta ROR\gamma t}$*Rag2*$^{-/-}$ and Cre-negative control littermates were stimulated for 16 h with IL-23 and IL-1β. IL-23 is a known activator of ILC3s[109,213,214] and IL-1β has been shown to have synergistic effects on IL-23-mediated ILC3 activation[111,116]. Efficiency of *Rptor* and *Rictor* deletion was measured by analyzing phosphorylation of mTOR (S2448), mTORC1-specific target sites in S6 protein (Ser235/236) and mTORC2-specific target site in Akt (Ser473).

Activation of ILC3s induced phosphorylation of mTOR, S6 and Akt (Fig.7) demonstrating that mTORC1 and mTORC2 were induced after IL-23/IL-1β stimulation. mTOR phosphorylation was reduced but not completely abrogated in *Rptor*- and *Rictor*-deficient ILC3s (Fig.7). This was consistent with the expectation that ILC3s with single deletion of *Rptor* or *Rictor* still contain one mTORC. All *Rptor* - and *Rictor*-deficient ILC3s failed to upregulate phosphorylation of pS6 and Akt, respectively (Fig.7). These results demonstrate that the respective target gene was efficiently deleted from all ILC3s in knockout mice. Interestingly, pAkt was also reduced in activated *Rptor* -deficient ILC3s. pS6 was lower in *Rictor*-deficient ILC3s. This finding indicates that mTORC1 and mTORC2 signaling mutually support each other. Similarly, mTORC2 was shown to promote mTORC1 in NK cells.[215] In contrast, mTORC1 was mostly reported to negatively regulate mTORC2.[184,188,215] Therefore, the finding that mTORC1 might positively regulate mTORC2 in ILC3s was unexpected.
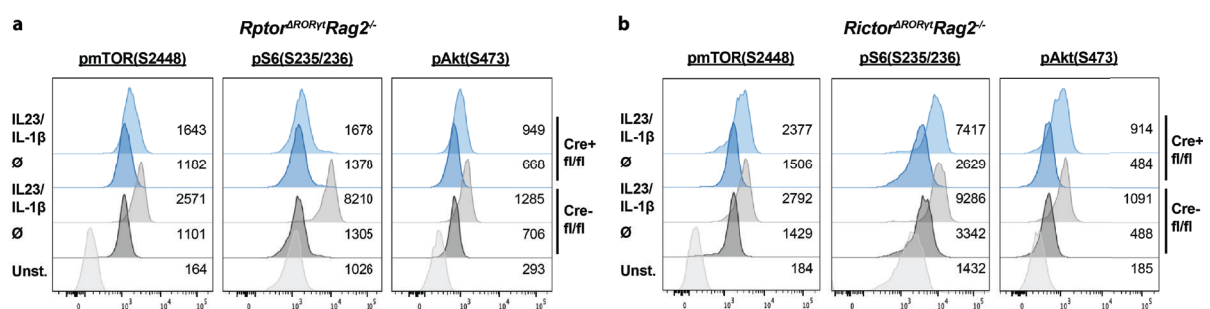
Fig.7 IL-23/IL-1β induce mTORC1- and mTORC2-dependent phosphorylation of S6 and Akt. Sort-purified Lin$^-$CD90.2$^+$KLRG1$^-$ ILC3s isolated from the SI LP of *Rptor*$^{\Delta ROR\gamma t}$*Rag2*$^{-/-}$ (a), *Rictor*$^{\Delta ROR\gamma t}$*Rag2*$^{-/-}$ (b) or control mice were cultured 17 h with or without IL-23/IL-1β. phosphoFlow was used to determine phosphorylation of mTOR, mTORC1 target sites on S6 and mTORC2 target site on Akt. Lin: CD3, CD8, CD11c, CD19, B220, Gr-1, NK1.1, TCRβ, TCRγδ, Ter-119. Unst.: unstained. Exemplary histograms from 4-5 independent experiments are shown. (Data provided by Frank Michael Lehmann, UKBB and DBM Basel.)

5.1.2 Lymphoid tissue development in knockout mice

RORγt-expressing LTi cells are known to be important for PP and LN development.[216,217] Hence, numbers of LNs (inguinal, popliteal, superficial cervical, axillary, peri-aortic, mesenteric and pancreatic LNs) and PPs in *Rptor^{ΔRORγt}*, *Rictor^{ΔRORγt}*, *Rictor/Rptor^{ΔRORγt}*, *Rptor^{ΔRORγt}Rag2$^{-/-}$*, *Rictor^{ΔRORγt}Rag2$^{-/-}$* and *Rictor/Rptor^{ΔRORγt}Rag2$^{-/-}$* mice were compared to Cre-negative control littermates.

Knockout mice on a wildtype background developed normal numbers of LNs (data not shown). In wildtype mice with single deletion of *Rptor* or *Rictor*, PP numbers were unchanged (Fig.8a, b). Double-knockout mice showed a non-significant tendency towards reduced PP numbers (Fig.8c).

Knockout mice on a *Rag2*-deficient background developed normal LNs compared to Cre-negative littermates (data not shown). As expected, PPs were not macroscopically detectable in *Rag2*-deficient knockout and *Rag2*-deficient control mice (data not shown). The absence of macroscopic PPs is a result of the lack of B and T cells.

Collectively, these data show that the induction of LNs and PPs was not impaired by the single deletion of *Rptor* and *Rictor* in RORγt$^+$ ILCs. Dual knockout of *Rptor* and *Rictor*, however, led to a mild reduction in PPs. Thus, it could not be fully excluded that loss of *Rptor* and *Rictor* in RORγt$^+$ LTi cells affected the formation of secondary lymphoid structures in the intestine.
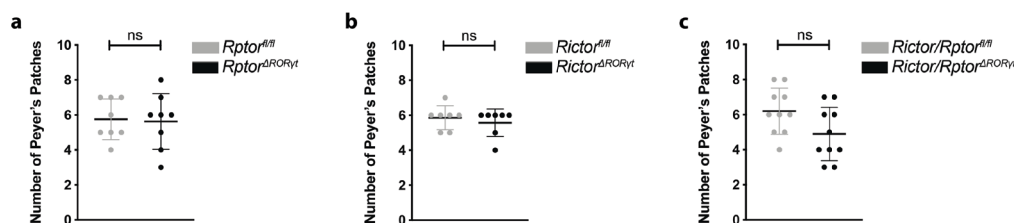
Fig.8 Peyer's patches in *Rptor^{ΔRORγt}*, *Rictor^{ΔRORγt}* and *Rictor/Rptor^{ΔRORγt}* mice. PPs were counted in a) *Rptor^{ΔRORγt}*, b) *Rictor^{ΔRORγt}* or c) *Rictor/Rptor^{ΔRORγt}* mice and age-matched Cre-negative littermates. Mice were 8-10 weeks old at analysis. n = 7-10. Two-tailed unpaired t test. *p ≤ 0.05, **p ≤ 0.01, ***p ≤ 0.001

5.1.3 Immune cell numbers in knockout mice

To determine if *RORc*-driven deletion of the respective target gene affected other cell subsets, the total cellularity of the thymus, mesenteric LNs (mLN), spleen, SI and colon was tested. In addition, the number of several immune cells including DCs, MΦ, granulocytes and B cells

was examined. Since RORγt is expressed in thymic T cell precursors, I further analyzed the T cell compartment. A detailed gating scheme of the described innate and adaptive immune cell subsets is shown in Fig.S1. Table 3 gives an overview of the surface markers applied to dissect immune cell subsets.

Cell Type	Subset	Markers
B cell (Spleen)	Germinal center B cell	CD3$^-$CD19$^+$B220$^+$GL-7$^+$
	Marginal zone B cell	CD3$^-$CD19$^+$B220$^+$CD21^{high}CD23$^{-/low}$IgD$^{-/low}$IgM$^+$
	Follicular B cell	CD3$^-$CD19$^+$B220$^+$CD21$^+$CD23$^+$IgD$^+$IgM$^+$
B cell (Intestine)	SI B cell	CD3$^-$CD19$^+$B220$^+$CD21$^+$CD23$^+$IgD$^+$IgM$^+$
	Colonic B cell	CD3$^-$CD19$^+$B220$^+$CD21^{low}CD23^{low}IgD$^+$IgM$^+$
Dendritic cell	Plasmacytoid DC	CD11c$^+$B220$^+$MHC-II$^{low/-}$Siglec-H$^+$
	Conventional DC1	CD11c$^+$B220$^-$MHC-II$^+$XCR1$^+$
	Conventional DC2	CD11c$^+$B220$^-$MHC-II$^+$Sirpα^+
Myeloid cell	Monocyte	CD11b$^+$F4/80$^+$Ly-6G$^-$Ly-6C$^+$
	MΦ	CD11b$^+$F4/80$^+$Ly-6G$^-$Ly-6C$^-$
	Granulocyte	CD11b$^+$Ly-6G$^+$Ly-6C$^+$
T cell	Treg	TCRβ$^+$CD4$^+$CD25$^+$FoxP3$^+$
	naïve CD4$^+$	TCRβ$^+$CD4$^+$CD62L$^+$CD44$^-$
	memory CD4$^+$	TCRβ$^+$CD4$^+$CD62L$^{low/-}$CD44$^+$
	naïve CD8$^+$	TCRβ$^+$CD8$^+$CD62L$^+$CD44$^-$
	central memory CD8$^+$	TCRβ$^+$CD8$^+$CD62L$^+$CD44$^+$
	effector memory CD8$^+$	TCRβ$^+$CD8$^+$CD62L$^-$CD44$^+$
	TCRγδ	TCRγδ$^+$

Table 3 Discrimination of innate and adaptive immune cell subsets by flow cytometry.

First, I compared the cellularity and the immune cell composition of knockout mice on a wildtype background to control littermates. In *Rptor^{ΔRORγt}*, *Rictor^{ΔRORγt}* and *Rictor/Rptor^{ΔRORγt}* mice cellularity of thymus, LN, spleen, SI and colon was normal (Fig.9a, c, e). There was no difference in splenic germinal center B cells (GC B cell), marginal zone B cells (MZB cells) or follicular B cells and SI B cells of knockout mice (Fig.9b, d, f). *RORc*-driven deletion of *Rptor* resulted in a minor reduction of B cells in the colon (Fig.9b, right panel). Mice with *Rictor* and dual *Rictor*/*Rptor* deletion displayed a significant 2-fold and 3-fold reduction of colonic B cells (Fig.9d, f, right panel). Numbers of plasmacytoid DCs (pDC), conventional DC1s (cDC1), conventional DC2 (cDC2), neutrophil granulocytes, monocytes and MΦ were normal in all knockout mice (Fig.9g-l).

Those results suggest that *RORc*-driven deletion of *Rptor* and *Rictor* had no indirect impact on innate immune cell numbers. However, B cell numbers were specifically reduced in the colon of mice with conditional knockout of *Rictor* or both *Rptor* and *Rictor*. This finding raises the

possibility that disruption of mTORC2 and dual mTORC signaling in ILC3s or T cells indirectly affected maintenance or recruitment of colonic B cells.
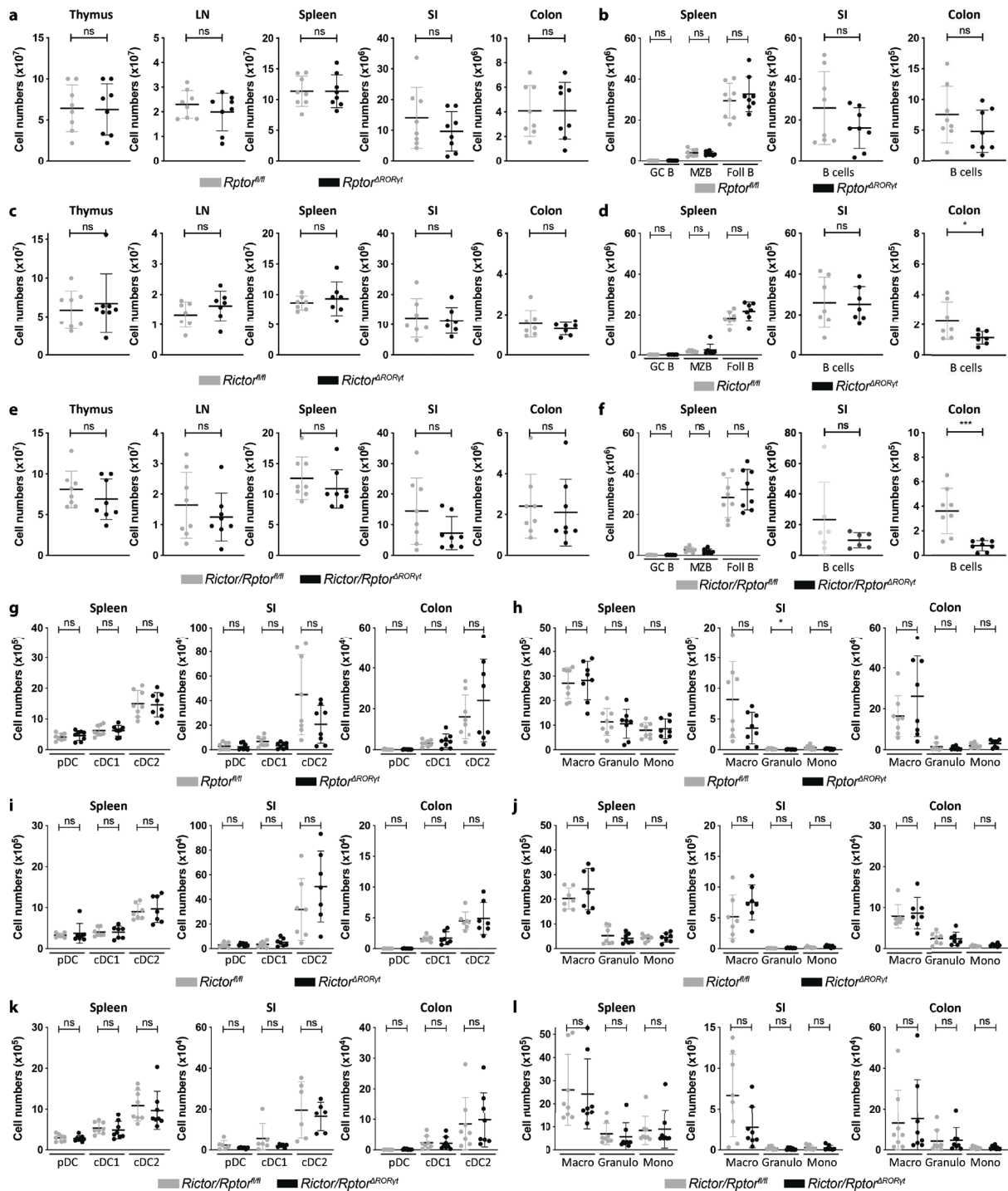
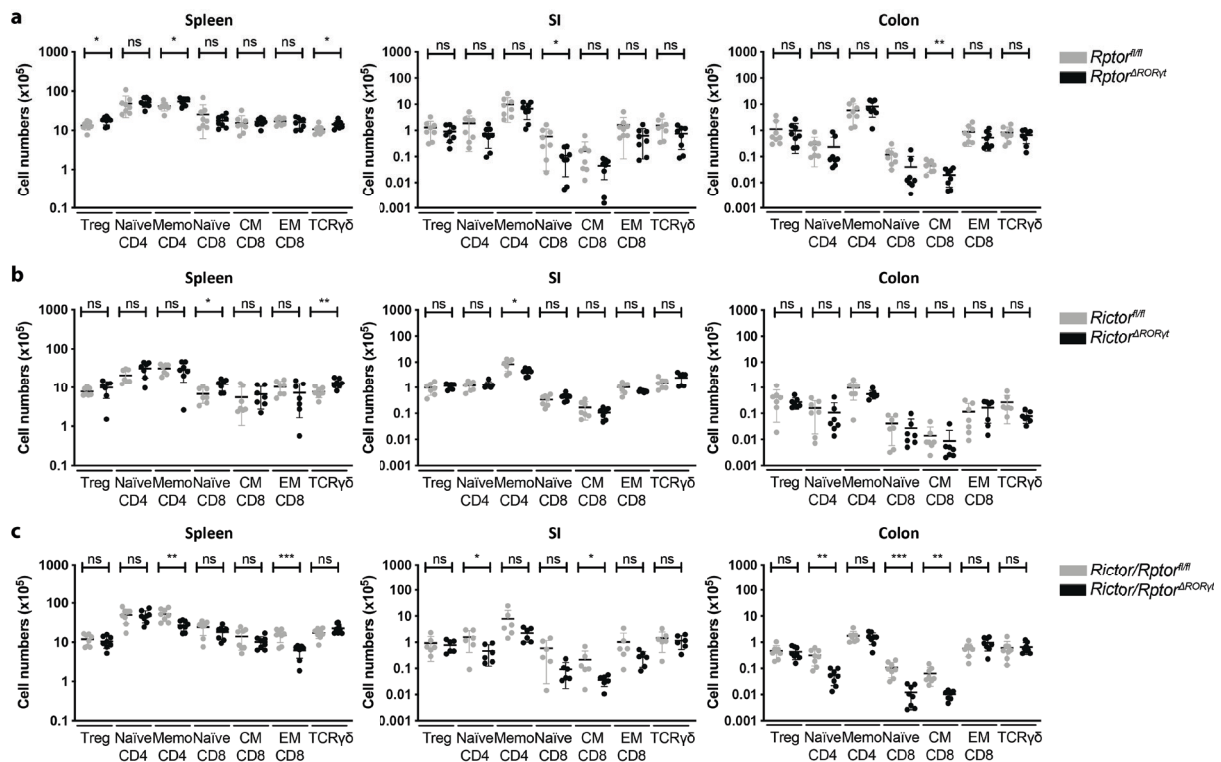
Fig.9 Innate immune cell and B cell subsets in wildtype mice with *RORc*-driven deletion of *Rptor* and/or *Rictor*. Cells were isolated from thymus, mLN, spleen, SI LP and cLP of $Rptor^{\Delta ROR \gamma t}$ (a, b, g, h), $Rictor^{\Delta ROR \gamma t}$ (c, d, i, j) or $Rictor/Rptor^{\Delta ROR \gamma t}$ (e, f, k, l) mice and age-matched Cre-negative littermates. a, c, e) Total count of living cells. Cell numbers of B cell (b, d, f), DC (g, I, k) and myeloid cell (h, j, l) subsets were determined in indicated organs. Mice were 8-10 weeks old at analysis. GC B: germinal center B cell, MZB: marginal zone B cell, Foll B: follicular B cell, pDC: plasmacytoid DC, cDC1: conventional DC1, cDC2: conventional DC2, Macro: macrophage, Granulo: granulocyte, Mono: monocyte. n = 6-8. Two-tailed unpaired t test or Mann-Whitney U test. *p ≤ 0.05, **p ≤ 0.01, ***p ≤ 0.001

Since RORγt is expressed in double-positive thymocytes, the observation of changes in all T cell subsets was not surprising. As described in chapter 2.4.2, mTORC1 and mTORC2 are critically involved in T cell differentiation, function and memory formation. The particular changes in T cell composition are displayed in Fig.10 and summarized in Table 4. Interestingly, alterations in the T cell compartment were heterogenous between spleen, SI and colon. Thus, mTORC1 and mTORC2 dependency of T cells appeared to be tissue-specific.

Fig.10 T cell subsets in wildtype mice with *RORc*-driven deletion of *Rptor* and/or *Rictor*. Cells were isolated from spleen, SI LP and cLP of *Rptor*$^{\Delta ROR\gamma t}$ (a), *Rictor*$^{\Delta ROR\gamma t}$ (b) or *Rictor/Rptor*$^{\Delta ROR\gamma t}$ (c) mice and age-matched Cre-negative littermates. Cell numbers of T cell subsets were determined in indicated organs. Mice were 8-10 weeks old at analysis. Memo CD4: memory CD4 T cell, CM CD8: central memory CD8 T cell, EM CD8: effector memory CD8 T cell. n = 6-8. Two-tailed unpaired t test or Mann-Whitney U test. *p ≤ 0.05, **p ≤ 0.01, ***p ≤ 0.001

	Rptor$^{\Delta ROR\gamma t}$			*Rictor*$^{\Delta ROR\gamma t}$			*Rictor/Rptor*$^{\Delta ROR\gamma t}$		
Subset	Spleen	SI	Colon	Spleen	SI	Colon	Spleen	SI	Colon
Treg	↑	=	=	=	=	=	=	=	=
naïve CD4$^+$	=	=	=	=	=	=	=	=	↓
memory CD4$^+$	↑	=	=	=	↓	=	↓	↓	=
naïve CD8$^+$	=	↓	=	↑	=	=	=	=	↓
central memory CD8$^+$	=	=	↓	=	=	=	=	↓	↓
effector memory CD8$^+$	=	=	=	=	=	=	↓	=	=
TCRγδ	↑	=	=	↑	=	=	=	=	=

Table 4 Changes in T cell subsets upon *RORc*-driven deletion of *Rptor* or *Rictor* compared to control animals.

Next, I analyzed $Rptor^{\Delta ROR\gamma t}Rag2^{-/-}$, $Rictor^{\Delta ROR\gamma t}Rag2^{-/-}$, $Rictor/Rptor^{\Delta ROR\gamma t}Rag2^{-/-}$ mice and Cre-negative control littermates to determine whether cellularity and innate immune cells are affected by a specific loss of *Rptor* and/or *Rictor* in the absence of B and T cells.
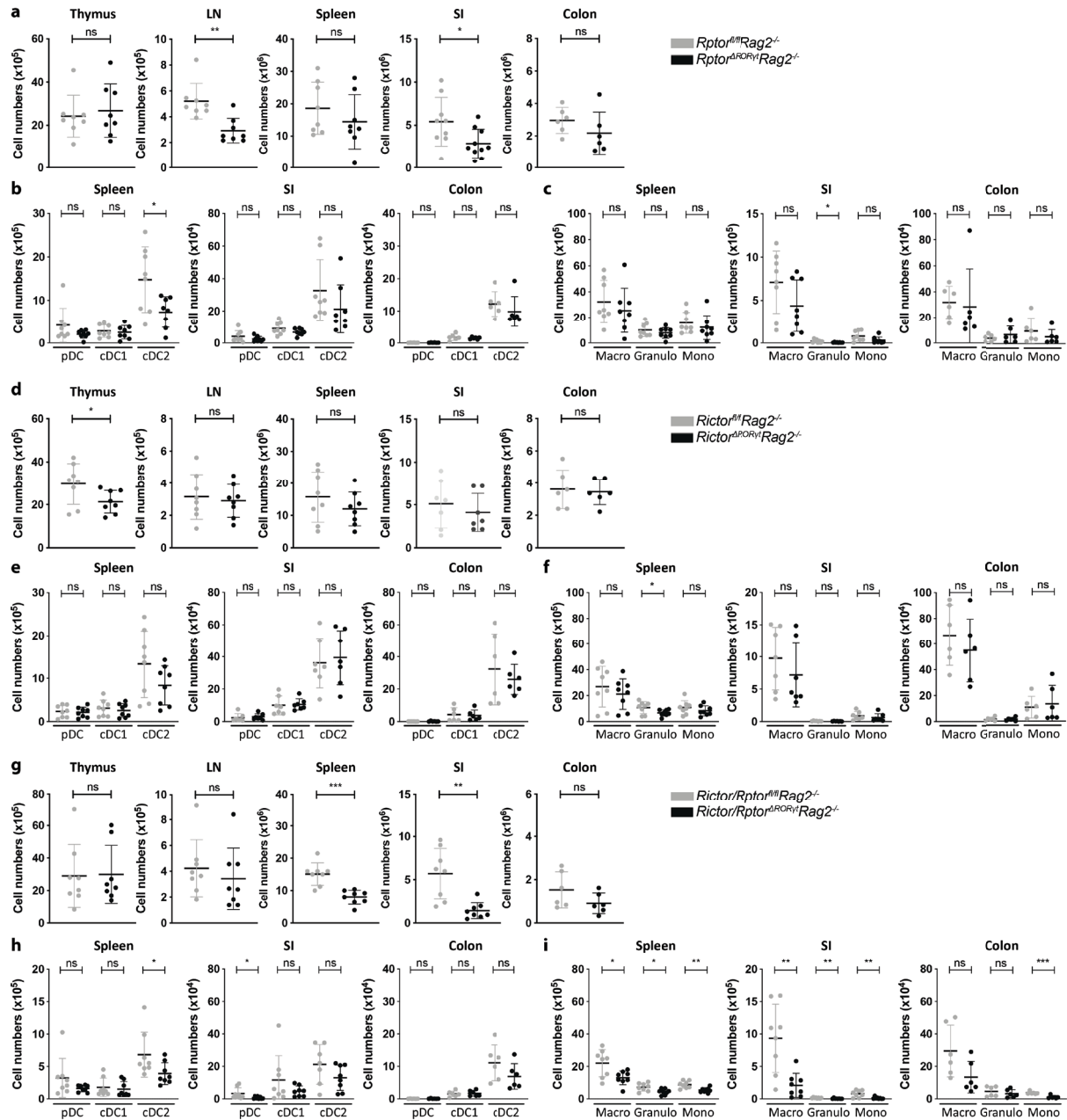
Fig.11 Innate immune cell subsets in $Rptor^{\Delta ROR\gamma t}Rag2^{-/-}$, $Rictor^{\Delta ROR\gamma t}Rag2^{-/-}$ and $Rictor/Rptor^{\Delta ROR\gamma t}Rag2^{-/-}$ mice. Cells were isolated from thymus, inguinal LN, spleen, SI LP and cLP of $Rptor^{\Delta ROR\gamma t}Rag2^{-/-}$ (a-c), $Rictor^{\Delta ROR\gamma t}Rag2^{-/-}$ (d-f) or $Rictor/Rptor^{\Delta ROR\gamma t}Rag2^{-/-}$ (g-i) mice and age-matched Cre-negative littermates. a, d, g) Total count of living cells. Cell numbers of DC (b, e, h) and myeloid cell (c, f, i) subsets were determined in indicated organs. Mice were 8-10 weeks old at analysis. pDC: plasmacytoid DC, cDC1 conventional DC1, cDC2 conventional DC2, Macro: macrophage, Granulo: granulocyte, Mono: monocyte. n = 6-8. Two-tailed unpaired t test or Mann-Whitney U test. *p ≤ 0.05, **p ≤ 0.01, ***p ≤ 0.001

Deletion of *Rptor* did not affect cellularity of thymus, spleen and colon (Fig.11a). The cellularity of LN and SI was reduced (Fig.11a). cDC2s were decreased in the spleen (Fig.11b) and granulocyte numbers were diminished in the SI (Fig.11c). However, it should be noted here that granulocyte numbers were below 0.4 % and 1.2 % in non-inflamed SI and colon.

In mice with ILC3-specific knockout of *Rictor*, the cellularity of LN, spleen, SI and colon remained normal, but the cellularity of the thymus was slightly decreased (Fig.11d). With exception of a modest reduction of granulocytes in the spleen, DCs (Fig.11e) and myeloid cells (Fig.11f) were unchanged.

Cellularity of spleen and SI was significantly reduced upon dual deletion of *Rptor* and *Rictor* (Fig.11g). The numbers of cDC2s, MΦ, monocytes and granulocytes were reduced in the spleen and the SI (reduction of ~40 % in the spleen and ~75 % in the SI, respectively) (Fig.11h, i). In the colon, only monocyte numbers were significantly diminished.

Taken together, mice lacking *Rptor* in ILC3s displayed a modest reduction of splenic cDCs and SI granulocytes. It is therefore possible that recruitment or retention of these subsets was affected, but I did not study this question further in detail. Double-knockout mice had a more pronounced reduction in myeloid cells as compared to single knockout mice.

5.1.4 ILC subsets in knockout mice

To investigate the effect of *RORc*-driven deletion of *Rptor* and/or *Rictor* on ILCs, I analyzed numbers and ratios of NK cell, ILC1, ILC2 and ILC3 subsets. My analysis was focused on the SI and the colon, as ILC3s are most abundant at mucosal barrier sites. The defining ILC subset-specific markers are summarized in Table 5.

Cell Type	Markers
NK cell	Lin$^-$CD90.2$^+$NKp46$^+$T-bet$^+$EOMES$^+$
ILC1	Lin$^-$CD90.2$^+$NKp46$^+$T-bet$^+$EOMES$^-$
ILC2	Lin$^-$CD90.2$^+$KLRG1$^+$CD25$^+$CD127$^{+/low}$
CD4$^+$ ILC3	Lin$^-$CD90.2$^+$RORγt$^+$CD4$^+$NKp46$^-$
NCR$^+$ ILC3	Lin$^-$CD90.2$^+$RORγt$^+$CD4$^-$NKp46$^+$
NCR$^-$ ILC3	Lin$^-$CD90.2$^+$RORγt$^+$CD4$^-$NKp46$^-$

Table 5 Discrimination of ILC subsets by flow cytometry. Lin: CD3, CD8, CD11c, CD19, B220, Gr-1, TCRβ, TCRγδ, Ter-119.

The SI and colon of wildtype mice harbored at least three different subsets of ILC3s: CD4$^+$ ILC3s, NCR$^-$ ILC3s and NCR$^+$ ILC3s. In both SI and colon, NCR$^-$ ILC3s were most abundant

(Fig.12). *Rictor^ΔRORγt* mice showed no significant changes in total ILC3s in the SI and colon (Fig.12d, e). However, the number of NCR⁺ ILC3s in the SI was significantly diminished in *Rptor^ΔRORγt* and *Rictor/Rptor^ΔRORγt* mice (Fig.12b, c, f, g). Numbers of NK cells, ILC1s and ILC2s remained normal in the SI and colon of knockout mice (Fig.13).
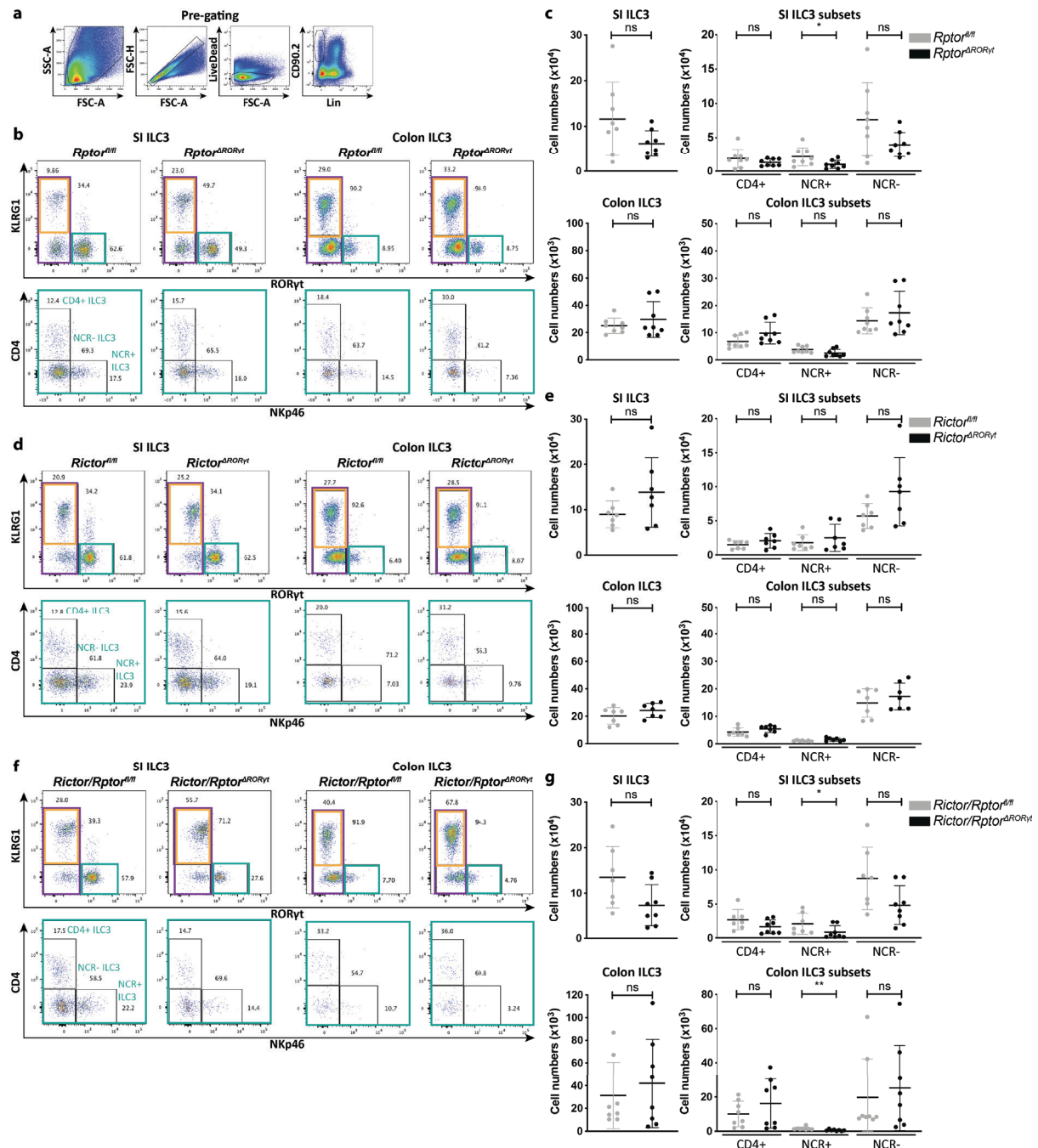
Fig.12 NCR⁺ ILC3 subsets in wildtype mice are reduced upon loss of mTORC1 signaling. Cells were isolated from SI LP and cLP of *Rptor^ΔRORγt* (b, c), *Rictor^ΔRORγt* (d, e) or *Rictor/Rptor^ΔRORγt* (f, g) mice and age-matched Cre-negative littermates and analyzed by flow cytometry. a) Pre-gating for ILCs. b, d, f) Exemplary blots of ILC3 subsets in SI and colon. c, e, g) Total ILC3 numbers and numbers of ILC3 subsets. Lin: CD3, CD8, CD11c, CD19, B220, Gr-1, TCRβ, TCRγδ, Ter-119. Mice were 8-10 weeks old at analysis. n = 7-8. Two-tailed unpaired t test or Mann-Whitney U test. *p ≤ 0.05, **p ≤ 0.01, ***p ≤ 0.001
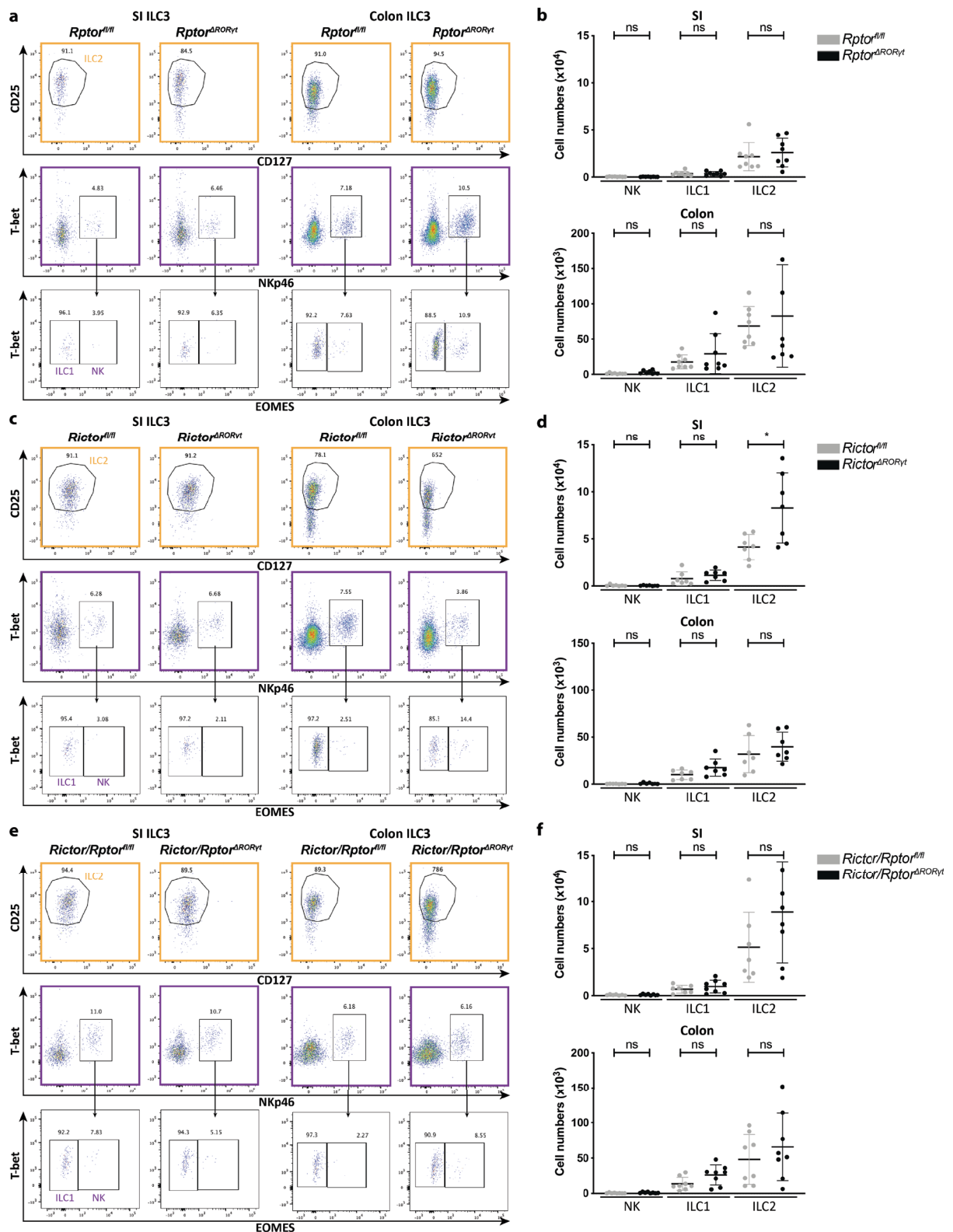
Fig.13 Numbers of NK cells, ILC1s and ILC2s in wildtype mice with *RORc*-driven deletion of *Rptor* and/or *Rictor*. Cells were isolated from SI LP and cLP of *Rptor*^{ΔRORγt} (a, b), *Rictor*^{ΔRORγt} (c, d) or *Rictor/Rptor*^{ΔRORγt} (e, f) mice and age-matched Cre-negative littermates and analyzed by flow cytometry. a, c, e) Exemplary blots of NK cell, ILC1 and ILC2 subsets in SI and colon. NK cells and ILC1s were pre-gated on Lin⁻CD90.2⁺KLRG1⁺/⁻ cells (purple frame). ILC2s were pre-gated as Lin⁻CD90.2⁺KLRG1⁺ cells (yellow frame). b, d, f) Total NK cell, ILC1 and ILC2 numbers. Mice were 8-10 weeks old at analysis. n = 7-8. Two-tailed unpaired t test or Mann-Whitney U test. *p ≤ 0.05, **p ≤ 0.01, ***p ≤ 0.001

These findings show that mTORC1 signaling and combined mTORC1/2 signaling were involved in maintaining SI NCR$^+$ ILC3s in wildtype mice. There were no indirect effects on numbers of other ILC subsets. Although the numbers of ILCs were not significantly changed, the percentage of NK cell, ILC1 and ILC2 subsets was increased in some organs of knockout mice (Fig.S2). Whether the proportional changes in these ILCs might reflect a developmental switch or peripheral transition will be discussed later.

There was a striking difference in ILC3 numbers of *Rag2*$^{-/-}$ knockout mice as compared to wildtype knockout mice. In *Rptor*$^{\Delta ROR\gamma t}$*Rag2*$^{-/-}$, *Rictor*$^{\Delta ROR\gamma t}$*Rag2*$^{-/-}$, *Rictor/Rptor*$^{\Delta ROR\gamma t}$*Rag2*$^{-/-}$ mice, numbers of NCR$^+$ and NCR$^-$ ILC3 subsets in the SI were reduced to different degrees (*Rptor* knockout: ~ 50 %, *Rictor* knockout: ~ 30 %, *Rptor/Rictor* knockout: ~ 80 %) (Fig.14c, e, g). Furthermore, deletion of *Rictor* and dual deletion of *Rptor* and *Rictor* decreased the number of CD4$^+$ ILC3s. Accordingly, the percentage of CD4$^+$, NCR$^+$ and NCR$^-$ ILC3s in the SI decreased (Fig.S3). The reduction of ILC3 numbers might at least in part explain the reduction of SI cellularity observed before (Fig.11). ILC3 numbers and percentage were not altered in the colon of knockout mice (Fig.14b-g and Fig.S3).

SI ILC1s and ILC2s showed a significant increase in the SI of *Rptor*$^{\Delta ROR\gamma t}$*Rag2*$^{-/-}$ and *Rictor*$^{\Delta ROR\gamma t}$*Rag2*$^{-/-}$ mice (Fig.15a-d). Concomitantly, percentage of ILC1s and ILC2s was elevated in the SI (Fig.S3). *Rictor/Rptor*$^{\Delta ROR\gamma t}$*Rag2*$^{-/-}$ mice displayed normal numbers of SI ILC1s and SI ILC2s. The number and percentage of ILC1s and ILC2s was not altered in the colon of knockout mice (Fig.15 and Fig.S3).

Collectively, these results demonstrate that mTORC1 and mTORC2 signaling were crucial to maintain normal numbers of SI ILC3s in the absence of B and T cells. In contrast, colonic ILC3 numbers seemed to be largely independent from mTOR signaling.

All in all, both single and dual loss of *Rptor* and *Rictor* in RORγt-expressing cells had an impact on ILC3 numbers in the SI of wildtype and lymphopenic mice. However, ILC3 numbers were more dependent on mTOR in a *Rag2*$^{-/-}$ background. Unexpectedly, the loss of ILC3s was accompanied by expansion of SI ILC1s and ILC2s. Whether this effect was due to altered ILC plasticity or changes in the immunological niches of the SI will be further addressed. In contrast to numbers of SI ILC3s, colonic ILC3 numbers were largely independent from mTORC1 and mTORC2 signaling suggesting tissue-specific differences in mTOR-dependency of ILC3s.
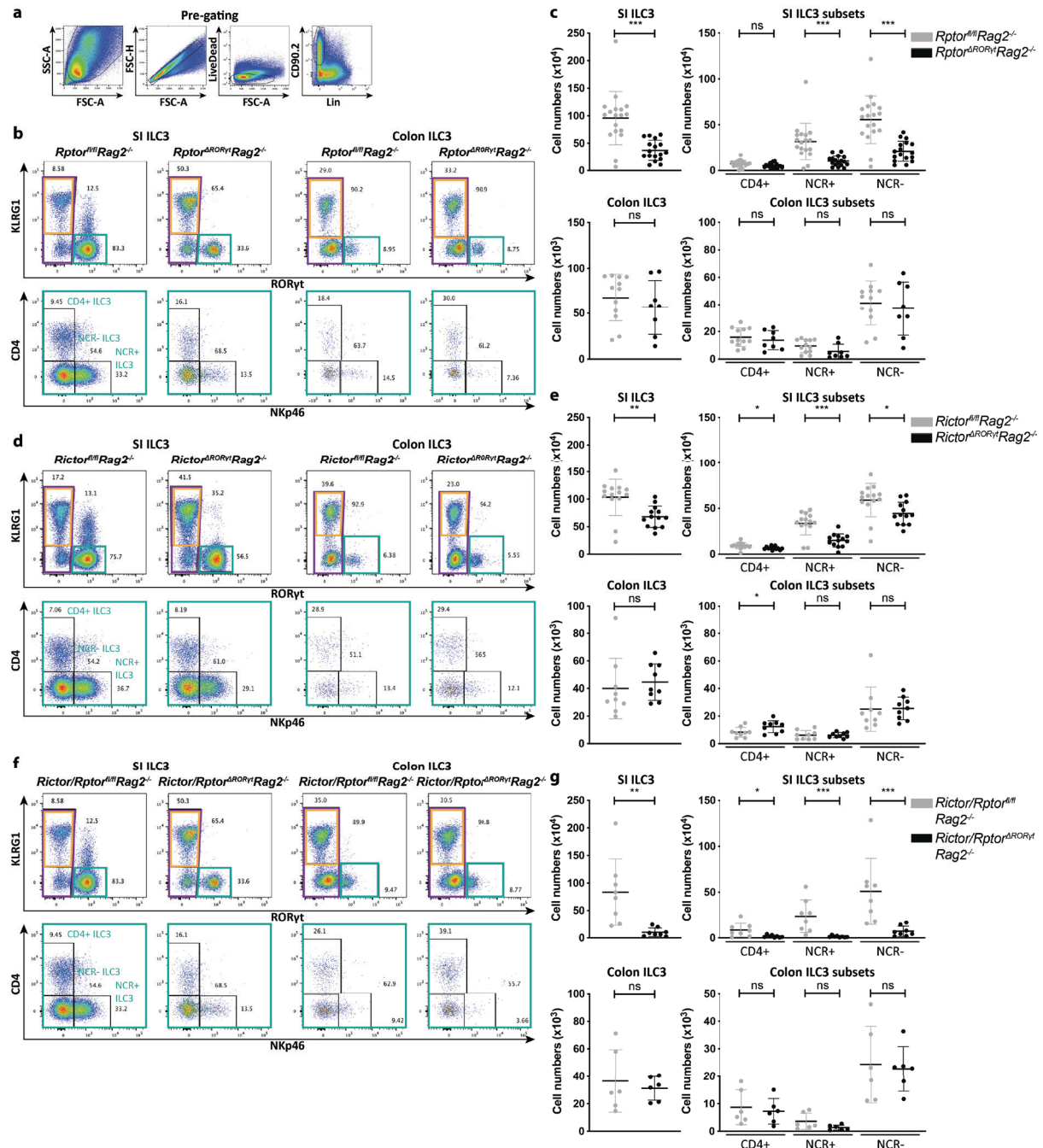
Fig.14 ILC3 subsets in *Rag2^{-/-}* mice are dependent on mTORC1 and mTORC2 signaling *in vivo*. Cells were isolated from SI LP and cLP of *Rptor^{ΔRORγt}Rag2^{-/-}* (b, c), *Rictor^{ΔRORγt}Rag2^{-/-}* (d, e) or *Rictor/Rptor^{ΔRORγt}Rag2^{-/-}* (f, g) mice and age-matched Cre-negative littermates and analyzed by flow cytometry. a) Pre-gating for ILCs. b, d, f) Exemplary blots of ILC3 subsets in SI and colon. c, e, g) Total ILC3 numbers and numbers of ILC3 subsets. Lin: CD3, CD8, CD11c, CD19, B220, Gr-1, TCRβ, TCRγδ, Ter-119. Mice were 8-10 weeks old at analysis. n = 8-17. Two-tailed unpaired t test or Mann-Whitney U test. *p ≤ 0.05, **p ≤ 0.01, ***p ≤ 0.001
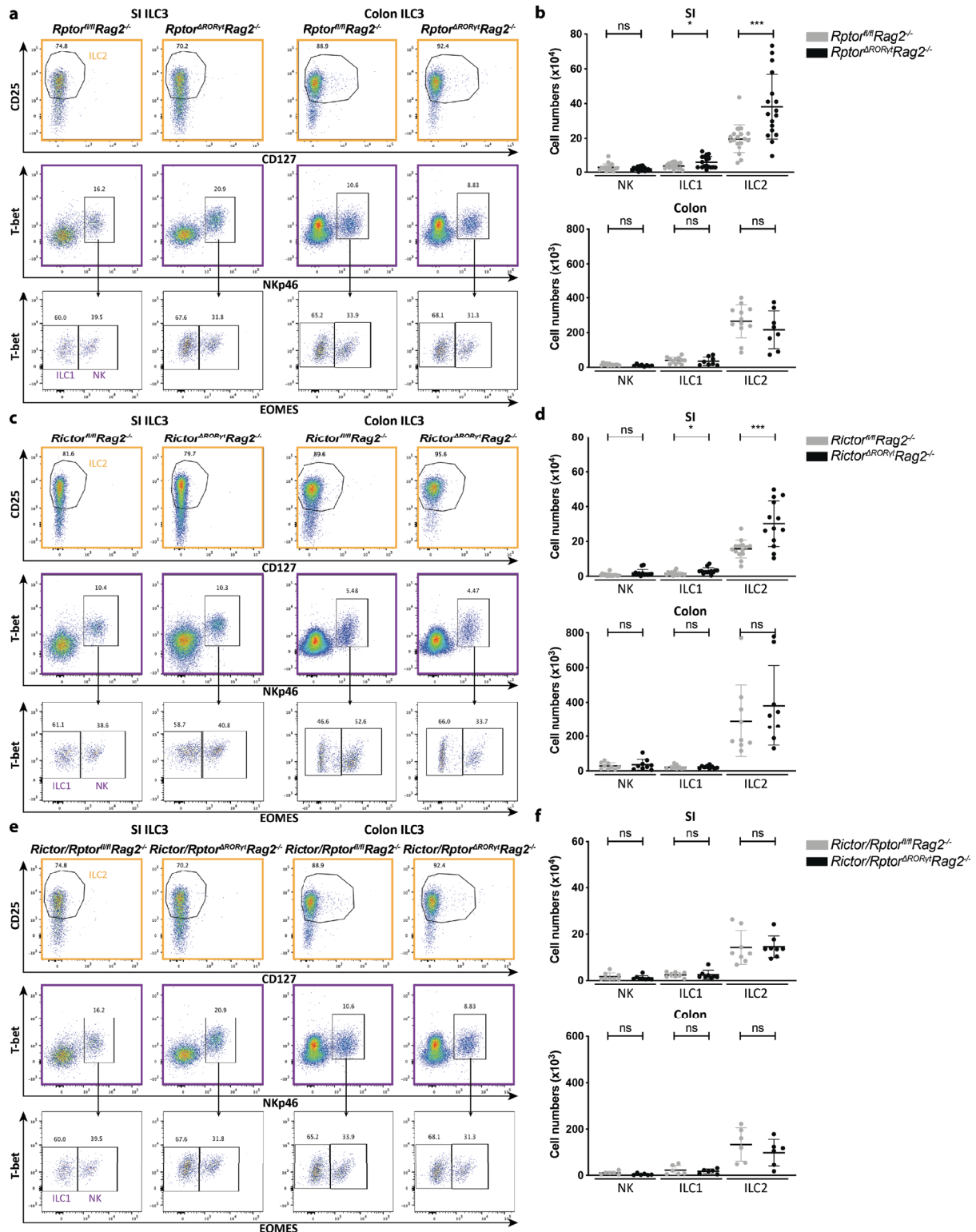
Fig.15 SI ILC1s and ILC2s are increased in *Rag2⁻/⁻* mice with single deletion of *Rptor* or *Rictor*. Cells were isolated from SI LP and cLP of *Rptor^ΔRORγt^Rag2⁻/⁻* (a, b), *Rictor^ΔRORγt^Rag2⁻/⁻* (c, d) or *Rictor/Rptor^ΔRORγt^Rag2⁻/⁻* (e, f) mice and age-matched Cre-negative littermates and analyzed by flow cytometry. a, c, e) Exemplary blots of NK cell, ILC1 and ILC2 subsets in SI and colon. NK cells and ILC1s were pre-gated on Lin⁻CD90.2⁺KLRG1⁺/⁻ cells (purple frame). ILC2s were pre-gated as Lin⁻CD90.2⁺KLRG1⁺ cells (yellow frame). b, d, f) Total NK cell, ILC1 and ILC2 numbers. Mice were 8-10 weeks old at analysis. n = 9-14. Two-tailed unpaired t test or Mann-Whitney U test. *p ≤ 0.05, **p ≤ 0.01, ***p ≤ 0.001

5.1.5 Bone marrow ILC progenitors in knockout mice

The previous data demonstrated that the number of SI NCR⁺ ILC3s was decreased in wildtype mice with *RORc*-driven deletion of *Rptor* and/or *Rictor*. Furthermore, conditional knockout of *Rptor* and/or *Rictor* resulted in a reduction of all SI ILC3s in *Rag2⁻/⁻* mice. To investigate if these alterations in ILC3s were a result of a developmental defect in BM progenitor cells, numbers and percentage of Lin⁻cKit⁺CD127⁺Flt3⁺Sca1⁺/⁻ common lymphoid progenitors (CLPs), Lin⁻α4β7⁺CD127⁺CD25⁻Flt3⁻ common helper ILC progenitors (CHILPs) and Lin⁻CD90.2⁺CD25⁺ ILC2 progenitors (ILC2ps) were analyzed in the BM of knockout strains. The gating strategy is displayed in Fig.16a. As depicted in Fig.16, no striking change in progenitor cells number could be observed in any of the conditional knockout strains.
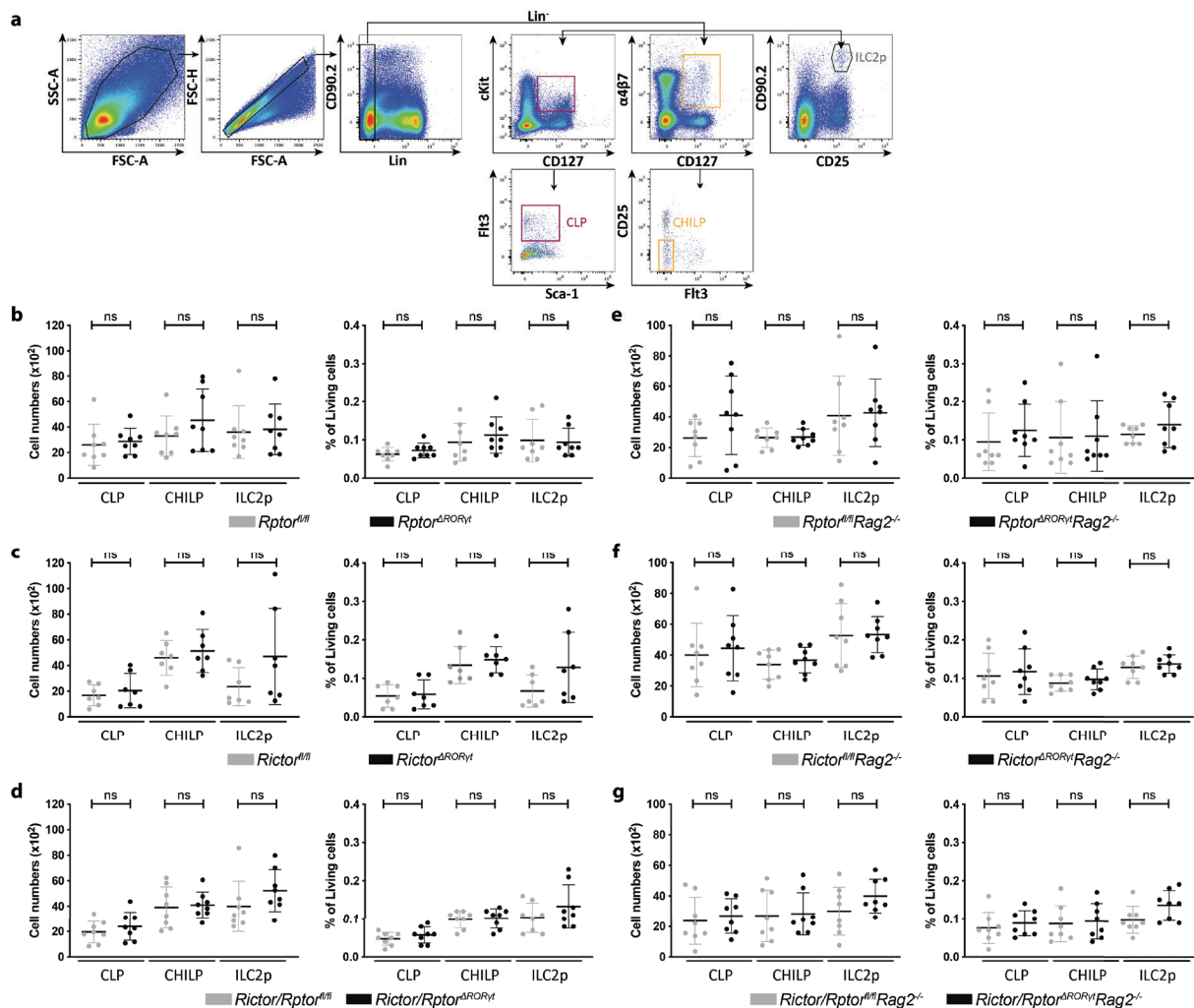
Fig.16 ILC progenitors in the bone marrow are not affected by *RORc*-driven deletion of *Rptor* and *Rictor in vivo*. Cells were isolated from the tibia and femur of one hind leg and analyzed for number of common lymphoid progenitors (CLPs), common helper ILC progenitors (CHILPs) and ILC2 progenitors (ILC2ps). a) Gating strategy for hematopoietic progenitors, BM from *Rag2⁻/⁻* mouse. Lin: CD3, CD8, CD11c, CD19, B220, Gr-1, NK1.1, TCRβ, TCRγδ, Ter-119. b) *Rptor^ΔRORγt*, c) *Rictor^ΔRORγt*, d) *Rictor/Rptor^ΔRORγt*, e) *Rptor^ΔRORγtRag2⁻/⁻*, f) *Rictor^ΔRORγtRag2⁻/⁻* or f) *Rictor/Rptor^ΔRORγtRag2⁻/⁻* mice and age-matched Cre-negative littermates. Mice were 8-10 weeks old at analysis. n = 7-8. Two-tailed unpaired t test or Mann-Whitney U test. *p ≤ 0.05, **p ≤ 0.01, ***p ≤ 0.001

Altogether, the presented *in vivo* data indicate that the reduction of ILC3 numbers was not a result of a decrease in CLPs and CHILPs. This is in line with the fact that RORγt is not expressed in these progenitor cells.[11,59] However, it could not be excluded that the differentiation of ILC3s from CHILPs or an unidentified RORγt⁺ ILC3 precursor was impaired by loss of mTORC1 or mTORC2 signaling.

5.2 mTORC1 and mTORC2 in ILC3 differentiation, survival and proliferation

The failure to maintain normal SI ILC3 numbers upon conditional deletion of *Rptor* and/or *Rictor* in RORγt-expressing cells of *Rag2⁻/⁻* mouse strains could have several explanations. Firstly, disruption of mTORCs could impair the differentiation of a RORγt⁺ ILC3 progenitor towards mature ILC3s. Secondly, the lack of mTOR signaling could reduce the survival of mature ILC3s. Finally, loss of mTORC1 or mTORC2 signaling could lower the capacity of ILC3s to proliferate. The fact that ILC3 subsets were reduced in the SI but not in the colon upon loss of *Rptor*, *Rictor* and both *Rptor* and *Rictor* also suggested that tissue-specific niche factors or homing properties contributed to the organ-specific reduction of ILC3s.

5.2.1 *RORc*-driven deletion of *Rptor* but not *Rictor* impairs ILC3 reconstitution in bone marrow chimeras

To determine whether BM progenitors from *Rptor^ΔRORγt^Rag2⁻/⁻* and *Rictor^ΔRORγt^Rag2⁻/⁻* mice could equally reconstitute SI and colonic ILC3s of immunodeficient recipient mice, mixed BM chimera experiments were performed. This model also allowed to exclude indirect *trans* effects of the mutation in ILC3s during development. BM cells from *Rag2⁻/⁻Ly5.1* mice and BM cells from *Rptor^ΔRORγt^Rag2⁻/⁻* mice, *Rictor^ΔRORγt^Rag2⁻/⁻* mice or respective littermate controls were injected in a 1:1 ratio into lethally irradiated *Rag2⁻/⁻Ly5.1/Ly5.2* recipients (Fig.17a). As both knockout strains and their Cre-negative littermates uniformly express Ly5.2 on hematopoietic cells, they could be discriminated from Ly5.1-positive *Rag2⁻/⁻* donor cells and from recipient cells expressing both isoforms of the congenic marker (Fig.17d, e).
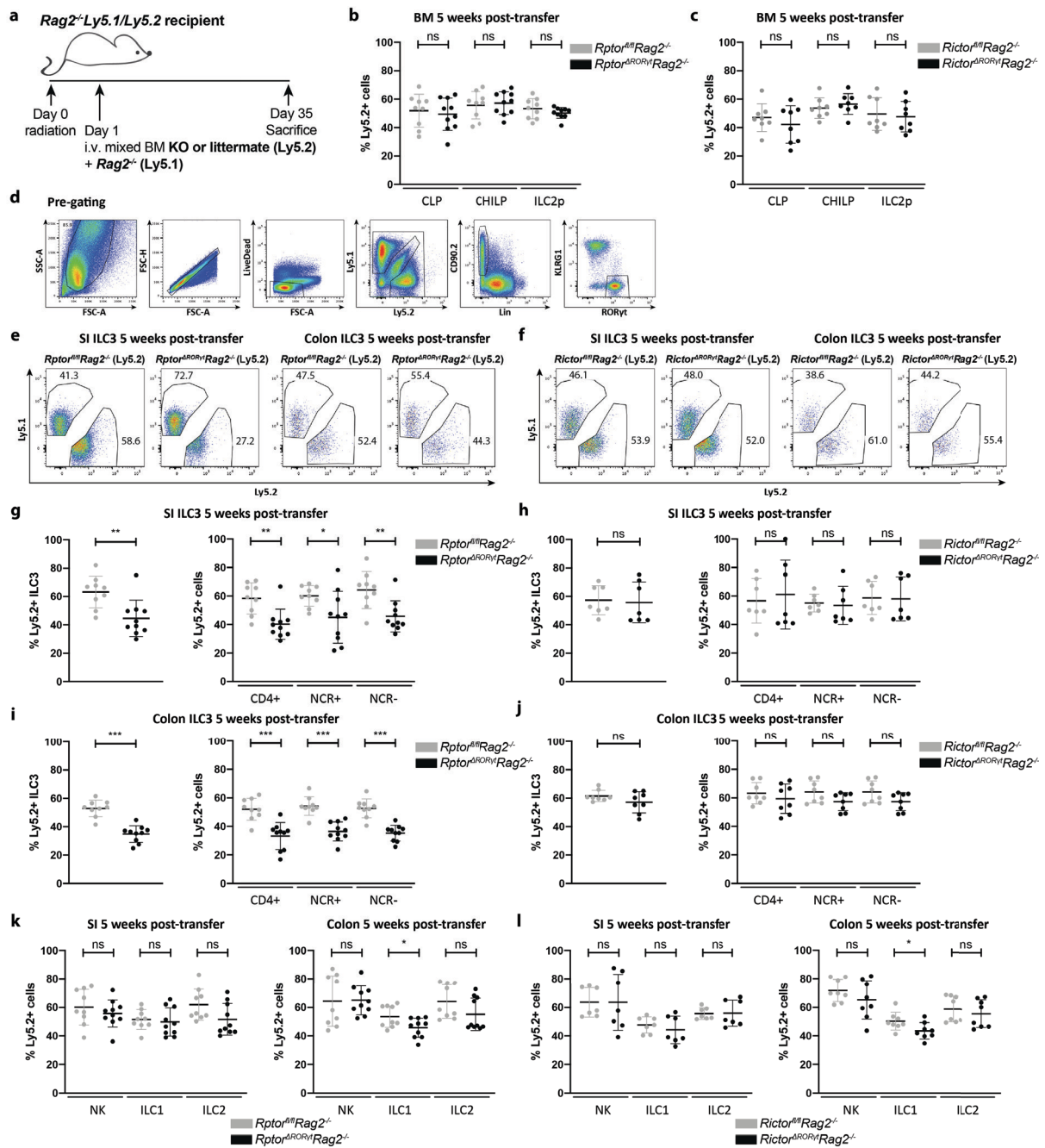
Fig.17 Competitive reconstitution of ILC3s in bone marrow chimeras is impaired by _RORc_-driven deletion of _Rptor_ but not _Rictor_. a) Bone marrow chimera model timeline. BM from _Rag2^-/-Ly5.1_ mice was mixed with BM from either _Rptor^ΔRORγtRag2^-/-_ mice (b, e, g, I, k), _Rictor^ΔRORγtRag2^-/-_ (c, f, h, j, l) mice or Cre-negative littermates, respectively. Five weeks after transplantation, mice were sacrificed. Cells were extracted from the SI LP, the cLP and the tibia and femur of one hind leg (BM). b, c) Percentage of Ly5.2^+Ly5.1^- common lymphoid progenitors (CLPs), common helper ILC progenitors (CHILPs) and ILC2 progenitors in the BM was determined by flow cytometry. d) Gating strategy for donor-derived ILCs. e) Exemplary blots of Ly5.1 and Ly5.2 percentages within the donor-derived ILC3 population. Percentage of Ly5.2^+Ly5.1^- ILC3s was determined in the SI (g, h) and colon (I, j). k, l) Percentage of Ly5.2^+Ly5.1^- NK cells, ILC1s and ILC2s was determined in the SI (left) and the colon (right). n = 8-10 mice from 2-3 independent experiments. Two-tailed unpaired t test. *p ≤ 0.05, **p ≤ 0.01, ***p ≤ 0.001

Five weeks after BM transfer, equal percentages of CLPs, CHILPs and ILC2p were derived from Ly5.1- and Ly5.2-positive donor cells (Fig.17b, c). These data confirm previous findings that CLPs, CHILPs and ILC2ps were normal in knockout mice (see chapter 5.2.4). However, _Rptor_ deletion resulted in a significant reduction of ILC3s both in SI and colon (Fig.17g, i). Loss of

Rictor had no effect on the efficiency of ILC3 reconstitution (Fig.17h, j). With the exception of modestly reduced reconstitution of ILC1s in the colon, reconstitution of other ILC subsets was normal (Fig.17k, l)

These findings show that the reconstitution of ILC3s after BM transplantation was impaired when *Rptor* was deleted in ILC3s. Moreover, they indicate that the effect of *Rptor* deletion on ILC3 numbers was cell-intrinsic. The transition of ILC3s into ILC1s (exILC3s) has been described (see chapter 2.2.3). It can therefore not be excluded that the modest reduction of ILC1s (Fig.17k, l) was a result of reduced ILC3 numbers.

5.2.2 mTORC1 and mTORC2 mediate ILC3 proliferation under steady state and activating conditions

To examine whether the observed decline in ILC3 numbers in the SI occurred due to impaired cell survival or proliferation, freshly isolated ILC3s from the SI and colon of $Rptor^{\Delta ROR\gamma t}Rag2^{-/-}$ and $Rictor^{\Delta ROR\gamma t}Rag2^{-/-}$ mice were analyzed for active Caspase-3, an indicator of active apoptosis, and Ki-67, a marker for cells undergoing proliferation (Fig.18a, b).
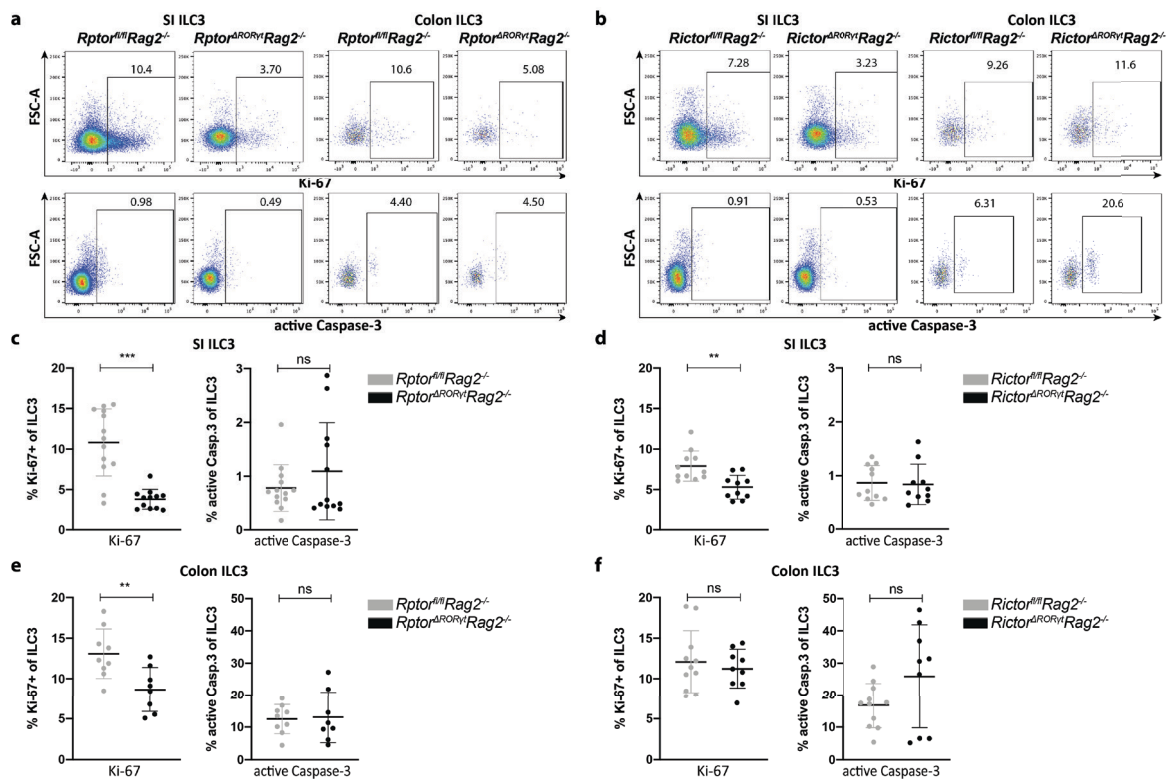
Fig.18 Loss of mTORC1 or mTORC2 signaling affects ILC3 proliferation but not survival *in vivo*. Cells were isolated from the SI LP and cLP of $Rptor^{\Delta ROR\gamma t}Rag2^{-/-}$ (a, c, e) or $Rictor^{\Delta ROR\gamma t}Rag2^{-/-}$ (b, d, f) mice and age-matched Cre-negative littermates. a, b) Exemplary blots of SI and colonic ILC3s. c-f) Percentage of Ki-67-positive ILC3s and ILC3s positive for active Caspase-3 was determined by flow cytometry. n = 10-12. Two-tailed unpaired t test. *p ≤ 0.05, **p ≤ 0.01, ***p ≤ 0.001

Approximately 10 % of SI ILC3s and 15 % of colonic ILC3s from littermate controls were positive for Ki-67 (Fig.18). In comparison, less than 5 % of SI ILC3s and 10 % of colonic ILC3s from $Rptor^{\Delta ROR\gamma t}Rag2^{-/-}$ mice were positive for Ki-67 indicating a severe reduction of proliferation (Fig.18a, c). The percentage of Ki-67$^+$ ILC3s from the SI of $Rictor^{\Delta ROR\gamma t}Rag2^{-/-}$ mice was also significantly reduced compared to littermate controls (Fig.18b, d). The proliferation of colonic ILC3s from $Rictor^{\Delta ROR\gamma t}Rag2^{-/-}$ mice was not impaired (Fig.18e, f). The percentage of active Caspase-3$^+$ ILC3s was equal in both knockout strains and control littermates (Fig.18c-f). These results indicate that ILC3 proliferation but not ILC3 survival was regulated by mTORC1 and mTORC2 signaling. Thus, the decrease of ILC3s in knockout mice or in BM chimeras was likely a result of impaired expansion rather than survival.

IL-2 has been previously reported to have an effect on ILC proliferation.[50,83,84,218] Furthermore, IL-2 has been described as an upstream activator of mTORC1-dependent proliferation in T cells and T-cell lymphoma cell lines.[219,220] To assess whether ILC3s in the SI and colon of $Rptor^{\Delta ROR\gamma t}Rag2^{-/-}$ and $Rictor^{\Delta ROR\gamma t}Rag2^{-/-}$ could proliferate in response to IL-2 *in vivo*, knockout and control mice received one single intraperitoneal (i.p.) injection of IL-2/α-IL-2 complex. IL-2/α-IL-2 complexes enhance the biological activity of IL-2 and induce robust proliferation of T cells *in vivo*.[219]

One day after IL-2/α-IL-2 complex injection, 30 % of ILC3s proliferated in the SI of control animals (Fig.19a-d). ILC3s *in* $Rptor^{\Delta ROR\gamma t}Rag2^{-/-}$ mice utterly failed to proliferate (Fig.19a, b). In $Rictor^{\Delta ROR\gamma t}Rag2^{-/-}$ mice, the proliferation capacity of SI ILC3s was reduced by 50 % compared to littermate controls (Fig.19c, d). These results demonstrate that loss of both mTORC1 and mTORC2 signaling impaired IL-2-dependent ILC3 proliferation in the SI. In the colon of $Rptor^{\Delta ROR\gamma t}Rag2^{-/-}$ mice, $Rictor^{\Delta ROR\gamma t}Rag2^{-/-}$ mice and littermate controls, IL-2/α-IL-2 complex treatment did not induce ILC3 proliferation (Fig.19b, d) compared to untreated mice (Fig.18e, f). Thus, treatment with IL-2/α-IL-2 complex selectively enhanced ILC3 proliferation in the SI. The reduced capacity of SI ILC3s to proliferate could not be explained by lack of IL-2 receptor as CD25, a subunit of the IL-2 receptor, was expressed on ILC3s of untreated $Rptor^{\Delta ROR\gamma t}Rag2^{-/-}$ and $Rictor^{\Delta ROR\gamma t}Rag2^{-/-}$ mice (Fig.19e, f).

In summary, these findings show that *in vivo* proliferation but not survival of SI ILC3s depends on mTORC1 and to a lower extent on mTORC2. The decreased proliferation of SI ILC3s could explain the observed reduction of ILC3s in *Rptor* and *Rictor* knockout mice. In line with the

finding that colonic ILC3 numbers were not affected by loss of *Rptor* and *Rictor*, proliferation of colonic ILC3s was less dependent on mTOR signaling. IL-2/α-IL-2 complex treatment revealed that in particular SI ILC3s proliferate in response to activation. This activation-induced proliferation required both mTORC1 and mTORC2 signaling. It cannot be excluded that the colon was less accessible to IL-2/α-IL-2 complexes and that factors other than IL-2 contribute to ILC3 proliferation in the SI.
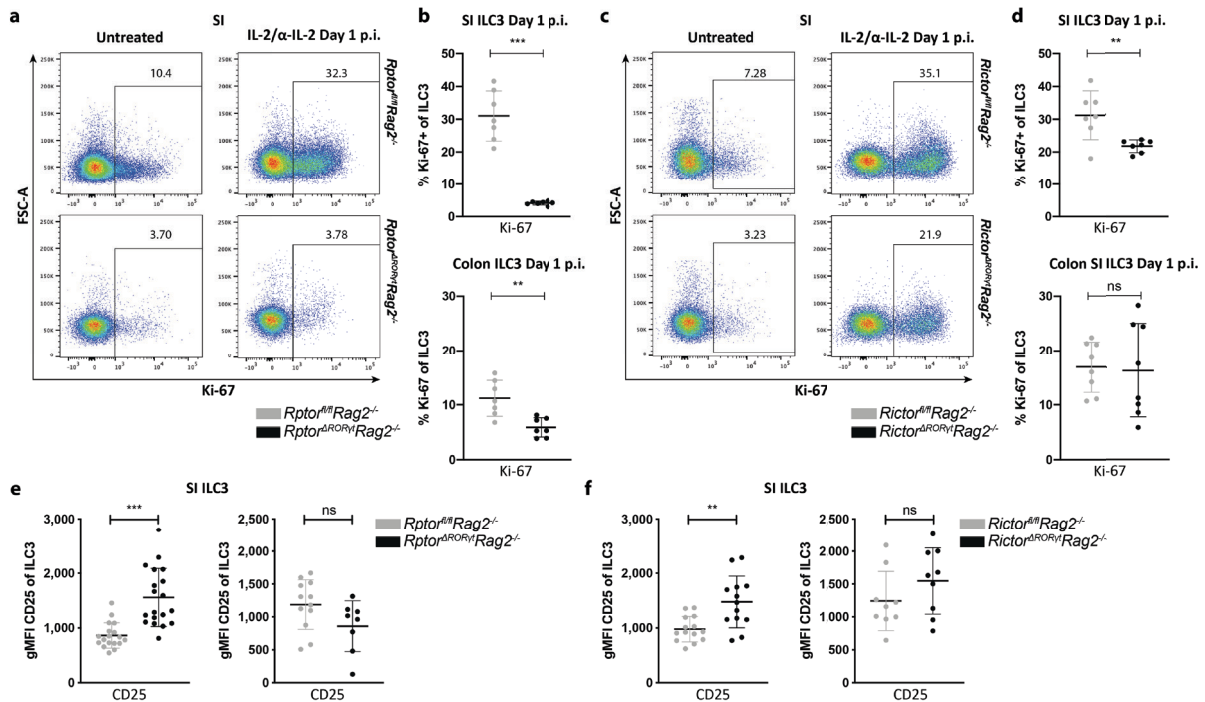
Fig.19 Loss of mTORC1 or mTORC2 signaling impairs IL-2/α-IL-2 complex-mediated ILC3 proliferation *in vivo*. *Rptor$^{\Delta ROR\gamma t}$Rag2$^{-/-}$* (a, b) or *Rictor$^{\Delta ROR\gamma t}$Rag2$^{-/-}$* (b, d) mice and Cre-negative littermates were injected with one single dose of IL-2/α-IL-2 complex. After one day, cells from the SI LP and cLP were isolated and the percentage of Ki-67-positive ILC3s was analyzed. Exemplary blots from untreated and treated animals are shown on the left side. n = 7 mice from 2-3 independent experiments. e, f) CD25 surface expression was determined on ILC3s isolated from the SI LP of untreated *Rptor$^{\Delta ROR\gamma t}$Rag2$^{-/-}$* (e) or *Rictor$^{\Delta ROR\gamma t}$Rag2$^{-/-}$* (f) mice and Cre-negative littermates. gMFI: geometric mean fluorescence intensity. n= 12-19. Two-tailed unpaired t test. *p ≤ 0.05, **p ≤ 0.01, ***p ≤ 0.001

5.2.3 mTORC1 in ILC3 plasticity

Immunophenotyping of mTOR knockout mice revealed that the loss of ILC3s in the SI of *Rptor$^{\Delta ROR\gamma t}$Rag2$^{-/-}$* and *Rictor$^{\Delta ROR\gamma t}$Rag2$^{-/-}$* mice was accompanied by an increase of ILC1s and ILC2s. This effect was not observed in *Rictor/Rptor$^{\Delta ROR\gamma t}$Rag2$^{-/-}$* mice, which had an even more pronounced loss of ILC3s.

On one hand, this might indicate that ILC1s, ILC2s and ILC3s were competing for the same niche in the SI. This niche might be disturbed in mice deficient in both mTORCs. On the other

hand, it is possible that loss of mTORC1 signaling in intestinal RORγt-expressing cells might divert a RORγt-expressing ILC3 progenitor towards ILC1 and ILC2 fate. Plasticity between ILC subsets has been repeatedly described in the past.[70,80,221] Moreover, RORγt-expressing ILC progenitor with the potential to develop into ILC1s and ILC2s have been found in human blood.[222] While the ILC1 population has been reported to contain "exILC3s" generated by ILC3s[77,80], ILC2s have so far not been described as expressing RORγt under homeostatic conditions. However, a recent publication showed that inflammatory ILC2s can upregulate RORγt and transform into ILC3-like cells.[17]

To test whether other intestinal ILC subsets had a history of *RORc*-driven Cre-expression, NK cells, ILC1s, ILC2s and ILC3s from the SI of *Rptor*^{ΔRORγt}*Rag2*$^{-/-}$ and control mice were sorted and tested for excision of the floxed target region. As depicted in Fig.20a, all ILCs derived from Cre-negative animals showed only an 800 bp band, which indicates that the floxed region has not been genetically removed. DNA isolated from ILC3s of Cre-positive animals showed only a 200 bp fragment demonstrating that the floxed region has been excised. ILC1s from both Cre-positive samples and ILC2s from one Cre-positive sample showed a 200 bp band. This finding is in line with the previous reports that ILC1s contain exILC3s with a history of RORγt expression.[11] The recent reports that a similar plasticity exists also between ILC3s and ILC2s (chapter 2.2.3) might explain the incomplete excision of the floxed allele in one out of two *Rptor*^{ΔRORγt}*Rag2*$^{-/-}$ animals. Of note, the PCR results on target excision in ILC2s might also be caused by a leakage of the Cre-driving promoter.

To further investigate the effect of ILC3 deficiency on other ILC subsets, SI ILC numbers were determined in *RORγt*$^{-/-}$ mice. As described previously[23], ILC3s were not detected in *RORγt*$^{-/-}$ mice. In addition, ILC1s were almost absent in the SI of those mice (Fig.20b). The reduction in SI ILC1s was not unexpected, given the fact that previous reports described the presence of exILC3s within the SI ILC1 population.[11,77] Interestingly, SI ILC2s were also decreased in *RORγt*$^{-/-}$ mice (Fig.20b). The reduction in ILC2s might indicate that SI ILC2s depend on ILC3s by a so far unknown mechanism. All in all, it can be concluded that a complete block in the development of RORγt$^+$ ILC3s does not automatically lead to a compensatory increase in other ILC family member subsets in the SI.

To further test whether loss of mTORC1 signaling promotes ILC3 plasticity or ILC1 and ILC2 expansion from a RORγt-positive precursor, I injected *RORγt*^{eYFP}*Rag2*$^{-/-}$ FM reporter mice

every other day with 2.5 mg/kg rapamycin for three weeks (Fig.20c). In these mice, the stop sequence of an eYFP-reporter is irreversibly removed in all RORγt-expressing cells at any developmental stage. Rapamycin treatment significantly reduced NCR[+] ILC3s and modestly but significantly increased ILC2s (Fig.20d). SI NK cells and ILC1s were unchanged. Independent of rapamycin treatment, approximately 30 % of ILC1s, 5 % of ILC2s and 99 % of ILC3s were eYFP-positive (Fig.20e). These data confirm our previous finding that a substantial proportion of ILC1s belong to the exILC3 subset described by Vonarbourg et al.[77] Furthermore, it demonstrates that few ILC2s also show a history of RORγt expression. The percentage of eYFP-positive cells in rapamycin-treated animals was not increased compared to PBS treatment suggesting that both the classical ILC2s and ILC2-like exILC3s increased upon mTORC1 suppression.
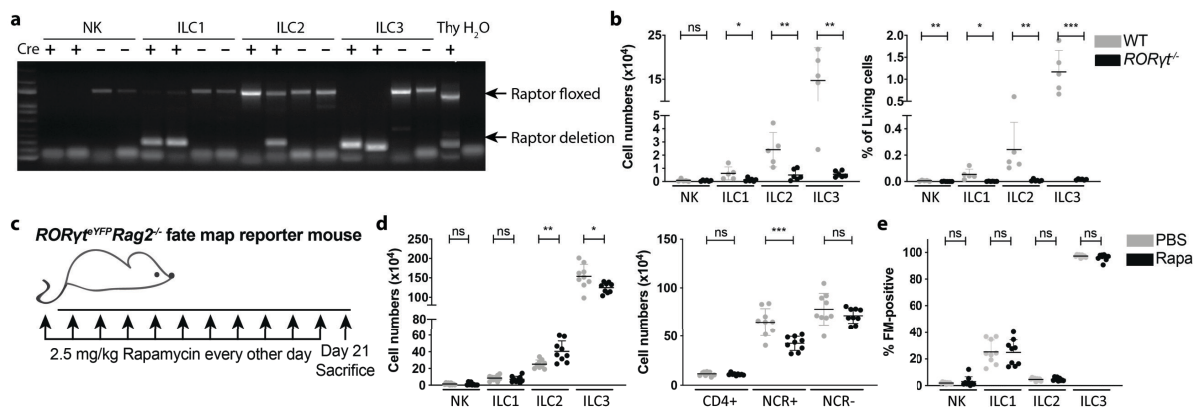
Fig.20 A subset of intestinal ILC1s and ILC2s show a history of RORγt expression and dependency on RORγt. a) Excision of floxed *Rptor* sequence in ILC subsets in the SI. NK cells, ILC1s, ILC2s and ILC3s were sorted from the SI LP of *Rptor^{ΔRORγt}Rag2^{-/-}* mice. DNA was extracted from all subsets, followed by a PCR enclosing one loxP site of *Rptor*. 200 bp fragments are equivalent to excised target sequence. 800 bp fragments indicate preserved *Rptor* sequence. Thy: thymus from *Rptor^{ΔRORγt}* mouse. n = 2. b) Cells were isolated from the SI LP of C57BL/6 wildtype mice and *RORγt^{-/-}* mice. Cells were stained *ex vivo* for NK cell, ILC1, ILC2 and ILC3 markers. n = 5-6. c-e) *RORγt^{eYFP}Rag2^{-/-}* FM reporter mice were injected with 2.5 mg/kg rapamycin every other day for three weeks. Mice were sacrificed and the cells from the SI LP were isolated. ILC subsets were stained with lineage specific markers and analyzed by flow cytometry. d) Number and percentage of ILC subsets. n = 9 mice from 3 independent experiments. e) Percentage of eYFP-positive cells in each ILC subset. Mice were 8-10 weeks old at analysis. Two-tailed unpaired t test or Mann-Whitney U test. *p ≤ 0.05, **p ≤ 0.01, ***p ≤ 0.001

In conclusion, these data confirm that mTORC1 deficiency affects ILC3 cell numbers. Nevertheless, there is so far no solid evidence that the increase in intestinal ILC1s and ILC2s in *Rptor^{ΔRORγt}Rag2^{-/-}* mice was based on an alternative fate of RORγt-positive precursors in the absence of mTORC1, although it could not be entirely excluded.

5.3 Effect of mTORC1 and mTORC2 on ILC3 cytokine production

One of the important effector functions of ILC3s is their capacity to produce cytokines and other signaling molecules, which modulate the responses of other hematopoietic and non-hematopoietic cells in the gastrointestinal tract. Though ILC3 numbers were altered upon conditional deletion of *Rptor* and *Rictor*, the functionality of the remaining ILC3s might not be affected. The following experiments addressed the question whether cytokine production of ILC3s depends on mTORC1 and mTORC2 signaling.

5.3.1 Under steady state conditions, IL-22 and IFN-γ production in ILC3s is not affected by loss of mTORC1 and mTORC2 signaling *in vivo*

To examine whether loss of mTORC1 or mTORC2 signaling alters cytokine release under homeostatic conditions *in vivo*, the percentage of IL-22 and of IFN-γ-producing ILC3s from SI and colon of *Rptor^{ΔRORγt}Rag2$^{-/-}$* and *Rictor^{ΔRORγt}Rag2$^{-/-}$* mice and control animals was determined directly *ex vivo*.

Neither ILC3s from *Rptor^{ΔRORγt}Rag2$^{-/-}$* nor from *Rictor^{ΔRORγt}Rag2$^{-/-}$* mice displayed differences in the percentage of IL-22$^+$ or IFN-γ$^+$ ILC3s (Fig.21). This indicates that IL-22 and IFN-γ production in the SI and colon did not require mTORC1 and mTORC2 signaling in resting ILC3s.
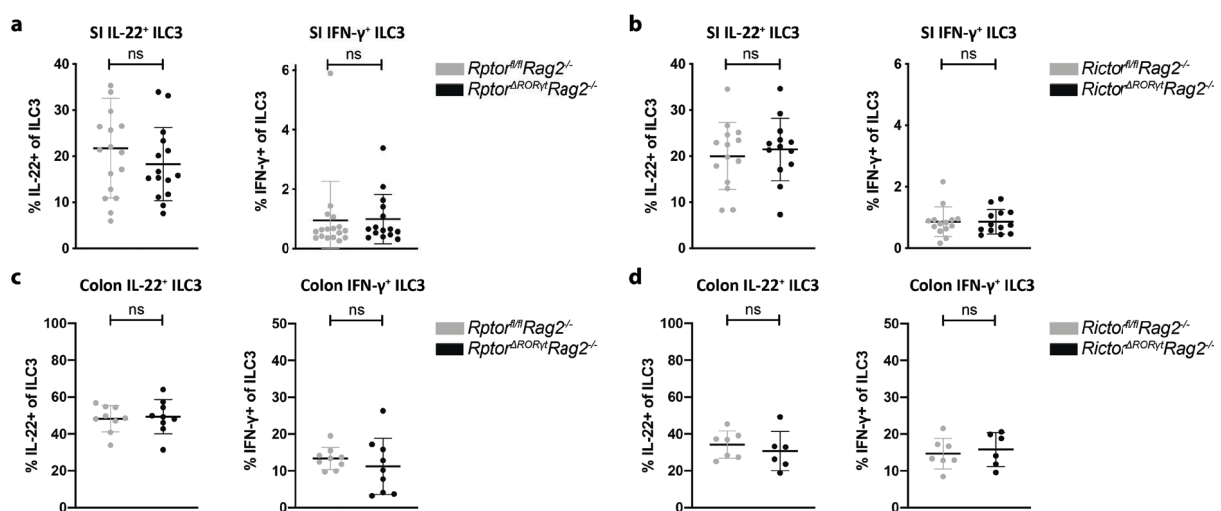
Fig.21 Deletion of *Rptor* or *Rictor* does not affect the percentage of IL-22$^+$ ILC3s and IFN-γ$^+$ ILC3s under steady state conditions. Cells were isolated from the SI LP or cLP and cultured in medium with 10 μg/ml Brefeldin A for 2 h. Cells were stained for ILC3 markers and cytokines and analyzed by flow cytometry. *Rptor^{ΔRORγt}Rag2$^{-/-}$* (a, c) or *Rictor^{ΔRORγt}Rag2$^{-/-}$* (b, d) and age-matched Cre-negative littermates. Mice were 8-10 weeks old at analysis. n = 8 - 16. Two-tailed unpaired t test or Mann Whitney U test. *p ≤ 0.05, **p ≤ 0.01, ***p ≤ 0.001

5.3.2 Activation-induced IFN-γ production but not IL-22 production by ILC3s requires mTORC1 and mTORC2 signaling *in vitro*

The phosphoFlow (Fig.7) and In-Cell Western analysis (Fig.S4) showed that IL-23/IL-1β stimulation induced phosphorylation of mTORC1 target S6 and mTORC2 target Akt in ILC3s. These results suggested that mTOR signaling was involved in activation-induced immune responses of ILC3s. To investigate whether mTOR signaling is required for activation-induced cytokine production in ILC3s, SI LP cells were isolated from $Rptor^{\Delta ROR\gamma t}Rag2^{-/-}$ and $Rictor^{\Delta ROR\gamma t}Rag2^{-/-}$ mice and control littermates. ILC3s were sort-purified by FACS and cultured with IL-23 and IL-1β.

48 h after stimulation, 30 % and 85 % of SI ILC3s from control animals produced IFN-γ and IL-22, respectively (Fig.22a, b). In cultures derived from $Rptor^{\Delta ROR\gamma t}Rag2^{-/-}$ and $Rictor^{\Delta ROR\gamma t}Rag2^{-/-}$ mice, IL-23/IL-1β-induced IFN-γ$^+$ ILC3s were decreased by 80 % and 40 % (Fig.22a, b). Analysis of the supernatant of *in vitro* cultures of activated ILC3s from $Rptor^{\Delta ROR\gamma t}Rag2^{-/-}$ and $Rictor^{\Delta ROR\gamma t}Rag2^{-/-}$ mice confirmed the reduction of IFN-γ release (Fig.22c, d). IL-22$^+$ ILC3s were modestly but significantly reduced in cultures from $Rptor^{\Delta ROR\gamma t}Rag2^{-/-}$ mice, but not in cultures from $Rictor^{\Delta ROR\gamma t}Rag2^{-/-}$ mice (Fig.22a, b). IL-22 protein levels in the supernatant of *Rptor*-deficient cells were also slightly but not significantly reduced (Fig.22c). The supernatant from cultures with *Rictor*-deficient cells did not display altered IL-22 levels (Fig.22d). These results suggest that, on one hand, IFN-γ production by IL-23/IL-1β-stimulated ILC3s depended both on mTORC1 and mTORC2 signaling. On the other hand, IL-22 production seemed to be less dependent on mTOR signaling.

In line with results from knockout animals, mTORC1 inhibitor rapamycin and mTORC1/2 inhibitor PP242 reduced the percentage of activation-induced IFN-γ$^+$ ILC3s. IL-22$^+$ ILC3s were modestly but significantly decreased (Fig.22e, f).

Altogether, these data suggest that stimulation of ILC3s activated mTORC1 and mTORC2. mTORC1 and mTORC2 were required for activation-induced IFN-γ production. IL-22 was only marginally affected by the loss of mTORC1 but not mTORC2 signaling suggesting that activation-mediated IL-22 production was largely regulated via signaling cascades other than mTOR.
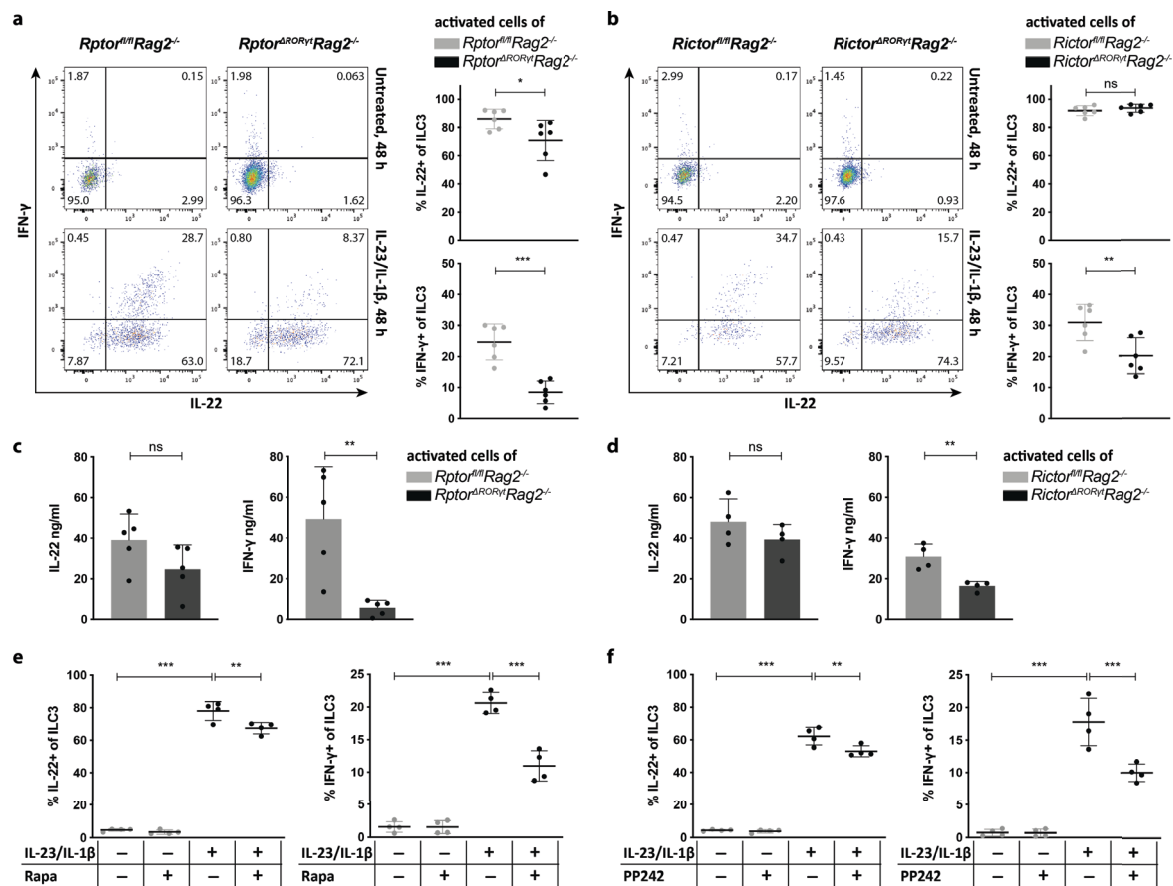
Fig.22 Loss of mTORC1 and mTORC2 signaling impairs IFN-γ but not IL-22 release in ILC3s *in vitro*. a-d) Lin⁻CD90.2⁺KLRG1⁻ ILC3s were sorted from the SI LP of *Rptor*^ΔRORγt*Rag2*^-/- (a, c) or *Rictor*^ΔRORγt*Rag2*^-/- (b, d) mice and control littermates and cultured with 20 ng/ml IL-23 and IL-1β for 2 days. Intracellular IL-22 and IFN-γ was measured by flow cytometry (a, b) and IL-22 and IFN-γ levels in the supernatant were measured by using Th Cytokine LEGENDplex Kit (c, d). For each experiment, cells from 1-3 mice per group were pooled. n = 6 experiments. Unpaired t-test. e, f) Cells were isolated from the SI LP of C57BL/6J mice. Lin⁻CD90.2⁺KLRG1⁻ ILC3s were sorted and cultured with 20 ng/ml IL-23 and IL-1β or medium. Where indicated, 10 nM rapamycin (e) or 1 μM PP242 (f) was added. After 2 days, cells were stained for intracellular IL-22 and IFN-γ. For each experiment, cells from 8-10 mice were pooled. n = 4 experiments. One-Way ANOVA with multiple comparison test (Dunnett). Lin: CD3, CD8, CD11c, CD19, B220, Gr-1, NK1.1, TCRβ, TCRγδ, Ter-119. *p ≤ 0.05, **p ≤ 0.01, ***p ≤ 0.001

5.3.3 Cytokine responses and changes in metabolism of ILC3s are differentially regulated by mTORC1 *in vitro*

It is well established that mTOR is involved in metabolic changes upon stimulation of T cells, DCs or MΦ.[176-181] Changes between oxidative phosphorylation and glycolysis are relevant and required for effector function and differentiation of immune cells.

The Agilent Seahorse platform was used to determine whether stimulation of sorted ILC3s leads to a change in cell metabolism. Moreover, the method allowed to test whether blockade of mTORC1 was associated with changes in oxidative phosphorylation and glycolysis. Due to limitation of cell numbers and requirement of high cell numbers, ILC3s were isolated from the SI of Flt3 transgenic (*Flt3*^tg^) mice. Flt3 ligand promotes ILC production and DC development in

these mice.[223] Importantly, differentiated ILCs do not express Flt3 receptor. Instead, the expansion of ILCs in this mouse model is based on an effect on ILC precursors.[223]

IL-23/IL-1β stimulation of ILC3s resulted in a strong increase in extracellular acidification rate (ECAR), a surrogate marker of glycolysis (Fig.23a). This upregulation of glycolysis was markedly reduced upon treatment with rapamycin. The oxygen consumption rate (OCR) was enhanced upon stimulation indicating an upregulation of mitochondrial oxidative respiration (Fig.23a). The upregulation of the OCR was independent of mTORC1 as rapamycin did not affect OCR in stimulated ILC3s.
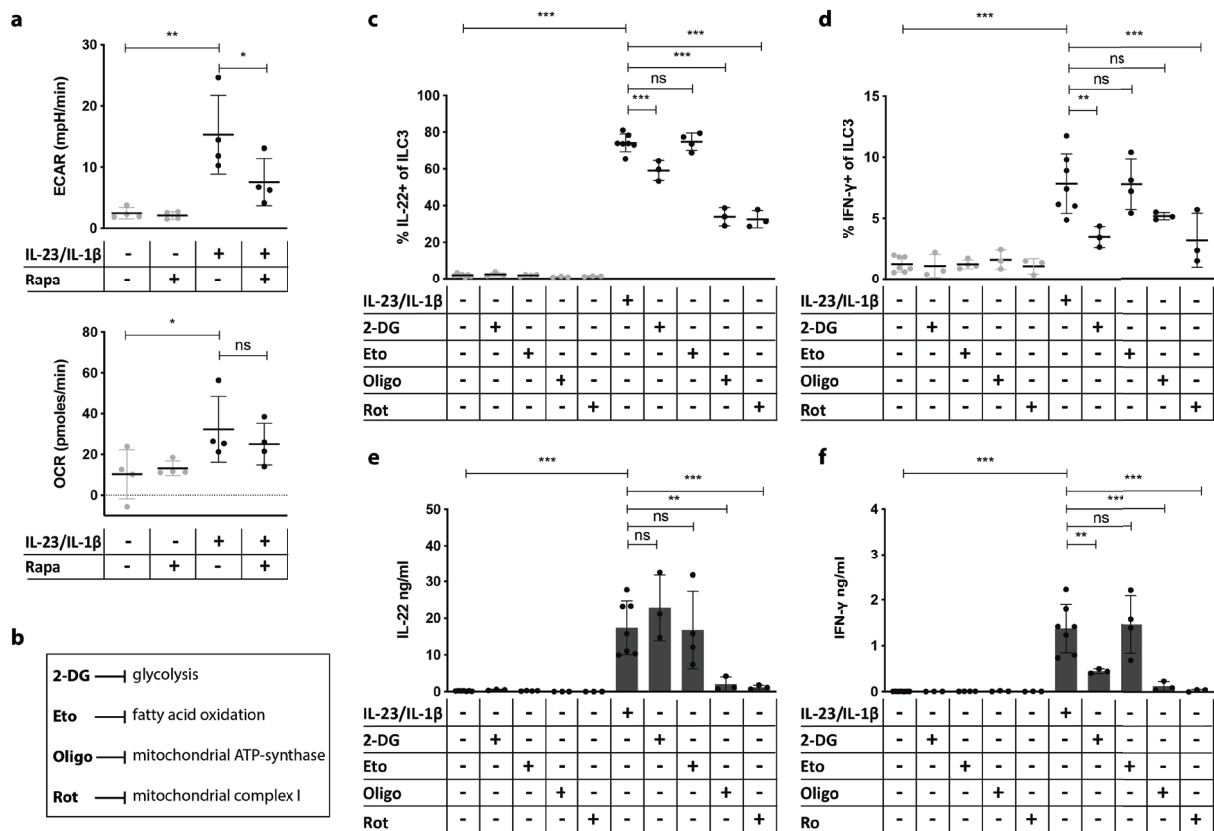
Fig.23 IFN-γ and IL-22 production in ILC3s depends on different metabolic pathways *in vitro*. a) Sort-purified Lin⁻CD90.2⁺KLRG1⁻ ILC3s from the SI LP of *Flt3^tg* mice were analyzed for changes in metabolic activity after 48 h in culture with IL-23/IL-1β or medium only with or without rapamycin. Extracellular Acidification Rate (ECAR) as glycolysis readout (top). Baseline Oxygen Consumption Rate (OCR) (bottom) as readout of oxidative respiration. Metabolic activities were measured using Seahorse XFe96 Analyzer (Agilent Technologies). In each experiment, measurements were done in duplicates or triplicates for each condition. b) Metabolic inhibitors and targeted metabolic pathways. 2-deoxy-D-glucose (2-DG), etomoxir (Eto), oligomycin (Oligo) or rotenone (Rot). c-e) Cells were isolated from the SI LP of C57BL/6 wildtype mice. Lin⁻CD90.2⁺KLRG1⁻ ILC3s were sorted and cultured 16 h with or without IL -23/ IL-1β. Where indicated, metabolic inhibitors were added. Cells were then stained for intracellular IFN-γ (c) and IL-22 (d). IFN-γ (e) and IL-22 (f) was analyzed in the supernatant using Th Cytokine LEGENDplex Kit. Lin: CD3, CD8, CD11c, CD19, B220, Gr-1, NK1.1, TCRβ, TCRγδ, Ter-119. n = 3-7. One-Way ANOVA with multiple comparison test (Dunnett). *p ≤ 0.05, **p ≤ 0.01, ***p ≤ 0.001

These findings demonstrated that glycolysis and IFN-γ release seemed to be almost fully dependent on mTORC1. On the other hand, IL-22 production and OCR were mTORC1-independent. Those data suggested that IFN-γ production required glycolysis *in vitro*. Instead,

IL-22 production could depend rather on oxygen-consuming metabolic switches, which was apparently less dependent on mTORC1. To test this hypothesis, wildtype SI ILC3s were activated with IL-23 and IL-1β with or without glycolysis inhibitor 2-Deoxy-D-glucose (2-DG), fatty acid oxidation inhibitor etomoxir, mitochondrial ATP synthase inhibitor oligomycin or mitochondrial complex I inhibitor rotenone for 16 h (Fig.23b).

2-DG reduced the percentage of activation-induced IL-22$^+$ ILC3s only modestly but significantly (Fig.23c). Oligomycin and rotenone severely diminished the percentage of IL-22$^+$ ILC3s (Fig.23c). Etomoxir had no significant effect on intracellular IL-22 production. Accordingly, oligomycin or rotenone but not 2-DG or etomoxir significantly reduced extracellular amount of IL-22 measured in supernatants of those ILC3 cultures (Fig.23e).

The percentage of IFN-γ$^+$ ILC3s was strongly reduced in the presence of 2-DG, oligomycin and rotenone (Fig.23d). Etomoxir had no significant effect on intracellular IFN-γ (Fig.23d). In line with flow cytometric results of intracellular cytokines, IFN-γ protein levels in ILC3 culture supernatants were significantly decreased by suppression of glycolysis and mitochondrial respiration, but not by inhibition of fatty acid oxidation (Fig.23f).

Taken together, IL-23/IL-1β-mediated IFN-γ release by ILC3s required both glycolysis and mitochondrial respiration. In contrast, activation-induced IL-22 production depended mostly on mitochondrial oxidative respiration as the overall IL-22 release into the supernatant was only efficiently blocked by inhibitors of the mitochondrial respiration chain. The observation that the percentage of IL-22$^+$ ILC3s was slightly decreased at 16 h of culture with 2-DG might indicate the involvement of glycolysis in sustained IL-22 production. This effect might be explained by the fact that intermediate products of glycolysis fuel mitochondrial respiration.[178]

Of note, both oligomycin and rotenone reduced the percentage of living cells after 16 h of culture (data not shown). Hence, addition of inhibitors of the mitochondrial respiration chain might also reflect a complete shutdown of cytokine release due to induction of apoptosis or cell death.

In summary, release of IFN-γ was almost fully dependent on mTORC1 signaling and glycolysis. Furthermore, the data presented here indicate that initial IL-22 production of ILC3s rather depends on oxygen-consuming metabolic switches and is less dependent on mTORC1 signaling. However, glycolysis might be involved in sustained IL-22 responses by ILC3s.

5.4 Effects of *RORc*-driven *Rptor* and *Rictor* deletion on α-CD40 colitis and defense against *C. rodentium* infection

As shown before, the secretion of IFN-γ by activated ILC3s, which has been assigned a pro-inflammatory role in murine colitis models[29,77,160,162], required mTORC1 and to lesser mTORC2. IL-22, which has been described to play a role in defense against *C. rodentium* infections[61,128,129], was less dependent on mTOR signaling. To further test whether mTORC1 and mTORC2 signaling was involved in ILC3 cytokine responses *in vivo*, two mouse models were applied: 1) the α-CD40 colitis model, and 2) the *Citrobacter rodentium*- (*C. rodentium*)-mediated colitis model.

5.4.1 Deficiency of mTORC1 or mTORC2 signaling in ILC3s reduces α-CD40 colitis

In the α-CD40 colitis model, acute colitis is induced through a single α-CD40 Ab injection into *Rag1*- or *Rag2*-deficient mice. Upon injection with low doses of α-CD40 Ab (100-200 μg/mouse), activation of innate cells causes a self-limiting colitis.[29,159] ILC3s have been shown to play an important role in colitis-induction in this model, as depletion of ILCs significantly reduces colitis.[29] Furthermore, it has been shown that IL-23, IFN-γ and IL-22 participate in the development of α-CD40 Ab-mediated colitis.[29,159-162] Importantly, IFN-γ produced by ILC3s has been shown to be sufficient to induce this form of experimental colitis.[159,160,162]

To test whether mTORC1 or mTORC2 deletion in ILC3s could prevent α-CD40 colitis, *Rptor*$^{\Delta ROR\gamma t}$*Rag2*$^{-/-}$ and *Rictor*$^{\Delta ROR\gamma t}$*Rag2*$^{-/-}$ mice and control animals were i.p. injected with 140 μg α-CD40 Ab. Weight loss was monitored daily and feces was collected at day 4 and day 10 post-injection to determine fecal Lipocalin-2 (LPC2), a marker for inflammation. Mice were sacrificed ten days after injection and histological colitis scores were determined after hematoxylin and eosin staining of paraffine-embedded sections from the cecum and the colon. As previously reported, Cre-negative littermate controls displayed a self-healing colitis with consecutive weight loss until day 3 post-injection, augmented fecal LPC2 and increased histopathological signs in colon and cecum at day 10 post-injection (Fig.24a-f).

Rptor^(ΔRORγt)Rag2^(-/-) and *Rictor^(ΔRORγt)*Rag2^(-/-) mice showed less severe weight loss, lower LPC2 expression and lower histopathological scores than littermate controls (Fig.24a-f). Thus, disruption of both mTORC1 and mTOR2 signaling ameliorated α-CD40 colitis.
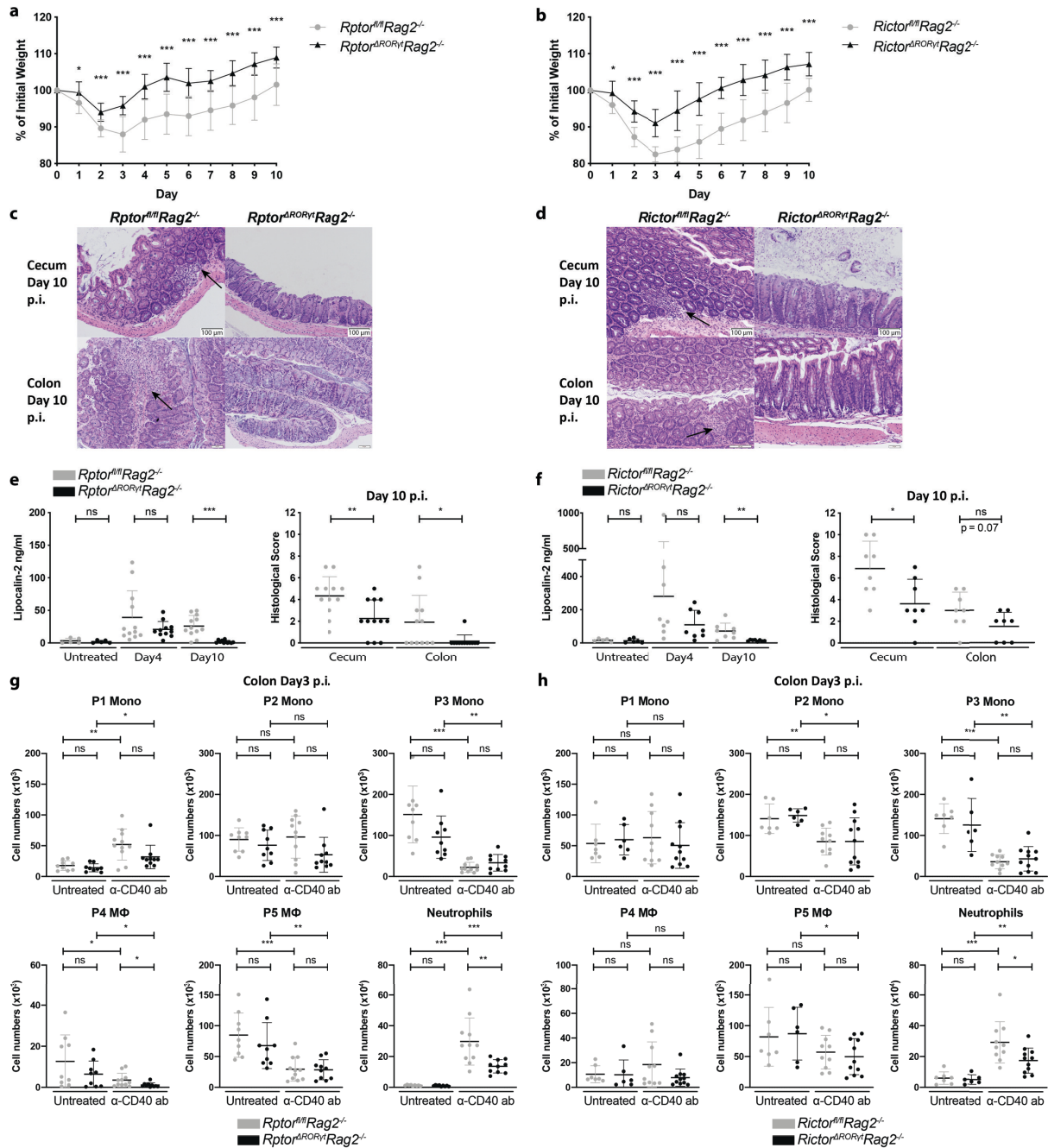
Fig.24 Single loss of mTORC1 or mTORC2 signaling in ILC3s protects *Rag2^(-/-)* mice from α-CD40 colitis. a-f) *Rptor^(ΔRORγt)Rag2^(-/-)* (a, c, e) or *Rictor^(ΔRORγt)Rag2^(-/-)* (b, d, f) mice and age-matched littermates were left untreated or were injected with a single dose of 140 μg α-CD40 Ab. Weight was monitored daily (a, b). Mice were sacrificed 10 days post-injection. Same parts of the colon and the whole cecum were sectioned and stained with hematoxylin and eosin. Exemplary histology picture from the cecum and colon are depicted (c, d). Histological colitis score was determined by an experienced gastroenterologist (e, f right panel). At day 4 and day 10, fecal Lipocalin-2 was determined from feces pellets diluted in PBS using ELISA (e, f, left panel). g, h) *Rptor^(ΔRORγt)Rag2^(-/-)* (g) or *Rictor^(ΔRORγt)Rag2^(-/-)* (h) mice and age-matched littermates were left untreated or received a single dose of 140 μg α-CD40 Ab. Weight was monitored daily. Mice were sacrificed 3 days post-injection and cells were isolated from the colon. Monocytes (P1-P3), macrophages (P4-P5) and neutrophils were analyzed by FACS. n = 8-13 from 3-4 independent experiments. Two-tailed unpaired t test or Mann-Whitney U test. *p ≤ 0.05, **p ≤ 0.01, ***p ≤ 0.001

In a previous study, activated ILC3s have been shown to recruit inflammatory monocytes and neutrophils.[224] Thereby, myeloid cell fostered α-CD40 Ab-mediated inflammation.[224] As *Rptor$^{\Delta ROR\gamma t}$Rag2$^{-/-}$* and *Rictor$^{\Delta ROR\gamma t}$Rag2$^{-/-}$* mice exhibited lower inflammation scores in the cecum and colon, myeloid cells and neutrophils were analyzed in the colon 3 days post-injection. According to previous publications, myeloid cells were subdivided into inflammatory monocyte subsets P1 to P3 and into tissue-resident MΦ subsets P4 and P5 cells.[225,226] An exemplary gating strategy is displayed in Fig.S5. Table 6 summarizes the subset defining cell markers.

Cell Type	Subset	Markers
Inflammatory monocyte	**P1**	Lin$^-$CD45$^+$CD11b$^+$CD24^{low}CD64$^+$CCR2$^+$Ly-6C$^+$MHC-II$^-$
	P2	Lin$^-$CD45$^+$CD11b$^+$CD24^{low}CD64$^+$CCR2$^+$Ly-6C$^+$MHC-II$^+$
	P3	Lin$^-$CD45$^+$CD11b$^+$CD24^{low}CD64$^+$CCR2$^+$Ly-6C$^-$MHC-II$^+$
Tissue-resident macrophage	**P4**	Lin$^-$CD45$^+$CD11b$^+$CD24^{low}CD64$^+$CCR2$^-$Ly-6C$^-$MHC-II$^-$
	P5	Lin$^-$CD45$^+$CD11b$^+$CD24^{low}CD64$^+$CCR2$^-$Ly-6C$^-$MHC-II$^+$
Granulocyte	**Neutrophil**	Lin^{high}CD45$^+$

Table 6 Myeloid cell subset markers Lin: CD3, CD19, NK1.1, Ly-6G.

Compared to untreated mice, the number of inflammatory P1 monocytes was modestly elevated in Cre-negative littermate controls 3 days after α-CD40 Ab injection (Fig.24g, h). Inflammatory P3 monocytes and tissue-resident P4 and P5 MΦ were reduced in α-CD40 Ab-treated mice (Fig.24g, h). In other inflammation models, it has been reported that inflammatory monocytes are recruited within the first two days of an insult and vanished shortly after.[226] Therefore, it cannot be excluded that pro-inflammatory monocyte numbers peaked before day 3 of colitis. There was no striking difference in the number of P1-P3 monocytes and P4-P5 MΦ in α-CD40 Ab-treated *Rptor$^{\Delta ROR\gamma t}$Rag2$^{-/-}$* and *Rictor$^{\Delta ROR\gamma t}$Rag2$^{-/-}$* mice compared to α-CD40 Ab-treated littermate controls (Fig.24g, h). This suggests that recruitment or retention of inflammatory monocytes and MΦ was normal in knockout mice. Compared to untreated animals, neutrophils were increased in the colon of α-CD40 Ab-treated control animals (Fig.24g, h). This α-CD40 Ab-mediated neutrophil influx was dampened in the colon of *Rptor$^{\Delta ROR\gamma t}$Rag2$^{-/-}$* and *Rictor$^{\Delta ROR\gamma t}$Rag2$^{-/-}$* mice (Fig.24g, h). This finding suggests that ILC3s were involved in the recruitment of neutrophils in an mTORC1- and mTORC2-dependent manner.

As described above, ILC3-derived IFN-γ has been reported to play an essential role in α-CD40 colitis.[29,159,160,162] Moreover, IL-22 might promote IFN-γ production in this colitis model.[161] My previous data demonstrated that ILC3s derived from $Rptor^{\Delta ROR\gamma t}Rag2^{-/-}$ and $Rictor^{\Delta ROR\gamma t}Rag2^{-/-}$ mice produced less IFN-γ but almost normal levels of IL-22 *in vitro*. Therefore, ILC3 cytokine production was tested in the colon 3 days post-injection.

In α-CD40 Ab-treated control animals, ~50 % and 30 % of colonic ILC3s produced IL-22 and IFN-γ, respectively (Fig.25a, b). The percentage of IL-22⁺ ILC3s in the colon of $Rptor^{\Delta ROR\gamma t}Rag2^{-/-}$ and $Rictor^{\Delta ROR\gamma t}Rag2^{-/-}$ mice was comparable to those in control littermates (Fig.25a, b). This supports the previous finding that IL-22 production by ILC3s displayed only a modest dependency on mTOR. In the colon of $Rptor^{\Delta ROR\gamma t}Rag2^{-/-}$ mice, the proportion of IFN-γ⁺ ILC3s was significantly decreased (Fig.25a). The ratio of colonic IFN-γ⁺ ILC3s was modestly but not significantly reduced in $Rictor^{\Delta ROR\gamma t}Rag2^{-/-}$ mice (Fig.25 b). These results demonstrated that mTORC1 and mTORC2 were involved in ILC3-mediated IFN-γ production upon α-CD40 Ab treatment. The finding that IFN-γ was more affected by loss of *Rptor* than by loss of *Rictor* was in line with the previous *in vitro* results.
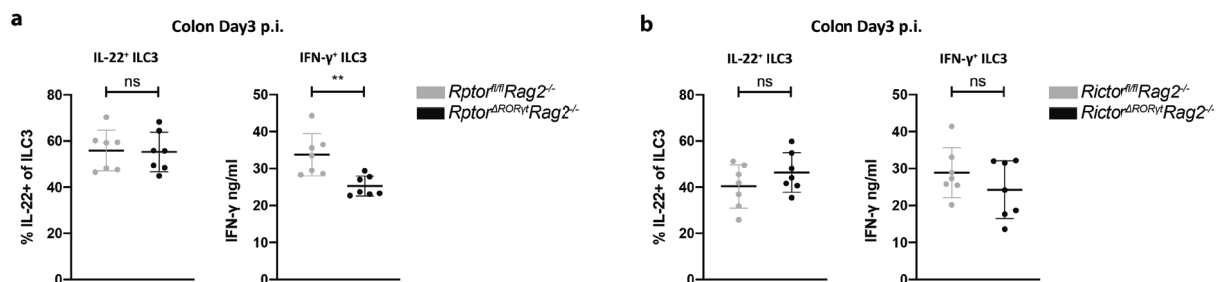
Fig.25 IL-22 and IFN-γ in α-CD40 colitis in $Rptor^{\Delta ROR\gamma t}Rag2^{-/-}$ and $Rictor^{\Delta ROR\gamma t}Rag2^{-/-}$ mice. $Rptor^{\Delta ROR\gamma t}Rag2^{-/-}$ (a) or $Rictor^{\Delta ROR\gamma t}Rag2^{-/-}$ (b) mice and age-matched littermates were left untreated or received a single dose of 140 µg α-CD40 Ab. Weight was monitored daily. Mice were sacrificed 3 days post-injection. a, b) Cells were isolated from the cLP. 1.0 - 1.5 x 10⁶ cLPs cells were cultured overnight. Brefeldin A was added 4 h before staining. Percentage of IL-22⁺ and IFN-γ⁺ ILC3s was determined by flow cytometry. n = 7 from 2-3 independent experiments. Two-tailed unpaired t test or Mann-Whitney U test. *p ≤ 0.05, **p ≤ 0.01, ***p ≤ 0.001

Taken together, loss of mTORC1 or mTORC2 signaling in ILC3s improved α-CD40 colitis and reduced neutrophil influx into the colon. A similar decrease in neutrophils accumulation has been previously correlated with amelioration of α-CD40 colitis.[224] α-CD40 Ab-mediated IFN-γ production was impaired in *Rptor*- and *Rictor*-deficient ILC3s. As IFN-γ produced by ILC3s essentially contributes to the development of α-CD40 colitis[160,162], the amelioration of colitis in knockout mice might in part be attributed to a decrease of IFN-γ release by ILC3s.

5.4.2 Early defense against *C. rodentium* is not impaired by mTORC1 and mTORC2 deficiency in ILC3s

In contrast to IFN-y production, IL-22 release by ILC3s was not impaired *in vivo* or *in vitro* upon specific deletion of *Rptor* or *Rictor*. This suggests that IL-22 responses by ILC3 during early bacterial infection might not be diminished. The defense against *C. rodentium* infection depends on IL-22 derived from ILC3s and Th17/22 cells.[128,129,152,214,227-229] In knockout mouse models lacking IL-22, control of *C. rodentium* infection has been shown to be severely impaired and has been associated with increased intestinal epithelial damage, a higher systemic bacterial load and higher mortality.[128,152,214,228-230] Therefore, the *C. rodentium* infection model was used to test whether loss of mTORC1 or mTORC2 signaling in RORγt-expressing cells has an impact on their capacity to respond to infection and leads to progression of infection.

Rptor^{ΔRORγt}Rag2$^{-/-}$ mice, *Rictor^{ΔRORγt}Rag2$^{-/-}$* mice and control littermates were orally infected with 2×10^9 CFU of a modified nalidixic acid-resistant *C. rodentium* strain containing a bioluminescence construct[113] (kindly provided by Dr. Jan Niess, University Hospital Basel). Mice were monitored for loss of weight and scored for symptomatic signs of colitis daily. Moreover, fecal bacterial loads and LPC2 levels were tested four and seven days after infection. Seven days after infection mice were sacrificed and splenic bacterial load, colon length and histological colitis score were determined.

In line with previous publications[128,230], *Rag2*-deficient control littermates did not lose weight during the first 7 days of infection (Fig.26a, c). The colon was slightly but non-significantly shortened compared to untreated controls and displayed intermediate signs of colitis (Fig.26b, d, e, g). Accordingly, fecal LPC2 was moderately increased at day 4 and 7 post-infection (Fig.26f, h). Infected *Rptor^{ΔRORγt}Rag2$^{-/-}$* and *Rictor^{ΔRORγt}Rag2$^{-/-}$* mice showed overall no change in weight and no difference in colon length and histological colitis scores compared to infected control littermates (Fig.26a-e, g). In comparison to infected control animals, *Rptor^{ΔRORγt}Rag2$^{-/-}$* mice produced significantly less fecal LPC2 upon infection (Fig.26f, h). Finally, *Rptor^{ΔRORγt}Rag2$^{-/-}$* mice and *Rictor^{ΔRORγt}Rag2$^{-/-}$* mice were not more susceptible to *C. rodentium* infection as they exhibited similar fecal bacterial loads and same levels of bacterial dissemination to the spleen as infected control littermates (Fig.26i, j). Results from *C. rodentium* experiments in *Rptor^{ΔRORγt} and Rictor^{ΔRORγt}* mice, in which RORγt-expressing

ILC3s and T cells were affected by the loss of the respective target gene, closely resembled the findings in *Rag2*-deficient mice (Fig.S6).

To summarize, the presented data demonstrates that single loss of mTORC1 or mTORC2 signaling in ILC3s does not impair early defense against infection with *C. rodentium* in both immune-competent and immune-compromised mice.

The observations from both the α-CD40 colitis model and the *C. rodentium*-induced colitis model imply that loss of either mTORC1 or mTORC2 signaling dampened ILC3-mediated inflammation in the colon. At the same time, mTORC1 or mTORC2 deficiency in ILC3s did not impair their capacity to protect the body from *C. rodentium* infection through the intestinal tract.
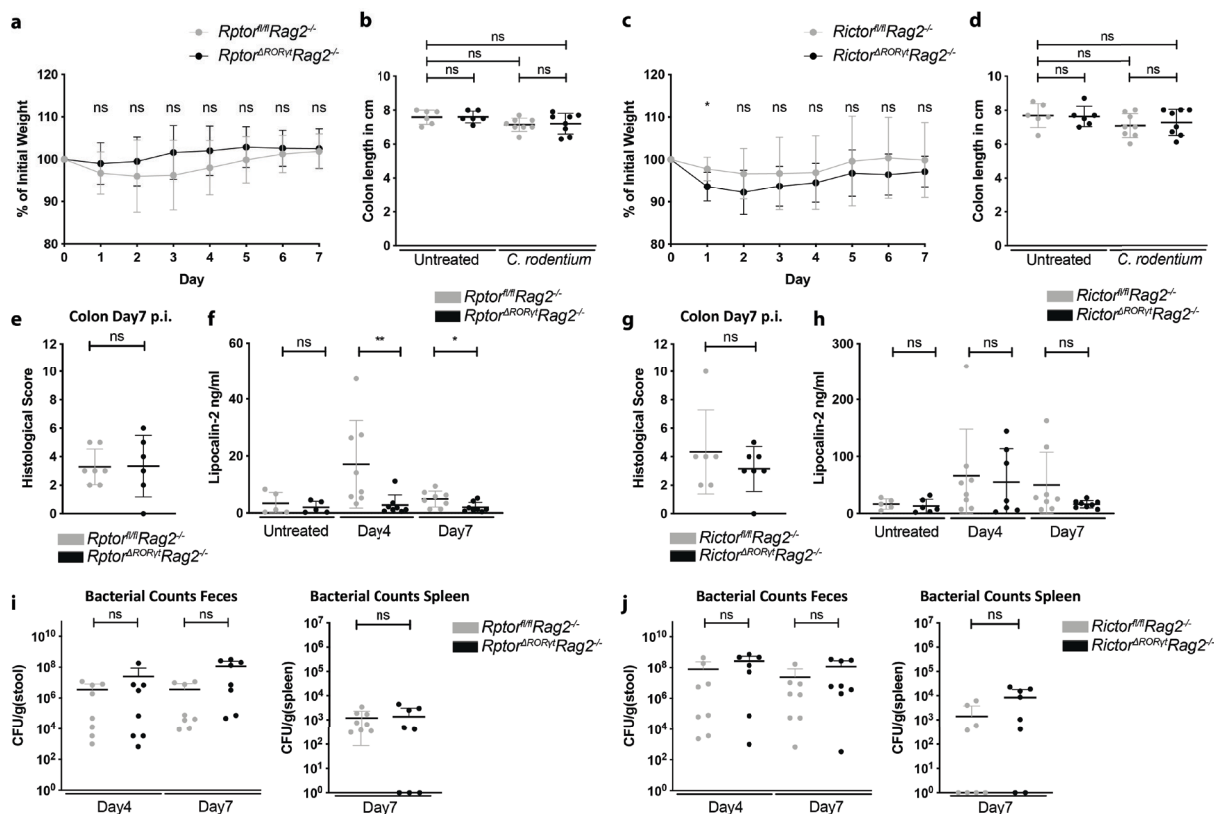
Fig.26 Loss of mTORC1 or mTORC2 in RORγt-expressing cells in *Rag2-/-* mice does not alter susceptibility to *C. rodentium*. *Rptor^ΔRORγt^Rag2-/-* (a, b, e, f, i) or *Rictor^ΔRORγt^Rag2-/-* (c, d, g, h, j) mice and age-matched littermates were left untreated or were orally infected with 2 x 10⁹ CFU *C. rodentium*. Weight was monitored daily (a, c). Mice were sacrificed 7 days post-infection. The colon length was measured (b, d) and same parts of the colon were sectioned and stained with hematoxylin and eosin. Histological colitis score was determined by an experienced gastroenterologist (e, g). At day 4 and day 7, fecal Lipocalin-2 was determined from feces pellets diluted in PBS using ELISA (f, h). Fecal bacterial load was tested at day 4 and day 7 post-infection (i, j, left). Spleen was homogenized to determine bacterial spreading (i, j, right). n = 6-8 from two independent experiments. Two-tailed unpaired t test or Mann-Whitney U test. *p ≤ 0.05, **p ≤ 0.01, ***p ≤ 0.001

6 Discussion

ILC3s populate lymphoid and non-lymphoid organs but are most abundant in the intestinal mucosa where they contribute to tissue homeostasis, repair and defense against extracellular pathogens. Beneficial effects of ILC3s on the mucosal barrier function are mediated by the release of cytokines, including IL-22 and IL-17. ILC3 cytokines, however, can also have inflammatory potential. For example, IFN-γ-producing exILC3s promote the progression of inflammatory diseases in humans such as IBD. Although the list of signals that influence ILC3 functions is constantly growing, it is not fully understood how the specific cytokine output of ILC3s is regulated. mTORC1 and mTORC2 have been reported to modulate survival, differentiation and cytokine release of various immune cells. In the first part of my thesis, I elucidated the role of mTORC1 and mTORC2 for ILC3 development, proliferation and survival in the presence and absence of adaptive immune cells. In the second part, I tested whether mTOR signaling has an impact on activation-induced ILC3 cytokine release and metabolic changes. Finally, I determined whether mTOR is involved in modulating IL-22 and IFN-γ responses of ILC3s during intestinal inflammation and bacterial infection of the gut.

In the first part, I showed that ILC3-intrinsic disruption of mTOR signaling altered SI ILC3 numbers in wildtype mice. mTOR-dependency of SI ILC3s was even greater in the absence of adaptive immune cells. *RORc*-driven deletion of *Rptor* but not *Rictor* impaired ILC3 reconstitution after BM transplantation. Furthermore, mTORC1 and mTORC2 were crucial for SI ILC3 proliferation but not survival. Surprisingly, reduction of ILC3s in the SI of knockout mice was accompanied by an increase in ILC1s and ILC2s. In the second part, I could show that loss of mTORC1 and mTORC2 signaling impairs IFN-γ but not IL-22 production in activated ILC3s. IL-23/IL-1β-activated ILC3s upregulated glycolysis and IFN-γ production in an mTOR-dependent manner *in vitro*. Activation-induced IL-22 production was largely dependent on oxidative phosphorylation but did not require mTOR. Consistently, *Rptor* or *Rictor* deficiency in ILC3s protected mice from IFN-γ-dependent α-CD40 colitis but did not impair IL-22-mediated protection against *C. rodentium* infection. Altogether, mTORC1 and mTORC2 play a critical role in the regulation of ILC3 proliferation and in the promotion of ILC3-mediated IFN-γ responses in the intestine.

6.1 Role of the adaptive immune system for mTOR-dependency of ILC3s

In *Rag2*^{-/-} mice, disruption of mTORC1 and mTORC2 signaling resulted in a strong reduction of SI ILC3s. In mice with an adaptive immune system, ILC3 numbers in the SI were affected to a lower degree by deletion of *Rptor* or *Rictor*. This different mTOR-dependency of ILC3s might be based on an altered ILC3 activation status in wildtype vs. *Rag2*^{-/-} mice. In line with this assumption, several groups demonstrated that ILC3 numbers and ILC3 proliferation were increased in *Rag2*^{-/-} mice when compared to wildtype mice.[95,231] It was shown that Tregs and Th17 cells could downmodulate ILC3 activation in the SI by suppressing IL-23 production in MNPs and by preventing the outgrowth of SFB, respectively.[121] Moreover, ILC3s are thought to compete with T cells for growth, proliferation and survival factors, e.g. for IL-2 and IL-7[148]. I could show that activation induced mTOR signaling in ILC3s. To determine whether mTORC1 and mTORC2 pathways were upregulated in *Rag2*^{-/-} mice compared to wildtype mice, our group started to assess the phosphorylation status of mTOR targets in SI ILC3s from wildtype and *Rag2*^{-/-} mice by flow cytometry. In addition, we started to establish an immunohistochemical staining to analyze the phosphorylation of mTOR targets in ILC3s *in situ*. These experiments are in progress.

Of note, our finding contradicts a recent report by Di Luccia *et al.* in which SI ILC3s were also severely depleted on a wildtype background.[209] My work shows that mTOR-dependency of ILC3s was closely linked to the degree of activation. Hence, this discrepancy in ILC3 phenotype might be due to variations in the activation status of ILCs observed in different mouse facilities.[30]

6.2 Tissue-specific mTOR-dependency of ILC3s

Interestingly, ILC3-specific deletion of *Rptor* and/or *Rictor* resulted in reduced ILC3 numbers in the SI but not in the colon of wildtype and *Rag2*^{-/-} mice. This finding raised the question of why colonic ILC3 numbers were independent of mTORC1 and/or mTORC2 signaling. It cannot be excluded that the mTOR pathway is less active in colonic ILC3s. The proliferation rate of SI and colonic ILC3s was comparable under homeostatic conditions. After IL-2 activation, however, there was a striking increase of proliferation in SI but not colonic ILC3s. This finding

suggests that activation-dependent mTOR signaling was induced in ILC3s in the SI but not in the colon. Similar to IL-2, other factors might differentially regulate mTOR in SI and colonic ILC3s.

As described in chapter 2.3.1, ILC3s are modulated by nutrient-derived ligands and microbiota. Both nutrients and microbiota species are non-uniformly distributed throughout the intestinal tract.[213,232-236] For example, the RAR-activating ligand retinol is more abundant in the SI than in the colon.[232] RAR-activation is also linked to enhanced mTORC1 and mTORC2 activity in T cells.[237] These findings suggest that the high SI level of RAR ligands might likewise induce mTOR in SI ILC3s. Moreover, short-chain fatty acids (SCFA), which have been shown to downregulate ILC3 activity, are higher in the terminal SI and colon than in the proximal SI.[158,233,234] Non-digestible carbohydrates derived mostly from fibers are fermented by specific microbiota species of the colon, which leads to locally increased SCFA levels.[233] Evidence from *in vitro* tests with cancer cell lines indicated that microbiota-derived SCFA could suppress mTOR activity.[238] This raises the possibility that SCFAs could restrain mTOR signaling in colonic ILC3s under homeostasis. To summarize, fluctuations in micro-environmental signals might cause the observed disparity in mTOR-dependency in the SI and colon.

6.3 Effect of *RORc*-driven deletion of *Rptor* and *Rictor* on other immune cells

The total lymphocyte counts in LN, spleen, SI and colon were overall normal in *Rptor* and/or *Rictor* knockout strains on a wildtype background. Accordingly, DCs and MΦ were not changed. With the exception of colonic B cells in mice with *RORc*-driven deletion of *Rictor* or *Rictor*/*Rptor*, peripheral B cells were normal. The expression of *RORc*-driven Cre expression can be excluded in germline or B cell lineages. However, differentiation of CD4^{+} T cells into specific Th subsets, which help to maintain B cell numbers, is dependent on mTORC1 and mTORC2.[177,180,182-184,187] Given that CD4^{+} T cells also harbor the deletion of *Rptor* and *Rictor*, it could not be excluded that the local reduction of colonic B cells was caused by alterations of the T cell compartment. Alternatively, the observed changes in the immune cell compartment might reflect disrupted ILC3-T cell regulatory circuits. Accordingly, a recent publication indicated a crosstalk between ILC3 and Tfh cells, which regulated B cell numbers in the colon.[137] This paper described that loss of MHC-II in ILC3s results in an increase of B

cells in the colonic lamina propria. Our group showed that *RORc*-driven loss of *Rptor* resulted in upregulation of MHC-II in intestinal ILC3s.[239] Those findings raise the possibility that loss of either mTORC1 and/or mTORC2 signaling in ILC3s might also directly affect colonic B cell numbers.

In contrast to wildtype mice, cellularity of the SI was reduced in *Rag2*^{-/-} mice with ILC3-specific deletion of *Rptor* and even more impaired in *Rag2*^{-/-} mice with loss of both *Rptor* and *Rictor* in ILC3s. The splenic cellularity of *Rictor/Rptor*[ΔRORγt]*Rag2*^{-/-} mice was also diminished. In line with the reduced number of lymphocytes, there were tissue-specific decreases in peripheral DCs and MΦ. In several organs including the intestine, ILC3s have been described as a source of GM-CSF or CCL8 both recruiting and activating myeloid cells.[91,94,108,119,240,241] Whether production of those cytokines and chemokines requires mTORC1 and mTORC2 in ILC3s is not known. To understand whether mTOR deficiency impairs ILC3-mediated myeloid cell recruitment, chemokine production by *Rptor*- and *Rictor*-deficient SI ILC3s remains to be tested.

Under homeostasis, naïve and memory T cells were partially reduced in wildtype mice carrying *RORc*-driven deletion of both mTORC1 and mTORC2. Effects of single *Rptor* and *Rictor* knockout were less pronounced. Similarly, T cell-specific deletion of mTOR signaling components such as *Tsc1/2*, *Rptor*, *Rictor*, *Rheb* or *mTOR* has been previously reported to affect memory formation.[177,180,183] Impairment of mTOR signaling is associated with failures in directed immune responses under polarizing conditions *in vitro* and after infection or inflammation *in vivo*.[177,180,183,185,186,197] Despite reports that disruption of mTOR signaling promotes Tregs *in vitro*, only a modest increase of Treg was observed in the spleen but not in other organs of *Rptor*-deficient mice. This is in line with an earlier report in which *mTOR* knockout in T cells did not change Treg numbers *in vivo*.[186] Changes in the T cell compartment could also be associated with functional changes in ILC3s. ILC3s have been reported to recruit T cells to the SI[143], to modulate T cell expansion and function in the intestinal tract[139,144-146] and to promote memory T cell formation in secondary lymphoid tissues[242]. It thus remains to be tested whether *RORc*-driven deletion also affects T cell differentiation by modulation of ILC3-T cells interactions.

6.4 mTORC1 and mTORC2 signaling regulate ILC3 differentiation and proliferation

To exclude indirect effects by T cells, further studies were performed with *Rptor* and *Rictor* knockout mice on a *Rag2⁻/⁻* background. BM chimera experiments demonstrated that *RORc*-driven loss of mTORC1 impaired the competitive reconstitution of ILC3s in the SI and large intestine. Under homeostatic conditions and after injection of IL-2/α-IL2 complex, the loss of mTORC1 in ILC3s blocked intestinal ILC3 proliferation in *Rag2⁻/⁻* mice. Proliferation was only partially reduced in the absence of mTORC2 signaling. Those results match the observation that ILC3 numbers are more affected in the SI of *Rag2⁻/⁻* mice with ILC3-specific deletion of *Rptor* than in those with *RORc*-driven deletion of *Rictor*. In line with the presented results, Di Luccia *et al.* reported that the mTORC1 inhibitor rapamycin impaired activation-induced proliferation of the ILC3-like cell line MNK3.[209]

Whether the *RORc*-driven loss of mTOR signaling only affects proliferation of mature ILC3s or whether RORγt-expressing progenitors are also affected remains to be elucidated. *RORc*-driven *Rptor* and *Rictor* deletion did not reduce the number of common ILC progenitors indicating that the observed loss of SI ILC3s is not associated with mTOR-dependent impairment of progenitor cell development. Accordingly, it has been reported that ILC progenitors develop independently of RORγt expression, as multipotent ILC progenitors are still present in *RORC*-deficient patients.[243] Studies with a polychromic reporter mouse, however, have unveiled the presence of a rare RORγt-expressing progenitor.[66] This progenitor harbors a restricted lineage potential and develops preferentially into ILC2s and ILC3s. Furthermore, RORγt-expressing ILC progenitors are circulating in the blood of humans and can differentiate into ILC3s.[222] Mass cytometry results revealed the presence of a multipotent ILC progenitor in the human fetal intestine and RORγt-expressing progenitor cells have been discovered in pediatric and adult human SI and tonsil.[222,244,245] Importantly, the promiscuous RORγt⁺ progenitor cells cannot be phenotypically distinguished from mature ILC3s with classical ILC panels used in flow cytometry.[66,222] It can therefore not be excluded that RORγt⁺ progenitors are accumulating in distinct tissues. Deficiency in mTORC1 and/or mTORC2 might modulate the survival, proliferation or differentiation of those RORγt⁺ progenitors and thereby might lead to diminished ILC3 numbers in specific tissues. To test this, it would be

necessary to establish an *in vitro* assay of such RORγt$^+$ progenitors or to test their differentiation after adoptive transfer *in vivo*. Given that the described RORγt$^+$ progenitor was extremely rare and could only be unambiguously defined by a combination of surface markers and transcription factors[66], such assays would be technically challenging.

Despite the fact that ILC3 numbers were normal in the colon of mice with *RORc*-driven deletion of *Rptor*, BM cells from *Rptor^{ΔRORγt}Rag2$^{-/-}$* mice lost some of their competitive reconstitution capacity in the colon. It cannot be excluded that ILC3s in the colon have not yet filled up the immunological niche 5 weeks after transplantation. Alternatively, RORγt$^+$ progenitor cells derived from *Rptor^{ΔRORγt}Rag2$^{-/-}$* and *Rictor^{ΔRORγt}Rag2$^{-/-}$* mice could display alterations in their homing properties. This could lead to an inefficient colonization of the colon. To solve this question, BM chimeras could be analyzed after a recovery period of several months.

6.5 mTORC1 and mTORC2 signaling in plasticity of RORγt$^+$ ILCs

Unexpectedly, ILC2 numbers were drastically increased in the SI of mice with a single deletion of mTORC1 or mTORC2. In line with this result, rapamycin treatment of *RORγt^{eYFP}Rag2$^{-/-}$* FM reporter mice enhanced both SI eYFP$^+$ and eYFP$^-$ ILC2 numbers. This effect might be explained by mTOR-mediated regulation of RORγt function. In maturing Th17 cells, it has been shown that mTORC1 activated S6K2.[246] pS6K2 promoted translocation of RORγt into the nucleus. Deletion of *Rptor* did not affect activation-induced RORγt expression[246,247], but abrogated nuclear import of RORγt and Th17 cell maturation[246]. Furthermore, mTORC1 signaling in activated T cells suppressed the expression of Gfi, a negative regulator of Th17 differentiation.[246] Disruption of mTOR signaling in RORγt$^+$ progenitor cells[66,222] or maturing ILC3s might lead to a similar failure of RORγt nuclear translocation. As suggested by Pokrovskii *et al.* (2.2.3), the activation level of lineage-repressing transcription factors might be crucial to prevent phenotypic shifts of ILCs in the SI and colon.[71] A loss of RORγt translocation might therefore promote ILC3-ILC2 transition in the SI in the absence of mTOR signaling.[71] Analysis of the ILC2 marker KLRG1 and ILC3 marker RORγt within the Lin$^-$CD90.2$^+$ ILC subset revealed a KLRG1$^+$RORγt$^+$ ILC population, which was strikingly reduced in knockout mice with *RORc*-driven deletion of *Rptor* and or *Rictor* (compare Fig.12 and Fig.14). Approximately 45 % of this

KLRG1$^+$RORγt$^+$ ILC population was also negative for the ILC1 markers T-bet and NKp46 suggesting that this population might contain ILC3-ILC2 intermediate cells. Impaired RORγt translocation could render these cells more prone to become ILC2s. The cellular localization of RORγt in RORγt$^+$ ILCs from *Rptor* and *Rictor* knockout animals could be tested using the ImageStream platform. ImageStream combines flow cytometry with imaging of single cells and allows one to visualize whether a transcription factor is retained in the cytoplasm or has translocated to the nucleus.[248,249] Moreover, *RORγt^{eYFP}* FM reporter mice were used to trace all ILCs that had a history of RORγt expression.[11] Our *RORγt^{eYFP}Rag2$^{-/-}$* FM reporter mice could be crossed to *Rptor$^{\Delta ROR\gamma t}$Rag2$^{-/-}$* and *Rictor$^{\Delta ROR\gamma t}$Rag2$^{-/-}$* mice. Analysis of SI eYFP$^+$ ILC2s in the resulting mouse strains would allow to unambiguously define whether the expanding ILC2 population shows a history of RORγt expression.

Besides the major increase in SI ILC2 numbers, there was also a minor increase in SI ILC1s. It is known that the ILC1 pool contains ILC3-derived exILC3s, in particular in the intestine.[11,77] Thus, mTOR-mediated defect in RORγt function might also promote ILC3-ILC1 transition in *Rptor*- and *Rictor*-deficient ILC3s.

It cannot be excluded that the loss of ILC3s opens an immunological niche in the SI, which is then occupied by ILC1s and ILC2s. However, ILC1s and ILC2s were not increased in mice with dual *Rptor/Rictor* knockout. This observation renders it unlikely that higher ILC1 and ILC2 numbers were only caused by an increased niche availability.

6.6 mTORC1 and mTORC2 regulate activation-induced glycolysis and IFN-γ production *in vitro*

IL-23 and IL-1β synergistically induce ILC3-mediated IL-22 and IL-17 production *in vivo* and *in vitro*.[109,111-115,153,213,214] I could accordingly show that IL-23/IL-1β stimulation of primary SI ILC3s elicited robust IFN-γ and IL-22 responses. Genetic abrogation of mTORC1 and mTORC2 signaling impaired IFN-γ release by ILC3s. IL-22 production was modestly reduced in *Rptor*-deficient ILC3s, but not in *Rictor*-deficient ILC3s. This data was confirmed in activated ILC3s cultured in the presence of the mTORC1 inhibitor rapamycin and the mTORC1/2 inhibitor PP242. In line with my results, a previous publication showed that mTORC1 was required for maximal IL-22 production in ILC3s.[209]

Metabolic changes often provide the means for activation-induced effector functions including cytokine production. Th17 cells and ILC3s overlap in function and respond to similar cytokines. Similar to Th17 cells,[178,182,246,250], ILC3s upregulated glycolysis and oxidative respiration in response to IL-23/IL-1β stimulation. This is in line with the finding that IL-23/IL-1β induced glycolysis and mitochondrial oxidative phosphorylation in the MNK3 cell line.[209] The activation-induced increase in glycolysis and IFN-γ production was largely dependent on mTORC1 signaling. Conversely, the enhanced mitochondrial oxidative respiration and IL-22 production was only modestly dependent on mTORC1. Altogether, these findings suggest that IL-23/IL-1β-induced IFN-γ production was directly linked to mTOR-mediated upregulation of glycolysis. IL-22 production, on the other hand, was mediated by mTOR-independent processes, in particular mitochondrial respiration. It has to be considered that intermediate products of glycolysis build substrates used in other metabolic pathways such as the pentose phosphate pathway or the mitochondrial tricarboxylic acid (TCA) cycle. Thereby, glycolysis indirectly promotes oxidative phosphorylation.[178,182] Accordingly, long-term-suppression of glycolysis might also disturb functions associated with mitochondrial respiration. Of note, inhibition of mitochondrial respiration impaired the viability of ILC3 *in vitro*. Although the intracellular analysis was focused on non-apoptotic cells, it cannot be excluded that the observed downmodulation of cytokine production could be partially linked to viability. In contrast to the results presented here, Di Luccia *et al.* found that mitochondrial respiration and ROS production was upregulated in activated MNK3 cells in a mTORC1-dependent manner.[209] This accumulation of ROS promoted IL-22 and IL-17 production.[209] It cannot be excluded that the MNK3 cell line and primary ILC3s display distinct kinetics in cytokine production. Moreover, Di Luccia *et al.* applied lower doses of IL-23 and IL-1β for *in vitro* stimulation and rapamycin concentration were higher.[209]

Whether fatty acid oxidation (FAO) also contributes to activation-induced ILC3 cytokine production remains controversial. ILC3s have been shown to take up fatty acids.[206,209] Di Luccia *et al.* observed a modest reduction of IL-22 and IL-17 production in activated MNK3 cells upon treatment with the FAO inhibitor etomoxir[209]. However, as demonstrated here, etomoxir treatment of activated primary ILC3s did not affect IL-22 and IFN-γ production. The discrepancy between my data and data from Luccia *et al.* might be explained by the different etomoxir concentrations applied in the two studies: 200 μM etomoxir in the study by Di Luccia

et al. and 10 μM etomoxir in the present study. Raud *et al.* recently published a paper comparing the effects of etomoxir and genetic deletion of the etomoxir target carnitine palmitoyltransferase I (CPT1) on T cell memory formation.[251] Following up on contradicting findings between pharmacological and genetic FAO inhibition, they discovered that etomoxir concentrations beyond 100 μM resulted in off-target inhibition of the mitochondrial adenine nucleotide translocator (ANT), an accumulation of ATP in the mitochondrial matrix and block mitochondrial respiration. As the concentration used in the present study was already close to the threshold, it is likely that FAO does not contribute to activation-mediated ILC3 cytokine responses *in vitro*, although further studies on FAO and fatty acid uptake would be needed.

6.7 Downstream effects of mTOR signaling in ILC3s

It is not entirely clear how mTOR regulates IFN-γ production without disrupting IL-22 release in activated ILC3s *in vitro*. One option might be that IL-23 and IL-1β differentially modulate post-transcriptional regulation and mRNA stability of IL-22 and IFN-γ transcripts. I found a 100-fold increase in IFN-γ transcripts versus a 1.500-fold increase of IL-22 transcripts in ILC3s activated for 16 h (data not shown). Nevertheless, IL-22 and IFN-γ reached comparable protein levels in the supernatant after *in vitro* stimulation for 2 days. Inhibition of glycolysis has been previously shown to impair IFN-γ production in activated T cells via binding of unoccupied glyceraldehyde-3-phosphate dehydrogenase (GAPDH) to the AU-rich 3-prime untranslated region of IFN-γ mRNA.[252] Given that the upregulation of IFN-γ was almost fully dependent on mTORC1 and to a large degree on glycolysis, such post-transcriptional regulation might also occur in activated ILC3s. Moreover, IL-1β supports IL-23-mediated priming of cytokine responses in memory T cells by stabilizing cytokine transcripts including IL-22, IL-17 and IFN-γ.[253] This might suggest that cytokine production is at least in part modulated through post-transcriptional regulation. This assumption would need to be tested in more detail by analysis of mRNA transcript stability and by testing recruitment of GAPDH to cytokine transcripts in activated ILC3s.

Rptor deletion partially reduced both activation-induced IFN-γ and IL-22 transcript levels in activated ILC3s (data not shown). This indicates that mTOR might also regulate transcription of IFN-γ and IL-22. In Th17 cells, γδT cells and ILC3s, the transcription factors STAT3 and STAT4

are regulated by IL-23[79,254,255] and IL-1β[256]. The level of STAT3 and STAT4 activation modulates the cytokine profile in all three immune cell subsets.[79,129,156,253-255,257,258] It has been shown that STAT3 binds the IL-22 locus on DNA and directly promotes IL-22 transcription in ILC3s.[129] In NK cells, STAT3 also binds the IFN-γ promoter.[259] The degree of STAT4 activity directly correlated with the capacity of ILC3s to produce IFN-γ *in vitro* and *in vivo*.[79,156] Collectively, those various findings implicate that the level of STAT3 and STAT4 activation might be crucial to modulate IL-22 versus IFN-γ production in ILC3s. Activation-induced mTOR signaling might in turn regulate STAT3/4 signaling.

Our group confirmed that IL-23/IL-1β stimulation strongly activated STAT3 and STAT4 in ILC3s *in vitro* (chapter 9.3, Fig.4, manuscript in preparation). ILC3-specific deletion of *Rptor* resulted in impaired activation-induced STAT3 phosphorylation and completely abrogated STAT4 phosphorylation. *Rictor* deficiency only affected STAT4 phosphorylation. In conclusion, our data implies that both mTORCs might modulate IL-22 and IFN-γ expression through regulation of the degree of STAT3 and STAT4 activity.

6.8 mTORC1 and mTORC2 selectively inhibit ILC3-mediated IFN-γ responses during intestinal inflammation

ILC3-mediated IL-22 production is important for defense against extracellular pathogens like *C. rodentium*.[61,128,129] In contrast, induction of ILC3- and exILC3-derived IFN-γ has been frequently associated with exacerbation of intestinal inflammatory disease models including the α-CD40 colitis model.[29,77,159,160,162] It is therefore of particular interest to find pathways which differentially regulate protective versus inflammatory programs in ILC3s. The *in vitro* data presented here indicated that mTORC1 and mTORC2 were crucial for the induction of IFN-γ production by ILC3s but might be dispensable for IL-22 production. To assess whether *RORc*-driven deletion of *Rptor* and *Rictor* can specifically divert inflammatory responses *in vivo*, I tested both the α-CD40 colitis model and the *C. rodentium* infection model in mTOR knockout mice.

Indeed, mice with ILC3-specific deletion of *Rptor* or *Rictor* were equally protected against α-CD40 colitis. In line with the dampened disease severity, IFN-γ[+] ILC3s were decreased in α-CD40 Ab-treated knockout animals while IL-22 production was not affected. These results

demonstrate that single inhibition of mTORC1 or mTORC2 could specifically suppress IFN-γ responses by ILC3s. It is not entirely clear why both mTORC1 and mTORC2 signaling abrogation dampened α-CD40 colitis to a similar scope. It is known that mTORC1 and mTORC2 modulate each other in a cell-type specific manner.[173,174] In NK cells, positive mTORC1-mTORC2 feedback and negative mTORC2-mTORC1 feedback loops are governed by cytokine signals. The balance of mTORC1 and mTORC2 signaling determines NK cell maturation and effector functions.[215] Phosphorylation data of mTORC1 and mTORC2 targets in *in vitro* activated ILC3s indicate that disruption of mTORC1 signaling also reduced mTORC2 signaling. Conversely, abrogation of mTORC2 signaling reduced mTORC1 signaling. It is possible that mTORC1 and mTORC2 display positive feedback loops in ILC3s. This might explain the close resemblance of the phenotype in knockout mice with *RORc*-driven deletion of *Rptor* and *Rictor*.

The decreased α-CD40 Ab-mediated inflammation in knockout mice was accompanied by lowered amounts of neutrophils. Two recent studies demonstrated that ILC3s promote α-CD40 colitis through GM-CSF release and subsequent recruitment of neutrophils.[224,240] ILC3s are one major source of GM-CSF in the SI and colon of mice.[119] Although not analyzed in detail, it is possible that mTOR signaling regulates the production of GM-CSF or other cytokines that are essential for recruitment and activation of myeloid cells during inflammation.

As expected by the modest effect of mTORC1 and mTORC2 on IL-22 production by ILC3s *in vitro*, mice with *RORc*-driven deletion of *Rptor* or *Rictor* did not exhibit defects in protection against *C. rodentium* infection. It was surprising that the reduction of ILC3 numbers in knockout mice with *Rag2*^{-/-} background did not increase the susceptibility to *C. rodentium* infection. However, results from other studies imply that a certain threshold of IL-22 might be sufficient to maintain the intestinal barrier function and to protect against infection. Rankin *et al.*[230] and Song *et al.*[260] described that the specific loss of NCR+ ILC3s did not render wildtype mice more susceptible to *C. rodentium* infection although complete ablation of ILC3s impaired the defense against infection. At the same time, loss of NCR+ ILC3s was a minor survival disadvantage in *C. rodentium*-infected *Rag2*^{-/-} mice.[230] The loss of ILC3s seemed to be compensated by an increase in percentage of IL-22 producing ILC3s in response to *C. rodentium* infection in wildtype mice. Similarly, fingolimod-treated mice displayed reduced

ILC numbers in the SI but did not exhibit a reduction of IL-22, IL-17A, GM-CSF or antimicrobial peptides.[44] Whether IL-22 responses are equally preserved in mice with ILC3-specific knockout of *Rptor* or *Rictor* remains to be determined. In contrast to the data presented here, Di Luccia *et al.* published that loss of mTORC1 was sufficient to impair ILC3 responses during *C. rodentium* infection.[209] As described before, my data implies that effects of mTOR only become obvious in activated ILC3s. Under homeostasis, ILC3s might be less activated in our mouse models. This would explain the discrepancy between the two data sets.

The data presented here suggest that mTOR signaling is involved in the maintenance of quiescent SI ILC3s. Accordingly, *RORc*-driven loss of mTOR signaling altered SI ILC3 numbers in wildtype mice. The activation of ILC3s in the SI of lymphopenic mice rendered ILC3s more sensitive to a defect in mTOR signaling. Colonic ILC3s numbers were surprisingly not affected by loss of mTOR signaling under homeostatic conditions. This observation implies that mTOR signaling in SI and colonic ILC3s are differentially regulated under homeostatic conditions. It remains to be tested whether the level of mTOR signaling in the SI and the colon are truly divergent.

In line with the assumption that mTOR signaling is only important in activated ILC3s, *in vivo* stimulation of ILC3 proliferation was mTOR-dependent. The disruption of mTOR signaling preferentially inhibited IFN-γ responses by ILC3s stimulated *in vitro*, but had minor effects on IL-22 production. Consistently, *Rptor*- and *Rictor* deficiency in ILC3s protected *Rag2*$^{-/-}$ mice in the IFN-γ-mediated α-CD40 colitis model. The same mouse strains were not more susceptible to *C. rodentium* infection. These findings suggest that both mTORC1 and mTORC2 promote pro-inflammatory ILC3-mediated IFN-γ responses without altering protective ILC3 properties in the intestinal tract. Interestingly, the rapamycin analogues sirolimus and everolimus led to clinical remission in 4 cases of pediatric CD, 5 cases of pediatric UC and 1 case of adult CD, which became previously refractory to conventional treatments.[261-263] Moreover, everolimus alleviated colitis and suppressed IFN-γ responses in IL-10 deficient mice, an experimental model of CD.[264] Application of mTOR inhibitors might therefore ameliorate IFN-γ-mediated intestinal inflammatory diseases without compromising protective immune responses. Rapamycin analogues in clinical studies were combined with other drugs. Hence, the therapeutic potential of specific mTOR inhibitors in human colitis would need to be confirmed in murine colitis models and clinical studies.

7 Acknowledgments

8 References

1   Spits, H. *et al.* Innate lymphoid cells--a proposal for uniform nomenclature. *Nat Rev Immunol* **13**, 145-149, doi:10.1038/nri3365 (2013).

2   Vivier, E. *et al.* Innate Lymphoid Cells: 10 Years On. *Cell* **174**, 1054-1066, doi:10.1016/j.cell.2018.07.017 (2018).

3   McKenzie, A. N., Spits, H. & Eberl, G. Innate lymphoid cells in inflammation and immunity. *Immunity* **41**, 366-374, doi:10.1016/j.immuni.2014.09.006 (2014).

4   Klose, C. S. & Artis, D. Innate lymphoid cells as regulators of immunity, inflammation and tissue homeostasis. *Nat Immunol* **17**, 765-774, doi:10.1038/ni.3489 (2016).

5   Shikhagaie, M. M., Germar, K., Bal, S. M., Ros, X. R. & Spits, H. Innate lymphoid cells in autoimmunity: emerging regulators in rheumatic diseases. *Nat Rev Rheumatol* **13**, 164-173, doi:10.1038/nrrheum.2016.218 (2017).

6   Kiessling, R., Klein, E. & Wigzell, H. "Natural" killer cells in the mouse. I. Cytotoxic cells with specificity for mouse Moloney leukemia cells. Specificity and distribution according to genotype. *Eur J Immunol* **5**, 112-117, doi:10.1002/eji.1830050208 (1975).

7   Rosenau, W. & Moon, H. D. Lysis of homologous cells by sensitized lymphocytes in tissue culture. *Journal of the National Cancer Institute* **27**, 471-483 (1961).

8   Abel, A. M., Yang, C., Thakar, M. S. & Malarkannan, S. Natural Killer Cells: Development, Maturation, and Clinical Utilization. *Front Immunol* **9**, 1869, doi:10.3389/fimmu.2018.01869 (2018).

9   Weizman, O. E. *et al.* ILC1 Confer Early Host Protection at Initial Sites of Viral Infection. *Cell* **171**, 795-808.e712, doi:10.1016/j.cell.2017.09.052 (2017).

10   Wagner, M. & Koyasu, S. Cancer Immunoediting by Innate Lymphoid Cells. *Trends Immunol* **40**, 415-430, doi:10.1016/j.it.2019.03.004 (2019).

11   Klose, C. S. N. *et al.* Differentiation of type 1 ILCs from a common progenitor to all helper-like innate lymphoid cell lineages. *Cell* **157**, 340-356, doi:10.1016/j.cell.2014.03.030 (2014).

12   Robinette, M. L. *et al.* Transcriptional programs define molecular characteristics of innate lymphoid cell classes and subsets. *Nat Immunol* **16**, 306-317, doi:10.1038/ni.3094 (2015).

13   Yudanin, N. A. *et al.* Spatial and Temporal Mapping of Human Innate Lymphoid Cells Reveals Elements of Tissue Specificity. *Immunity* **50**, 505-519 e504, doi:10.1016/j.immuni.2019.01.012 (2019).

14   Colonna, M. Innate Lymphoid Cells: Diversity, Plasticity, and Unique Functions in Immunity. *Immunity* **48**, 1104-1117, doi:10.1016/j.immuni.2018.05.013 (2018).

15   Cortez, V. S. & Colonna, M. Diversity and function of group 1 innate lymphoid cells. *Immunol Lett* **179**, 19-24, doi:10.1016/j.imlet.2016.07.005 (2016).

16   Simoni, Y. & Newell, E. W. Dissecting human ILC heterogeneity: more than just three subsets. *Immunology* **153**, 297-303, doi:10.1111/imm.12862 (2018).

17   Huang, Y. *et al.* IL-25-responsive, lineage-negative KLRG1(hi) cells are multipotential 'inflammatory' type 2 innate lymphoid cells. *Nat Immunol* **16**, 161-169, doi:10.1038/ni.3078 (2015).

18   Simoni, Y. *et al.* Human Innate Lymphoid Cell Subsets Possess Tissue-Type Based Heterogeneity in Phenotype and Frequency. *Immunity* **46**, 148-161, doi:10.1016/j.immuni.2016.11.005 (2017).

19   Mebius, R. E., Streeter, P. R., Michie, S., Butcher, E. C. & Weissman, I. L. A developmental switch in lymphocyte homing receptor and endothelial vascular addressin expression regulates lymphocyte homing and permits CD4+ CD3- cells to colonize lymph nodes. *Proc Natl Acad Sci U S A* **93**, 11019-11024, doi:10.1073/pnas.93.20.11019 (1996).

20   Mebius, R. E., Rennert, P. & Weissman, I. L. Developing lymph nodes collect CD4+CD3- LTbeta+ cells that can differentiate to APC, NK cells, and follicular cells but not T or B cells. *Immunity* **7**, 493-504, doi:10.1016/s1074-7613(00)80371-4 (1997).

21   Yoshida, H. *et al.* IL-7 receptor alpha+ CD3(-) cells in the embryonic intestine induces the organizing center of Peyer's patches. *Int Immunol* **11**, 643-655, doi:10.1093/intimm/11.5.643 (1999).

22   Yokota, Y. *et al.* Development of peripheral lymphoid organs and natural killer cells depends on the helix-loop-helix inhibitor Id2. *Nature* **397**, 702-706, doi:10.1038/17812 (1999).

23   Sun, Z. *et al.* Requirement for RORgamma in thymocyte survival and lymphoid organ development. *Science* **288**, 2369-2373, doi:10.1126/science.288.5475.2369 (2000).

24   Kim, D. *et al.* Regulation of peripheral lymph node genesis by the tumor necrosis factor family member TRANCE. *J Exp Med* **192**, 1467-1478, doi:10.1084/jem.192.10.1467 (2000).

25   Eberl, G. *et al.* An essential function for the nuclear receptor RORgamma(t) in the generation of fetal lymphoid tissue inducer cells. *Nat Immunol* **5**, 64-73, doi:10.1038/ni1022 (2004).

26   Meier, D. *et al.* Ectopic lymphoid-organ development occurs through interleukin 7-mediated enhanced survival of lymphoid-tissue-inducer cells. *Immunity* **26**, 643-654, doi:10.1016/j.immuni.2007.04.009 (2007).

27   Schmutz, S. *et al.* Cutting Edge: IL-7 Regulates the Peripheral Pool of Adult RORγ+ Lymphoid Tissue Inducer Cells. *The Journal of Immunology* **183**, 2217-2221, doi:10.4049/jimmunol.0802911 (2009).

28   Zhong, C. *et al.* Differential Expression of the Transcription Factor GATA3 Specifies Lineage and Functions of Innate Lymphoid Cells. *Immunity* **52**, 83-95.e84, doi:10.1016/j.immuni.2019.12.001 (2020).

29   Buonocore, S. *et al.* Innate lymphoid cells drive interleukin-23-dependent innate intestinal pathology. *Nature* **464**, 1371-1375, doi:10.1038/nature08949 (2010).

30   Thiemann, S. *et al.* Enhancement of IFNgamma Production by Distinct Commensals Ameliorates Salmonella-Induced Disease. *Cell Host Microbe* **21**, 682-694.e685, doi:10.1016/j.chom.2017.05.005 (2017).

31   Klose, C. S. *et al.* A T-bet gradient controls the fate and function of CCR6-RORgammat+ innate lymphoid cells. *Nature* **494**, 261-265, doi:10.1038/nature11813 (2013).

32   Gury-BenAri, M. *et al.* The Spectrum and Regulatory Landscape of Intestinal Innate Lymphoid Cells Are Shaped by the Microbiome. *Cell* **166**, 1231-1246.e1213, doi:10.1016/j.cell.2016.07.043 (2016).

33   Bar-Ephraim, Y. E. *et al.* Cross-Tissue Transcriptomic Analysis of Human Secondary Lymphoid Organ-Residing ILC3s Reveals a Quiescent State in the Absence of Inflammation. *Cell Rep* **21**, 823-833, doi:10.1016/j.celrep.2017.09.070 (2017).

34   Ohnmacht, C. Tolerance to the Intestinal Microbiota Mediated by ROR(gammat)(+) Cells. *Trends Immunol* **37**, 477-486, doi:10.1016/j.it.2016.05.002 (2016).

35   Vonarbourg, C. & Diefenbach, A. Multifaceted roles of interleukin-7 signaling for the development and function of innate lymphoid cells. *Semin Immunol* **24**, 165-174, doi:10.1016/j.smim.2012.03.002 (2012).

36   Robinette, M. L. *et al.* IL-15 sustains IL-7R-independent ILC2 and ILC3 development. *Nat Commun* **8**, 14601, doi:10.1038/ncomms14601 (2017).

37   Huang, Y., Mao, K. & Germain, R. N. Thinking differently about ILCs—Not just tissue resident and not just the same as CD4+ T-cell effectors. *Immunological Reviews* **286**, 160-171, doi:10.1111/imr.12704 (2018).

38   Shih, H. Y. *et al.* Developmental Acquisition of Regulomes Underlies Innate Lymphoid Cell Functionality. *Cell* **165**, 1120-1133, doi:10.1016/j.cell.2016.04.029 (2016).

39   Koues, O. I. *et al.* Distinct Gene Regulatory Pathways for Human Innate versus Adaptive Lymphoid Cells. *Cell* **165**, 1134-1146, doi:10.1016/j.cell.2016.04.014 (2016).

40   Ercolano, G. *et al.* Distinct and shared gene expression for human innate versus adaptive helper lymphoid cells. *J Leukoc Biol*, doi:10.1002/jlb.5ma0120-209r (2020).

41 Mowel, W. K. *et al.* Group 1 Innate Lymphoid Cell Lineage Identity Is Determined by a cis-Regulatory Element Marked by a Long Non-coding RNA. *Immunity* **47**, 435-449.e438, doi:10.1016/j.immuni.2017.08.012 (2017).

42 Gasteiger, G., Fan, X., Dikiy, S., Lee, S. Y. & Rudensky, A. Y. Tissue residency of innate lymphoid cells in lymphoid and nonlymphoid organs. *Science* **350**, 981-985, doi:10.1126/science.aac9593 (2015).

43 Huang, Y. *et al.* S1P-dependent interorgan trafficking of group 2 innate lymphoid cells supports host defense. *Science* **359**, 114-119, doi:10.1126/science.aam5809 (2018).

44 Eken, A. *et al.* Fingolimod Alters Tissue Distribution and Cytokine Production of Human and Murine Innate Lymphoid Cells. *Front Immunol* **10**, 217, doi:10.3389/fimmu.2019.00217 (2019).

45 Boos, M. D., Yokota, Y., Eberl, G. & Kee, B. L. Mature natural killer cell and lymphoid tissue-inducing cell development requires Id2-mediated suppression of E protein activity. *J Exp Med* **204**, 1119-1130, doi:10.1084/jem.20061959 (2007).

46 Zook, E. C. & Kee, B. L. Development of innate lymphoid cells. *Nat Immunol* **17**, 775-782, doi:10.1038/ni.3481 (2016).

47 Cherrier, D. E., Serafini, N. & Di Santo, J. P. Innate Lymphoid Cell Development: A T Cell Perspective. *Immunity* **48**, 1091-1103, doi:10.1016/j.immuni.2018.05.010 (2018).

48 Geiger, T. L. *et al.* Nfil3 is crucial for development of innate lymphoid cells and host protection against intestinal pathogens. *J Exp Med* **211**, 1723-1731, doi:10.1084/jem.20140212 (2014).

49 Seehus, C. R. *et al.* The development of innate lymphoid cells requires TOX-dependent generation of a common innate lymphoid cell progenitor. *Nat Immunol* **16**, 599-608, doi:10.1038/ni.3168 (2015).

50 Seillet, C. *et al.* Nfil3 is required for the development of all innate lymphoid cell subsets. *J Exp Med* **211**, 1733-1740, doi:10.1084/jem.20140145 (2014).

51 Yu, X. *et al.* The basic leucine zipper transcription factor NFIL3 directs the development of a common innate lymphoid cell precursor. *eLife* **3**, doi:10.7554/eLife.04406 (2014).

52 Yang, Q. *et al.* TCF-1 upregulation identifies early innate lymphoid progenitors in the bone marrow. *Nat Immunol* **16**, 1044-1050, doi:10.1038/ni.3248 (2015).

53 Harly, C. *et al.* The transcription factor TCF-1 enforces commitment to the innate lymphoid cell lineage. *Nat Immunol* **20**, 1150-1160, doi:10.1038/s41590-019-0445-7 (2019).

54 Harly, C., Cam, M., Kaye, J. & Bhandoola, A. Development and differentiation of early innate lymphoid progenitors. *J Exp Med* **215**, 249-262, doi:10.1084/jem.20170832 (2018).

55 Ebihara, T. *et al.* Runx3 specifies lineage commitment of innate lymphoid cells. *Nat Immunol* **16**, 1124-1133, doi:10.1038/ni.3272 (2015).

56 Yagi, R. *et al.* The transcription factor GATA3 is critical for the development of all IL-7Ralpha-expressing innate lymphoid cells. *Immunity* **40**, 378-388, doi:10.1016/j.immuni.2014.01.012 (2014).

57 Hoyler, T. *et al.* The transcription factor GATA-3 controls cell fate and maintenance of type 2 innate lymphoid cells. *Immunity* **37**, 634-648, doi:10.1016/j.immuni.2012.06.020 (2012).

58 Tufa, D. M. *et al.* Transient Expression of GATA3 in Hematopoietic Stem Cells Facilitates Helper Innate Lymphoid Cell Differentiation. *Front Immunol* **10**, 510, doi:10.3389/fimmu.2019.00510 (2019).

59 Constantinides, M. G., McDonald, B. D., Verhoef, P. A. & Bendelac, A. A committed precursor to innate lymphoid cells. *Nature* **508**, 397-401, doi:10.1038/nature13047 (2014).

60 Li, S. *et al.* Ikaros Inhibits Group 3 Innate Lymphoid Cell Development and Function by Suppressing the Aryl Hydrocarbon Receptor Pathway. *Immunity* **45**, 185-197, doi:10.1016/j.immuni.2016.06.027 (2016).

61 Satoh-Takayama, N. *et al.* Microbial flora drives interleukin 22 production in intestinal NKp46+ cells that provide innate mucosal immune defense. *Immunity* **29**, 958-970, doi:10.1016/j.immuni.2008.11.001 (2008).

62   Goverse, G. *et al.* Vitamin A Controls the Presence of RORgamma+ Innate Lymphoid Cells and Lymphoid Tissue in the Small Intestine. *J Immunol* **196**, 5148-5155, doi:10.4049/jimmunol.1501106 (2016).

63   Wong, S. H. *et al.* Transcription factor RORalpha is critical for nuocyte development. *Nat Immunol* **13**, 229-236, doi:10.1038/ni.2208 (2012).

64   Walker, J. A. *et al.* Bcl11b is essential for group 2 innate lymphoid cell development. *J Exp Med* **212**, 875-882, doi:10.1084/jem.20142224 (2015).

65   Califano, D. *et al.* Transcription Factor Bcl11b Controls Identity and Function of Mature Type 2 Innate Lymphoid Cells. *Immunity* **43**, 354-368, doi:10.1016/j.immuni.2015.07.005 (2015).

66   Walker, J. A. *et al.* Polychromic Reporter Mice Reveal Unappreciated Innate Lymphoid Cell Progenitor Heterogeneity and Elusive ILC3 Progenitors in Bone Marrow. *Immunity* **51**, 104-118.e107, doi:10.1016/j.immuni.2019.05.002 (2019).

67   Xu, W. *et al.* An Id2(RFP)-Reporter Mouse Redefines Innate Lymphoid Cell Precursor Potentials. *Immunity* **50**, 1054-1068.e1053, doi:10.1016/j.immuni.2019.02.022 (2019).

68   Di Santo, J. P., Lim, A. I. & Yssel, H. 'ILC-poiesis': generating tissue ILCs from naive precursors. *Oncotarget* **8**, 81729-81730, doi:10.18632/oncotarget.21046 (2017).

69   Lim, A. I. & Di Santo, J. P. ILC-poiesis: Ensuring tissue ILC differentiation at the right place and time. *Eur J Immunol* **49**, 11-18, doi:10.1002/eji.201747294 (2019).

70   Bal, S. M., Golebski, K. & Spits, H. Plasticity of innate lymphoid cell subsets. *Nat Rev Immunol*, doi:10.1038/s41577-020-0282-9 (2020).

71   Pokrovskii, M. *et al.* Characterization of Transcriptional Regulatory Networks that Promote and Restrict Identities and Functions of Intestinal Innate Lymphoid Cells. *Immunity* **51**, 185-197.e186, doi:10.1016/j.immuni.2019.06.001 (2019).

72   Silver, J. S. *et al.* Inflammatory triggers associated with exacerbations of COPD orchestrate plasticity of group 2 innate lymphoid cells in the lungs. *Nat Immunol* **17**, 626-635, doi:10.1038/ni.3443 (2016).

73   Bal, S. M. *et al.* IL-1beta, IL-4 and IL-12 control the fate of group 2 innate lymphoid cells in human airway inflammation in the lungs. *Nat Immunol* **17**, 636-645, doi:10.1038/ni.3444 (2016).

74   Ohne, Y. *et al.* IL-1 is a critical regulator of group 2 innate lymphoid cell function and plasticity. *Nat Immunol* **17**, 646-655, doi:10.1038/ni.3447 (2016).

75   Bernink, J. H. *et al.* c-Kit-positive ILC2s exhibit an ILC3-like signature that may contribute to IL-17-mediated pathologies. *Nat Immunol* **20**, 992-1003, doi:10.1038/s41590-019-0423-0 (2019).

76   Golebski, K. *et al.* IL-1beta, IL-23, and TGF-beta drive plasticity of human ILC2s towards IL-17-producing ILCs in nasal inflammation. *Nat Commun* **10**, 2162, doi:10.1038/s41467-019-09883-7 (2019).

77   Vonarbourg, C. *et al.* Regulated expression of nuclear receptor RORgammat confers distinct functional fates to NK cell receptor-expressing RORgammat(+) innate lymphocytes. *Immunity* **33**, 736-751, doi:10.1016/j.immuni.2010.10.017 (2010).

78   Rankin, L. C. *et al.* The transcription factor T-bet is essential for the development of NKp46+ innate lymphocytes via the Notch pathway. *Nat Immunol* **14**, 389-395, doi:10.1038/ni.2545 (2013).

79   Mikami, Y. *et al.* NCR(+) ILC3 maintain larger STAT4 reservoir via T-BET to regulate type 1 features upon IL-23 stimulation in mice. *Eur J Immunol* **48**, 1174-1180, doi:10.1002/eji.201847480 (2018).

80   Bernink, J. H. *et al.* Interleukin-12 and -23 Control Plasticity of CD127(+) Group 1 and Group 3 Innate Lymphoid Cells in the Intestinal Lamina Propria. *Immunity* **43**, 146-160, doi:10.1016/j.immuni.2015.06.019 (2015).

81   Bernink, J. H. *et al.* Human type 1 innate lymphoid cells accumulate in inflamed mucosal tissues. *Nat Immunol* **14**, 221-229, doi:10.1038/ni.2534 (2013).

82   Cella, M. *et al.* Subsets of ILC3-ILC1-like cells generate a diversity spectrum of innate lymphoid cells in human mucosal tissues. *Nat Immunol* **20**, 980-991, doi:10.1038/s41590-019-0425-y (2019).

83   Crellin, N. K. *et al.* Regulation of cytokine secretion in human CD127(+) LTi-like innate lymphoid cells by Toll-like receptor 2. *Immunity* **33**, 752-764, doi:10.1016/j.immuni.2010.10.012 (2010).

84   Cella, M., Otero, K. & Colonna, M. Expansion of human NK-22 cells with IL-7, IL-2, and IL-1beta reveals intrinsic functional plasticity. *Proc Natl Acad Sci U S A* **107**, 10961-10966, doi:10.1073/pnas.1005641107 (2010).

85   Wang, S. *et al.* Regulatory Innate Lymphoid Cells Control Innate Intestinal Inflammation. *Cell* **171**, 201-216.e218, doi:10.1016/j.cell.2017.07.027 (2017).

86   Bando, J. K. *et al.* ILC2s are the predominant source of intestinal ILC-derived IL-10. *J Exp Med* **217**, doi:10.1084/jem.20191520 (2020).

87   Seehus, C. R. *et al.* Alternative activation generates IL-10 producing type 2 innate lymphoid cells. *Nat Commun* **8**, 1900, doi:10.1038/s41467-017-02023-z (2017).

88   Eberl, G. & Littman, D. R. Thymic origin of intestinal alphabeta T cells revealed by fate mapping of RORgammat+ cells. *Science* **305**, 248-251, doi:10.1126/science.1096472 (2004).

89   Cella, M. *et al.* A human natural killer cell subset provides an innate source of IL-22 for mucosal immunity. *Nature* **457**, 722-725, doi:10.1038/nature07537 (2009).

90   Sanos, S. L. *et al.* RORgammat and commensal microflora are required for the differentiation of mucosal interleukin 22-producing NKp46+ cells. *Nat Immunol* **10**, 83-91, doi:10.1038/ni.1684 (2009).

91   Magri, G. *et al.* Innate lymphoid cells integrate stromal and immunological signals to enhance antibody production by splenic marginal zone B cells. *Nat Immunol* **15**, 354-364, doi:10.1038/ni.2830 (2014).

92   Mackley, E. C. *et al.* CCR7-dependent trafficking of RORgamma(+) ILCs creates a unique microenvironment within mucosal draining lymph nodes. *Nat Commun* **6**, 5862, doi:10.1038/ncomms6862 (2015).

93   Kobayashi, T. *et al.* Homeostatic Control of Sebaceous Glands by Innate Lymphoid Cells Regulates Commensal Bacteria Equilibrium. *Cell* **176**, 982-997.e916, doi:10.1016/j.cell.2018.12.031 (2019).

94   Croxatto, D. *et al.* Group 3 innate lymphoid cells regulate neutrophil migration and function in human decidua. *Mucosal Immunol* **9**, 1372-1383, doi:10.1038/mi.2016.10 (2016).

95   Sawa, S. *et al.* RORgammat+ innate lymphoid cells regulate intestinal homeostasis by integrating negative signals from the symbiotic microbiota. *Nat Immunol* **12**, 320-326, doi:10.1038/ni.2002 (2011).

96   Lee, J. S. *et al.* AHR drives the development of gut ILC22 cells and postnatal lymphoid tissues via pathways dependent on and independent of Notch. *Nat Immunol* **13**, 144-151, doi:10.1038/ni.2187 (2011).

97   Miani, M. *et al.* Gut Microbiota-Stimulated Innate Lymphoid Cells Support beta-Defensin 14 Expression in Pancreatic Endocrine Cells, Preventing Autoimmune Diabetes. *Cell Metab* **28**, 557-572.e556, doi:10.1016/j.cmet.2018.06.012 (2018).

98   Qi, X. *et al.* Gut microbiota-bile acid-interleukin-22 axis orchestrates polycystic ovary syndrome. *Nat Med* **25**, 1225-1233, doi:10.1038/s41591-019-0509-0 (2019).

99   Nakamoto, N. *et al.* Commensal Lactobacillus Controls Immune Tolerance during Acute Liver Injury in Mice. *Cell Rep* **21**, 1215-1226, doi:10.1016/j.celrep.2017.10.022 (2017).

100   Rothhammer, V. & Quintana, F. J. The aryl hydrocarbon receptor: an environmental sensor integrating immune responses in health and disease. *Nat Rev Immunol* **19**, 184-197, doi:10.1038/s41577-019-0125-8 (2019).

101   Zhou, L. AHR Function in Lymphocytes: Emerging Concepts. *Trends Immunol* **37**, 17-31, doi:10.1016/j.it.2015.11.007 (2016).

102   Kiss, E. A. *et al.* Natural aryl hydrocarbon receptor ligands control organogenesis of intestinal lymphoid follicles. *Science* **334**, 1561-1565, doi:10.1126/science.1214914 (2011).

103   Schiering, C. *et al.* Feedback control of AHR signalling regulates intestinal immunity. *Nature* **542**, 242-245, doi:10.1038/nature21080 (2017).

104 Li, S. *et al.* Aryl Hydrocarbon Receptor Signaling Cell Intrinsically Inhibits Intestinal Group 2 Innate Lymphoid Cell Function. *Immunity* **49**, 915-928.e915, doi:10.1016/j.immuni.2018.09.015 (2018).

105 Huh, J. R. & Veiga-Fernandes, H. Neuroimmune circuits in inter-organ communication. *Nat Rev Immunol*, doi:10.1038/s41577-019-0247-z (2019).

106 Ibiza, S. *et al.* Glial-cell-derived neuroregulators control type 3 innate lymphoid cells and gut defence. *Nature* **535**, 440-443, doi:10.1038/nature18644 (2016).

107 Seillet, C. *et al.* The neuropeptide VIP confers anticipatory mucosal immunity by regulating ILC3 activity. *Nat Immunol* **21**, 168-177, doi:10.1038/s41590-019-0567-y (2020).

108 Dalli, J., Colas, R. A., Arnardottir, H. & Serhan, C. N. Vagal Regulation of Group 3 Innate Lymphoid Cells and the Immunoresolvent PCTR1 Controls Infection Resolution. *Immunity* **46**, 92-105, doi:10.1016/j.immuni.2016.12.009 (2017).

109 Takatori, H. *et al.* Lymphoid tissue inducer-like cells are an innate source of IL-17 and IL-22. *J Exp Med* **206**, 35-41, doi:10.1084/jem.20072713 (2009).

110 Kinnebrew, M. A. *et al.* Interleukin 23 production by intestinal CD103(+)CD11b(+) dendritic cells in response to bacterial flagellin enhances mucosal innate immune defense. *Immunity* **36**, 276-287, doi:10.1016/j.immuni.2011.12.011 (2012).

111 Longman, R. S. *et al.* CX(3)CR1(+) mononuclear phagocytes support colitis-associated innate lymphoid cell production of IL-22. *J Exp Med* **211**, 1571-1583, doi:10.1084/jem.20140678 (2014).

112 Savage, A. K., Liang, H. E. & Locksley, R. M. The Development of Steady-State Activation Hubs between Adult LTi ILC3s and Primed Macrophages in Small Intestine. *J Immunol* **199**, 1912-1922, doi:10.4049/jimmunol.1700155 (2017).

113 Manta, C. *et al.* CX(3)CR1(+) macrophages support IL-22 production by innate lymphoid cells during infection with Citrobacter rodentium. *Mucosal Immunol* **6**, 177-188, doi:10.1038/mi.2012.61 (2013).

114 Friedrich, C. *et al.* MyD88 signaling in dendritic cells and the intestinal epithelium controls immunity against intestinal infection with C. rodentium. *PLoS Pathog* **13**, e1006357, doi:10.1371/journal.ppat.1006357 (2017).

115 Wang, B. *et al.* Macrophage beta2-Integrins Regulate IL-22 by ILC3s and Protect from Lethal Citrobacter rodentium-Induced Colitis. *Cell Rep* **26**, 1614-1626.e1615, doi:10.1016/j.celrep.2019.01.054 (2019).

116 Castleman, M. J. *et al.* Commensal and Pathogenic Bacteria Indirectly Induce IL-22 but Not IFNgamma Production From Human Colonic ILC3s via Multiple Mechanisms. *Front Immunol* **10**, 649, doi:10.3389/fimmu.2019.00649 (2019).

117 Martinez-Lopez, M. *et al.* Microbiota Sensing by Mincle-Syk Axis in Dendritic Cells Regulates Interleukin-17 and -22 Production and Promotes Intestinal Barrier Integrity. *Immunity* **50**, 446-461.e449, doi:10.1016/j.immuni.2018.12.020 (2019).

118 Takayama, T. *et al.* Imbalance of NKp44(+)NKp46(-) and NKp44(-)NKp46(+) natural killer cells in the intestinal mucosa of patients with Crohn's disease. *Gastroenterology* **139**, 882-892, 892.e881-883, doi:10.1053/j.gastro.2010.05.040 (2010).

119 Mortha, A. *et al.* Microbiota-dependent crosstalk between macrophages and ILC3 promotes intestinal homeostasis. *Science* **343**, 1249288, doi:10.1126/science.1249288 (2014).

120 Bauche, D. *et al.* LAG3(+) Regulatory T Cells Restrain Interleukin-23-Producing CX3CR1(+) Gut-Resident Macrophages during Group 3 Innate Lymphoid Cell-Driven Colitis. *Immunity* **49**, 342-352.e345, doi:10.1016/j.immuni.2018.07.007 (2018).

121 Mao, K. *et al.* Innate and adaptive lymphocytes sequentially shape the gut microbiota and lipid metabolism. *Nature* **554**, 255-259, doi:10.1038/nature25437 (2018).

122 Domingues, R. G. & Hepworth, M. R. Immunoregulatory Sensory Circuits in Group 3 Innate Lymphoid Cell (ILC3) Function and Tissue Homeostasis. *Front Immunol* **11**, 116, doi:10.3389/fimmu.2020.00116 (2020).

123 Zenewicz, L. A. *et al.* Innate and adaptive interleukin-22 protects mice from inflammatory bowel disease. *Immunity* **29**, 947-957, doi:10.1016/j.immuni.2008.11.003 (2008).

124 Sabat, R., Ouyang, W. & Wolk, K. Therapeutic opportunities of the IL-22-IL-22R1 system. *Nature reviews. Drug discovery* **13**, 21-38, doi:10.1038/nrd4176 (2014).

125 Sonnenberg, G. F. *et al.* Innate lymphoid cells promote anatomical containment of lymphoid-resident commensal bacteria. *Science* **336**, 1321-1325, doi:10.1126/science.1222551 (2012).

126 Gronke, K. *et al.* Interleukin-22 protects intestinal stem cells against genotoxic stress. *Nature* **566**, 249-253, doi:10.1038/s41586-019-0899-7 (2019).

127 Pickert, G. *et al.* STAT3 links IL-22 signaling in intestinal epithelial cells to mucosal wound healing. *J Exp Med* **206**, 1465-1472, doi:10.1084/jem.20082683 (2009).

128 Zheng, Y. *et al.* Interleukin-22 mediates early host defense against attaching and effacing bacterial pathogens. *Nat Med* **14**, 282-289, doi:10.1038/nm1720 (2008).

129 Guo, X. *et al.* Induction of innate lymphoid cell-derived interleukin-22 by the transcription factor STAT3 mediates protection against intestinal infection. *Immunity* **40**, 25-39, doi:10.1016/j.immuni.2013.10.021 (2014).

130 Goto, Y. *et al.* Innate lymphoid cells regulate intestinal epithelial cell glycosylation. *Science* **345**, 1254009, doi:10.1126/science.1254009 (2014).

131 Pickard, J. M. *et al.* Rapid fucosylation of intestinal epithelium sustains host-commensal symbiosis in sickness. *Nature* **514**, 638-641, doi:10.1038/nature13823 (2014).

132 Pham, T. A. *et al.* Epithelial IL-22RA1-mediated fucosylation promotes intestinal colonization resistance to an opportunistic pathogen. *Cell Host Microbe* **16**, 504-516, doi:10.1016/j.chom.2014.08.017 (2014).

133 Zhang, Y. *et al.* Type 3 innate lymphoid cell-derived lymphotoxin prevents microbiota-dependent inflammation. *Cell Mol Immunol* **15**, 697-709, doi:10.1038/cmi.2017.25 (2018).

134 Kinugasa, T., Sakaguchi, T., Gu, X. & Reinecker, H. C. Claudins regulate the intestinal barrier in response to immune mediators. *Gastroenterology* **118**, 1001-1011, doi:10.1016/s0016-5085(00)70351-9 (2000).

135 Aparicio-Domingo, P. *et al.* Type 3 innate lymphoid cells maintain intestinal epithelial stem cells after tissue damage. *J Exp Med* **212**, 1783-1791, doi:10.1084/jem.20150318 (2015).

136 Lindemans, C. A. *et al.* Interleukin-22 promotes intestinal-stem-cell-mediated epithelial regeneration. *Nature* **528**, 560-564, doi:10.1038/nature16460 (2015).

137 Melo-Gonzalez, F. *et al.* Antigen-presenting ILC3 regulate T cell-dependent IgA responses to colonic mucosal bacteria. *J Exp Med* **216**, 728-742, doi:10.1084/jem.20180871 (2019).

138 von Burg, N. *et al.* Activated group 3 innate lymphoid cells promote T-cell-mediated immune responses. *Proc Natl Acad Sci U S A* **111**, 12835-12840, doi:10.1073/pnas.1406908111 (2014).

139 Hepworth, M. R. *et al.* Innate lymphoid cells regulate CD4+ T-cell responses to intestinal commensal bacteria. *Nature* **498**, 113-117, doi:10.1038/nature12240 (2013).

140 He, Y., Franchi, L. & Nunez, G. TLR agonists stimulate Nlrp3-dependent IL-1beta production independently of the purinergic P2X7 receptor in dendritic cells and in vivo. *J Immunol* **190**, 334-339, doi:10.4049/jimmunol.1202737 (2013).

141 Tsuji, M. *et al.* Requirement for lymphoid tissue-inducer cells in isolated follicle formation and T cell-independent immunoglobulin A generation in the gut. *Immunity* **29**, 261-271, doi:10.1016/j.immuni.2008.05.014 (2008).

142 Reboldi, A. *et al.* IgA production requires B cell interaction with subepithelial dendritic cells in Peyer's patches. *Science* **352**, aaf4822, doi:10.1126/science.aaf4822 (2016).

143 Kruglov, A. A. *et al.* Nonredundant function of soluble LTalpha3 produced by innate lymphoid cells in intestinal homeostasis. *Science* **342**, 1243-1246, doi:10.1126/science.1243364 (2013).

144 Hepworth, M. R. *et al.* Immune tolerance. Group 3 innate lymphoid cells mediate intestinal selection of commensal bacteria-specific CD4(+) T cells. *Science* **348**, 1031-1035, doi:10.1126/science.aaa4812 (2015).

145 Goto, Y. *et al.* Segmented filamentous bacteria antigens presented by intestinal dendritic cells drive mucosal Th17 cell differentiation. *Immunity* **40**, 594-607, doi:10.1016/j.immuni.2014.03.005 (2014).

146 Qiu, J. *et al.* Group 3 innate lymphoid cells inhibit T-cell-mediated intestinal inflammation through aryl hydrocarbon receptor signaling and regulation of microflora. *Immunity* **39**, 386-399, doi:10.1016/j.immuni.2013.08.002 (2013).

147 Wagage, S. *et al.* The Group 3 Innate Lymphoid Cell Defect in Aryl Hydrocarbon Receptor Deficient Mice Is Associated with T Cell Hyperactivation during Intestinal Infection. *PLoS One* **10**, e0128335, doi:10.1371/journal.pone.0128335 (2015).

148 Martin, C. E. *et al.* Interleukin-7 Availability Is Maintained by a Hematopoietic Cytokine Sink Comprising Innate Lymphoid Cells and T Cells. *Immunity* **47**, 171-182.e174, doi:10.1016/j.immuni.2017.07.005 (2017).

149 Zhou, L. *et al.* Innate lymphoid cells support regulatory T cells in the intestine through interleukin-2. *Nature* **568**, 405-409, doi:10.1038/s41586-019-1082-x (2019).

150 Hernandez, P., Gronke, K. & Diefenbach, A. A catch-22: Interleukin-22 and cancer. *Eur J Immunol* **48**, 15-31, doi:10.1002/eji.201747183 (2018).

151 Vely, F. *et al.* Evidence of innate lymphoid cell redundancy in humans. *Nat Immunol* **17**, 1291-1299, doi:10.1038/ni.3553 (2016).

152 Bouladoux, N., Harrison, O. J. & Belkaid, Y. The Mouse Model of Infection with Citrobacter rodentium. *Curr Protoc Immunol* **119**, 19 15 11-19 15 25, doi:10.1002/cpim.34 (2017).

153 Sonnenberg, G. F., Monticelli, L. A., Elloso, M. M., Fouser, L. A. & Artis, D. CD4(+) lymphoid tissue-inducer cells promote innate immunity in the gut. *Immunity* **34**, 122-134, doi:10.1016/j.immuni.2010.12.009 (2011).

154 Ardain, A. *et al.* Group 3 innate lymphoid cells mediate early protective immunity against tuberculosis. *Nature* **570**, 528-532, doi:10.1038/s41586-019-1276-2 (2019).

155 Gladiator, A., Wangler, N., Trautwein-Weidner, K. & LeibundGut-Landmann, S. Cutting edge: IL-17-secreting innate lymphoid cells are essential for host defense against fungal infection. *J Immunol* **190**, 521-525, doi:10.4049/jimmunol.1202924 (2013).

156 Dulson, S. J., Watkins, E. E., Crossman, D. K. & Harrington, L. E. STAT4 Directs a Protective Innate Lymphoid Cell Response to Gastrointestinal Infection. *J Immunol* **203**, 2472-2484, doi:10.4049/jimmunol.1900719 (2019).

157 Coccia, M. *et al.* IL-1beta mediates chronic intestinal inflammation by promoting the accumulation of IL-17A secreting innate lymphoid cells and CD4(+) Th17 cells. *J Exp Med* **209**, 1595-1609, doi:10.1084/jem.20111453 (2012).

158 Bhatt, B. *et al.* Gpr109a Limits Microbiota-Induced IL-23 Production To Constrain ILC3-Mediated Colonic Inflammation. *J Immunol* **200**, 2905-2914, doi:10.4049/jimmunol.1701625 (2018).

159 Uhlig, H. H. *et al.* Differential activity of IL-12 and IL-23 in mucosal and systemic innate immune pathology. *Immunity* **25**, 309-318, doi:10.1016/j.immuni.2006.05.017 (2006).

160 Visekruna, A. *et al.* Transcription factor c-Rel plays a crucial role in driving anti-CD40-mediated innate colitis. *Mucosal Immunol* **8**, 307-315, doi:10.1038/mi.2014.68 (2015).

161 Eken, A., Singh, A. K., Treuting, P. M. & Oukka, M. IL-23R+ innate lymphoid cells induce colitis via interleukin-22-dependent mechanism. *Mucosal Immunol* **7**, 143-154, doi:10.1038/mi.2013.33 (2014).

162 Brasseit, J. *et al.* Divergent Roles of Interferon-gamma and Innate Lymphoid Cells in Innate and Adaptive Immune Cell-Mediated Intestinal Inflammation. *Front Immunol* **9**, 23, doi:10.3389/fimmu.2018.00023 (2018).

163 Castellanos, J. G. *et al.* Microbiota-Induced TNF-like Ligand 1A Drives Group 3 Innate Lymphoid Cell-Mediated Barrier Protection and Intestinal T Cell Activation during Colitis. *Immunity* **49**, 1077-1089.e1075, doi:10.1016/j.immuni.2018.10.014 (2018).

164 Fuchs, A. *et al.* Intraepithelial type 1 innate lymphoid cells are a unique subset of IL-12- and IL-15-responsive IFN-gamma-producing cells. *Immunity* **38**, 769-781, doi:10.1016/j.immuni.2013.02.010 (2013).

165 Li, J. *et al.* Enrichment of IL-17A(+) IFN-gamma(+) and IL-22(+) IFN-gamma(+) T cell subsets is associated with reduction of NKp44(+) ILC3s in the terminal ileum of Crohn's disease patients. *Clin Exp Immunol* **190**, 143-153, doi:10.1111/cei.12996 (2017).

166 Geremia, A. *et al.* IL-23-responsive innate lymphoid cells are increased in inflammatory bowel disease. *J Exp Med* **208**, 1127-1133, doi:10.1084/jem.20101712 (2011).

167 Li, J., Doty, A. & Glover, S. C. Aryl hydrocarbon receptor signaling involves in the human intestinal ILC3/ILC1 conversion in the inflamed terminal ileum of Crohn's disease patients. *Inflammation and cell signaling* **3**, doi:10.14800/ics.1404 (2016).

168 Kunz, J. *et al.* Target of rapamycin in yeast, TOR2, is an essential phosphatidylinositol kinase homolog required for G1 progression. *Cell* **73**, 585-596, doi:10.1016/0092-8674(93)90144-f (1993).

169 Cafferkey, R. *et al.* Dominant missense mutations in a novel yeast protein related to mammalian phosphatidylinositol 3-kinase and VPS34 abrogate rapamycin cytotoxicity. *Molecular and cellular biology* **13**, 6012-6023, doi:10.1128/mcb.13.10.6012 (1993).

170 Brown, E. J. *et al.* A mammalian protein targeted by G1-arresting rapamycin-receptor complex. *Nature* **369**, 756-758, doi:10.1038/369756a0 (1994).

171 Sabatini, D. M., Erdjument-Bromage, H., Lui, M., Tempst, P. & Snyder, S. H. RAFT1: a mammalian protein that binds to FKBP12 in a rapamycin-dependent fashion and is homologous to yeast TORs. *Cell* **78**, 35-43, doi:10.1016/0092-8674(94)90570-3 (1994).

172 Sabers, C. J. *et al.* Isolation of a protein target of the FKBP12-rapamycin complex in mammalian cells. *J Biol Chem* **270**, 815-822, doi:10.1074/jbc.270.2.815 (1995).

173 Laplante, M. & Sabatini, D. M. mTOR signaling in growth control and disease. *Cell* **149**, 274-293, doi:10.1016/j.cell.2012.03.017 (2012).

174 Shimobayashi, M. & Hall, M. N. Making new contacts: the mTOR network in metabolism and signalling crosstalk. *Nat Rev Mol Cell Biol* **15**, 155-162, doi:10.1038/nrm3757 (2014).

175 Dai, H. & Thomson, A. W. The "other" mTOR complex: New insights into mTORC2 immunobiology and their implications. *Am J Transplant* **19**, 1614-1621, doi:10.1111/ajt.15320 (2019).

176 Weichhart, T., Hengstschlager, M. & Linke, M. Regulation of innate immune cell function by mTOR. *Nat Rev Immunol* **15**, 599-614, doi:10.1038/nri3901 (2015).

177 Keating, R. & McGargill, M. A. mTOR Regulation of Lymphoid Cells in Immunity to Pathogens. *Front Immunol* **7**, 180, doi:10.3389/fimmu.2016.00180 (2016).

178 Dimeloe, S., Burgener, A. V., Grahlert, J. & Hess, C. T-cell metabolism governing activation, proliferation and differentiation; a modular view. *Immunology* **150**, 35-44, doi:10.1111/imm.12655 (2017).

179 Kelly, B. & O'Neill, L. A. Metabolic reprogramming in macrophages and dendritic cells in innate immunity. *Cell Res* **25**, 771-784, doi:10.1038/cr.2015.68 (2015).

180 Jones, R. G. & Pearce, E. J. MenTORing Immunity: mTOR Signaling in the Development and Function of Tissue-Resident Immune Cells. *Immunity* **46**, 730-742, doi:10.1016/j.immuni.2017.04.028 (2017).

181 Zeng, H. mTOR signaling in immune cells and its implications for cancer immunotherapy. *Cancer Lett* **408**, 182-189, doi:10.1016/j.canlet.2017.08.038 (2017).

182 Bantug, G. R., Galluzzi, L., Kroemer, G. & Hess, C. The spectrum of T cell metabolism in health and disease. *Nat Rev Immunol* **18**, 19-34, doi:10.1038/nri.2017.99 (2018).

183 Powell, J. D., Heikamp, E. B., Pollizzi, K. N. & Waickman, A. T. A modified model of T-cell differentiation based on mTOR activity and metabolism. *Cold Spring Harb Symp Quant Biol* **78**, 125-130, doi:10.1101/sqb.2013.78.020214 (2013).

184 Pollizzi, K. N. & Powell, J. D. Regulation of T cells by mTOR: the known knowns and the known unknowns. *Trends Immunol* **36**, 13-20, doi:10.1016/j.it.2014.11.005 (2015).

185 Delgoffe, G. M. *et al.* The kinase mTOR regulates the differentiation of helper T cells through the selective activation of signaling by mTORC1 and mTORC2. *Nature Immunology* **12**, 295-303, doi:10.1038/ni.2005 (2011).

186 Delgoffe, G. M. *et al.* The mTOR kinase differentially regulates effector and regulatory T cell lineage commitment. *Immunity* **30**, 832-844, doi:10.1016/j.immuni.2009.04.014 (2009).

187 Zeng, H. *et al.* mTORC1 and mTORC2 Kinase Signaling and Glucose Metabolism Drive Follicular Helper T Cell Differentiation. *Immunity* **45**, 540-554, doi:10.1016/j.immuni.2016.08.017 (2016).

188 Zeng, H. *et al.* mTORC1 couples immune signals and metabolic programming to establish T(reg)-cell function. *Nature* **499**, 485-490, doi:10.1038/nature12297 (2013).

189 Chapman, N. M. *et al.* mTOR coordinates transcriptional programs and mitochondrial metabolism of activated T(reg) subsets to protect tissue homeostasis. *Nat Commun* **9**, 2095, doi:10.1038/s41467-018-04392-5 (2018).

190 Shi, H. *et al.* Amino Acids License Kinase mTORC1 Activity and Treg Cell Function via Small G Proteins Rag and Rheb. *Immunity* **51**, 1012-1027.e1017, doi:10.1016/j.immuni.2019.10.001 (2019).

191 Sun, I. H. *et al.* mTOR Complex 1 Signaling Regulates the Generation and Function of Central and Effector Foxp3(+) Regulatory T Cells. *J Immunol* **201**, 481-492, doi:10.4049/jimmunol.1701477 (2018).

192 Shrestha, S. *et al.* Treg cells require the phosphatase PTEN to restrain TH1 and TFH cell responses. *Nat Immunol* **16**, 178-187, doi:10.1038/ni.3076 (2015).

193 Huynh, A. *et al.* Control of PI(3) kinase in Treg cells maintains homeostasis and lineage stability. *Nature Immunology* **16**, 188-196, doi:10.1038/ni.3077 (2015).

194 Hu, S. *et al.* Beneficial effects of dual TORC1/2 inhibition on chronic experimental colitis. *International immunopharmacology* **70**, 88-100, doi:10.1016/j.intimp.2019.02.022 (2019).

195 Pollizzi, K. N. *et al.* Asymmetric inheritance of mTORC1 kinase activity during division dictates CD8(+) T cell differentiation. *Nat Immunol* **17**, 704-711, doi:10.1038/ni.3438 (2016).

196 Zhang, L. *et al.* Mammalian Target of Rapamycin Complex 2 Controls CD8 T Cell Memory Differentiation in a Foxo1-Dependent Manner. *Cell Rep* **14**, 1206-1217, doi:10.1016/j.celrep.2015.12.095 (2016).

197 Chen, L. C., Nicholson, Y. T., Rosborough, B. R., Thomson, A. W. & Raimondi, G. A Novel mTORC1-Dependent, Akt-Independent Pathway Differentiates the Gut Tropism of Regulatory and Conventional CD4 T Cells. *J Immunol* **197**, 1137-1147, doi:10.4049/jimmunol.1600696 (2016).

198 Ip, W. K. E., Hoshi, N., Shouval, D. S., Snapper, S. & Medzhitov, R. Anti-inflammatory effect of IL-10 mediated by metabolic reprogramming of macrophages. *Science* **356**, 513-519, doi:10.1126/science.aal3535 (2017).

199 Cheng, S. C. *et al.* mTOR- and HIF-1α-mediated aerobic glycolysis as metabolic basis for trained immunity. *Science* **345**, 1250684, doi:10.1126/science.1250684 (2014).

200 Braza, M. S. *et al.* Inhibiting Inflammation with Myeloid Cell-Specific Nanobiologics Promotes Organ Transplant Acceptance. *Immunity* **49**, 819-828.e816, doi:10.1016/j.immuni.2018.09.008 (2018).

201 Bekkering, S. *et al.* Metabolic Induction of Trained Immunity through the Mevalonate Pathway. *Cell* **172**, 135-146.e139, doi:10.1016/j.cell.2017.11.025 (2018).

202 Joseph, A. M., Monticelli, L. A. & Sonnenberg, G. F. Metabolic regulation of innate and adaptive lymphocyte effector responses. *Immunol Rev* **286**, 137-147, doi:10.1111/imr.12703 (2018).

203 O'Sullivan, T. E. & Sun, J. C. Innate Lymphoid Cell Immunometabolism. *J Mol Biol* **429**, 3577-3586, doi:10.1016/j.jmb.2017.08.014 (2017).

204 Donnelly, R. P. *et al.* mTORC1-dependent metabolic reprogramming is a prerequisite for NK cell effector function. *J Immunol* **193**, 4477-4484, doi:10.4049/jimmunol.1401558 (2014).

205 Marçais, A. *et al.* The metabolic checkpoint kinase mTOR is essential for IL-15 signaling during the development and activation of NK cells. *Nat Immunol* **15**, 749-757, doi:10.1038/ni.2936 (2014).

206 Wilhelm, C. *et al.* Critical role of fatty acid metabolism in ILC2-mediated barrier protection during malnutrition and helminth infection. *J Exp Med* **213**, 1409-1418, doi:10.1084/jem.20151448 (2016).

207 Wilhelm, C., Kharabi Masouleh, S. & Kazakov, A. Metabolic Regulation of Innate Lymphoid Cell-Mediated Tissue Protection-Linking the Nutritional State to Barrier Immunity. *Front Immunol* **8**, 1742, doi:10.3389/fimmu.2017.01742 (2017).

208 Karagiannis, F. *et al.* Lipid-Droplet Formation Drives Pathogenic Group 2 Innate Lymphoid Cells in Airway Inflammation. *Immunity* **52**, 620-634.e626, doi:10.1016/j.immuni.2020.03.003 (2020).

209 Di Luccia, B., Gilfillan, S., Cella, M., Colonna, M. & Huang, S. C. ILC3s integrate glycolysis and mitochondrial production of reactive oxygen species to fulfill activation demands. *J Exp Med*, doi:10.1084/jem.20180549 (2019).

210 Bentzinger, C. F. *et al.* Differential response of skeletal muscles to mTORC1 signaling during atrophy and hypertrophy. *Skelet Muscle* **3**, 6, doi:10.1186/2044-5040-3-6 (2013).

211 Srinivas, S. *et al.* Cre reporter strains produced by targeted insertion of EYFP and ECFP into the ROSA26 locus. *BMC developmental biology* **1**, 4, doi:10.1186/1471-213x-1-4 (2001).

212 Tsapogas, P. *et al.* In vivo evidence for an instructive role of fms-like tyrosine kinase-3 (FLT3) ligand in hematopoietic development. *Haematologica* **99**, 638-646, doi:10.3324/haematol.2013.089482 (2014).

213 Sano, T. *et al.* An IL-23R/IL-22 Circuit Regulates Epithelial Serum Amyloid A to Promote Local Effector Th17 Responses. *Cell* **164**, 324, doi:10.1016/j.cell.2015.12.047 (2016).

214 Sonnenberg, G. F., Fouser, L. A. & Artis, D. Border patrol: regulation of immunity, inflammation and tissue homeostasis at barrier surfaces by IL-22. *Nat Immunol* **12**, 383-390, doi:10.1038/ni.2025 (2011).

215 Wang, F. *et al.* Crosstalks between mTORC1 and mTORC2 variagate cytokine signaling to control NK maturation and effector function. *Nat Commun* **9**, 4874, doi:10.1038/s41467-018-07277-9 (2018).

216 Mebius, R. E. Organogenesis of lymphoid tissues. *Nature Reviews Immunology* **3**, 292-303, doi:10.1038/nri1054 (2003).

217 Finke, D. Fate and function of lymphoid tissue inducer cells. *Current Opinion in Immunology* **17**, 144-150, doi:https://doi.org/10.1016/j.coi.2005.01.006 (2005).

218 Nussbaum, J. C. *et al.* Type 2 innate lymphoid cells control eosinophil homeostasis. *Nature* **502**, 245-248, doi:10.1038/nature12526 (2013).

219 Boyman, O., Kovar, M., Rubinstein, M. P., Surh, C. D. & Sprent, J. Selective stimulation of T cell subsets with antibody-cytokine immune complexes. *Science* **311**, 1924-1927, doi:10.1126/science.1122927 (2006).

220 Marzec, M. *et al.* IL-2- and IL-15-induced activation of the rapamycin-sensitive mTORC1 pathway in malignant CD4+ T lymphocytes. *Blood* **111**, 2181-2189, doi:10.1182/blood-2007-06-095182 (2008).

221 Melo-Gonzalez, F. & Hepworth, M. R. Functional and phenotypic heterogeneity of group 3 innate lymphoid cells. *Immunology* **150**, 265-275, doi:10.1111/imm.12697 (2017).

222 Scoville, S. D. *et al.* A Progenitor Cell Expressing Transcription Factor RORgammat Generates All Human Innate Lymphoid Cell Subsets. *Immunity* **44**, 1140-1150, doi:10.1016/j.immuni.2016.04.007 (2016).

223 Baerenwaldt, A. *et al.* Flt3 Ligand Regulates the Development of Innate Lymphoid Cells in Fetal and Adult Mice. *J Immunol* **196**, 2561-2571, doi:10.4049/jimmunol.1501380 (2016).

224 Li, J. *et al.* Activation of DR3 signaling causes loss of ILC3s and exacerbates intestinal inflammation. *Nat Commun* **10**, 3371, doi:10.1038/s41467-019-11304-8 (2019).

225 Bain, C. C. & Schridde, A. Origin, Differentiation, and Function of Intestinal Macrophages. *Front Immunol* **9**, 2733, doi:10.3389/fimmu.2018.02733 (2018).

226 Desalegn, G. & Pabst, O. Inflammation triggers immediate rather than progressive changes in monocyte differentiation in the small intestine. *Nat Commun* **10**, 3229, doi:10.1038/s41467-019-11148-2 (2019).

227 Backert, I. *et al.* STAT3 activation in Th17 and Th22 cells controls IL-22-mediated epithelial host defense during infectious colitis. *J Immunol* **193**, 3779-3791, doi:10.4049/jimmunol.1303076 (2014).

228 Chandrakesan, P. *et al.* Utility of a bacterial infection model to study epithelial-mesenchymal transition, mesenchymal-epithelial transition or tumorigenesis. *Oncogene* **33**, 2639-2654, doi:10.1038/onc.2013.210 (2014).

229 Higgins, L. M., Frankel, G., Douce, G., Dougan, G. & MacDonald, T. T. Citrobacter rodentium infection in mice elicits a mucosal Th1 cytokine response and lesions similar to those in murine inflammatory bowel disease. *Infect Immun* **67**, 3031-3039 (1999).

230 Rankin, L. C. *et al.* Complementarity and redundancy of IL-22-producing innate lymphoid cells. *Nat Immunol* **17**, 179-186, doi:10.1038/ni.3332 (2016).

231 Korn, L. L. *et al.* Conventional CD4+ T cells regulate IL-22-producing intestinal innate lymphoid cells. *Mucosal Immunol* **7**, 1045-1057, doi:10.1038/mi.2013.121 (2014).

232 Jaensson-Gyllenbäck, E. *et al.* Bile retinoids imprint intestinal CD103+ dendritic cells with the ability to generate gut-tropic T cells. *Mucosal Immunology* **4**, 438-447, doi:10.1038/mi.2010.91 (2011).

233 den Besten, G. *et al.* The role of short-chain fatty acids in the interplay between diet, gut microbiota, and host energy metabolism. *Journal of lipid research* **54**, 2325-2340, doi:10.1194/jlr.R036012 (2013).

234 Kim, S. H., Cho, B. H., Kiyono, H. & Jang, Y. S. Microbiota-derived butyrate suppresses group 3 innate lymphoid cells in terminal ileal Peyer's patches. *Sci Rep* **7**, 3980, doi:10.1038/s41598-017-02729-6 (2017).

235 James, K. R. *et al.* Distinct microbial and immune niches of the human colon. *Nature Immunology* **21**, 343-353, doi:10.1038/s41590-020-0602-z (2020).

236 Bunker, J. J. *et al.* Innate and Adaptive Humoral Responses Coat Distinct Commensal Bacteria with Immunoglobulin A. *Immunity* **43**, 541-553, doi:10.1016/j.immuni.2015.08.007 (2015).

237 Hall, J. A. *et al.* Essential role for retinoic acid in the promotion of CD4(+) T cell effector responses via retinoic acid receptor alpha. *Immunity* **34**, 435-447, doi:10.1016/j.immuni.2011.03.003 (2011).

238 Noureldein, M. H. & Eid, A. A. Gut microbiota and mTOR signaling: Insight on a new pathophysiological interaction. *Microb Pathog* **118**, 98-104, doi:10.1016/j.micpath.2018.03.021 (2018).

239 Lehmann, F. M. *et al.* Microbiota-induced tissue signals regulate ILC3-mediated antigen presentation. *Nature Communications* **11**, 1794, doi:10.1038/s41467-020-15612-2 (2020).

240 Pearson, C. *et al.* ILC3 GM-CSF production and mobilisation orchestrate acute intestinal inflammation. *eLife* **5**, e10066, doi:10.7554/eLife.10066 (2016).

241 Mortha, A. & Burrows, K. Cytokine Networks between Innate Lymphoid Cells and Myeloid Cells. *Front Immunol* **9**, 191, doi:10.3389/fimmu.2018.00191 (2018).

242 Withers, D. R. *et al.* Cutting edge: lymphoid tissue inducer cells maintain memory CD4 T cells within secondary lymphoid tissue. *J Immunol* **189**, 2094-2098, doi:10.4049/jimmunol.1201639 (2012).

243 Lim, A. I. *et al.* Systemic Human ILC Precursors Provide a Substrate for Tissue ILC Differentiation. *Cell* **168**, 1086-1100 e1010, doi:10.1016/j.cell.2017.02.021 (2017).

244 Li, N. *et al.* Mass cytometry reveals innate lymphoid cell differentiation pathways in the human fetal intestine. *J Exp Med* **215**, 1383-1396, doi:10.1084/jem.20171934 (2018).

245 Montaldo, E. *et al.* Human RORγt(+)CD34(+) cells are lineage-specified progenitors of group 3 RORγt(+) innate lymphoid cells. *Immunity* **41**, 988-1000, doi:10.1016/j.immuni.2014.11.010 (2014).

246 Kurebayashi, Y. *et al.* PI3K-Akt-mTORC1-S6K1/2 axis controls Th17 differentiation by regulating Gfi1 expression and nuclear translocation of RORγ. *Cell Rep* **1**, 360-373, doi:10.1016/j.celrep.2012.02.007 (2012).

247 Chang, J. *et al.* MyD88 is essential to sustain mTOR activation necessary to promote T helper 17 cell proliferation by linking IL-1 and IL-23 signaling. *Proc Natl Acad Sci U S A* **110**, 2270-2275, doi:10.1073/pnas.1206048110 (2013).

248 Zuba-Surma, E. K., Kucia, M., Abdel-Latif, A., Lillard, J. W., Jr. & Ratajczak, M. Z. The ImageStream System: a key step to a new era in imaging. *Folia histochemica et cytobiologica* **45**, 279-290 (2007).

249 Maguire, O., Collins, C., O'Loughlin, K., Miecznikowski, J. & Minderman, H. Quantifying nuclear p65 as a parameter for NF-kappaB activation: Correlation between ImageStream cytometry, microscopy, and Western blot. *Cytometry A* **79**, 461-469, doi:10.1002/cyto.a.21068 (2011).

250 Gerriets, V. A. *et al.* Metabolic programming and PDHK1 control CD4+ T cell subsets and inflammation. *J Clin Invest* **125**, 194-207, doi:10.1172/jci76012 (2015).

251 Raud, B. *et al.* Etomoxir Actions on Regulatory and Memory T Cells Are Independent of Cpt1a-Mediated Fatty Acid Oxidation. *Cell Metab* **28**, 504-515.e507, doi:10.1016/j.cmet.2018.06.002 (2018).

252 Chang, C. H. *et al.* Posttranscriptional control of T cell effector function by aerobic glycolysis. *Cell* **153**, 1239-1251, doi:10.1016/j.cell.2013.05.016 (2013).

253 Jain, A., Song, R., Wakeland, E. K. & Pasare, C. T cell-intrinsic IL-1R signaling licenses effector cytokine production by memory CD4 T cells. *Nat Commun* **9**, 3185, doi:10.1038/s41467-018-05489-7 (2018).

254 Parham, C. *et al.* A receptor for the heterodimeric cytokine IL-23 is composed of IL-12Rbeta1 and a novel cytokine receptor subunit, IL-23R. *J Immunol* **168**, 5699-5708, doi:10.4049/jimmunol.168.11.5699 (2002).

255 Lankford, C. S. & Frucht, D. M. A unique role for IL-23 in promoting cellular immunity. *J Leukoc Biol* **73**, 49-56 (2003).

256 Cai, Y. *et al.* Differential Roles of the mTOR-STAT3 Signaling in Dermal γδ T Cell Effector Function in Skin Inflammation. *Cell Rep* **27**, 3034-3048.e3035, doi:10.1016/j.celrep.2019.05.019 (2019).

257 Mathur, A. N. *et al.* Stat3 and Stat4 direct development of IL-17-secreting Th cells. *J Immunol* **178**, 4901-4907, doi:10.4049/jimmunol.178.8.4901 (2007).

258 Chun, E. *et al.* Metabolite-Sensing Receptor Ffar2 Regulates Colonic Group 3 Innate Lymphoid Cells and Gut Immunity. *Immunity* **51**, 871-884.e876, doi:10.1016/j.immuni.2019.09.014 (2019).

259 Gotthardt, D. *et al.* Loss of STAT3 in murine NK cells enhances NK cell-dependent tumor surveillance. *Blood* **124**, 2370-2379, doi:10.1182/blood-2014-03-564450 (2014).

260 Song, C. *et al.* Unique and redundant functions of NKp46+ ILC3s in models of intestinal inflammation. *J Exp Med* **212**, 1869-1882, doi:10.1084/jem.20151403 (2015).

261 Mutalib, M. *et al.* The use of sirolimus (rapamycin) in the management of refractory inflammatory bowel disease in children. *J Crohns Colitis* **8**, 1730-1734, doi:10.1016/j.crohns.2014.08.014 (2014).

262 Massey, D. C., Bredin, F. & Parkes, M. Use of sirolimus (rapamycin) to treat refractory Crohn's disease. *Gut* **57**, 1294-1296, doi:10.1136/gut.2008.157297 (2008).

263 Dumortier, J. *et al.* Everolimus for refractory Crohn's disease: A case report. *Inflammatory Bowel Diseases* **14**, 874-877, doi:10.1002/ibd.20395 (2008).

264 Matsuda, C. *et al.* Therapeutic effect of a new immunosuppressive agent, everolimus, on interleukin-10 gene-deficient mice with colitis. *Clin Exp Immunol* **148**, 348-359, doi:10.1111/j.1365-2249.2007.03345.x (2007).

9 Appendix

9.1 Abbreviations and symbols

9.1.1 Abbreviations

2-DG	2-Deoxy-D-glucose
Ab	antibody
Ach	acetylcholine
Ag	antigen
AhR	aryl hydrocarbon receptor
AMPK	AMP activated protein kinase
ARNT	AhR nuclear translocator
αLP	α-lymphoid progenitor
ATP	adenosine triphosphate
BAFF	B cell-activation factor
BCL11	B cell lymphoma-leukemia 11b protein
bp	base pair
BSA	Bovine Serum Albumin
CD	Crohn's disease
cDC1	conventional DC1
cDC2	conventional DC2
CF	cystic fibrosis
CFU	colony-forming units
CHILP	common helper innate lymphoid cell progenitor
CILCPs	common ILC precursors
cLP	colonic lamina propria
CLP	common lymphoid progenitor
CMP	common myeloid progenitor
COPD	chronic obstructive pulmonary disease
CP	cryptopatch
CRSwNP	chronic rhino-sinusitis with nasal polyps
DAMPs	damage-associated molecular patterns
DC	dendritic cell
ddH$_2$O	double-distilled water
DDR	DNA damage response
Deptor	DEP domain containing mTOR-interacting protein
DLL1	Delta-like 1
DMEM	Dulbecco's Modified Eagle medium
DMSO	dimethyl sulfoxide
dNTP	Deoxynucleoside Triphosphate

DMEM	Dulbecco's Modified Eagle medium
DSS	dextran sulfate sodium
ECAR	extracellular acidification rate
EDTA	Ethylenediaminetetraacetic acid
EHEC	enterohemorrhagic *Escherichia coli*
EILP	early innate lymphoid progenitor
EOMES	Eomesodermin
EPEC	enteropathogenic *Escherichia coli*
FACS	fluorescence-activated cell sorting
FBS	fetal bovine serum
FKB12	12-kDa FK506-binding protein
FM	fate map
Foll B cell	follicular B cell
Fwd primer	forward primer
GATA3	GATA binding protein 3
GC B cell	germinal center B cell
GDNF	glial-derived neurotrophic factor
GFL	GDNF family ligand
GM-CSF, CSF2	granulocyte-macrophage colony-stimulating factor
HSC	hematopoietic stem cell
HSCT	hematopoietic stem cell transplantation
iBALT	inducible bronchus-associated lymphoid tissues
IBD	inflammatory bowel disease
IL	interleukin
ILC	Innate lymphoid cell
ILC1	group 1 ILCs
ILC2	group 2 ILCs
ILC2p	ILC2-committed precursor
ILC3	group 3 ILCs
ILCP	ILC precursor
ILCregs	regulatory ILCs
IFN	interferon
IgA	immunoglobulin A
IgG	immunoglobulin G
ILF	isolated lymphoid follicle
IMDM	Iscove's Modified Dulbecco's Media
i.p.	intraperitoneal
ISC	intestinal epithelial stem cells
JAK	Janus kinase
KO	knockout
LB	Luria-Bertani

Lin⁻	lineage-negative
LN	lymph node
LP	lamina propria
LP2	lipocalin-2
Lt	lymphotoxin
LTi cell	lymphoid tissue inducer cell
MAMPs	microbe-associated molecular patterns
MHC	major histocompatibility complex
mLST8	mammalian lethal with sec-13 protein 8
mLN	mesenteric lymph node
MNP	mononuclear phagocyte
MΦ	macrophage
mSIN1	mammalian stress-activated map kinase-interacting protein
mTOR	mechanistic target of rapamycin
mTORC1	mTOR complex 1
mTORC2	mTOR complex 2
MYD88	myeloid differentiation primary response 88
MZB	marginal zone B cell
NCR	natural cytotoxicity receptor
NFIL3	nuclear factor interleukin-3 regulated protein
NK cell	natural killer cell
NKP	NK cell progenitors
NK cells	natural killer cells
NLR	NOD-like receptor
NMU	neuromedin U
NSG mice	NOD *SCID IL2rγ$^{/-}$* mice
OCR	oxygen consumption rate
PAMP	pathogen-associated patterns
PBS	phosphate-buffered saline
PCTR1	protectin conjugates in tissue regeneration1
pDC	plasmacytoid dendritic cell
PP	Peyer's patch
PRAS40	prolin-rich Akt substrate 40 kDa
PRR	pattern recognition receptor
Protor1/2	protein observed with Rictor 1 and 2
RA	retinoic acid
RAR	retinoic acid receptor
Raptor	regulatory-associated protein of mTOR
Reg	regenerating islet-derived proteins
Rev primer	reverse primer
Rheb	Ras homolog enriched in brain

Rictor	rapamycin-insensitive companion of mTOR
RLR	RIG-I-like receptors
RORα	RAR-related orphan receptor alpha
RORγt	RAR-related orphan receptor gamma t
RT qPCR	quantitative real-time polymerase chain reaction
RUNX3	runt related transcription factor 3
SCFA	short-chain fatty acid
SFB	segmented filamentous bacteria
SI	small intestine, small intestinal
SI LP	small intestinal lamina propria
SPF	specific-pathogen-free
STAT	signal transducer and activator of transcription
TCF1	T cell factor
Tfh cells	follicular T helper cells
Th	T helper
TL1A	TNF-like ligand 1A
TLR	Toll-like receptor
TNF	tumor necrosis factor
TOX	thymocyte selection-associated high mobility group box protein
TLR	Toll-like receptor
Treg	regulatory T cell
TSC1/2	tuberous sclerosis 1/2
UC	ulcerative colitis
VIPR	vasoactive intestinal peptide receptor
wt	wildtype
XRE	xenobiotic response elements

9.1.2 Symbols

g/L	gram per liter
M	molar
μm	micrometer
mM	millimolar
mg/ml	milligram per milliliter
μM	micromolar
μg/ml	microgram per milliliter
nM	nanomolar
ng/ml	nanogram per milliliter

9.2   Supplemental figures
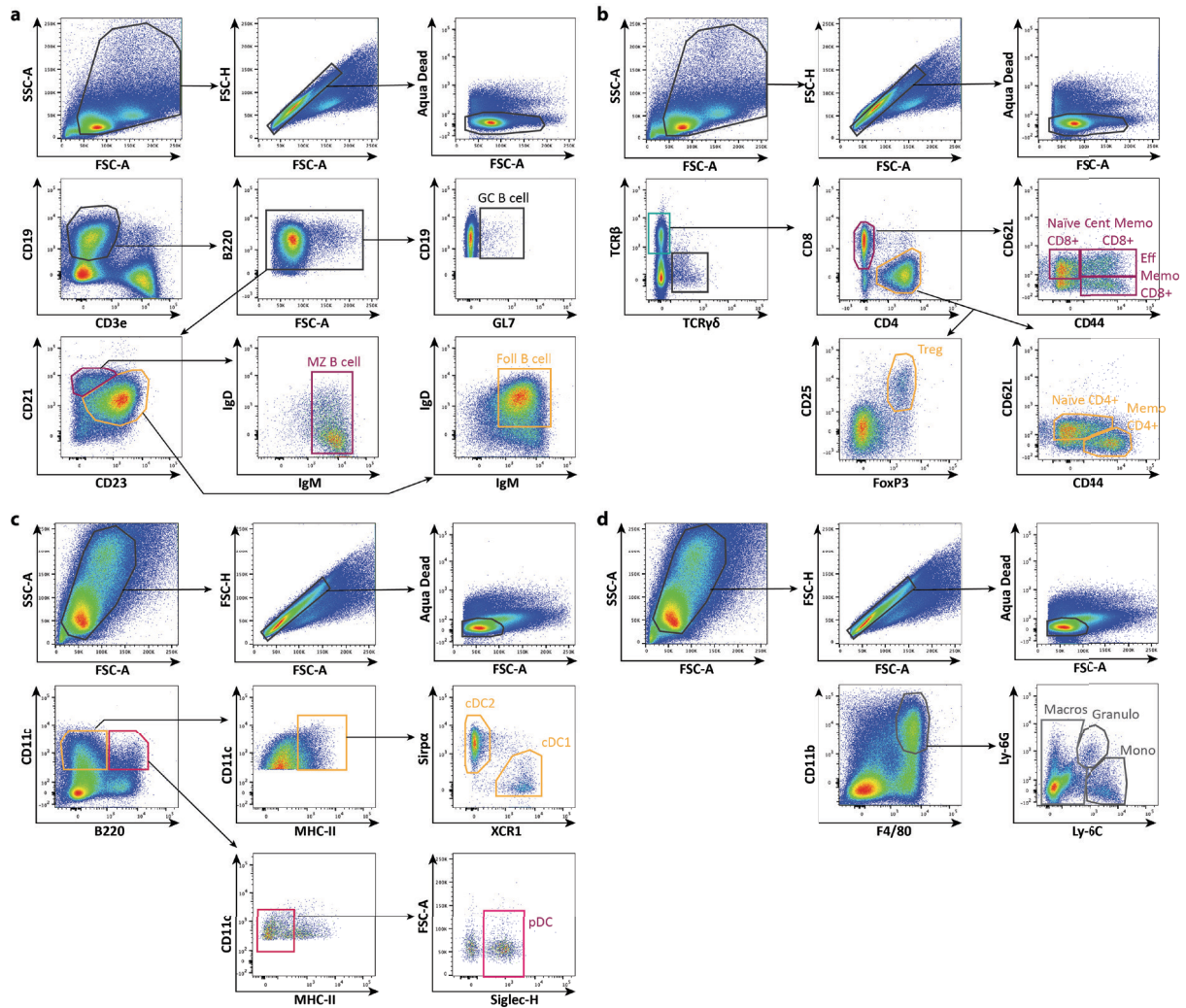
Fig.S1 Gating strategies for immunophenotyping of knockout mice. a) Exemplary B cell gating, spleen from wildtype mouse. b) Exemplary T cell gating, spleen from wildtype mouse. c) Exemplary DC gating, SI from *Rag2-/-* mouse. d) Exemplary myeloid cell gating, SI from *Rag2-/-* mouse. GC B: germinal center B cell, MZB: marginal zone B cell, Foll B: follicular B cell, Memo CD4: memory CD4 T cell, CM CD8: central memory CD8 T cell, EM CD8: effector memory CD8 T cell, pDC: plasmacytoid DC, cDC1 conventional DC1, cDC2 conventional DC2, Macro: macrophage, Granulo: granulocyte, Mono: monocyte.
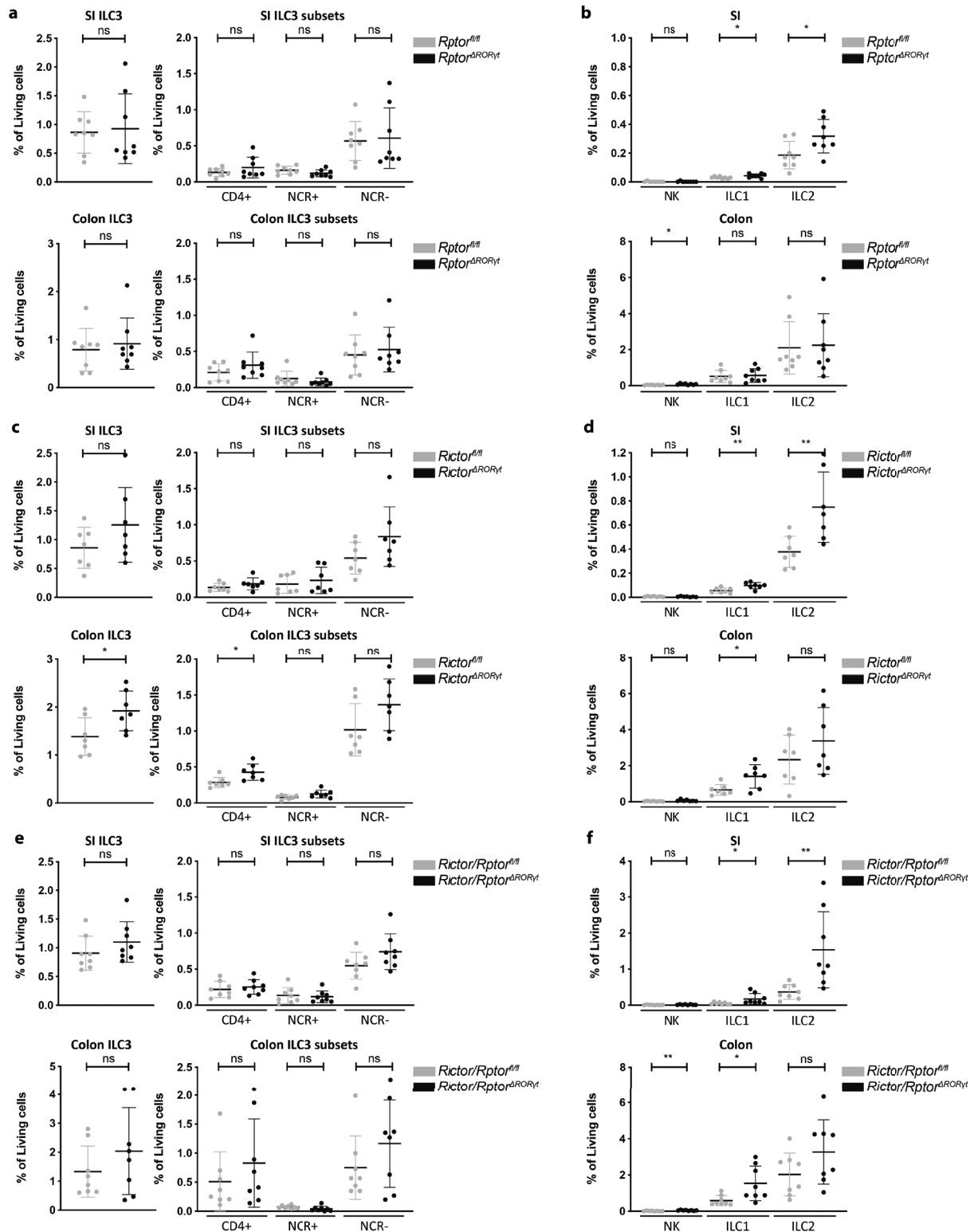
Fig.S2 Percentage of ILC3 subsets in wildtype mice is not affected by loss of mTORC1 and mTORC2. Cells were isolated from SI LP and cLP and analyzed for percentage of total ILC3s and three ILC3 subsets (a, c, e). Percentage of other ILC subsets were further dissected (b, d, f). $Rptor^{\Delta ROR\gamma t}$ (a, b), $Rictor^{\Delta ROR\gamma t}$ (c, d) or $Rictor/Rptor^{\Delta ROR\gamma t}$ (e, f) mice and age-matched Cre-negative littermates. Mice were 8-10 weeks old at analysis. n = 7-8. Two-tailed unpaired t test or Mann-Whitney U test. *p ≤ 0.05, **p ≤ 0.01, ***p ≤ 0.001

Fig.S3 Percentage of ILC3 subsets differs in *Rptor^ΔRORγt^Rag2^-/-^*, *Rictor^ΔRORγt^Rag2^-/-^* and *Rictor/Rptor^ΔRORγt^Rag2^-/-^* mice. Cells were isolated from SI LP and cLP and analyzed for percentage of total ILC3s and three ILC3 subsets (a, c, e). Percentage of other ILC subsets was further dissected (b, d, f). *Rptor^ΔRORγt^Rag2^-/-^* (a, b), *Rictor^ΔRORγt^Rag2^-/-^* (c, d) or *Rictor/Rptor^ΔRORγt^Rag2^-/-^* (e, f) mice and age-matched Cre-negative littermates. Mice were 8-10 weeks old at analysis. n = 6-17. Two-tailed unpaired t test or Mann-Whitney U test. *p ≤ 0.05, **p ≤ 0.01, ***p ≤ 0.001
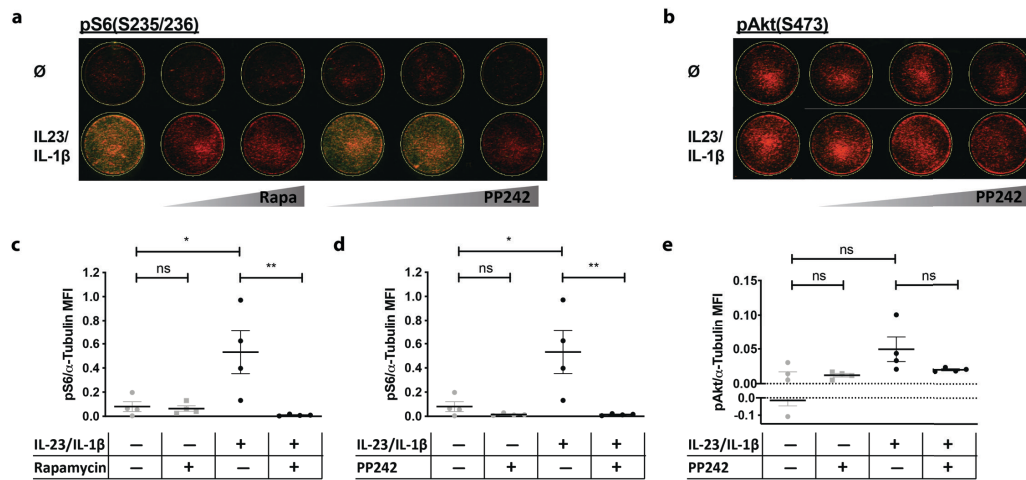
Fig.S4 IL-23/IL-1β induce mTOR-dependent phosphorylation of S6 and Akt. Sort-purified Lin⁻CD90.2⁺KLRG1⁻ ILC3s derived from the SI LP of *Flt3^tg* mice were cultured 48 h with or without IL23/IL-1β in the presence or absence of rapamycin (10 nM or 100 nM) or PP242 (10 nM, 100 nM or 1 μM). a, b) Exemplary In-Cell Western blot. Red: α-Tubulin, green: pS6 (a) or pAkt (b). c, d) Ratio of pS6 fluorescence signal normalized to α-Tubulin fluorescence signal. Rapamycin: 10 nM, PP242: 1 μM. e) Ratio of pAkt fluorescence signal normalized to α-Tubulin fluorescence signal. Rapamycin: 10 nM, PP242: 1 μM. n = 4. One-Way ANOVA with multiple comparison test (Dunnett). *p ≤ 0.05, **p ≤ 0.01, ***p ≤ 0.001
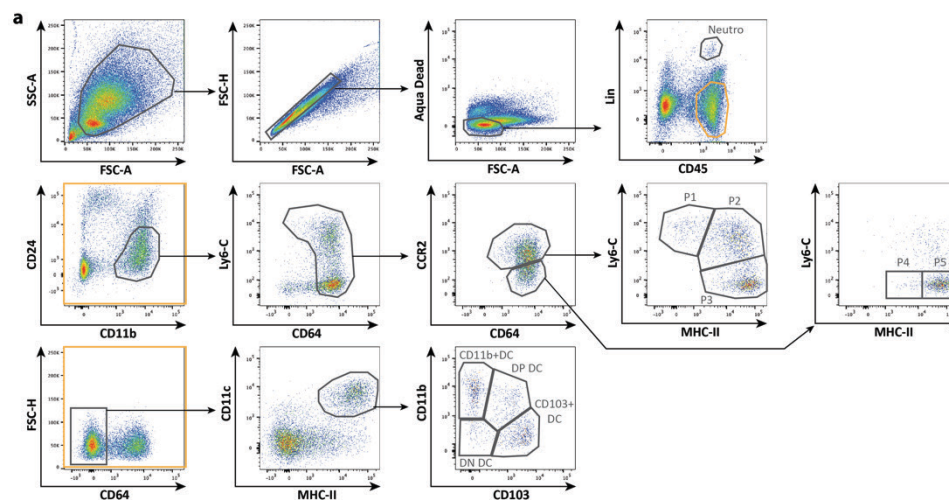
Fig.S5 Gating strategy for inflammatory monocytes, macrophages and neutrophils. a) Exemplary monocyte waterfall plot. Colon from *Rag2^-/-* mouse. Lin: CD3, CD19, NK1.1, Ly-6G.
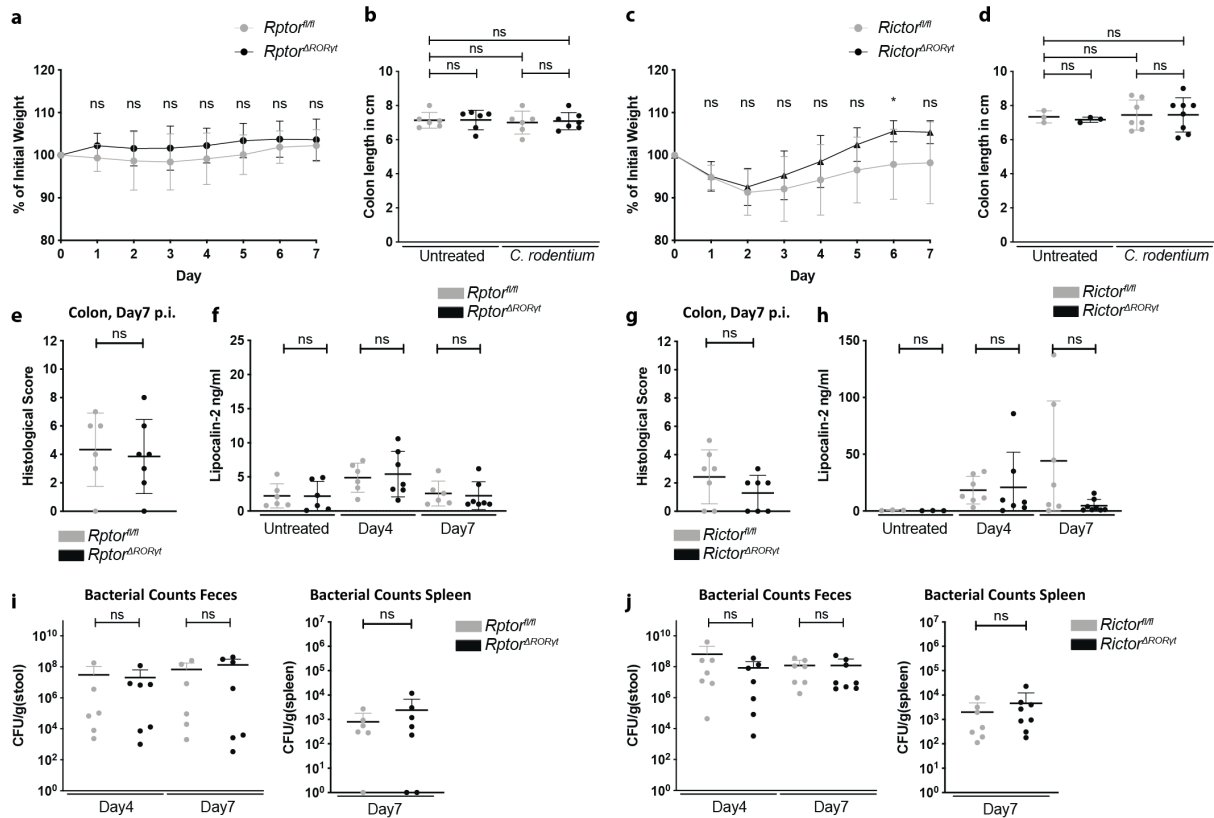
Fig.S6 Single loss of mTORC1 or mTORC2 in RORγt-expressing cells in immune-competent mice does not impair protection against infection with *C. rodentium*. *Rptor^{ΔRORγt}* (a, b, e, f, i) or *Rictor^{ΔRORγt}* (c, d, g, h, j) mice and age-matched littermates were left untreated or were orally infected with 2 x 10^9 CFU *C. rodentium*. Weight was monitored daily (a, c). Mice were sacrificed 7 days post-infection. The colon length was measured (b, d) and same parts of the colon were sectioned and stained with hematoxylin and eosin. Histological colitis score was determined by an experienced gastroenterologist (e, g). At day 4 and day 7, fecal Lipocalin-2 was determined from feces pellets diluted in PBS using ELISA (f, h). Fecal bacterial load was tested at day 4 and day 7 post-infection (i, j, left). Spleen was homogenized to determine bacterial spreading (i, j, right). n = 6-8. Two-tailed unpaired t test or Mann-Whitney U test. *p ≤ 0.05, **p ≤ 0.01, ***p ≤ 0.001

9.3 Publications/Manuscript in preparation

1. Microbiota-induced Tissue Signals Regulate ILC3-mediated Antigen Presentation.

Frank Michael Lehmann[1,9], Nicole von Burg[1,2,9], Robert Ivanek[3,4], Claudia Teufel[1], Edit Horvath[1], Annick Peter[1], Gleb Turchinovich[1], Daniel Staehli[1], Tobias Eichlisberger[5], Mercedes Gomez de Agüero[6], Mairene Coto-Llerena[3], Michaela Prchal-Murphy[7], Veronika Sexl[7], Mohamed Bentires-Alj[3], Christoph Mueller[8], Daniela Finke[1]

[1]Department of Biomedicine and University Children's Hospital of Basel, University of Basel, 4058, Basel, Switzerland; [2]Department of Health Technology, Technical University of Denmark, 2800, Kgs. Lyngby, Denmark; [3]Department of Biomedicine, University of Basel, 4056, Basel, Switzerland; [4]Swiss Institute of Bioinformatics, 4053, Basel, Switzerland; [5]Friedrich Miescher Institute for Biomedical Research, 4058, Basel, Switzerland; [6]Maurice Müller Laboratories, Department for BioMedical Research, Universitätsklinik für Viszerale Chirurgie und Medizin Inselspital, University of Bern, 3010, Bern, Switzerland; [7]Institute of Pharmacology and Toxicology, Department for Biomedical Sciences, University of Veterinary Medicine Vienna, Vienna, Austria; [8]Institute of Pathology, University of Bern, 3008, Bern, Switzerland; [9]These authors contributed equally: Frank Michael Lehmann, Nicole von Burg

Microbiota-induced tissue signals regulate ILC3-mediated antigen presentation

Frank Michael Lehmann [1,9], Nicole von Burg [1,2,9], Robert Ivanek [3,4], Claudia Teufel [1], Edit Horvath[1], Annick Peter[1], Gleb Turchinovich[1], Daniel Staehli[1], Tobias Eichlisberger [5], Mercedes Gomez de Agüero [6], Mairene Coto-Llerena[3], Michaela Prchal-Murphy[7], Veronika Sexl[7], Mohamed Bentires-Alj[3], Christoph Mueller [8] & Daniela Finke [1✉]

Although group 3 innate lymphoid cells (ILC3s) are efficient inducers of T cell responses in the spleen, they fail to induce CD4+ T cell proliferation in the gut. The signals regulating ILC3-T cell responses remain unknown. Here, we show that transcripts associated with MHC II antigen presentation are down-modulated in intestinal natural cytotoxicity receptor (NCR)⁻ ILC3s. Further data implicate microbiota-induced IL-23 as a crucial signal for reversible silencing of MHC II in ILC3s, thereby reducing the capacity of ILC3s to present antigen to T cells in the intestinal mucosa. Moreover, IL-23-mediated MHC II suppression is dependent on mTORC1 and STAT3 phosphorylation in NCR⁻ ILC3s. By contrast, splenic interferon-γ induces MHC II expression and CD4+ T cell stimulation by NCR⁻ ILC3s. Our results thus identify biological circuits for tissue-specific regulation of ILC3-dependent T cell responses. These pathways may have implications for inducing or silencing T cell responses in human diseases.

[1] Department of Biomedicine and University Children's Hospital of Basel, University of Basel, 4058 Basel, Switzerland. [2] Department of Health Technology, Technical University of Denmark, 2800 Kgs. Lyngby, Denmark. [3] Department of Biomedicine, University of Basel, 4056 Basel, Switzerland. [4] Swiss Institute of Bioinformatics, 4053 Basel, Switzerland. [5] Friedrich Miescher Institute for Biomedical Research, 4058 Basel, Switzerland. [6] Maurice Müller Laboratories, Department for BioMedical Research, Universitätsklinik für Viszerale Chirurgie und Medizin Inselspital, University of Bern, 3010 Bern, Switzerland. [7] Institute of Pharmacology and Toxicology, Department for Biomedical Sciences, University of Veterinary Medicine Vienna, Vienna, Austria. [8] Institute of Pathology, University of Bern, 3008 Bern, Switzerland. [9] These authors contributed equally: Frank Michael Lehmann, Nicole von Burg. ✉email: daniela.finke@unibas.ch

136

LC3s are primarily tissue-resident cells, which rapidly respond to infections and inflammation by cytokine secretion. They express and depend on the transcription factor RAR-related orphan receptor gamma t(RORγt)[1,2] and can be subdivided into natural cytotoxicity receptor (NCR)+ and NCR− cells[3]. Similar to T helper (TH)22 and TH17 cells, ILC3s secrete interleukin (IL)-22 and IL-17[4–6] and play a role in defense against *Citrobacter rodentium* infection and in tissue regeneration[7–11]. In addition to their function as early cytokine producers, recent analysis has revealed that ILC3 subsets can present antigen (Ag) to CD4+ T cells, but the quality and strength of T-cell response is tissue-dependent[12–14]. How ILC3-T-cell responses are regulated remains poorly defined.

In adults, ILC3s are abundant in mucosal tissues, e.g., the small intestine (SI) and colon, and mucosa-associated lymphoid organs[3,15]. In addition, ILC3s are found in the spleen (SP) and peripheral lymph nodes[6,15]. It is now increasingly recognized that ILCs exhibit heterogenous phenotypes across different tissues[16–19]. The exposure to environmental signals including microbial and nutrient-derived metabolites has been suggested to be relevant for the regulation of IL-22 and IL-17 responses of intestinal ILC3s[7,20–23]. The nature of signals that regulate Ag presentation and T-cell stimulation by ILC3s, however, is largely unknown. Moreover, data on a direct comparison of ILC3s among different organs are limited and often based on a sorting strategy not considering subsets. Single-cell transcriptome profiling of SI ILCs revealed that major histocompatibility complex (MHC) class II (MHC II) is mainly found in a NCR− ILC3 subset that lacks the T-box transcription factor T-bet (encoded by *Tbx21*) and is only partially overlapping with IL-22-producing ILC3s[20]. In the SP, Ag-presenting NCR− ILC3s elicit specific CD4+ T-cell responses and support the maintenance of CD4+ memory T cells[14,24]. In the SI, however, MHC II+ ILC3s are considered as negative regulators of commensal bacteria-specific CD4+ T-cell responses[12,13,25]. A central question that has not been addressed concerns the tissue-specific signals that regulate the capacity of ILC3 subsets to present Ag to CD4+ T cells.

We demonstrate here that NCR− ILC3s isolated from the SP and the SI of mice have a fundamentally distinct transcriptional signature. SP NCR− ILC3s harbor MHC II+ ILC3s with the capacity to elicit cognate CD4+ T-cell responses. In contrast, the majority of SI NCR− ILC3s lack MHC II and fail to induce T-cell proliferation. This is due to the fact that the gut microbiota and IL-23 inhibit expression of MHC II on ILC3s via pathways engaging mammalian target of rapamycin complex 1 (mTORC1) and signal transducer and activator of transcription 3 (STAT3). On the contrary, interferon γ (IFN-γ) enhances the expression of MHC II on ILC3s in the SP. Finally, we show that the functional inhibition of ILC3s by the SI environment is reversible both in vitro and in vivo. Together our data uncover the basic molecular requirements of ILC3s to control T-cell responses and highlight the role of the local environment in shaping tissue-specific ILC3-T-cell interactions.

Results

SP and SI ILC3s have a different transcriptional signature. SP and SI ILC3s differ in their capacity to induce Ag-dependent CD4+ T-cell responses[12,14]. To study the tissue-specific regulation of SP vs. SI NCR− ILC3 transcriptional programs, we profiled the transcriptome of the two subsets. To this end, lin −CD117+Thy1.2+eYFP+ cells from SP and SI of *RORc(γt)-Cre^{tg} Rosa26R^{eYFP/+}* (*Rorγt^{fm+}*) mice were sort-purified and subjected to RNA-sequencing (Supplementary Fig. 1a). The principal component analysis (PCA) of SP and SI NCR− ILC3s revealed a different transcriptional profile of the two subsets (Fig. 1a). A

total set of 1286 genes was differentially expressed with specific signature of SP and SI ILC3s for genes encoding transcription factors (e.g., *Epas1*, *Arnt2*, or *Runx1t1*), cytokines (e.g., *Il22* and *Il17a*) and genes involved in IL-23, hypoxia, or IFN-α responses (Fig. 1b, c, Supplementary Fig. 1b, c). Importantly, transcripts relevant for MHC II-dependent Ag presentation and costimulation (e.g., *H2-Aa*, *H2-Ab*, *Cd74*, *Cd80*, *Cd86*, and *Ctse*) were enriched in SP ILC3s (Fig. 1d). Flow cytometry analysis confirmed the enhanced expression of MHC II, CD80, and CD86 of SP NCR− ILC3s (Fig. 1e). A subset of naive MHC II+ and MHC II−NCR− ILC3s produced IL-22 (Supplementary Fig. 1d). In line with previous publications only the C-C chemokine receptor type 6 (CCR6)+ subset of NCR− ILC3s expressed MHC II (Supplementary Fig. 1d)[12,20].

SP and SI ILC3s differ in their capacity to activate T cells. As transcripts required for Ag presentation were enriched in SP ILC3s, we measured the capacity of activated SP and SI ILC3s to process and present Ag to induce CD4+ T-cell activation and proliferation. SP and SI NCR− ILC3s from *Rag2^{−/−}* mice (Supplementary Fig. 2a, b) and bone marrow-derived dendritic cells (BMDCs) as positive control were stimulated with IL-1β and cultured in the presence of Ovalbumin (Ova) protein or peptide with Ova-specific T-cell receptor (TCR) transgenic CD4+ T cells (*OT-II^{tg}* CD4+ T cells). Pre-activation of Ag-presenting cells (APCs) was chosen to simulate immunogenic conditions under which T-cell responses toward foreign Ag are elicited in vivo. IL-1β boosts the capacity of SP ILC3s to induce T-cell responses in vitro by upregulation of CD80, CD86 and MHC II[14]. IL-1β also induced the expression of *Tnfsf4* and its product OX40L by SP and SI ILC3s (Supplementary Fig. 2c, d).

In the presence of either Ova protein or peptide SP NCR− ILC3s induced significant CD69 upregulation and proliferation of *OT-II^{tg}* CD4+ T cells (Fig. 2a, b). Only a weak T-cell proliferation was observed with SI ILC3s and Ova protein, whereas almost 50% of T cells proliferated with Ova peptide. The observed difference between SP and SI NCR− ILC3s might be explained by two potential mechanisms: (I) SI NCR− ILC3s are less efficient at Ag uptake and processing and/or (II) NCR− ILC3s with properties of APCs are enriched in the SP. The finding that a higher percentage of freshly isolated SP NCR− ILC3s expressed MHC II, CD80, and CD86 as compared with SI NCR− ILC3s (Fig. 1e) supports the latter hypothesis. To explore this further, we studied the protein processing capacity of MHC II+ and MHC II− NCR− ILC3s from the SI and the SP (Fig. 2c). For this purpose, ILC3s from *Rag2^{−/−}* mice were cultured with Eα-GFP protein. Eα-peptide presented by MHC II molecules was detected by staining with the antibody clone YAe. As expected the YAe antibody did not stain MHC II− ILC3s. Interestingly, comparable frequencies of SI and SP MHC II+ NCR− ILC3s presented the Eα peptide. Sort-purified SP and SI MHC II+ ILC3s were also equally efficient at inducing T-cell activation and proliferation in the presence of Ova protein (Fig. 2d and Supplementary Fig. 2e). MHC II− SP ILC3s were superior of MHC II− SI ILC3s at inducing T-cell activation, most likely because IL-1β stimulation induced MHC II expression in MHC II−-sorted SP ILC3s, but not in SI ILC3s (Supplementary Fig. 2f)[14]. Together these data demonstrate that both SP and SI harbor a MHC II+ ILC3 subset that equally processes and presents Ag and induces proliferation of CD4+ T cells. Furthermore, this subset is significantly enriched in SP NCR− ILC3s ex vivo and after in vitro stimulation with IL-1β.

Since Ova protein pulsed DCs exceeded ILC3s in their capacity to induce T-cell proliferation (Fig. 2a, b), we asked whether DCs and ILC3s also differ in the quality of T-cell responses. Therefore, the cytokine production of *OT-II^{tg}* CD4+ T cells in co-cultures
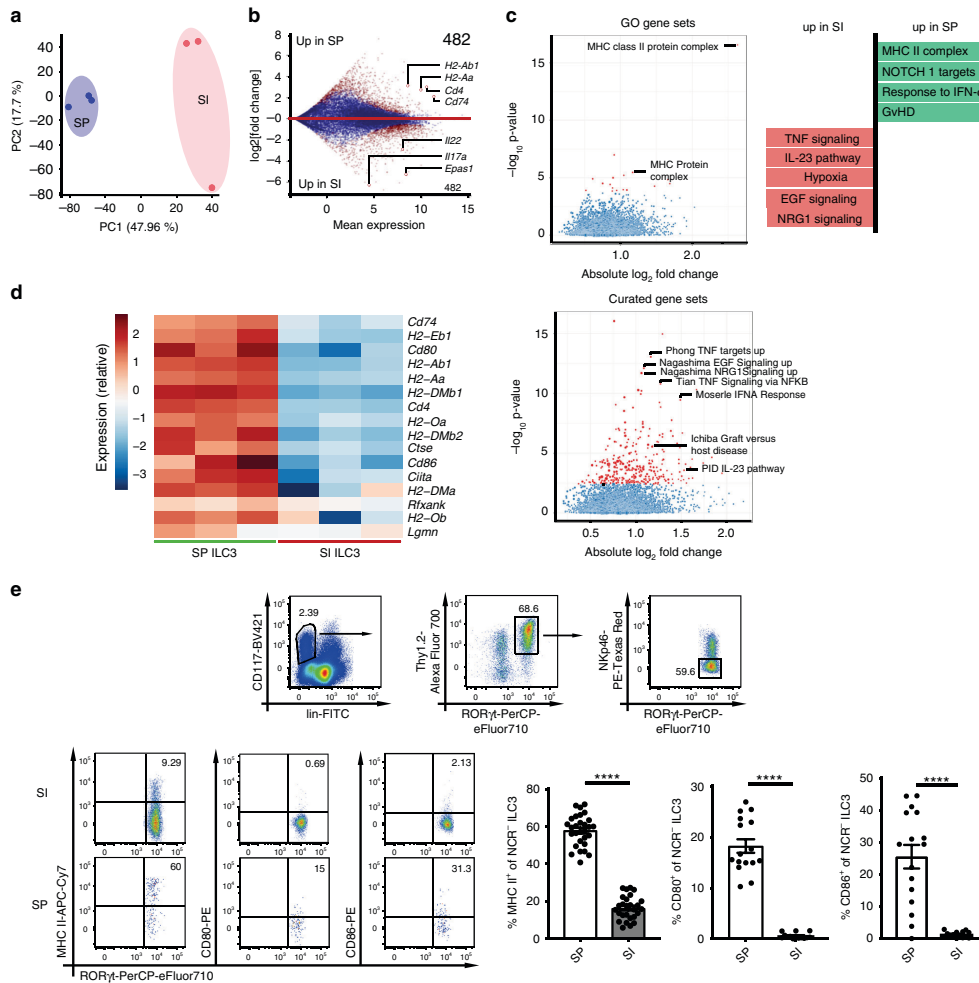
Fig. 1 SP and SI NCR⁻ ILC3s exhibit a different transcriptional signature. a PCA of RNA sequencing data of SI and SP NCR⁻ ILC3s isolated from *Rorγt*ᶠᵐ⁺ mice. Cells were sort-purified as depicted in Supplementary Fig. 1a. **b** Mean expression and log 2(fold change) of all detected genes. Genes with a significant difference are highlighted in red (FDR < 0.05). Numbers indicate the total amount of genes significantly higher expressed (log2(fold change) >1.5) in SP ILC3s or SI ILC3s. **c** Gene set enrichment analysis of gene ontology (GO) and curated gene sets. Gene sets with a significant difference are highlighted in red (FDR < 0.05). **d** Heatmap of genes associated with MHC II Ag presentation. **e** CD117⁺lin⁻Thy1.2⁺RORγt⁺NKp46⁻ ILC3s were analyzed for surface expression of MHC II ($n = 29$(SP) and $n = 27$(SI) mice), CD80 ($n = 16$(SP) and $n = 14$(SI) mice), and CD86 ($n = 16$(SP) and $n = 14$(SI) mice). Six to eight independent experiments. Each symbol represents a sample and the bar graph represents the mean ± s.e.m. ****$P \leq 0.0001$, calculated with unpaired two-tailed Student's *t* test. Source data are provided as a Source Data File.

with pre-activated DCs, SP ILC3s and SI ILC3s was measured. T cells stimulated with ILC3s produced less IFN-γ and more TNF (Supplementary Fig. 2g) as compared with co-cultures with Ag-pulsed DC. The IL-22 secretion of T cells was comparable when ILC3s or DCs were added as APCs (Supplementary Fig. 2g).

It has been previously reported that naive SI ILC3s induce T-cell death of commensal bacteria-specific T cells at steady state[13]. We therefore performed a SI ILC3-CD4⁺ T cell assay and incubated T cells with Annexin V which stains apoptotic cells.

The percentage of Annexin V⁺ *OT-II*ᵗᵍ CD4⁺ T cells after co-culture with IL-1β-pre-activated SI ILC3s and Ova Ag was reduced as compared with controls without Ova (Supplementary Fig. 2h). It is hence possible that the activation state and the type of Ag determine the effect of ILC3s on T-cell death.

Tissue localization determines the APC phenotype of ILC3s. To analyse whether the APC properties of ILC3s are fixed or can be
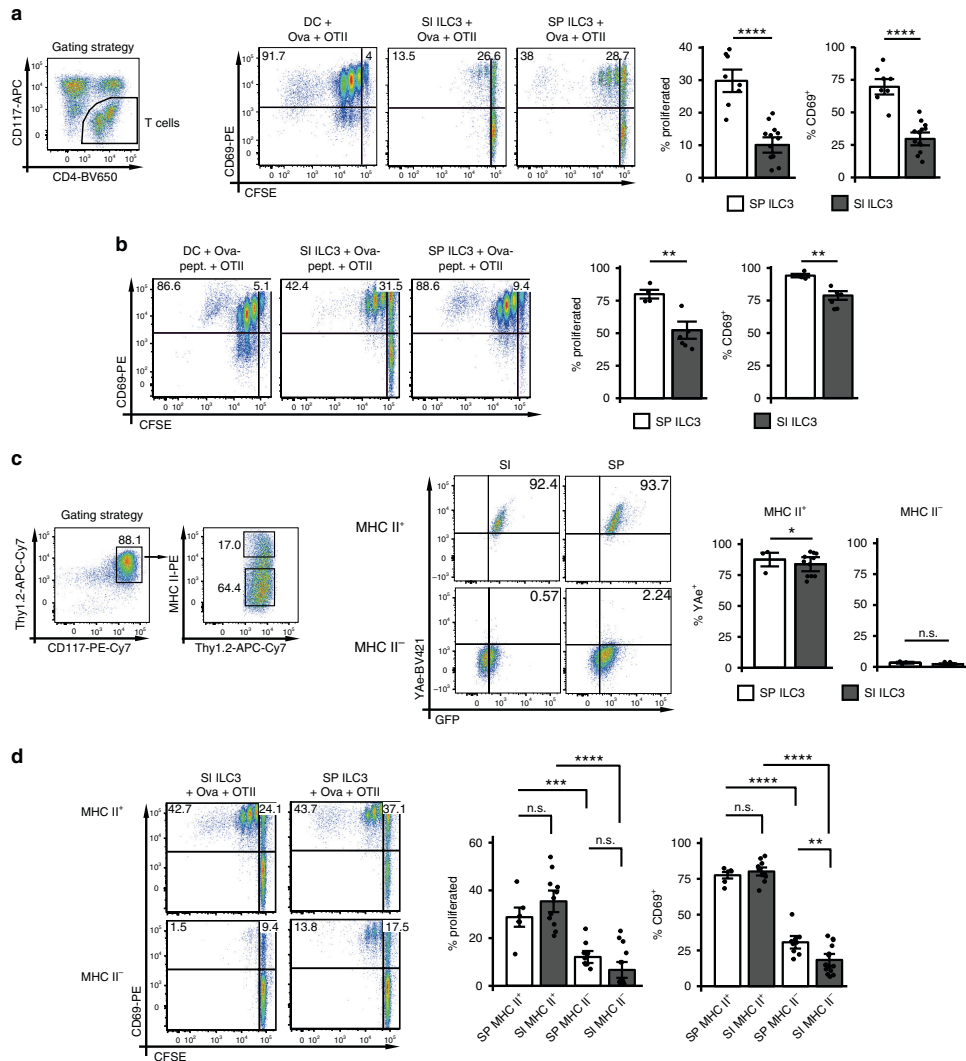
Fig. 2 SP and SI NCR⁻ ILC3s differ in their capacity to stimulate CD4⁺ T cells. Naive CFSE-labeled *OT-II^tg* CD4⁺ T cells were cultured either with 5×10^4 BMDCs, SP or SI ILC3s (*Rag2⁻/⁻*) pre-activated with IL-1β, in the presence of Ova protein (**a**) or peptide (**b**) for 72 h. ILC3s were sorted as depicted in Supplementary Fig. 2a. T cells were gated as CD3⁺ or CD117⁻. In (**a**), $n = 8$ (SP) and $n = 13$ (SI) distinct samples. Six independent experiments. In (**b**), $n = 4$ (SP) and $n = 6$ (SI) distinct samples. Three independent experiments. **c** SP or SI ILC3s (*Rag2⁻/⁻*) were cultured with Eα-GFP protein for 72 h. ILC3s were sorted as depicted in Supplementary Fig. 2a. Surface presentation of Eα peptide was analyzed by flow cytometry with antibody clone YAe. ILC3s were gated either on MHC II⁺ or MHC II⁻CD117⁺Thy1.2⁺ cells (gating strategy is depicted for SI ILC3s). $n = 3$ (SP) and $n = 11$ (SI) distinct samples of three independent experiments. **d** MHC II⁺ ($n = 6$ (SP) and $n = 11$ (SI) distinct samples) and MHC II⁻ ($n = 10$ (SP) and $n = 15$ (SI) distinct samples) ILC3s from SP and SI (*Rag2⁻/⁻*) were stimulated with IL-1β and used for T-cell stimulation in the presence of Ova protein. Five independent experiments. ILC3s were sorted as depicted in Supplementary Fig. 2a, e. T cells were gated as CD3⁺ or CD117⁻. Each symbol represents a sample and the bar graph represents the mean ± s.e.m. n.s., not significant; *$P \leq 0.05$; **$P \leq 0.01$; ***$P \leq 0.001$; ****$P \leq 0.0001$, calculated with mixed-effects models (two-sided) using lmerTest. Source data are provided as a Source Data File.
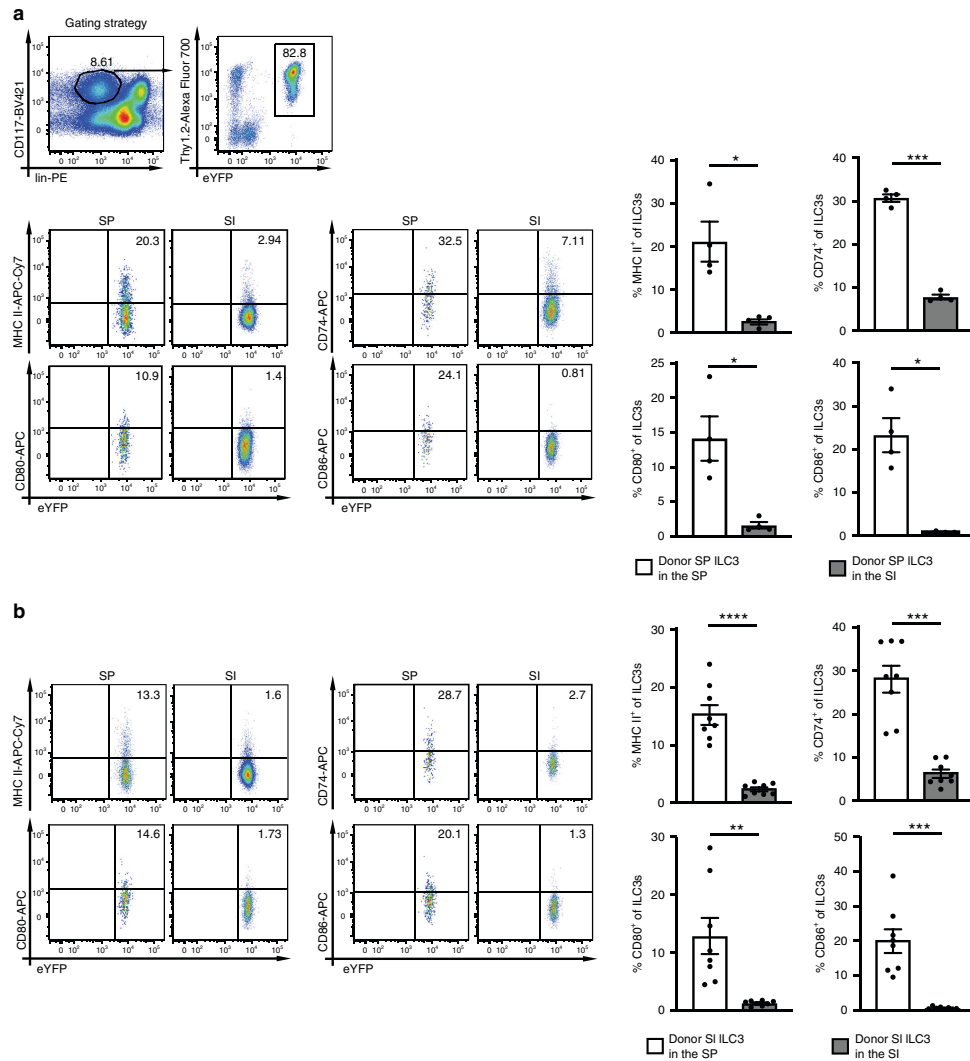
Fig. 3 The tissue localization determines the frequency of ILC3s with an APC phenotype. SP ILC3s (**a**) or SI ILC3s (**b**) from $Ror\gamma t^{fm+}Rag2^{-/-}$ mice were i.v. injected into $Rag2^{-/-}Il2rg^{-/-}$ mice. Cells were sort-purified as depicted in Supplementary Fig. 1a. Five weeks after transfer the expression of MHC II, CD80, CD86, and CD74 on donor derived ILC3s in the SP and SI of recipient mice was analyzed. ILC3s were gated as depicted in (**a**). **a** $n = 4$ distinct samples of four independent experiments and **b** $n = 8$ distinct samples of five independent experiments. Each symbol represents a sample and the bar graph represents the mean ± s.e.m. *$P \leq 0.05$; **$P \leq 0.01$; ***$P \leq 0.001$; ****$P \leq 0.0001$, calculated with two-tailed paired Student's t test. Source data are provided as a Source Data File.

altered by environmental signals, SP and SI ILC3s from $Ror\gamma t^{fm+}$ $Rag2^{-/-}$ mice were adoptively transferred into $Rag2^{-/-}Il2rg^{-/-}$ mice. Five weeks after transfer, eYFP+ donor ILC3s isolated from the SP and the SI of recipient mice were analyzed for the expression of CD80, CD86, CD74, and MHC II. There was no tissue-origin-specific bias of ILC3s homing to SP and SI.

Importantly, SP donor ILC3s isolated from the SI of recipients had down-modulated CD80, CD86, CD74, and MHC II (Fig. 3a). Conversely, SI donor ILC3s isolated from the SP of recipients had upregulated these molecules (Fig. 3b). Similar results were obtained 7 days after adoptive transfer of total splenocytes or intestinal lymphocytes into $Rag2^{-/-}Il2rg^{-/-}$ mice

(Supplementary Fig. 3a, b). In addition, the retention marker CD69 was downregulated in SI ILC3s after migration to the SP and upregulated in SP ILC3s after migration to the SI.

In order to test if retention or survival of MHC II$^+$ ILC3s was superior in the SP, SI CD45.1$^+$MHC II$^-$ and SI eYFP$^+$MHC II$^+$ ILC3s were injected into $Rag2^{-/-}Il2rg^{-/-}$ mice (Supplementary Fig. 3c, d). Five weeks later the two donor cell subsets were discriminated by anti-CD45.1 staining and eYFP. The input ratios of donor ILC3 subsets did not differ from the ratios in recipient SP. This strongly suggests that MHC II$^+$ and MHC II$^-$ ILC3s were comparable in retention or survival in the SP (Supplementary Fig. 3d). In line with previous results MHC II$^+$ ILC3s lost MHC II expression in the intestine and MHC II$^-$ ILC3s gained MHC II expression in the SP (Supplementary Fig. 3e).

Altogether the SI environment suppressed the expression of molecules required for MHC II Ag presentation and T-cell activation. Our data suggest that NCR$^-$ ILC3s exhibit certain plasticity and that tissue-specific factors condition the capacity of ILC3s to act as APCs for CD4$^+$ T cells.

In vitro culture reverses functional polarization of ILC3s. Our in vivo data showed that SI NCR$^-$ ILC3s, when migrating to the SP, upregulated molecules required for Ag presentation and activation of CD4$^+$ T cells. To further explore their plasticity, sort-purified SI ILC3s from $Rag2^{-/-}$ mice were cultured with IL-2, IL-7, and stem cell factor (SCF) for 7 days and used for RNA sequencing, flow cytometric analysis and stimulation of $OT-II^{tg}$ CD4$^+$ T cells. PCA of RNA sequencing data showed that samples from cultured SI ILC3s clustered with freshly isolated (ex vivo) SP ILC3 samples (Fig. 4a). Importantly, transcripts associated with MHC II Ag presentation were upregulated in SI ILC3s after culture (Fig. 4b). In addition, in vitro culture of SI ILC3s resulted in increased MHC II protein expression and accumulation of a CD74$^+$ MHC II$^+$ population of NCR$^-$ ILC3s, a subset existing only at low frequency within ex vivo SI ILC3s (Fig. 4c). These data demonstrate that SI ILC3s acquire a SP-like phenotype upon in vitro culture.

To test the capacity of cultured SI NCR$^-$ ILC3s to present Ag and stimulate CD4$^+$ T cells, ex vivo and cultured SI ILC3s were incubated with $OT-II^{tg}$ CD4$^+$ T cells and Ova protein (Fig. 4d) or Ova peptide (Fig. 4e). Our data show that cultured SI ILC3s were significantly better at CD4$^+$ T-cell stimulation compared with ex vivo SI ILC3s, suggesting that environmental factors in the intestine may negatively affect the Ag presentation capacity of ILC3s.

IL-23 negatively regulates Ag presentation by ILC3s. To investigate whether microbial products negatively regulated the capacity of SI ILC3s to induce T-cell responses, ILC3s from germ-free (GF) mice were assessed for their ability to stimulate CD4$^+$ T cells in vitro and to express MHC II. SI NCR$^-$ ILC3s from GF mice were significantly better at inducing Ova-specific CD4$^+$ T-cell proliferation in vitro and had a higher expression of MHC II as compared with NCR$^-$ ILC3s from conventional specific pathogen-free (SPF) mice (Fig. 5a, b and Supplementary Fig. 8). Together, in the absence of microbiota the capacity of SI ILC3s to stimulate CD4$^+$ T cells was enhanced.

Interestingly, gnotobiotic sDMDMm2 mice colonized with a mixture of 12 bacterial strains covering the five major phyla of procaryotes (see Table 1) showed no increased expression of MHC II on SI ILC3s as compared with conventional SPF mice, indicating that these bacteria were sufficient to repress MHC II expression (Supplementary Figs. 4a and 8)[26].

ILC3s isolated from $RORc(\gamma t)$-$Cre^{tg}Myd88^{fl/fl}$($Myd88^{ILC3-/-}$) mice and littermate controls expressed similar MHC II levels

indicating that TLR signaling via MyD88 was not responsible for downregulation of MHC II (Supplementary Figs. 4b and 8).

Our observations prompted us to study the effect of IL-23 on MHC II expression of ILC3s, since gut microbes can induce the expression of IL-23 by dendritic cells (DCs)[27]. Indeed, $Il23p19$ expression was significantly higher in the SI compared with the SP of SPF mice (Supplementary Fig. 5a). In line with a previous report, the expression of $Il12b$ and $Il23p19$ encoding the subunits of IL-23 were reduced in the terminal ileum of GF compared with SPF mice (Fig. 5c)[28]. To analyse whether IL-23 is involved in shaping the MHC II$^+$ to MHC II$^-$ ratio of NCR$^-$ ILC3s in the SI, IL-23 deficient ($Il23p19^{-/-}$) mice were used. Interestingly, a higher percentage of MHC II$^+$ cells was found in SI NCR$^-$ ILC3s of $Il23p19^{-/-}$ compared with wild-type (WT) mice (Fig. 5d and Supplementary Fig. 8). IL-23 deficiency did not increase the expression of MHC II on ILC3s in the spleen (Supplementary Fig. 5b and 8) most likely because IL-23 is not abundant in the spleen. CD80 and CD86 expression was not significantly affected by the lack of IL-23 (Supplementary Fig. 5c). SI ILC3s from $Il23p19^{-/-}$ mice showed a significant increase in their capacity to induce Ova-specific $OT-II^{tg}$ CD4$^+$ T-cell responses (Fig. 5e and Supplementary Fig. 5d). Conversely MHC II expression was reduced in WT SI or SP ILC3s after in vitro culture with IL-23 for 7 days (Fig. 5f). IL-23 also repressed the MHC II expression of SI ILC3s isolated from $Il23p19^{-/-}$ mice, indicating that ILC3s have no intrinsic defect in $Il23p19^{-/-}$ mice (Supplementary Fig. 5e). Finally, IL-23 added to 7 day cultures of SI ILC3s diminished their capacity to stimulate $OT-II^{tg}$ CD4$^+$ T cells (Fig. 5g, Supplementary Fig. 5f, g).

Collectively these data suggest that microbe-induced IL-23 negatively affects the capacity of NCR$^-$ ILC3s to induce CD4$^+$ T-cell responses.

IL-23 reduces MHC II expression through mTORC1 and STAT3. mTORC1 and STAT3 have been shown to be activated in innate immune cells upon IL-23 stimulation[29–31]. We therefore asked, whether IL-23-mediated silencing of MHC II in SI ILC3s requires mTORC1 and STAT3 signaling. IL-23 stimulation of NCR$^-$ ILC3s induced phosphorylation of the mTORC1 signaling kinase S6, mTOR and of STAT3 (Fig. 6a, b and Supplementary Fig. 6a). When ILC3s were incubated with Rapamycin or isolated from mice with a conditional deletion of $Rptor$ in ILC3s ($Rptor^{ILC3-/-}$, $Rag2^{-/-}$ background) (Fig. 6a and Supplementary Fig. 6a), IL-23 failed to activate mTORC1. Interestingly, the percentage of ex vivo MHC II$^+$ SI NCR$^-$ ILC3s from $Rptor^{ILC3-/-}$ mice was twice as high as in control mice ($Rptor^{fl/fl}$) suggesting that IL-23-mediated mTORC1 signaling suppressed the expression of MHC II on SI ILC3s (Fig. 6c and Supplementary Fig. 8). This was confirmed by stimulating SI and SP ILC3 from $Rptor^{ILC3-/-}$ mice for 7 days with IL-23 in vitro (Supplementary Fig. 6b). In the SI of mice with a $Stat3$ deletion in hematopoietic cells ($VAV1$-$Cre^{tg}Stat3^{fl/fl}$) a significantly higher percentage of MHC II$^+$ NCR$^-$ ILC3s was observed as compared with control mice (Fig. 6d and Supplementary Fig. 8). Notably, in vivo deletion of $Il23p19$, $Rptor$ or $Stat3$ had no effect on the MHC II$^+$ NCR$^-$ ILC3s percentage in the SP further emphasizing the fact that MHC II downregulation was specific for the gut (Supplementary Fig. 8).

It was recently shown that IL-23 promotes dermal $\gamma\delta$ T-cell differentiation and effector functions via STAT3 phosphorylation independently of the mTOR pathway[32]. Strikingly, IL-23-activated ILC3s from $Rptor^{ILC3-/-}$ mice showed a reduced STAT3 phosphorylation indicating that in ILC3s the IL-23/STAT3 axis was partially dependent on mTORC1 (Supplementary Fig. 6c). Following IL-23-stimulation S6 phosphorylation
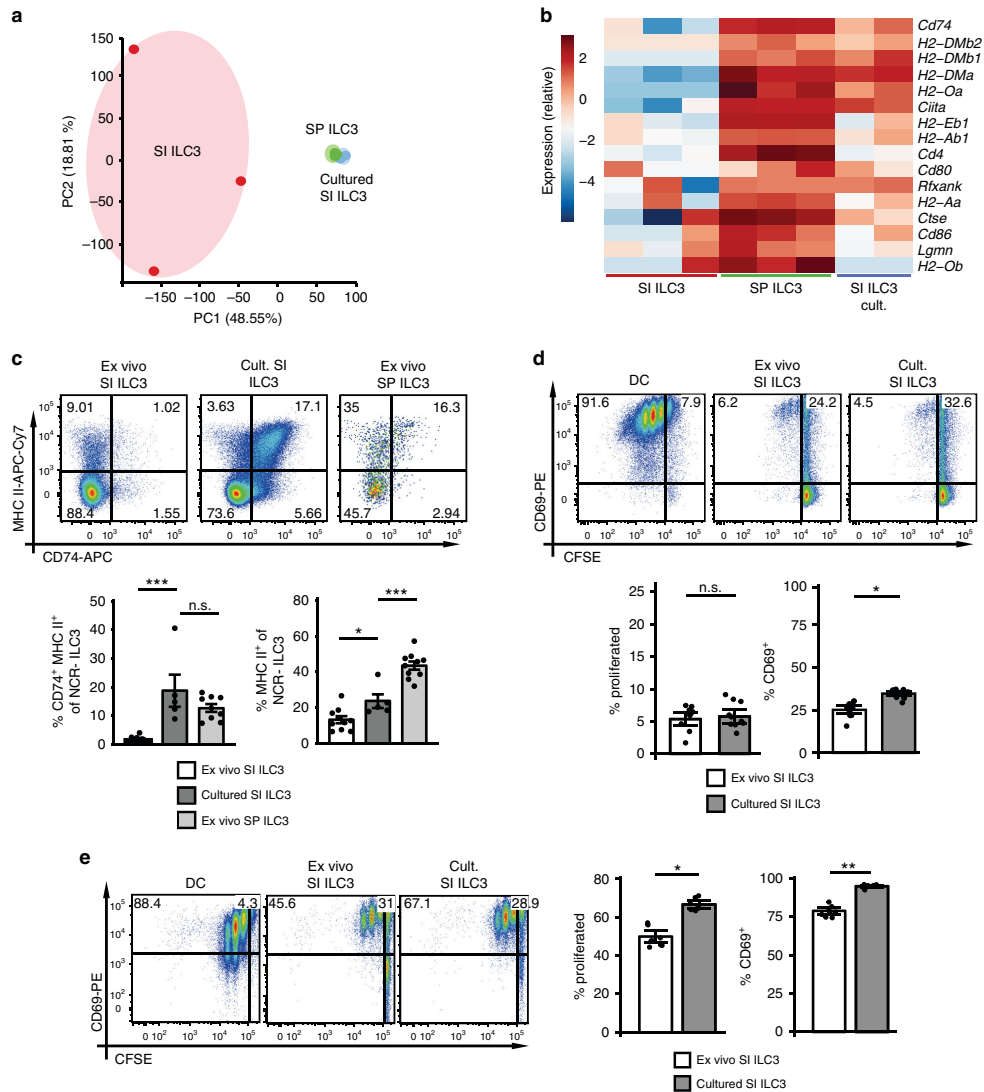
Fig. 4 MHC II downregulation of SI ILC3s is reversible upon in vitro culture. CD117$^+$Thy1.2$^+$lin$^-$ (CD3ε, CD8α, CD11b, CD11c, CD19, B220, Gr-1, TCR-β, TCR-γ/δ, TER119, NK1.1) KLRG1$^-$ ILC3s were isolated from SP or SI of $Rag2^{-/-}$ mice (Supplementary Fig. 2a). Freshly isolated (ex vivo) SP (green) or SI ILC3s (red) and SI ILC3s cultured for 7 days with IL-2, IL-7, and SCF (blue) were used for RNA sequencing. **a** PCA of RNA sequencing samples. **b** Heatmap of genes associated with MHC II Ag presentation. **c** Expression of MHC II and CD74 by cultured ILC3s ($n = 5$ distinct samples) or ex vivo SI ($n = 9$–10 distinct samples) and SP ($n = 9$–10 distinct samples) ILC3s of $Rag2^{-/-}$ mice. Five independent experiments. **d, e** Naïve CFSE-labeled OT-II^{tg} CD4$^+$ T cells were cultured either with 5×10^4 BMDCs, ex vivo or cultured SI ILC3s from $Rag2^{-/-}$ mice in the presence of Ova protein (**d**) or peptide (**e**). In (**d**), $n = 9$ (ex vivo SI ILC3) and $n = 10$ (cultured SI ILC3) distinct samples of four independent experiments. In (**e**), $n = 8$ distinct samples of three independent experiments. T cells were gated as in Fig. 2. Each symbol represents a sample and the bar graph represents the mean ± .e.m. n.s., not significant; *$P \leq 0.05$; **$P \leq 0.01$; ***$P \leq 0.001$, calculated with one-way ANOVA (two-tailed) and Bonferroni's multiple comparisons test (**c**) or with mixed-effects models (two-sided) using lmerTest (**d** and **e**). Source data are provided as a Source Data File.
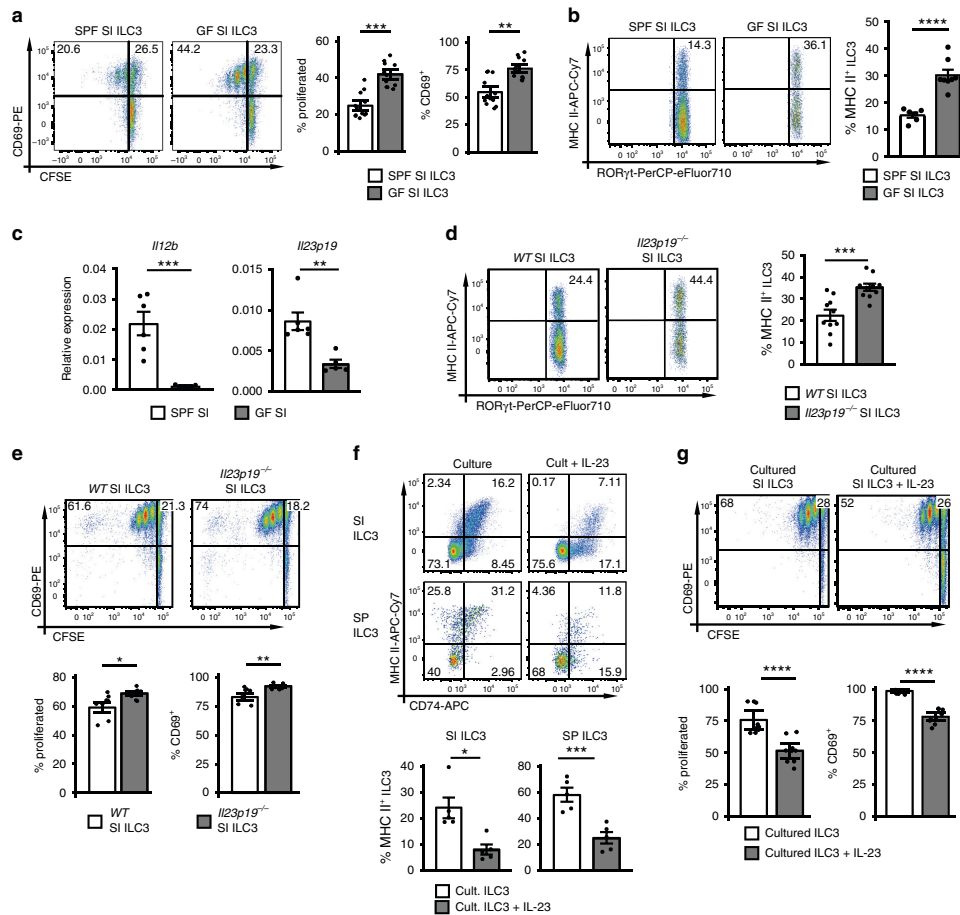
Fig. 5 The microbiota and IL-23 negatively regulate Ag presentation by ILC3s. a CFSE-labeled *OT-II^tg* CD4+ T cells were stimulated with 1×10^4 SPF or GF ILC3s (*Rag^{-/-}* background) in the presence of Ova peptide. $n = 12$ distinct samples of three independent experiments. ILC3s were sorted as depicted in Supplementary Fig. 2a. **b** MHC II expression of SI ILC3s from SPF ($n = 6$ mice) and GF ($n = 8$ mice) mice on *Rag^{-/-}* background. NCR− ILC3s were gated as shown in Fig. 1. Two independent experiments. **c** Relative expression of *Il12b* and *Il23p19* in the terminal ileum of SPF ($n = 6$ mice) and GF ($n = 5$ mice) mice on *Rag^{-/-}* background analyzed by qRT PCR. Two independent experiments. **d** MHC II expression of SI ILC3s from WT and *Il23p19^{-/-}* mice ($n = 10$ mice). NCR− ILC3s were gated as shown in Fig. 1. Five independent experiments. **e** Naive CFSE-labeled *OT-II^tg* CD4+ T cells were cultured either with 5×10^4 SI ILC3s of WT ($n = 8$ distinct samples) or *Il23p19^{-/-}* ($n = 10$ distinct samples) mice in the presence of Ova peptide. Four independent experiments. ILC3s were sorted as depicted in Supplementary Fig. 2a. **f** Surface expression of MHC II and CD74 on ILC3s of *Rag2^{-/-}* mice cultured 7 days with or without IL-23 in addition to IL-2, IL-7, and SCF ($n = 5$ distinct samples). NCR− ILC3s were gated as shown in Fig. 1. Five independent experiments. **g** SI ILC3s were sort-purified from *Rag2^{-/-}* mice (Supplementary Fig. 2a) and cultured 7 days with or without IL-23 in addition to IL-2, IL-7, and SCF. CFSE-labeled *OT-II^tg* CD4+ T cells were stimulated with 5×10^4 cultured ILC3s in the presence of Ova peptide. $n = 9$ distinct samples of three independent experiments. Each symbol represents a sample and the bar graph represents the mean ± s.e.m. *$P \leq 0.05$; **$P \leq 0.01$; ***$P \leq 0.001$; ****$P \leq 0.0001$, calculated with mixed-effects models (two-sided) using lmerTest (**a**, **e**, and **g**) or two-tailed unpaired (**b**, **c** *Il12b*, and **d**) or two-tailed paired (**f**) Student's *t* test or two-tailed Mann–Whitney test (**c** *Il23p19*). Source data are provided as a Source Data File.

was almost normal in *Stat3*-deficient ILC3s as compared with controls indicating that the majority of IL-23-induced mTORC1 signaling occurs independently of STAT3 (Supplementary Fig. 6d). Together these data demonstrate that the IL-23-mTORC1-STAT3 axis mediates downregulation of MHC II in SI ILC3s.

IFN-γ positively regulates MHC II expression of ILC3s. Adoptively transferred SI ILC3s displayed increased levels of MHC II in the SP of recipient mice (Fig. 3b). Since the major transcriptional regulator of MHC II expression is CIITA (class II MHC transactivator), these results suggest that splenic factors may induce or intestinal factors may repress CIITA. We therefore

Table 1 Microbial organisms used for sDMDMm2 mice.

Organism	DSM no.
Lachnoclostridium sp. YL32	DSM 26114
Ruminiclostridium sp. KB18	DSM 26090
Bacteroides sp. I48	DSM 26085
Parabacteroides sp. YL27	DSM 28989
Burkholderiales bacterium YL45	DSM 26109
Erysipelotrichaceae bacterium I46	DSM 26113
Blautia sp. YL58	DSM 26115
Flavonifractor plautii YL31	DSM 26117
Bifidobacterium animalis subsp. *animalis* YL2	DSM 26074
Lactobacillus reuteri I49	DSM 32035
Akkermansia muciniphila YL44	DSM 26127
Enterococcus faecalis KB1	DSM 32036

analyzed the expression of the three mRNA isoforms of the *Ciita* gene, which are regulated by different promoters (Fig. 7a)[33]. Indeed, freshly isolated SP ILC3s used *Ciita* promoters *pI*, *pIII*, and *pIV*, whereas ex vivo isolated SI ILC3s expressed only the *pI*-regulated isoform. These data indicate that there is a tissue-specific regulation of *Ciita* expression in ILC3s. IL-23 reduced the expression of promoter *pIII* in SP ILC3s (Supplementary Fig. 7a). It is hence possible that the IL-23-dependent repression of MHC II in vivo and in vitro was at least partially mediated by the reduction of *Ciita pIII*.

The promoter *pIV*, which was expressed in SP ILC3s, is inducible by IFN-γ[33]. IFN-γ expression was remarkably higher in the SP (Fig. 7b) pointing to its potential role in *Ciita pIV*-driven MHC II expression of SP ILC3s. To delineate the role of IFN-γ, we analyzed the expression of MHC II on SP and SI ILC3s of *Ifng*$^{-/-}$ mice and after stimulation of SI ILC3s with IFN-γ. SP NCR$^-$ ILC3s had a significantly lower expression of MHC II in *Ifng*$^{-/-}$ mice as compared with WT mice (Fig. 7c and Supplementary Fig. 8). CD80 and CD86 expression levels were not affected (Supplementary Fig. 7b). Conversely, stimulation with IFN-γ significantly increased the expression of MHC II molecules and *Ciita* promoter *pIV* by SI NCR$^-$ ILC3s (Fig. 7d, e). The effect on MHC II induction was abolished in cultures containing IFN-γ and IL-23 suggesting a dominant role of IL-23 in suppressing the expression of MHC II on ILC3s (Supplementary Fig. 7c). To analyse if IFN-γ also affects the capacity of ILC3s to stimulate T-cell responses, SI NCR$^-$ ILC3s were incubated with IFN-γ or left untreated and used for stimulation of CD4$^+$ T cells with Ova peptide (Fig. 7f). IFN-γ stimulated SI ILC3s were significantly better at inducing T-cell proliferation as compared with untreated cells.

In summary, we provide evidence that IFN-γ in the SP environment increases expression of MHC II molecules on NCR$^-$ ILC3s and enhances their potential to induce CD4$^+$ T-cell immune responses.

Discussion

We show here that NCR$^-$ ILC3s have a tissue-specific transcriptional signature. Transcripts associated with MHC II Ag presentation are relatively enriched in SP NCR$^-$ ILC3s. SP NCR$^-$ ILC3s are significantly more efficient in inducing CD4$^+$ T-cell activation and proliferation as compared with SI NCR$^-$ ILC3s. A subset of SI MHC II$^+$ NCR$^-$ ILC3s, however, can induce Ag-specific CD4$^+$ T-cell proliferation. The fact that SI ILC3s can adopt an APC phenotype upon in vitro culture or in vivo migration to the SP suggests that environmental signals determine the capacity of ILC3s to present Ag and to stimulate CD4$^+$ T cells. Indeed, we identified two essential pathways regulating ILC3-T-cell interactions in the SI vs. SP. One is mediated by

microbe-induced IL-23, which supresses MHC II expression of NCR$^-$ ILC3s through mTORC1 and STAT3 activation. The other pathway involves IFN-γ signaling, which induces the expression of MHC II on NCR$^-$ ILC3s and promotes NCR$^-$ ILC3-mediated CD4$^+$ T-cell activation and proliferation. The IFN-γ induced MHC II expression of NCR$^-$ ILC3s is reflected by the induction of *Ciita pIV* expression in ILC3s upon IFN-γ stimulation. The fact that the IFN-γ expression is low in the SI of WT mice explains why in *Ifng*$^{-/-}$ mice no significant reduction of MHC II expression by SI ILC3s was observed. Likewise, IL-23 expression is low in the SP and deletion of *Il23p19* does not alter MHC II expression of SP ILC3s.

SI ILC3s were shown to suppress commensal bacteria-specific T-cell responses[12]. The discrepancy to our data might be partially explained by the fact that we studied ILC3 APC function under activation conditions. Similarly, a study published in this issue demonstrates that upon activation human ILC3s acquire Ag-presenting properties for the induction of Ag-specific CD4$^+$ memory T-cell responses[34]. In mice upon IL-1β-stimulation both SI and SP ILC3s upregulate OX40L. OX40L has been described to be essential for the induction of pathogenic T-cell responses by TL1a-activated ILC3s in chronic colitis[35]. Our findings indicate that SI MHC II$^+$ ILC3s do not block CD4$^+$ T-cell immune responses per se. Under steady-state conditions, however, and under the local influence of microbiota and IL-23 the frequency of MHC II$^+$APC-like ILC3s is probably too low to elicit T-cell responses in the SI. Moreover, our data strongly suggests a dominant effect of IL-23 in repressing MHC II expression of ILC3s.

During the early phase of viral infections, innate immune cells can rapidly release high amounts of IFN-γ. This could result in the expansion of SP MHC II$^+$ ILC3s localized at the border between T and B-cell areas[36], where Ag uptake and presentation takes place. Our findings that SI ILC3s upregulate MHC II and induce CD4$^+$ T-cell proliferation after stimulation with IFN-γ demonstrate their potential to act as APCs under conditions where IFN-γ is released, e.g., during infections. Whether this is sufficient to promote CD4$^+$ T-cell responses in the gut remains to be investigated.

It has been previously reported that the microbiota promotes IL-23-induced phosphorylation of STAT3, thereby inducing IL-22 in ILC3s[29]. We describe here that microbe-induced IL-23 also limits the frequency of MHC II$^+$ NCR$^-$ ILC3s in the SI. NCR$^-$ ILC3s can be further subdivided into CCR6$^+$ and CCR6$^-$ cells. Interestingly, IL-23 has been shown to promote the development of T-bet$^+$CCR6$^-$NCR$^-$ ILC3s[37], which lack MHC II[12]. Our data strongly suggest that the IL-23-rich SI environment favors the accumulation of MHC II$^-$ ILC3s, but amongst this subset we found both CCR6$^+$ and CCR6$^-$ ILC3s. IL-23 signaling in NCR$^-$ ILC3s induced mTORC1 activation and STAT3 phosphorylation. We propose a model in which the collaborative mTORC1 and STAT3 signaling leads to downregulation of MHC II, most likely by the reduction of *Ciita* promoter *pIII* expression. In addition, IL-23 signaling may bypass mTORC1 to some extent and activate STAT3 via Janus kinases (JAK)[38]. We cannot exclude that other intestinal factors may prevent NCR$^-$ ILC3-mediated CD4$^+$ T-cell proliferation, in particular by inhibition of costimulatory or induction of coinhibitory molecules.

ILC3s are mainly tissue-resident cells and therefore exposed to local signals coming from other immune cell subsets, soluble factors, metabolites, and microbial products[39]. Recently, a tissue-specific imprinting has been reported for group 2 ILCs[18] and group 1 ILCs[40]. Furthermore, Nussbaum et al. showed that the tissue environment affects the expression of several surface markers, e.g., NKp46 and NK1.1, by total ILCs in SP and SI and that the SI environment inhibits the capacity of ILC3s to reject IL-
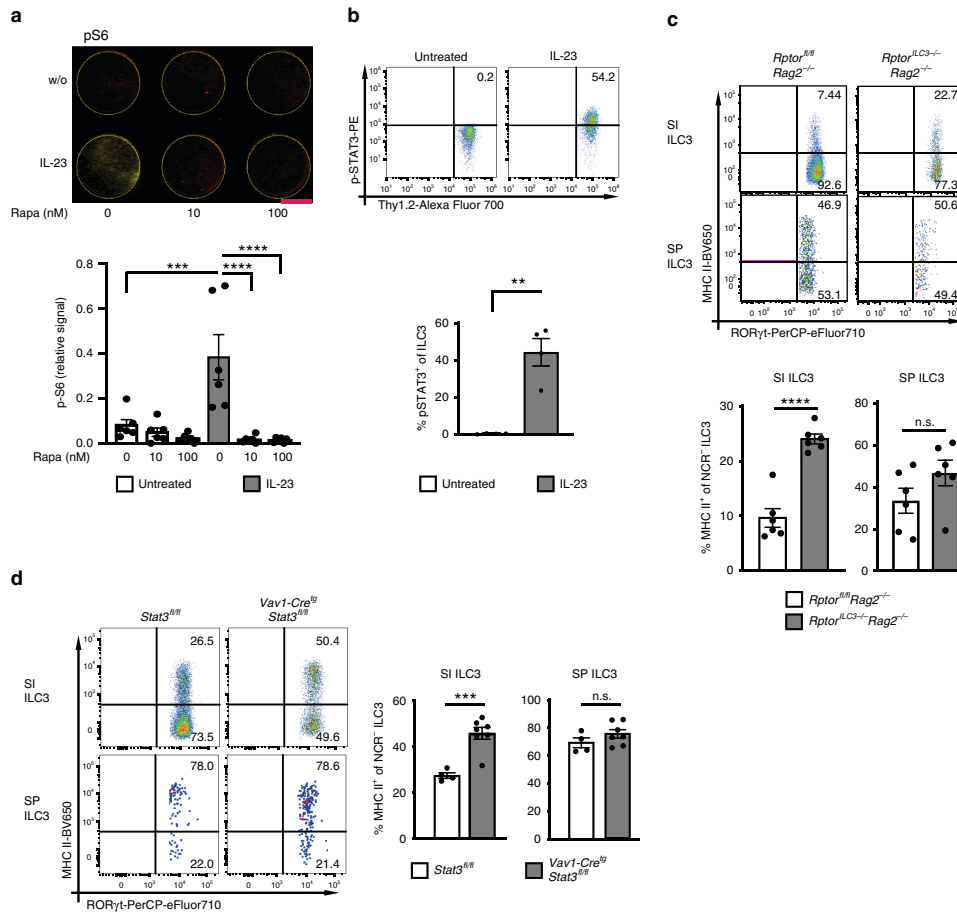
144

Fig. 6 IL-23 reduces MHC II expression through activation of mTORC1 and STAT3. a Phosphorylation of S6 of SI ILC3s (sorted from *Flt3L^tg* mice) after 48 h stimulation with or without IL-23 and 0, 10, or 100 nM Rapamycin (red = tubulin and green = p-S6). ILC3s were sorted as depicted in Supplementary Fig. 2a. Indicated is the relative phosphorylation of S6 (fluorescence signal for p-S6 normalized by fluorescence signal for tubulin). The indicated bar represents 3 mm. $n = 6$ distinct samples of five independent experiments. **b** Phosphorylation of STAT3(Tyr705) of sort-purified SI ILC3s (Supplementary Fig. 2a) from *Rag2^{−/−}* mice after 20 min stimulation with or without IL-23. $n = 4$ distinct samples of four independent experiments. **c** MHC II expression of SI and SP ILC3s from *Rptor^{fl/fl}Rag2^{−/−}* and *Rptor^{ILC3−/−}Rag2^{−/−}* mice. NCR− ILC3s were gated as shown in Fig. 1. $n = 6$ mice of two independent experiments. **d** MHC II expression of SI and SP ILC3s from *Stat3^{fl/fl}* ($n = 4$ mice) and *Vav1-Cre^{tg}Stat3^{fl/fl}* ($n = 7$ mice) mice. NCR− ILC3s were gated as shown in Fig. 1. Two independent experiments. Each symbol represents a sample and the bar graph represents the mean ± s.e.m. n.s. not significant; **$P ≤$ 0.01; ***$P ≤ 0.001$; ****$P ≤ 0.0001$, calculated with one-way ANOVA (two-tailed) and Bonferroni's multiple comparisons test (**a**) or two-tailed paired (**b**) or two-tailed unpaired (**c** and **d**) Student's t test. Source data are provided as a Source Data File.

12 secreting melanomas[17]. Our study provides a comprehensive comparison of transcriptomic profiles of NCR− ILC3s uncovering a tissue-specific signature responsible for Ag presentation and T-cell stimulation. We show that the ratio of NCR− ILC3 subsets with and without APC functions depends on IFN-γ and microbe-induced IL-23.

The discovery that APC properties of ILC3s are controlled by IFN-γ and microbe-induced IL-23 has important implications for our understanding of immune regulation in the gut. While the SP provides cytokines promoting the differentiation of MHC II+ ILC3s that are efficient inducers of T-cell responses, our data

extend the current model in which intestinal T-cell responses are limited by ILC3s. We propose that under steady-state conditions microbial commensals trigger constitutive IL-23 production by mononuclear cells and subsequently reduction of MHC II+ ILC3s in the SI. Altogether this might be essential to promote tissue protection and to prevent T-cell-dependent immune responses. Under chronic inflammatory conditions, however, intestinal ILC3s may promote pathogenic pro-inflammatory T-cell activation as previously suggested[35]. Therefore, tissue-specific alterations of the cytokine repertoire and microbial composition during infectious or inflammatory diseases should be considered as
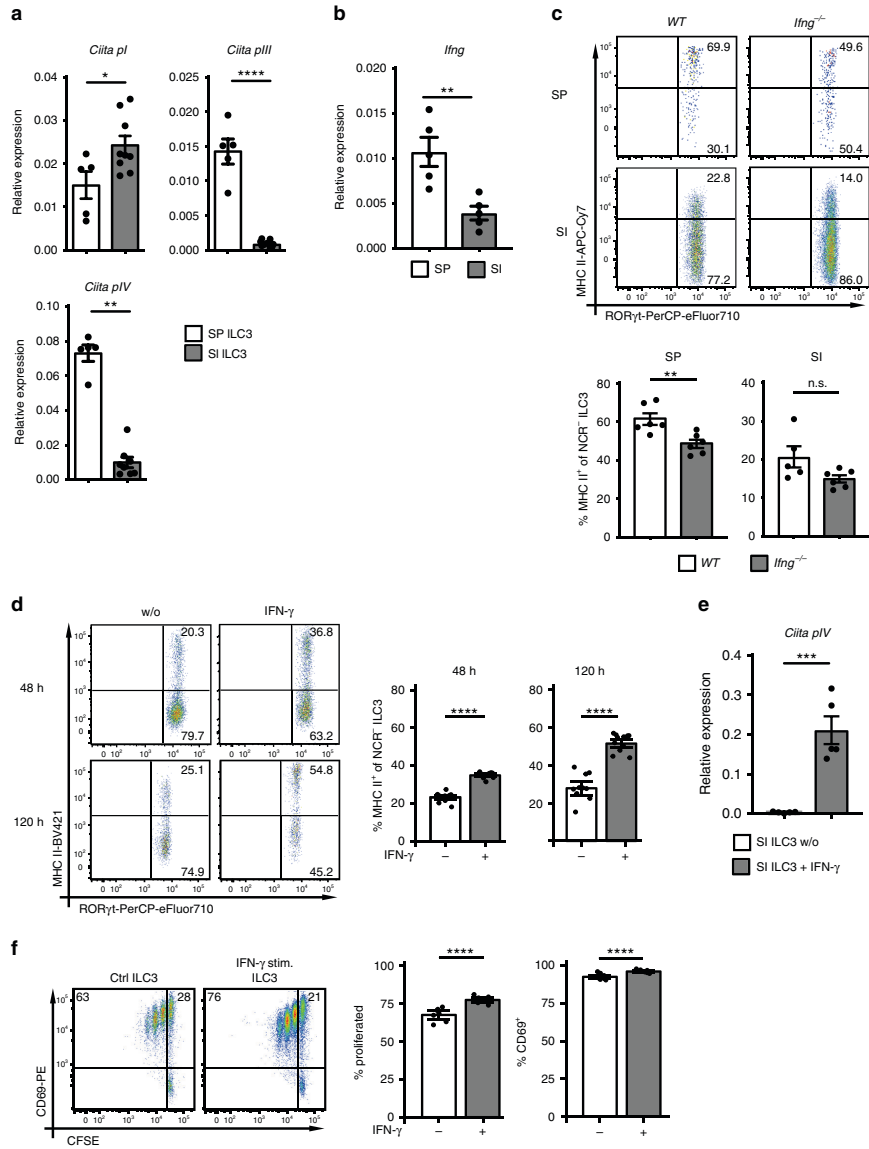
critical factors regulating ILC3-T-cell responses and disease outcome.

Methods

Antibodies. Fluorescent-labeled or biotin-conjugated antibodies (Abs) were purchased from BioLegend, eBioscience, Cell Signaling Technology, LI-COR Biosciences or BD Bioscience. The following Abs were used anti-CD3ε (145-2C11), anti-CD4 (RM4-5 or GK1.5), anti-CD8α (53-6.7), anti-CD11b (M1/70), anti-CD11c (N418), anti-CD19 (6D5), anti-CD45R (RA3-6B2, B220), anti-CD69 (H1.2F3), anti-CD74 (CLIP), anti-CD80 (16-10A1), anti-CD86 (GL1), anti-CD90.2 (Thy1.2, 30-H12), anti-CD117 (2B8), anti-Gr-1 (RB6-8C5, Ly-6G), anti-TCR-β (H57-597), anti-TCR-γδ (UC7-13D5), anti-TER-119 (TER-119), anti-MHC II (M5/114.15.2), anti-NKp46 (29A1.4), anti-NK1.1 (PK136), anti-KLRG1 (2F1), anti-Ea$_{52-68}$ (ebioYAe), anti-p-STAT3 (Tyr705) (13A3-1), anti-RORγt (AFKJS-9 or B2D), anti-OX40L (RM134L), anti-IFN-γ (XMG1.2), anti-TNF (MP6-XT22), anti-IL-22 (1H8PWSR), anti-tubulin (DM1A), anti-p-S6 (Ser235/236) (2F9), anti-p-S6 (Ser235/236) (D57.2.2E), anti-p-mTOR (Ser2448) (MRRBY), anti-mouse IgG IRDye680, and anti-rabbit IgG IRDye800.

Mice. Breeding and maintenance of SPF mice were performed in the animal facilities of the Department of Biomedicine (University of Basel, Switzerland) and the Institute for Pharmacology and Toxicology (University of Veterinary Medicine

146

Fig. 7 IFN-γ positively regulates MHC II expression of ILC3s. a Normalized expression of *Ciita* mRNA isoforms regulated by promoters *pI* ($n = 5$ distinct SP ILC3 samples and $n = 9$ distinct SI ILC3 samples), *pIII* ($n = 5$ distinct SP ILC3 samples and $n = 9$ distinct SI ILC3 samples), and *pIV* ($n = 5$ distinct SP ILC3 samples and $n = 8$ distinct SI ILC3 samples) in SP and SI ILC3s. ILC3s were sorted as depicted in Supplementary Fig. 2a. Five independent experiments. **b** Expression of IFN-γ in the SP and the SI of WT mice. $n = 5$ mice of two independent experiments. **c** MHC II expression of SI ILC3s from WT ($n = 6$ distinct samples) and *Ifng*$^{-/-}$ ($n = 6$ distinct samples) mice. NCR$^-$ ILC3s were gated as shown in Fig. 1. Two independent experiments. **d** MHC II expression of SI ILC3s (*Rag2*$^{-/-}$) stimulated for 48 h ($n = 9$ distinct samples of three independent experiments) or 120 h ($n = 10$ (w/o) distinct samples and $n = 11$ (IFN-γ stimulated) distinct samples of four independent experiments) with or without (w/o) IFN-γ. ILC3s were sorted as depicted in Supplementary Fig. 2a. **e** Normalized expression of *Ciita* mRNA isoform regulated by promoter *pIV* in SI ILC3s stimulated with or w/o IFN-γ for 120 h. $n = 5$ distinct samples of five independent experiments. ILC3s were sorted as depicted in Supplementary Fig. 2a. **f** SI ILC3s (sorted from *Rag2*$^{-/-}$ as depicted in Supplementary Fig. 2a) were stimulated for 120 h with or w/o IFN-γ. Naïve CFSE-labeled *OT-II*^{tg} CD4$^+$ T cells were cultured with 1×10^4 IFN-γ stimulated or unstimulated ILC3s in the presence of Ova peptide. $n = 7$ distinct samples of three independent experiments. Each symbol represents a sample and the bar graph represents the mean ± s.e.m. n.s., not significant; *$P \leq 0.05$; **$P \leq 0.01$; ***$P \leq 0.001$; ****$P \leq 0.0001$, calculated with two-tailed unpaired Student's *t* test (**a** *Ciita pI* and *pIII*, **b**, **c**, and **e**), Mann–Whitney test (**a** *Ciita pIV*) or with mixed-effects models (two-sided) using lmerTest (**d** and **f**). Source data are provided as a Source Data File.

Vienna, Austria; license: BMWFW-68.205/0093-WF/V/3b/2015). Germ-free (GF) mice and gnotobiotic sDMDMm2 mice were bred at the Clean Mouse Facility (University of Bern, Switzerland). GF mice were kept in flexible-film isolators or in individually ventilated cages (IVC). Routine monitoring by culture-dependent and -independent methods was done to confirm GF status. Gnotobiotic sDMDMm2 mice were generated by oral and rectal inoculation with a mixture of 12 bacterial strains (see Table 1)[26,41]. All animal experiments were conducted according to the Swiss Veterinary Law and Institutional Guidelines and were approved by the Cantonal Veterinary Office Basel City. Male or female mice of 8-13 weeks of age were used in all experiments. For all experiments, age- and sex-matched experimental groups of mice were used. Mice were housed under pathogen-free conditions in individually ventilated cages in a 22 °C temperature-controlled room with 12-h light–12-h dark cycles and free access to food and water. Experimental and control mice were co-housed and euthanized by terminal CO$_2$ inhalation.

Conventional *C57BL/6* mice (WT) were purchased from Janvier Labs (Saint Berthevin Cedex, France). The following transgenic mouse strains on *C57BL/6* background were used: OT-II T-cell receptor transgenic (*OT-II*^{tg}) mice (kindly provided by Antonius Rolink, University of Basel, Switzerland)[42], *Rag2*$^{-/-}$ mice (kindly provided by Georg Hollaender, University of Basel, Switzerland and Jesus College Oxford, UK)[43], *Rag1*$^{-/-}$ mice, *RORc(γt)-Cre*^{tg} mice (kindly provided by Andreas Diefenbach, Charité, Berlin, Germany)[44], *Rosa26R*$^{eYFP/+}$ (purchased from The Jackson Laboratory, JAX: 006148)[45], *Il23p19*$^{-/-}$ mice (kindly provided by B. Becher, University of Zurich, Switzerland)[46], *Rag2*$^{-/-}$*Il2rg*$^{-/-}$ mice (kindly provided by Joerg Kirberg, Paul-Ehrlich Institut, Langen, Germany)[47], *Flt3L*^{tg} mice (kindly provided by Antonius Rolink, University of Basel, Switzerland)[48], *Myd88*$^{fl/fl}$ mice (purchased from The Jackson Laboratory, JAX: 008888)[49], and *Ifng*$^{-/-}$ mice (kindly provided by Markus Heim, University of Basel, Switzerland)[50]. CD45.1$^+$ mice (purchased from The Jackson Laboratory, JAX: 002014) were bred to *Rag2*$^{-/-}$ mice.

To generate *Roryt*$^{fm+}$ mice, *RORc(γt)-Cre*^{tg} mice were bred to *Rosa26R*$^{eYFP/+}$ mice, as published before[44]. In addition, *Roryt*$^{fm+}$ mice were bred to *Rag2*$^{-/-}$ mice to generate *Roryt*$^{fm+}$*Rag2*$^{-/-}$. *RORc(γt)-Cre*^{tg} mice were bred to *Rptor*$^{fl/fl}$ mice (kindly provided by Michael N. Hall, University of Basel, Switzerland)[51] and backcrossed to *Rag2*$^{-/-}$ background to generate *Rptor*$^{ILC3-/-}$ mice. *VAV1-Cre*^{tg} mice[52] were bred to *Stat3*$^{fl/fl}$ mice[53] to generate *VAV1-Cre*^{tg}*Stat3*$^{fl/fl}$ mice. *RORc(γt)-Cre*^{tg} mice were bred to *Myd88*$^{fl/fl}$ mice to generate *Myd88*$^{ILC3-/-}$ mice.

Isolation of cells. SP and SI cells were isolated as published before[14]. In brief, the SI was opened longitudinally, incubated with 30 mM EDTA in 1 x PBS and washed several times with 1 x PBS to remove feces and mucus. Tissue pieces were digested in DMEM (Thermo Fisher Scientific) containing 0.025 mg per mL DNase I (Sigma-Aldrich) and 1 mg per mL collagenase D (Sigma-Aldrich) for 15 min at 37 °C. Supernatant was collected after washing with DMEM. Digestion steps were repeated three times with remaining tissue. After digestion SI cells were purified by Percoll density gradient (40/80%) centrifugation. The SP was cut into pieces and digested as the SI with DMEM containing DNase I and Collagenase D in 4 steps, each 15 min at 37 °C. Afterwards erythrolysis was performed.

Bone marrow-derived dendritic cells (BMDCs) were generated as published before[14]. In brief, femur and tibia were crushed. After erythrolysis bone marrow cells were cultured with Fms-related tyrosine kinase 3 ligand (Flt3lg)[54] (kindly provided by Antonius Rolink, University of Basel, Switzerland) for 7 days at 37 °C, 10% CO$_2$.

OT-II^{tg} CD4$^+$ T cells were isolated from secondary lymphoid organs as described elsewhere[14]. In brief, suspensions of SP and lymph nodes were generated and erythrolysis was performed. CD4$^+$ cells were enriched with CD4 Microbeads (Miltenyi Biotec) according to manufacturer's instructions. To obtain a pure CD4$^+$ T-cell population, CD11c$^-$CD4$^+$ T cells were sort-purified after enrichment. Sorted CD4$^+$ T cells were stained with 7.5 μM Carboxyfluorescein succinimidyl ester (CFSE, Molecular Probes) at room temperature (10 min) and used for Ag presentation assays.

Flow cytometry and cell sorting. Flow cytometry and cell sorting were done according to standard protocols. Single-cell suspensions were incubated with anti-FcγRII/RIII (cell culture supernatant of hybridoma cells producing clone 2.4G2[55] (kindly provided by Hans Acha-Orbea, University of Lausanne, Switzerland) and surface marker-specific Ab for 30 min on ice in 1 x PBS containing 3% FBS. Live/ dead staining was done with the fixable viability dyes eFluor 450 (eBioscience) or Zombie Aqua™ (BioLegend). For intracellular RORγt staining cells were fixed and permeabilized with the FoxP3 transcription factor staining buffer set (eBioscience) according to manufacturer's instructions. Cytokine staining was done after fixation with PBS containing 4% paraformaldehyde for 10 min on ice. For staining of p-STAT3 (Tyr705), p-mTOR (Ser2448) or p-S6 (Ser235/236) cells were fixed in PBS containing 4% paraformaldehyde for 15 min at 37 °C directly after stimulation. Permeabilization was done with True-Phos™ Perm Buffer (BioLegend) according to manufacturer's instructions. Afterward staining was done for 30 min on ice.

Annexin V staining was done with Annexin V APC (BD Biosciences) according to manufacturer's instructions.

To isolate NCR$^-$ ILC3s by cell sorting, SP and SI cells were stained with Abs specific for CD117, Thy1.2, KLRG1 and a lineage cocktail (lin) of Abs. Unless stated otherwise the following Abs were used for the lin cocktail: CD3ε, CD8α, CD11b, CD11c, CD19, B220, Gr-1, TCR-β, TCR-γ/δ, TER-119, NK1.1, and NKp46. To isolate MHC II$^+$ cells, additional staining with MHC II Ab was done.

Data were acquired with FACS Canto II (BD Bioscience), LSR Fortessa (BD Bioscience), or CytoFLEX (Beckman Coulter's). Sorting was done with a FACS Aria II (BD Bioscience). Diva Software (BD FACS Aria II, BD LSR Fortessa and BD FACS Canto II) and CytExpert Software (CytoFLEX, Beckman Coulter) were used for data collection. For analysis FlowJo (Tree Star) software was used.

Culture and stimulation of ILC3s. Cell culture was performed in IMDM medium (IMDM powder, Sigma-Aldrich), containing 3.02 g per L NaHCO$_3$ (Sigma-Aldrich), 1% Penicillin Streptomycin (Thermo Fisher Scientific), 1% Ciproxine Perfusion 0.2 g (Bayer), 0.1% Kanamycin (Sigma-Aldrich), 1% Insulin Transferrin Selenium (Thermo Fisher Scientific), 0.3% Primatone (Sigma-Aldrich), 1% MEM-NEAA (Thermo Fisher Scientific), 0.1% 2-mercaptoethanol (Thermo Fisher Scientific), and 5% FBS. Sort-purified SI ILC3s (CD117$^+$lin$^-$Thy1.2$^+$KLRG1$^-$) were cultured at 37 °C, 10% CO$_2$ for 7 days with 5% supernatant of IL-2 secreting cell line X63Ag8.653[56] (kindly provided by Antonius Rolink, University of Basel, Switzerland), IL-7 (30 ng per mL, Preprotech), SCF (20 ng per mL, Preprotech), 0.5 μg per mL Amphotericin B (Sigma-Aldrich), and 2% penicillin streptomycin solution (Thermo Fisher Scientific) in 24-well plates (0.5–1 × 10^6 cells per well). Medium was replaced by IMDM medium without Amphotericin B the next day. To analyse in vitro downregulation of MHC II and CD74 ILC3s were exposed to 20 ng per mL IL-23 (eBioscience) for 7 days at 37 °C, 10% CO$_2$ in addition to IL-2, IL-7, and SCF. Fresh IL-23 was added every 2–3 days.

For analysis of *Ciita* promoter usage, MHC II expression and T-cell stimulation capacity NCR$^-$ ILC3s (CD117$^+$lin$^-$Thy1.2$^+$KLRG1$^-$) were sort-purified from the SI and incubated in 24-well plates (0.5–1 × 10^6 cells per well) with 20 ng per mL IFN-γ (eBioscience) for 48 h or 120 h without additional cytokines at 37 °C, 10% CO$_2$. Combined stimulation with IFN-γ (20 ng per mL) and IL-23 (20 ng per mL) was done for 120 h without additional cytokines at 37 °C, 10% CO$_2$.

For phospho-flow staining sort-purified NCR$^-$ ILC3s (CD117$^+$lin$^-$Thy1.2$^+$KLRG1$^-$) were stimulated for the indicated time points with or without IL-23 (20 ng per mL) or IL-1β (20 ng per mL) in IMDM medium. To analyse *Ciita* promoter usage or induction of OX40L, ILC3s (CD117$^+$lin$^-$Thy1.2$^+$KLRG1$^-$) were isolated from *Rag2*$^{-/-}$ mice and stimulated for 18 h with IL-23 (20 ng per mL) or IL-1β (20 ng per mL) in IMDM medium.

Antigen presentation assay. ILC3s or in vitro generated BMDCs were stimulated overnight with 20 ng per mL IL-1β (Biovison Inc.). Unless otherwise indicated 5 × 10^4 ILC3s or BMDCs were cultured with 1.5 × 10^5 CFSE-labeled *OT-II*^{tg} CD4$^+$ T cells in the presence of Ova protein (100 μg per mL, Imject Ovalbumin, Thermo

147

Fisher Scientific, Inc.) or Ova$_{323-339}$ peptide (5 μg per mL, AnaSpec) or medium alone for 72 h at 37 °C, 10% CO_2. T cells were gated as CD3ε$^+$ or CD117$^-$; cells.

Eα-GFP assay. TOP10 *E. coli* bacteria were transformed with a plasmid (kindly provided by Marc Jenkins, University of Minnesota, USA) encoding His-tagged Eα-GFP[57]. After expansion and lysis of bacteria, the protein was purified with a nickel column (His-Select Nickel Affinity Gel, Sigma-Aldrich) according to manufacturer's instructions. Purity was controlled by polyacrylamid gel electrophoresis.

To analyse processing of Eα-GFP sort-purified NCR$^-$ ILC3s (CD117$^+$lin$^-$ Thy1.2$^+$KLRG1$^-$) from SP and SI were incubated with 100 μg per mL Eα-GFP protein in 96-well plates for 72 h at 37 °C, 10% CO_2. Surface presentation of Eα$_{52-68}$ peptide was analyzed by flow cytometry with the YAe antibody (ebioYAe).

Adoptive cell transfer. Lin$^-$Thy1.2$^+$eYFP$^+$ ILC3s of SP and SI was isolated from *RORγt^{fm+}Rag2$^{-/-}$* mice. 0.5–1 × 10^6 SI ILC3s and 1–2 × 10^5 SP ILC3s were intravenously (i.v.) injected into *Rag2$^{-/-}$Il2rg$^{-/-}$* mice. Five weeks after transfer SP and SI cells were isolated and analyzed by flow cytometry. For short-term migration assays (7 days), total splenocytes or total SI lymphocytes from *Rorγt^{fm}Rag2$^{-/-}$* mice were isolated following our protocols described before and i.v. injected into *Rag2$^{-/-}$Il2rg$^{-/-}$* mice (1 × 10^7 SI cells or 5 × 10^7 SP cells per mouse). Lin$^-$Thy1.2$^+$ KLRG1$^-$eYFP$^+$MHC II$^+$ and Lin$^-$Thy1.2$^+$KLRG1$^-$CD45.1$^+$MHC II$^-$ ILC3s were sort-purified from the SI of *Rorγt^{fm}Rag2$^{-/-}$* and CD45.1$^+$Rag2$^{-/-}$ mice, respectively. 1–2 × 10^5 MHC II$^+$ and MHC II$^-$ ILC3s were i.v. injected into *Rag2$^{-/-}$Il2rg$^{-/-}$* mice in a ratio of ~1:1. Five weeks after transfer SP and SI cells were isolated and analyzed by flow cytometry.

RNA sequencing. Cell suspensions were generated from SP and SI of *RORγt^{fm+}* mice. For T- and B-cell depletion of splenocytes 1 × 10^7 cells per mL were stained with CD3ε-biotin and B220-biotin Abs for 15 min on ice in PBS containing 3% FBS. Afterward, cells were incubated with Streptavidin Microbeads (Miltenyi Biotec) for 15 min on ice and depleted according to manufacturer's instructions. CD117$^+$lin$^-$ Thy1.2$^+$eYFP$^+$ NCR$^-$ ILC3s were sort-purified from SI and SP suspensions. RNA was isolated from 1–2 × 10^4 SP ILC3s and 0.5–3 × 10^5 SI ILC3s per sample with the PicoPure RNA isolation kit (Thermo Fisher Scientific) according to manufacturer's instructions. For each sample biological triplicates were generated.

Rag2$^{-/-}$ mice were used for RNA sequencing of cultured ILC3s. CD117$^+$ Thy1.2$^+$lin$^-$(CD3ε, CD8α, CD11b, CD11c, CD19, B220, Gr-1, TCR-β, TCR-γ/δ, TER119, NK1.1)KLRG1$^-$ ILC3s were sort-purified from SI and cultured for 7 days, as described above. RNA was isolated from cultured SI ILC3s (ca. 1 × 10^5 ILC3s per sample) and freshly isolated CD117$^+$lin$^-$Thy1.2$^+$KLRG1$^-$ ILC3s of SP (0.2–0.5 × 10^5 ILC3s per sample) and SI (ca. 1 × 10^5 ILC3s per sample) with the PicoPure RNA isolation kit (Thermo Fisher Scientific). For each sample biological replicates were generated. RNA sequencing and quality control were done by the genomics facility of the Friedrich Miescher Institute for Biomedical Research (Basel, Switzerland) using Hiseq 2500 system. Total RNA was amplified with NuGEN Ovation RNA Seq System V2. Library preparation was done with Illumina TruSeq DNA Nano kit, according to manufacturer's instructions. Base calling and quality scoring were performed with RTA software (Real-Time Analysis).

Obtained single-end RNA-seq reads were mapped to the mouse genome assembly, version mm9 (downloaded from genome.ucsc.edu), with RNA-STAR (2.5.0c)[58], with default parameters except for reporting for multi-mappers only one hit in the final alignment files (outFilterMultimapNmax=1) and filtering reads without evidence in spliced junction table (outFilterType="BySJout"). Subsequent gene expression data analysis was done within the R software (R Foundation for Statistical Computing, Vienna, Austria). Raw reads and mapping quality was assessed by the qQCreport function from the R/Bioconductor software package QuasR (version 1.14.0)[59].

Using RefSeq mRNA coordinates from UCSC (genome.ucsc.edu, downloaded in July 2013) and the qCount function from QuasR package, we quantified gene expression as the number of reads that started within any annotated exon of a gene. The differentially expressed genes were identified using the edgeR package (version 3.16.5)[60]. Pools of mice (indicated as a factor) were included as a covariate. Genes with a false discovery rate (FDR) smaller than 0.05 and minimum log2 (fold change) of 1.5 were considered as differentially expressed.

qRT PCR. For RNA isolation, tissue samples from duodenum, jejunum and terminal ileum of the SI and the whole SP were directly frozen in TRIzol (TRI Reagent, Thermo Fisher Scientific) in liquid N_2. Homogenization of tissue was done in microtubes containing Zirconia beads (BioSpec Products) using FastPrep-24 instrument (MP Biomedicals) for 1 min at 6.5 m/s. RNA was isolated according to manufacturer's instructions (TRi Reagent, Thermo Fisher Scientific). Quality and concentration were measured with a Nanodrop 2000c (Thermo Fisher Scientific). RNA of duodenum, jejunum, and ileum was pooled afterward, unless otherwise indicated.

Synthesis of the first-strand cDNA was done with Oligo dT (Promega), dNTPs (Roche), random hexamers (Sigma-Aldrich), and Superscript III Reverse Transcriptase (Invitrogen) according to manufacturer's instructions. Quantitative real-time PCR (qRT PCR) was done using Sensimix SYBR-Hi-Rox Kit (Bioline) on

a Rotor-Gene RG 3000A (Corbett Research). The following primer were used: *Tbp* fw (GGCACCACCCCCTTGTACCCT), *Tbp* rv (ACGCAGTTGTCCGTGGCTC T), *Il12b* fw (TGGGAGTACCCTGACTCCTG), *Il12b* rv (AGGAACGCACCTTTC TGGTT), *Tnfsf4* fw (ACTCTCTTCCTCTCCGGCAAA), *Tnfsf4* rv (TTGCCCATC CTCACATCTGG), *Il23p19* fw (CACCAGCGGGACATATGAATCT), *Il23p19* rv (CACTGGATACGGGGCACATT), *Ifng* fw (CTGAGACAATGAACGCTACAC), and *Ifng* rv (TTTCTTCCACATCTATGCCAC).

Gene expression was normalized to the gene encoding TATA box binding protein (Tbp) using the comparative threshold cycle method (ΔC$_T$).

To analyse the expression of *pI*, *pIII*, or *pIV* regulated *Ciita* mRNA isoforms qRT PCR was done. SI and SP NCR$^-$ ILC3s (Thy1.2$^+$lin$^-$KLRG1$^-$) were isolated from *Rag2$^{-/-}$* mice. RNA was isolated with the RNeasy Micro Kit (Qiagen) according to manufacturer's instructions. Quality control was done with a Nanodrop 2000c. cDNA synthesis and qRT PCR were done as described above. The following primer were used: *Ciita pI* fw (CAGGGACCATGGAGACCATA GT), *Ciita pI* rv (CAGGTAGCTGCCCTCTGGAG), *Ciita pIII* fw (CTGCATCA CTCTGCTCTCTAA), *Ciita pIII* rv (GTCATAGAGGTGGTAGAGATGT), *Ciita pIV* fw (CATGCAGGCAGCACTCAGAA), and *Ciita pIV* rv (GGGTCGGCAT CACTGTTAAGG). Rotor-Gene software (Corbett Research) was used for data collection and analysis.

In-Cell Western. Sort-purified lin$^-$CD90.2$^+$KLRG1$^-$SI LC3s from *Flt3^{tg}* were cultured 48 h with or without 20 ng per mL IL-23 in the presence or absence of rapamycin (10 or 100 nM). After stimulation, the cells were fixed in PBS containing 3.75% paraformaldehyde for 30 min at room temperature and washed twice with 1% BSA in PBS. Then, cells were permeabilized for 30 min with 0.1% Triton X100 in 1% BSA/PBS and washed once. After blocking with 1% goat serum in 1% BSA/ PBS, cells were incubated overnight with primary mouse α-tubulin (Sigma-Aldrich) and rabbit α-p-S6 Ser235/236 (Cell Signaling Technology) Abs. Finally, cells were washed three times with 0.1% Triton X100 in 1% BSA/PBS, incubated for 1 h with secondary goat α-mouse IgG IRDye680 (LI-COR Biosciences) and goat α-rabbit IgG IRDye800 (LI-COR Biosciences) Abs and washed five times with 0.1% Triton X100 in 1% BSA/PBS. Before scanning the cells with the Odyssey CLx Infrared Scanning System (LI-COR Biosciences), all supernatant was removed. Image Studio Software (LI-COR) using Odyssey CLx Infrared Scanning System (LI-COR Biosciences) was used for data collection.

Statistical analysis. GraphPad Prism 7 (GraphPad Software, Inc., La Jolla, CA, USA) was used to calculate P values with one-way ANOVA, Mann–Whitney test or two-tailed Student's *t* test with a 95% confidence interval, as outlined in each figure legend. In some experiments pools of mice were used for in vitro assays. Statistical analysis for these experiments was done with mixed-effects models (random effect: pool of mice, fixed effect: treatment, mouse strain or organ) and lmerTest package of R software with a Satterthwaite approximation[61]. For multiple comparisons with mixed effect models P values have been adjusted with Benjamini–Hochberg procedure.

Reporting summary. Further information on research design is available in the Nature Research Reporting Summary linked to this article.

Data availability

Sequencing data reported in this paper is accessible with the following accession code: GSE114751 (https://www.ncbi.nlm.nih.gov/geo/query/acc.cgi?acc=GSE114751). Data bases used in this study are accessible at UCSC Genome Browser (http://hgdownload.soe. ucsc.edu/goldenPath/mm9/bigZips/, http://hgdownload.soe.ucsc.edu/goldenPath/mm9/ database/). The data underlying Figs. 1e, 2a–d, 3a, b, 4c–e, 5a–g, 6a–d, 7a–f and Supplementary Figs. 2c, d, g, h, 3a, b, e, 4a, b, 5a, g, 6b, c, 7a–c and 8a, b are provided as a Source Data File.

Code availability

Data analyses codes have been published before and are available from the corresponding author on request[58–60].

References

1. Sun, Z. et al. Requirement for RORgamma in thymocyte survival and lymphoid organ development. *Science* **288**, 2369–2373 (2000).
2. Eberl, G. et al. An essential function for the nuclear receptor RORgamma(t) in the generation of fetal lymphoid tissue inducer cells. *Nat. Immunol.* **5**, 64–73 (2004).
3. Spits, H. et al. Innate lymphoid cells–a proposal for uniform nomenclature. *Nat. Rev. Immunol.* **13**, 145–149 (2013).

148

4. Cella, M. et al. A human natural killer cell subset provides an innate source of IL-22 for mucosal immunity. *Nature* **457**, 722–725 (2009).
5. Cupedo, T. et al. Human fetal lymphoid tissue-inducer cells are interleukin 17-producing precursors to RORC+ CD127+ natural killer-like cells. *Nat. Immunol.* **10**, 66–74 (2009).
6. Takatori, H. et al. Lymphoid tissue inducer-like cells are an innate source of IL-17 and IL-22. *J. Exp. Med.* **206**, 35–41 (2009).
7. Satoh-Takayama, N. et al. Microbial flora drives interleukin 22 production in intestinal NKp46+ cells that provide innate mucosal immune defense. *Immunity* **29**, 958–970 (2008).
8. Sonnenberg, G. F., Monticelli, L. A., Elloso, M. M., Fouser, L. A. & Artis, D. CD4(+) lymphoid tissue-inducer cells promote innate immunity in the gut. *Immunity* **34**, 122–134 (2011).
9. Tumanov, A. V. et al. Lymphotoxin controls the IL-22 protection pathway in gut innate lymphoid cells during mucosal pathogen challenge. *Cell Host Microbe* **10**, 44–53 (2011).
10. Zheng, Y. et al. Interleukin-22 mediates early host defense against attaching and effacing bacterial pathogens. *Nat. Med.* **14**, 282–289 (2008).
11. Hanash, A. M. et al. Interleukin-22 protects intestinal stem cells from immune-mediated tissue damage and regulates sensitivity to graft versus host disease. *Immunity* **37**, 339–350 (2012).
12. Hepworth, M. R. et al. Innate lymphoid cells regulate CD4+ T-cell responses to intestinal commensal bacteria. *Nature* **498**, 113–117 (2013).
13. Hepworth, M. R. et al. Immune tolerance. Group 3 innate lymphoid cells mediate intestinal selection of commensal bacteria-specific CD4+ T cells. *Science* **348**, 1031–1035 (2015).
14. von Burg, N. et al. Activated group 3 innate lymphoid cells promote T-cell-mediated immune responses. *Proc. Natl Acad. Sci. USA* **111**, 12835–12840 (2014).
15. Kim, C. H., Hashimoto-Hill, S. & Kim, M. Migration and tissue tropism of innate lymphoid cells. *Trends Immunol.* **37**, 68–79 (2016).
16. Simoni, Y. et al. Human innate lymphoid cell subsets possess tissue-type based heterogeneity in phenotype and frequency. *Immunity* **46**, 148–161 (2017).
17. Nussbaum, K. et al. Tissue microenvironment dictates the fate and tumor-suppressive function of type 3 ILCs. *J. Exp. Med.* jem.20162031, https://doi.org/10.1084/jem.20162031 (2017).
18. Ricardo-Gonzalez, R. R. et al. Tissue signals imprint ILC2 identity with anticipatory function. *Nat. Immunol.* https://doi.org/10.1038/s41590-018-0201-4 (2018).
19. Robinette, M. L. et al. Transcriptional programs define molecular characteristics of innate lymphoid cell classes and subsets. *Nat. Immunol.* **16**, 306–317 (2015).
20. Gury-BenAri, M. et al. The spectrum and regulatory landscape of intestinal innate lymphoid cells are shaped by the microbiome. *Cell* **166**, 1231–1246.e13 (2016).
21. Kiss, E. A. et al. Natural aryl hydrocarbon receptor ligands control organogenesis of intestinal lymphoid follicles. *Science* **334**, 1561–1565 (2011).
22. Qiu, J. et al. The aryl hydrocarbon receptor regulates gut immunity through modulation of innate lymphoid cells. *Immunity* **36**, 92–104 (2012).
23. van de Pavert, S. A. et al. Maternal retinoids control type 3 innate lymphoid cells and set the offspring immunity. *Nature* **508**, 123–127 (2014).
24. Withers, D. R. et al. Cutting edge: lymphoid tissue inducer cells maintain memory CD4 T cells within secondary lymphoid tissue. *J. Immunol.* **189**, 2094–2098 (2012).
25. Goto, Y. et al. Segmented filamentous bacteria antigens presented by intestinal dendritic cells drive mucosal Th17 cell differentiation. *Immunity* **40**, 594–607 (2014).
26. Uchimura, Y. et al. Complete genome sequences of 12 species of stable defined moderately diverse mouse microbiota 2. *Genome Announc.* **4**, 476–2 (2016).
27. Kinnebrew, M. A. et al. Interleukin 23 production by intestinal CD103(+) CD11b(+) dendritic cells in response to bacterial flagellin enhances mucosal innate immune defense. *Immunity* **36**, 276–287 (2012).
28. Becker, C. et al. Constitutive p40 promoter activation and IL-23 production in the terminal ileum mediated by dendritic cells. *J. Clin. Invest.* **112**, 693–706 (2003).
29. Guo, X. et al. Induction of innate lymphoid cell-derived interleukin-22 by the transcription factor STAT3 mediates protection against intestinal infection. *Immunity* **40**, 25–39 (2014).
30. Chen, F. et al. mTOR mediates IL-23 induction of neutrophil IL-17 and IL-22 production. *J. Immunol.* **196**, 4390–4399 (2016).
31. Mao, K. et al. Innate and adaptive lymphocytes sequentially shape the gut microbiota and lipid metabolism. *Nature* **554**, 255–259 (2018).
32. Cai, Y. et al. Differential roles of the mTOR-STAT3 signaling in dermal γδ T cell effector function in skin inflammation. *Cell Rep.* **27**, 3034–3048 (2019).
33. Reith, W., LeibundGut-Landmann, S. & Waldburger, J.-M. Regulation of MHC class II gene expression by the class II transactivator. *Nat. Rev. Immunol.* **5**, 793–806 (2005).
34. Rao, A. et al. Cytokines regulate the antigen-presenting characteristics of human circulating and tissue-resident intestinal ILCs. *Nat. Commun.* (2020).
35. Castellanos, J. G. et al. Microbiota-induced TNF-like ligand 1A drives group 3 innate lymphoid cell-mediated barrier protection and intestinal T cell activation during colitis. *Immunity* https://doi.org/10.1016/j.immuni.2018.10.014 (2018).
36. Kim, M.-Y. et al. CD4(+)CD3(-) accessory cells costimulate primed CD4 T cells through OX40 and CD30 at sites where T cells collaborate with B cells. *Immunity* **18**, 643–654 (2003).
37. Klose, C. S. N. et al. A T-bet gradient controls the fate and function of CCR6⁻RORγt+ innate lymphoid cells. *Nature* **494**, 261–265 (2013).
38. Parham, C. et al. A receptor for the heterodimeric cytokine IL-23 is composed of IL-12Rbeta1 and a novel cytokine receptor subunit IL-23R. *J. Immunol.* **168**, 5699–5708 (2002).
39. Gasteiger, G., Fan, X., Dikiy, S., Lee, S. Y. & Rudensky, A. Y. Tissue residency of innate lymphoid cells in lymphoid and nonlymphoid organs. *Science* **350**, 981–985 (2015).
40. Crinier, A. et al. High-dimensional single-cell analysis identifies organ-specific signatures and conserved NK cell subsets in humans and mice. *Immunity* https://doi.org/10.1016/j.immuni.2018.09.009 (2018).
41. Brugiroux, S. et al. Genome-guided design of a defined mouse microbiota that confers colonization resistance against *Salmonella enterica* serovar Typhimurium. *Nat. Microbiol.* **2**, 16215 (2016).
42. Barnden, M. J., Allison, J., Heath, W. R. & Carbone, F. R. Defective TCR expression in transgenic mice constructed using cDNA-based alpha- and beta-chain genes under the control of heterologous regulatory elements. *Immunol. Cell Biol.* **76**, 34–40 (1998).
43. Shinkai, Y. et al. RAG-2-deficient mice lack mature lymphocytes owing to inability to initiate V(D)J rearrangement. *Cell* **68**, 855–867 (1992).
44. Eberl, G. & Littman, D. R. Thymic origin of intestinal alphabeta T cells revealed by fate mapping of RORgammat+ cells. *Science* **305**, 248–251 (2004).
45. Srinivas, S. et al. Cre reporter strains produced by targeted insertion of EYFP and ECFP into the ROSA26 locus. *BMC Dev. Biol.* **1**, 4–8 (2001).
46. Ghilardi, N. et al. Compromised humoral and delayed-type hypersensitivity responses in IL-23-deficient mice. *J. Immunol.* **172**, 2827–2833 (2004).
47. Colucci, F. et al. Dissecting NK cell development using a novel alymphoid mouse model: investigating the role of the c-abl proto-oncogene in murine NK cell differentiation. *J. Immunol.* **162**, 2761–2765 (1999).
48. Tsapogas, P. et al. In vivo evidence for an instructive role of fms-like tyrosine kinase-3 (FLT3) ligand in hematopoietic development. *Haematologica* **99**, 638–646 (2014).
49. Hou, B., Reizis, B. & DeFranco, A. L. Toll-like receptors activate innate and adaptive immunity by using dendritic cell-intrinsic and -extrinsic mechanisms. *Immunity* **29**, 272–282 (2008).
50. Dalton, D. K. et al. Multiple defects of immune cell function in mice with disrupted interferon-gamma genes. *Science* **259**, 1739–1742 (1993).
51. Bentzinger, C. F. et al. Skeletal muscle-specific ablation of raptor, but not of rictor, causes metabolic changes and results in muscle dystrophy. *Cell Metab.* **8**, 411–424 (2008).
52. de Boer, J. et al. Transgenic mice with hematopoietic and lymphoid specific expression of Cre. *Eur. J. Immunol.* **33**, 314–325 (2003).
53. Alonzi, T. et al. Essential role of STAT3 in the control of the acute-phase response as revealed by inducible gene inactivation [correction of activation] in the liver. *Mol. Cell. Biol.* **21**, 1621–1632 (2001).
54. Brasel, K., De Smedt, T., Smith, J. L. & Maliszewski, C. R. Generation of murine dendritic cells from flt3-ligand-supplemented bone marrow cultures. *Blood* **96**, 3029–3039 (2000).
55. Unkeless, J. C. Characterization of a monoclonal antibody directed against mouse macrophage and lymphocyte Fc receptors. *J. Exp. Med.* **150**, 580–596 (1979).
56. Karasuyama, H. & Melchers, F. Establishment of mouse cell lines which constitutively secrete large quantities of interleukin 2, 3, 4 or 5, using modified cDNA expression vectors. *Eur. J. Immunol.* **18**, 97–104 (1988).
57. Itano, A. A. et al. Distinct dendritic cell populations sequentially present antigen to CD4 T cells and stimulate different aspects of cell-mediated immunity. *Immunity* **19**, 47–57 (2003).
58. Dobin, A. et al. STAR: ultrafast universal RNA-seq aligner. *Bioinformatics* **29**, 15–21 (2013).
59. Gaidatzis, D., Lerch, A., Hahne, F. & Stadler, M. B. QuasR: quantification and annotation of short reads in R. *Bioinformatics* **31**, 1130–1132 (2015).
60. Robinson, M. D., McCarthy, D. J. & Smyth, G. K. edgeR: a Bioconductor package for differential expression analysis of digital gene expression data. *Bioinformatics* **26**, 139–140 (2010).
61. Kuznetsova, A., Brockhoff, P. B. & Christensen, R. H. B. lmerTest Package: tests in linear mixed effects models. *J. Stat. Softw.* **82**, 1–26 (2017).

Competing interests

The authors declare no competing interests.

Additional information

Supplementary information is available for this paper at https://doi.org/10.1038/s41467-020-15612-2.

Correspondence and requests for materials should be addressed to D.F.

Peer review information *Nature Communications* thanks Andrew McKenzie and the other, anonymous, reviewer(s) for their contribution to the peer review of this work.

Reprints and permission information is available at http://www.nature.com/reprints

Publisher's note Springer Nature remains neutral with regard to jurisdictional claims in published maps and institutional affiliations.

150

2. Dual function of mTOR signalling in regulating ILC3 proliferation and Type 1 responses in the intestine.

Claudia Teufel[1], Edit Horvath[1], Annick Peter[1], Salvatore Piscuoglio[2], Caner Ercan[2], Michael N. Hall[3], Daniela Finke[1*], Frank Michael Lehmann[1*]

In preparation

[1]Department of Biomedicine and University Children's Hospital of Basel, University of Basel, 4058 Basel, Switzerland; [2]Institute of Pathology, University Hospital Basel, 4031 Basel, Switzerland [3]Biozentrum, University of Basel, 4056 Basel, Switzerland.

*equal contribution

Abstract

Group 3 innate lymphoid cells (ILC3s) support the integrity of the intestinal barrier through production of IL-22. Upon activation ILC3s can switch towards IFN-γ[+]ILCs, which have a pathogenic role in intestinal inflammation. The mechanism by which the activation-induced IFN-γ-release occurs is not completely understood. Using mice with a specific deletion of *Rptor* or *Rictor* we show here that under state conditions mTORC1 and to a lesser extent mTORC2 have a role in the regulation of ILC3 proliferation and cell numbers. In an IFN-γ-dependent colitis mouse model loss of mTORC1 or mTORC2 signaling in ILC3s ameliorated disease. In line, activation-induced phosphorylation of the transcription factor STAT4 and transition towards IFN-γ[+]ILCs were reduced in ILC3s deficient in mTORC1 or mTORC2 signaling.

These data collectively show a critical role for mTOR in controlling the number and IFN-γ-production of ILC3s and suggest that mTOR inhibitors might be protective in IFN-γ-mediated inflammatory diseases.
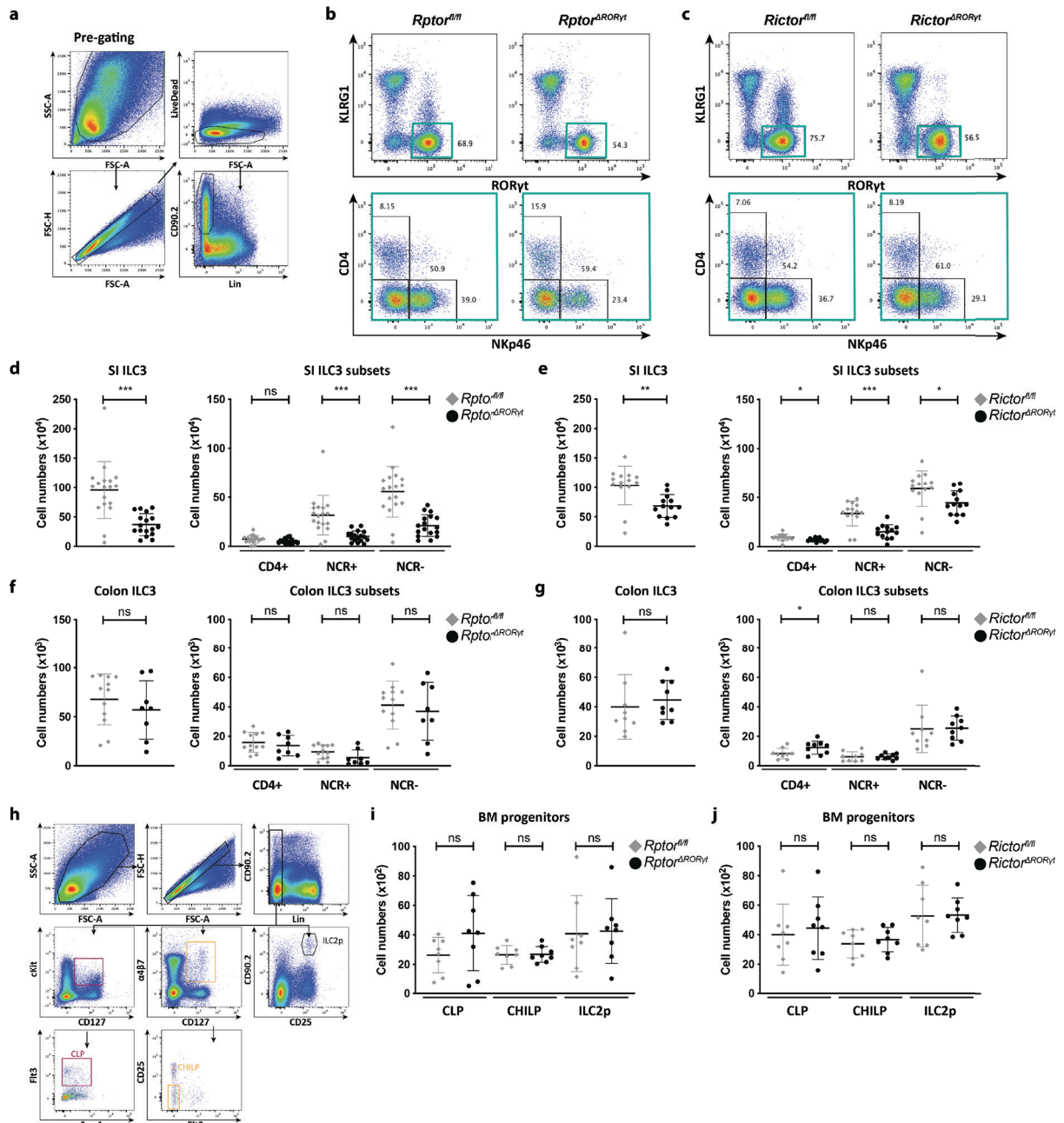
Fig.1 ILC3 subsets in *Rag2⁻/⁻* mice are dependent on mTORC1 and mTORC2 signaling *in vivo*. Cells were isolated from SI LP and cLP of *Rptor^ΔRORγt* (b, d, f) or *Rictor^ΔRORγt* (c, e, g) mice and age-matched Cre-negative littermates. a) Pre-gating for ILCs. Lin: CD3, CD8, CD11c, CD19, B220, Gr-1, TCRβ, TCRγδ, Ter-119. b, c) Exemplary blots of ILC3 subsets in the SI. The ILC3 subset (blue marked gate, upper panel) was separated into CD4⁺, NCR⁻ and NCR⁺ ILC3 subsets (lower panel). d-g) Total ILC3 numbers and numbers of CD4⁺, NCR⁻ and NCR⁺ ILC3s was analyzed in indicated organs. Mice were 8-10 weeks old at analysis. n = 8-17. h-j) Cells were isolated from the tibia and femur of one hind leg of *Rptor^ΔRORγt* (i) or *Rictor^ΔRORγt* (j) mice and age-matched Cre-negative littermates and analyzed for number of common lymphoid progenitors (CLPs), common helper ILC progenitors (CHILPs) and ILC2 progenitors (ILC2ps). Mice were 8-10 weeks old at analysis. n = 7-8. h) Gating strategy for hematopoietic progenitors. Lin: CD3, CD8, CD11c, CD19, B220, Gr-1, NK1.1, TCRβ, TCRγδ, Ter-119. i, j) Total numbers of CLPs, CHILPs and ILC2ps in indicated mouse strains. Two-tailed unpaired t test or Mann-Whitney U test. *p ≤ 0.05, **p ≤ 0.01, ***p ≤ 0.001
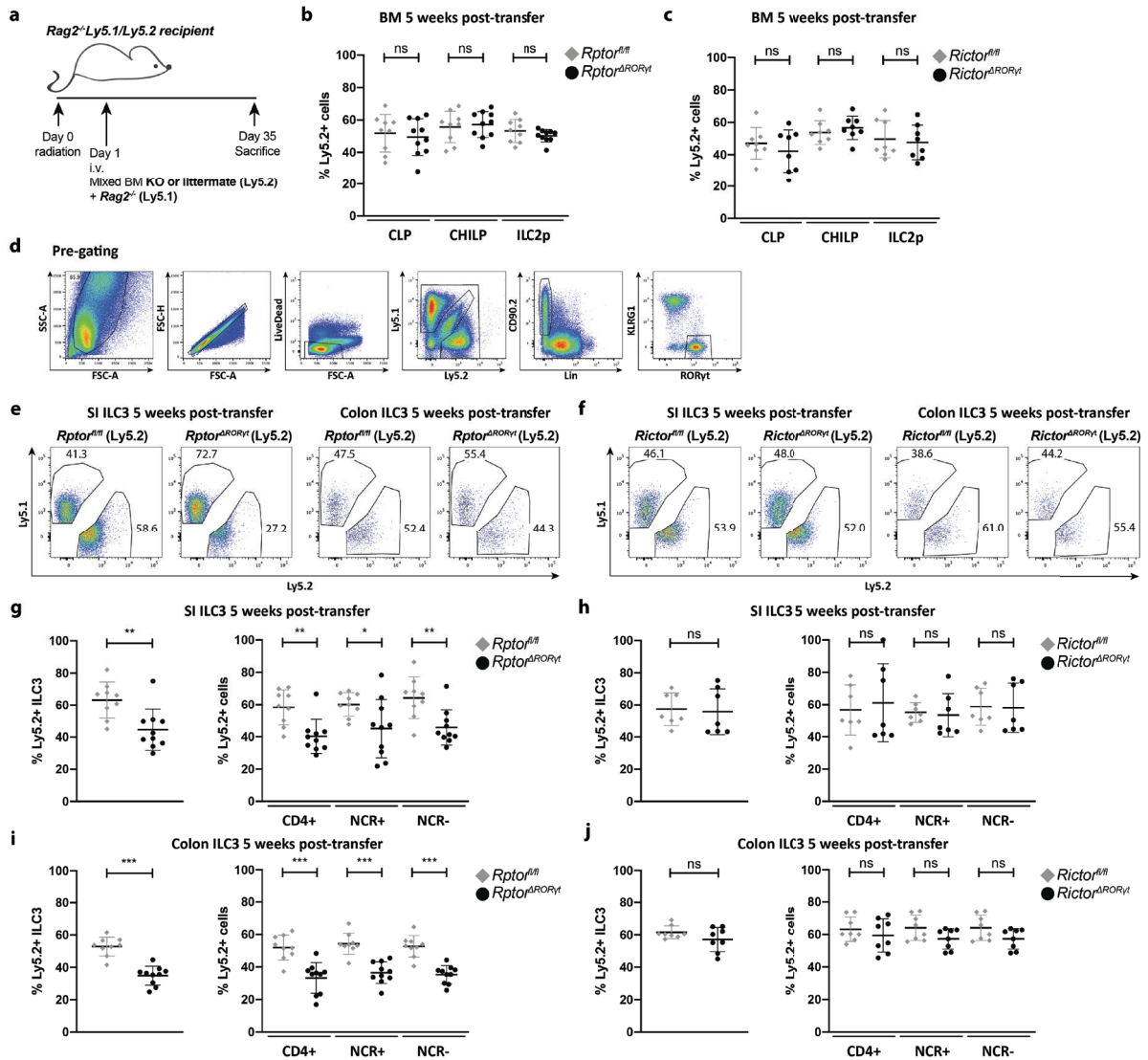
Fig.2 Competitive reconstitution of ILC3s in bone marrow chimeras is impaired by *RORc*-driven deletion of *Rptor* but not *Rictor*. a) Bone marrow chimera model: BM from *Rag2⁻/⁻Ly5.1* mice was mixed in a 1:1 ratio with BM from either *Rptor^ΔRORγt* mice (b, e, g, i), *Rictor^ΔRORγt* (c, f, h, j) mice or Cre-negative littermates, respectively. Five weeks after transplantation, mice were sacrificed. Cell were extracted from the SI LP, the cLP and the tibia and femur of one hind leg (BM). b, c) Percentage of Ly5.2⁺Ly5.1⁻ CLPs, CHILPs and ILC2ps in the BM was determined by flow cytometry. d) Gating strategy for donor-derived ILCs. Lin: CD3, CD8, CD11c, CD19, B220, Gr-1, TCRβ, TCRγδ, Ter-119. e, f) Exemplary blots of Ly5.1 and Ly5.2 percentages within donor-derived ILC3 population. g-j) Percentage of Ly5.2-positive ILC3s was determined in the SI (j, k) and colon (l, m). n = 8-10 mice from 2-3 independent experiments. Two-tailed unpaired t test or Mann-Whitney U test. *p ≤ 0.05, **p ≤ 0.01, ***p ≤ 0.001
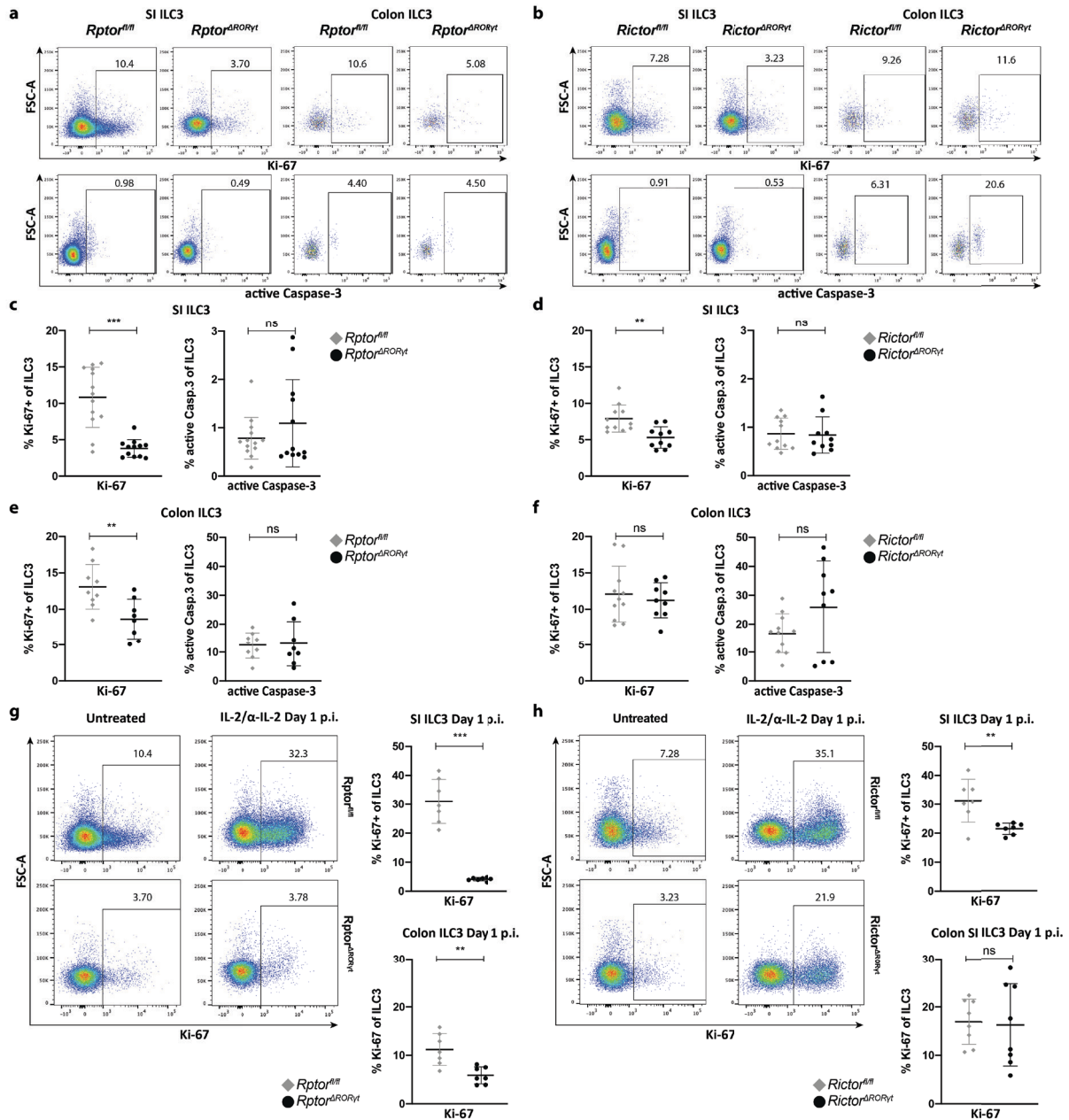
Fig.3 Disruption of mTORC1 or mTORC2 signaling impairs IL-2/α-IL-2 complex-mediated ILC3 proliferation *in vivo*. a-f) Cells were isolated from the SI LP and cLP of *Rptor^ΔRORγt* (a, c, e) or *Rictor^ΔRORγt* (b, d, f) mice and age-matched Cre-negative littermates. a, b) Exemplary blots of SI and colonic ILC3s. c-f) Percentage of Ki-67-positive ILC3s and ILC3s positive for active Caspase-3 was determined by flow cytometry. n = 10-12. g, h) *Rptor^ΔRORγt* (g) or *Rictor^ΔRORγt* (h) mice and Cre-negative littermates were injected with one single dose of IL-2/α-IL-2 complex. After one day, cells from the SI LP and cLP were isolated and the percentage of Ki-67-positive ILC3s was analyzed by flow cytometry. Exemplary blots from untreated and treated animals are shown on the left side. n = 7 mice from 2-3 independent experiments. Two-tailed unpaired t test. *p ≤ 0.05, **p ≤ 0.01, ***p ≤ 0.001

154
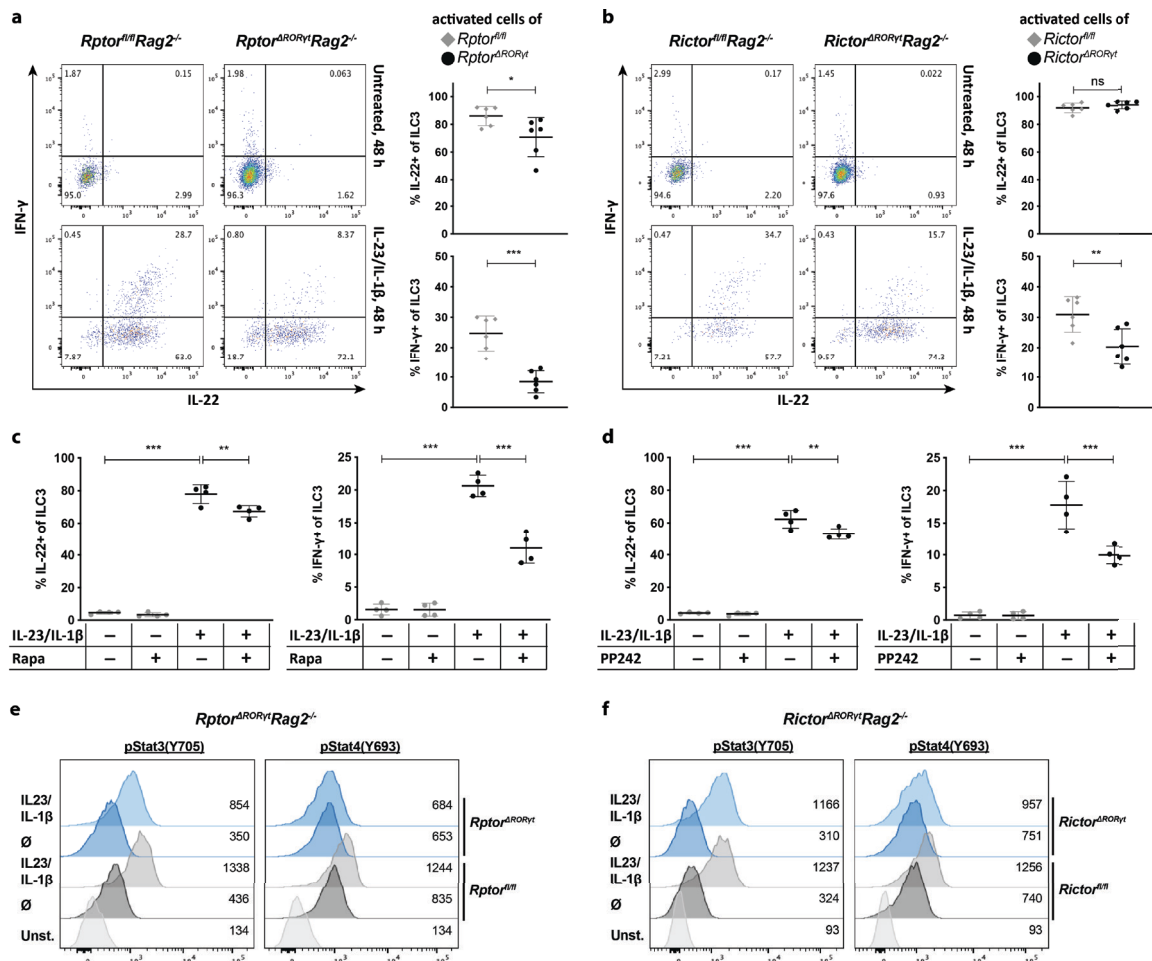
Fig.4 Loss of mTORC1 and mTORC2 signaling impairs IFN-γ but not IL-22 in ILC3s *in vitro*. a, b) Lin⁻CD90.2⁺KLRG1⁻ ILC3s were sorted from the SI of *Rptor^ΔRORγt* (a) or *Rictor^ΔRORγt* (b) mice and control littermates and cultured with 20 ng/ml IL-23 and IL-1β for 2 days. Intracellular IL-22 and IFN-γ was measured by flow cytometry. For each experiment, cells from 1-3 mice per group were pooled. n = 6 experiments. Two-tailed unpaired t-test. c, d) Cells were isolated from the SI of C57BL/6J mice. Lin⁻CD90.2⁺KLRG1⁻ ILC3s were sorted and cultured with 20 ng/ml IL-23 and IL-1β or medium. Where indicated, 10 nM rapamycin (c) or 1 μM PP242 (d) was added. After 2 days, cells were stained for intracellular IL-22 and IFN-γ. For each experiment, cells from 8-10 mice were pooled. n = 4 experiments. One-Way ANOVA with multiple comparison test (Dunnett). e, f) Lin⁻CD90.2⁺KLRG1⁻ ILC3s were sorted from the SI of *Rptor^ΔRORγt* (e) or *Rictor^ΔRORγt* (f) mice and control littermates and cultured with 20 ng/ml IL-23 and IL-1β for 17 h. Phosphorylation of STAT3 and STAT4 was determined by phosphoFlow analysis. Depicted histograms (modal view) are representative of 4-6 independent experiments. Lin: CD3, CD8, CD11c, CD19, B220, Gr-1, NK1.1, TCRβ, TCRγδ, Ter-119. *p ≤ 0.05, **p ≤ 0.01, ***p ≤ 0.001

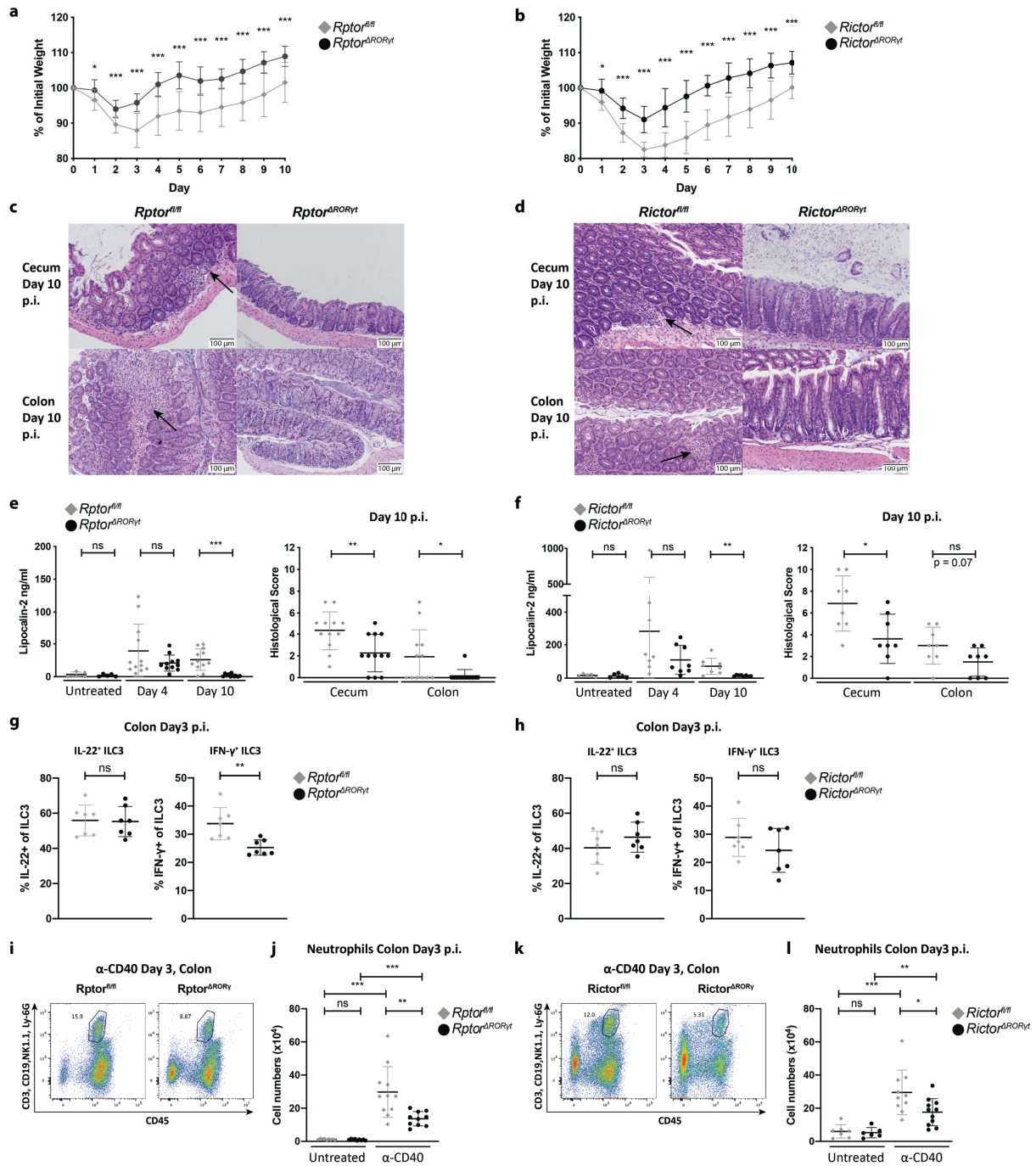**Fig.5 Single inhibition of mTORC1 or mTORC2 signaling in ILC3s protects *Rag2^{-/-}* mice from α-CD40 colitis.** a-f) *Rptor[ΔRORγt]* (a, c, e) or *Rictor[ΔRORγt]* (b, d, f) mice and age-matched littermates were left untreated or were injected with a single dose of 140 μg α-CD40 Ab. Weight was monitored daily (a, b). Mice were sacrificed 10 days post-injection. Same parts of the colon and the whole cecum were sectioned and stained with hematoxylin and eosin. Exemplary histology picture from the cecum and colon are depicted (c, d). Arrows indicate lymphocyte invasions. Histological colitis score was determined by an experienced gastroenterologist (e, f, right). At day 4 and day 10, fecal Lipocalin-2 was determined from feces pellets diluted in PBS using ELISA (e, f, left). g-l) *Rptor[ΔRORγt]* (g, i, j) or *Rictor[ΔRORγt]* (h, k, l) mice and age-matched littermates were left untreated or received a single dose of 140 μg α-CD40 Ab. Weight was monitored daily. Mice were sacrificed 3 days post-injection. Cells were isolated from the cLP. g, h) 1.0 - 1.5 x 10⁶ cLPs cells were cultured overnight. Brefeldin A was added 4 h before staining. Percentage of IL-22⁺ and IFN-γ⁺ ILC3s was determined by flow cytometry. i-l) Neutrophils were analyzed by FACS. Exemplary

FACS plots (g, i) and total neutrophil counts (h, j) are depicted. Lin: CD3, CD19, NK1.1, Ly-6G n = 6-13 from 2-4 independent experiments. Two-tailed unpaired t test or Mann-Whitney U test. *p ≤ 0.05, **p ≤ 0.01, ***p ≤ 0.001
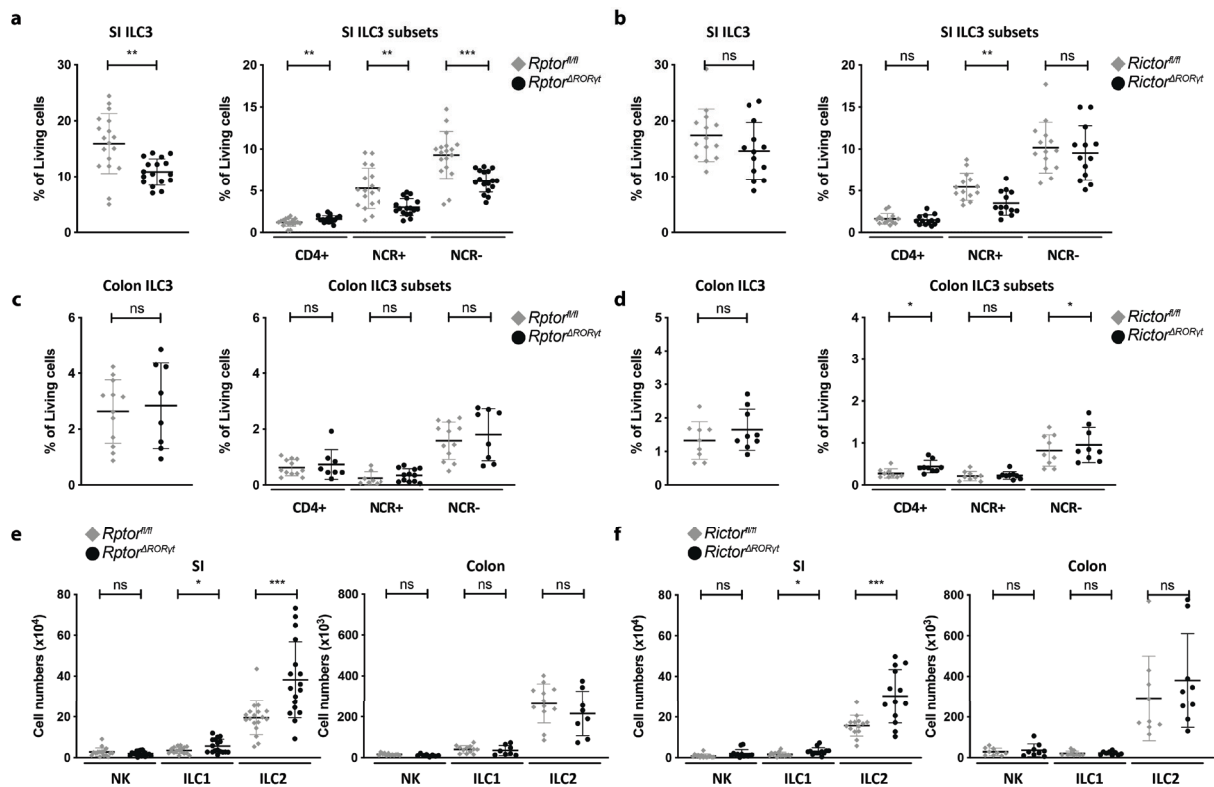

Fig.S1 Percentage of ILC3 subsets and total number of other ILCs in *Rptor^ΔRORγt* and *Rictor^ΔRORγt* mice. Cells were isolated from SI LP and cLP of *Rptor^ΔRORγt* (a, c, e) or *Rictor^ΔRORγt* (b, d, f) mice and age-matched Cre-negative littermates. a-d) Cell isolates were analyzed for percentage of total ILC3 and percentage of CD4+, NCR- and NCR+ ILC3 subsets within the ILC3 subset. e, f) Total number of NK cells (Lin-CD90.2+KLRG1+/-T-bet+Eomes+), ILC1s (Lin-CD90.2+KLRG1+/-T-bet+Eomes-) and ILC2s (Lin-CD90.2+KLRG1+ CD25+CD127+/low) was determined by flow cytometry. Lin: CD3, CD8, CD11c, CD19, B220, Gr-1, TCRβ, TCRγδ, Ter-119. Mice were 8-10 weeks old at analysis. n = 8-17. Two-tailed unpaired t test or Mann-Whitney U test. *p ≤ 0.05, **p ≤ 0.01, ***p ≤ 0.001
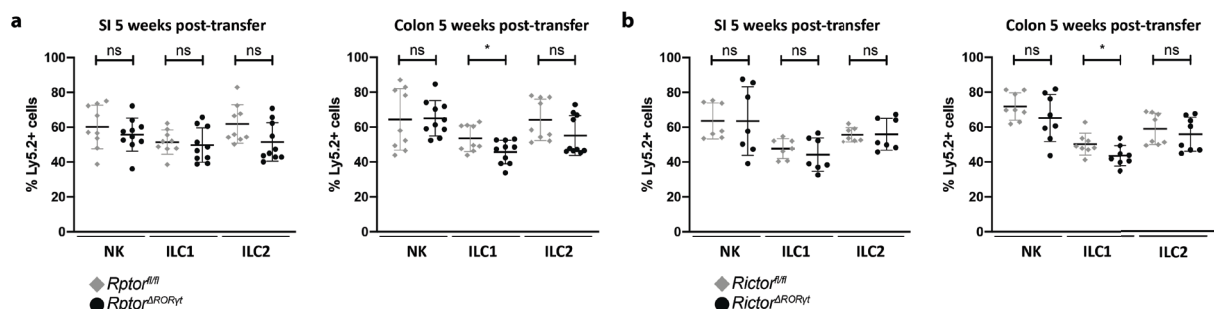

Fig.S2 Percentage of donor-derived NK cells, ILC1s and ILC2s in bone marrow chimeras. Bone marrow chimera model: BM from *Rag2^-/-Ly5.1* mice was mixed in a 1:1 ratio with BM from either *Rptor^ΔRORγt* mice (a), *Rictor^ΔRORγt* (b) mice or Cre-negative littermates, respectively. Five weeks after transplantation, mice were sacrificed. Cell were extracted from the SI LP and the cLP. a, b) Percentage of Ly5.2+Ly5.1- NK cells, ILC1s and ILC2s within donor-derived cells was determined by flow cytometry. n = 8-10 mice from 2-3 independent experiments. Two-tailed unpaired t test or Mann-Whitney U test. *p ≤ 0.05, **p ≤ 0.01, ***p ≤ 0.001
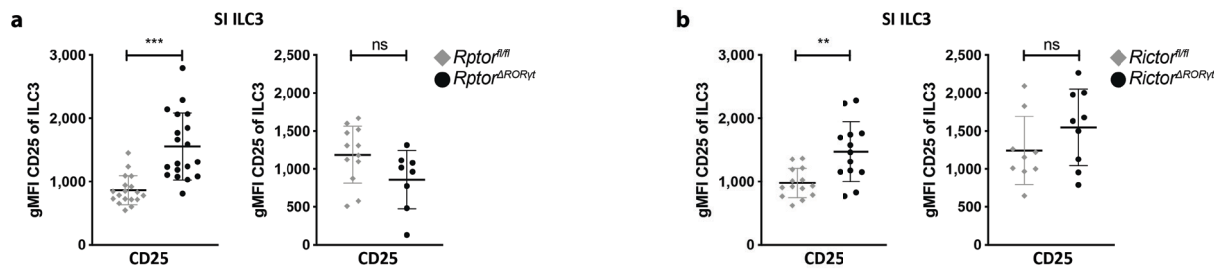
Fig.S3 CD25 expression in SI and colonic ILC3s derived from _Rptor^ΔRORγt_ and _Rictor^ΔRORγt_ mice. a-b) Cells were isolated from the SI LP and cLP of _Rptor^ΔRORγt_ (a) or _Rictor^ΔRORγt_ (b) mice and age-matched Cre-negative littermates. CD25 surface expression was determined on ILC3s. n= 12-19. Two-tailed unpaired t test. *p ≤ 0.05, **p ≤ 0.01, ***p ≤ 0.001
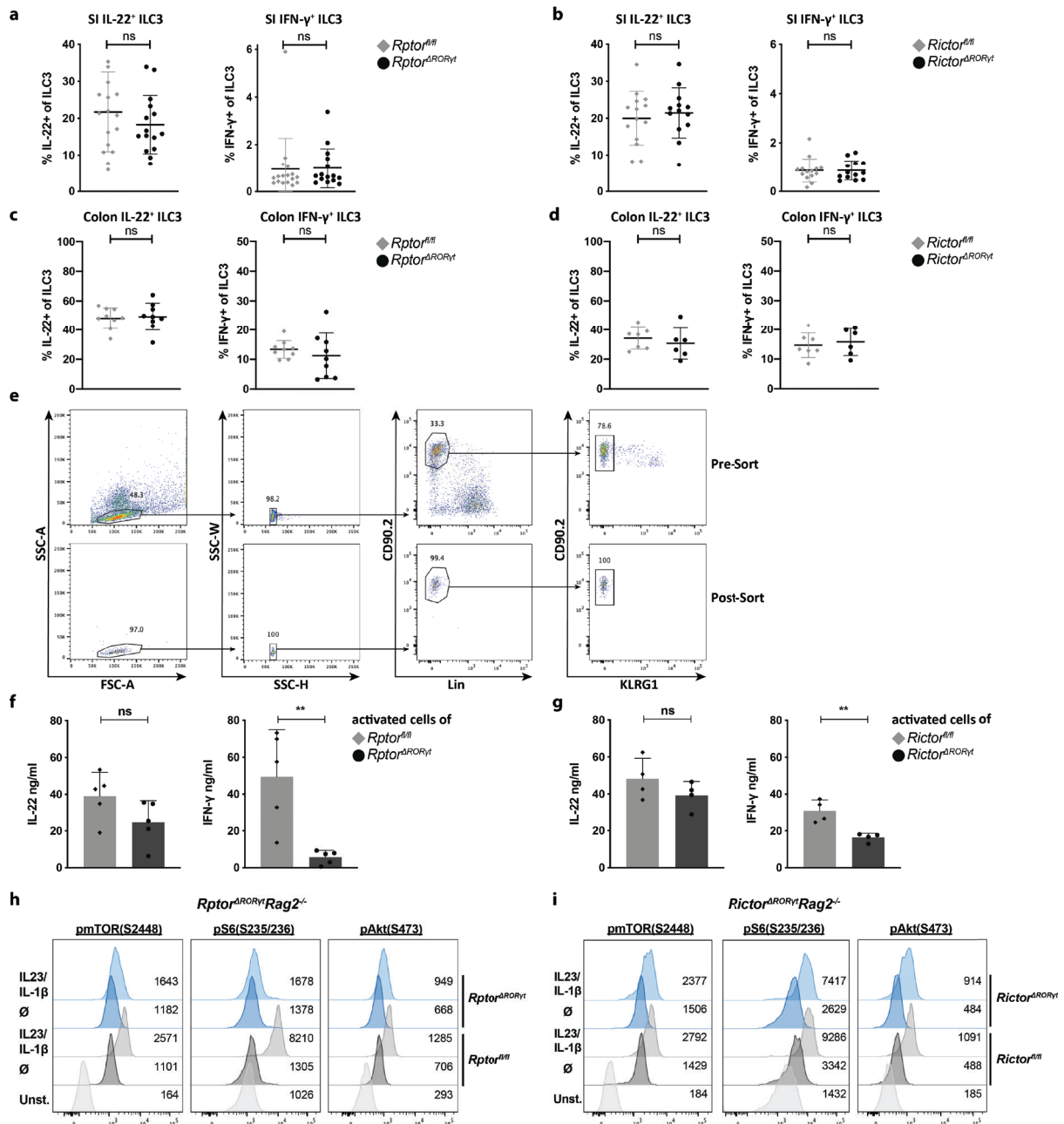

Fig.S4 Steady state cytokines in ILC3s _ex vivo_ and IFN-γ protein, IL-22 protein in and phosphorylation of mTOR targets in activated ILC3s _in vitro_. a-d) Cells were isolated from SI LP and cLP of _Rptor^ΔRORγt_ (a, c) or _Rictor^ΔRORγt_ (b,

d) mice and age-matched Cre-negative littermates. Naïve SI LP and cLP cells were cultured with Brefeldin A for 2 h and percentage of IL-22 and IFN-γ-producing ILC3s was determined by flow cytometry. Mice were 8-10 weeks old at analysis. n = 8-17. Two-tailed unpaired t test or Mann-Whitney U test. e) Sort strategy for ILC3s. f, g) Lin⁻CD90.2⁺KLRG1⁻ ILC3s were sorted from the SI of $Rptor^{\Delta ROR\gamma t}$ (f) or $Rictor^{\Delta ROR\gamma t}$ (g) mice and control littermates and cultured with 20 ng/ml IL-23 and IL-1β for 2 days. IL-22 and IFN-γ levels in the supernatant were measured using Th Cytokine LEGENDplex Kit. For each experiment, cells from 2-3 mice per group were pooled. n = 4-5 experiments. Two-tailed unpaired t test. h, i) Lin⁻CD90.2⁺KLRG1⁻ ILC3s were sorted from the SI of $Rptor^{\Delta ROR\gamma t}$ (h) or $Rictor^{\Delta ROR\gamma t}$ (i) mice and control littermates and cultured with 20 ng/ml IL-23 and IL-1β for 17 h. Phosphorylation of mTOR, mTORC1-target site in S6 protein and mTORC2-target site in Akt was determined by phosphoFlow analysis. Depicted histograms (modal view) are representative of 4-6 independent experiments. Lin: CD3, CD8, CD11c, CD19, B220, Gr-1, NK1.1, TCRβ, TCRγδ, Ter-119. *p ≤ 0.05, **p ≤ 0.01, ***p ≤ 0.001

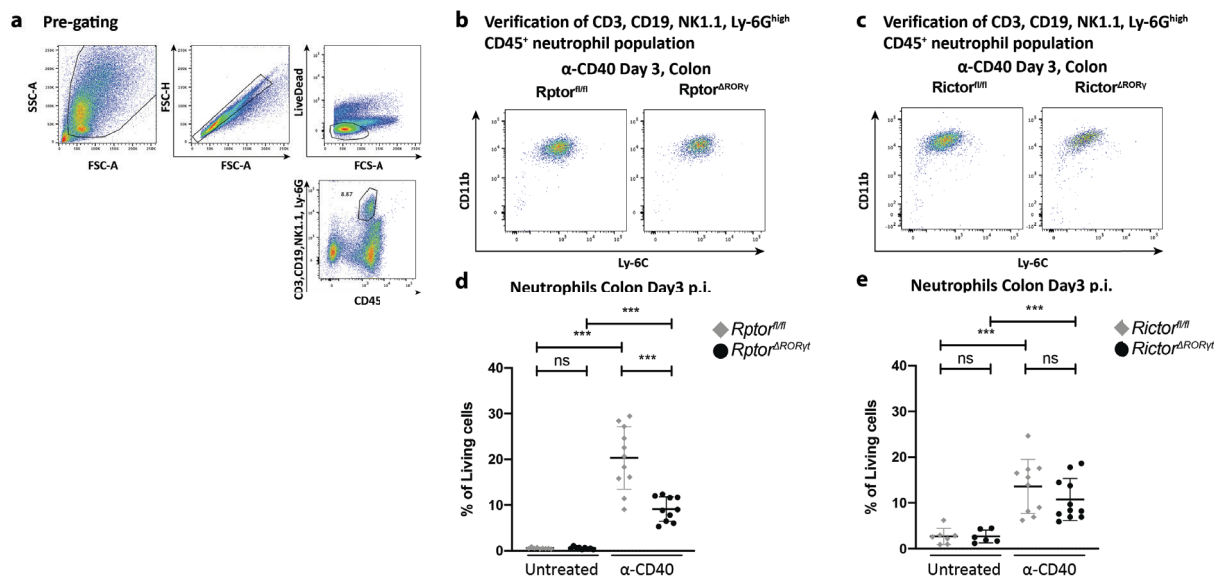**Fig.S5 Verification of neutrophils population.** $Rptor^{\Delta ROR\gamma t}$ (b) or $Rictor^{\Delta ROR\gamma t}$ (c) mice and age-matched littermates were left untreated or were injected with a single dose of 140 µg α-CD40 Ab. Mice were sacrificed 3 days post-injection and cells were isolated from the cLP. Neutrophils were analyzed by FACS. a) Gating of neutrophils. b, c) Exemplary plots verifying CD3, CD19, NK1.1, Ly-6G^high CD45⁺ population as CD11b⁺Ly-6C⁺ neutrophils. d, e) Percentage of neutrophils within living cells. 3-4 independent experiments. Two-tailed unpaired t test. *p ≤ 0.05, **p ≤ 0.01, ***p ≤ 0.001